# The Journal of Gemmology

Volume 35 / No. 4 / 2016

SSEF
SCHWEIZERISCHES GEMMOLOGISCHES INSTITUT
SWISS GEMMOLOGICAL INSTITUTE
INSTITUT SUISSE DE GEMMOLOGIE

Gem-A
THE GEMMOLOGICAL ASSOCIATION OF GREAT BRITAIN

The Gemmological Association of Great Britain

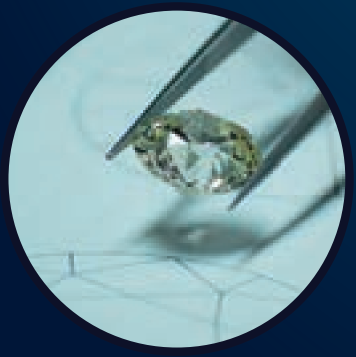

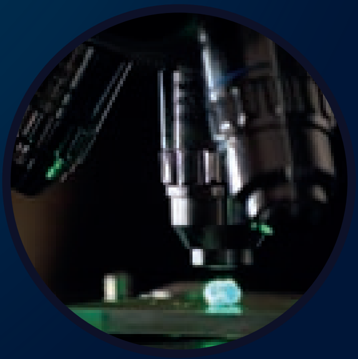

The Journal of
# Gemmology
Volume 35 / No. 4 / 2016

## COLUMNS

271 **What's New**
DiaPix Jewelry Imaging | DiaTrue screening system | GemTrue Experior tester | GLIS-3000 GEM Luminous Imaging System | J-Secure synthetic diamond detector | Solico and Synova diamond-cutting machines | CIBJO Congress 2016 presentations and special reports | GIT Lab Updates | USA lifts ban on Burmese ruby and jadeite | *Margaritologia* newsletter | David Friend Hall at the Yale Peabody Museum | Harvard Museum virtual tour | 'Jades for Life and Death' online

274 **Practical Gemmology**
Anomalous behaviour of a Sumitomo synthetic diamond on the reflectance meter

276 **Gem Notes**
Antigorite serpentine from northwestern Pakistan | 'Black' axinite | Beryl from Tanzania with phenakite inclusions | Clinohumite from Vietnam | Lace opal from Utah, USA | Pollucite from Pakistan with polylithionite inclusions | Large ruby matrix from Lục Yên, Vietnam | Scapolite from Badakhshan, Afghanistan | Tourmaline from Ife, Osun State, Nigeria | Cat's-eye väyrynenite from Pakistan | Quartzite and calcite bangles resembling jadeite | Large pink sapphire with diffusion-induced star | Mid-year 2016 Myanma Jade & Gems Emporium

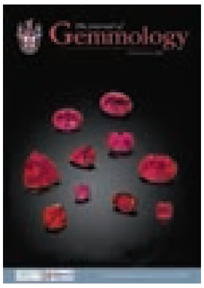

**Cover Photo:** Greenland is poised to become a significant producer of rubies and pink sapphires. These rubies recovered from the Aappaluttoq deposit weigh 0.29–2.53 ct and were characterized for an article appearing in this issue (see pp. 294–306). Photo by Bilal Mahmood, AGL.

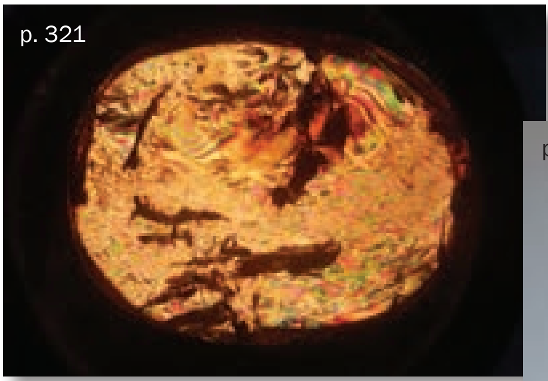

p. 321

p. 287

## ARTICLES

### Feature Articles

294 **Ruby and Pink Sapphire from Aappaluttoq, Greenland**
*By Christopher P. Smith, Andrew J. Fagan and Bryan Clark*

308 **Geology, Gemmological Properties and Preliminary Heat Treatment of Gem-Quality Zircon from the Central Highlands of Vietnam**
*By Le Thi-Thu Huong, Bui Sinh Vuong, Nguyen Thi Minh Thuyet, Nguyen Ngoc Khoi, Somruedee Satitkune, Bhuwadol Wanthanachaisaeng, Wolfgang Hofmeister, Tobias Häger and Christoph Hauzenberger*

320 **Identification of Reconstructed Amber from Different Periods**
*By Haibo Li, Jie Liang, Taijin Lu, Jun Zhang and Jun Zhou*

330 **Violet-to-Blue 'Nuummite' from Simiuttat, Greenland: Origin of Colour Appearance and Conditions of Formation**
*By Leander Franz, Tay Thye Sun, Richard Wirth, Christian de Capitani and Loke Hui Ying*

342 **Conferences**
2nd European Mineralogical Conference | HRD Antwerp Symposium | Geological Society of America | Gem-A Conference

349 **Gem-A Notices**

364 **Learning Opportunities**

367 **New Media**

370 **Literature of Interest**

*The Journal* is published by Gem-A in collaboration with SSEF and with the support of AGL and GIT.

Gem-A
THE GEMMOLOGICAL ASSOCIATION OF GREAT BRITAIN

SSEF
SCHWEIZERISCHES GEMMOLOGISCHES INSTITUT
SWISS GEMMOLOGICAL INSTITUTE
INSTITUT SUISSE DE GEMMOLOGIE

AGL

ISSN: 1355-4565, http://dx.doi.org/10.15506/JoG.2016.35.4

The Journal of
Gemmology

**Editor-in-Chief**
Brendan M. Laurs
brendan.laurs@gem-a.com

**Production Editor**
Mary A. Burland
mary.burland@gem-a.com

**Marketing Consultant**
Ya'akov Almor
bizdev@gem-a.com

**Editorial Assistant**
Carol M. Stockton

**Editor Emeritus**
Roger R. Harding

**Executive Editor**
Alan D. Hart

**Associate Editors**

Ahmadjan Abduriyim, *Tokyo, Japan;* Edward Boehm, *RareSource, Chattanooga, Tennessee, USA;* Maggie Campbell Pedersen, *Organic Gems, London;* Alan T. Collins, *King's College London;* John L. Emmett, *Crystal Chemistry, Brush Prairie, Washington, USA;* Emmanuel Fritsch, *University of Nantes, France;* Rui Galopim de Carvalho, *Portugal Gemas, Lisbon, Portugal;* Lee A. Groat, *University of British Columbia, Vancouver, Canada;* Thomas Hainschwang, *GGTL Laboratories, Balzers, Liechtenstein;* Henry A. Hänni, *GemExpert, Basel, Switzerland;* Jeff W. Harris, *University of Glasgow;* Alan D. Hart, *Gem-A, London;* Ulrich Henn, *German Gemmological Association, Idar-Oberstein;* Jaroslav Hyršl, *Prague, Czech Republic;* Brian Jackson, *National Museums Scotland, Edinburgh;* Stefanos Karampelas, *GRS Gemresearch Swisslab, Basel, Switzerland;* Lore Kiefert, *Gübelin Gem Lab Ltd., Lucerne, Switzerland;* Hiroshi Kitawaki, *Central Gem Laboratory, Tokyo, Japan;* Michael S. Krzemnicki, *Swiss Gemmological Institute SSEF, Basel;* Shane F. McClure, *Gemological Institute of America, Carlsbad, California;* Jack M. Ogden, *Striptwist Ltd., London;* Federico Pezzotta, *Natural History Museum of Milan, Italy;* Jeffrey E. Post, *Smithsonian Institution, Washington DC, USA;* Andrew H. Rankin, *Kingston University, Surrey;* George R. Rossman, *California Institute of Technology, Pasadena, USA;* Karl Schmetzer, *Petershausen, Germany;* Dietmar Schwarz, *AIGS Lab Co. Ltd., Bangkok, Thailand;* Menahem Sevdermish, *GemeWizard Ltd., Ramat Gan, Israel;* Guanghai Shi, *China University of Geosciences, Beijing;* James E. Shigley, *Gemological Institute of America, Carlsbad, California;* Christopher P. Smith, *American Gemological Laboratories Inc., New York, New York;* Evelyne Stern, *London;* Elisabeth Strack, *Gemmologisches Institut Hamburg, Germany;* Tay Thye Sun, *Far East Gemological Laboratory, Singapore;* Pornsawat Wathanakul, *Gem and Jewelry Institute of Thailand, Bangkok;* Chris M. Welbourn, *Reading, Berkshire;* Bert Willems, *Leica Microsystems, Wetzlar, Germany;* Bear Williams, *Stone Group Laboratories LLC, Jefferson City, Missouri, USA;* J.C. (Hanco) Zwaan, *National Museum of Natural History 'Naturalis', Leiden, The Netherlands.*

## Content Submission

The Editor-in-Chief is glad to consider original articles, news items, conference/excursion reports, announcements and calendar entries on subjects of gemmological interest for publication in *The Journal of Gemmology*. A guide to the various sections and the preparation of manuscripts is given at www.gem-a.com/index.php/news-publications/publications/journal-of-gemmology/submissions, or contact the Production Editor.

## Subscriptions

Gem-A members receive *The Journal* as part of their membership package, full details of which are given at www.gem-a.com/membership. Laboratories, libraries, museums and similar institutions may become Direct Subscribers to *The Journal*.

## Advertising

Enquiries about advertising in *The Journal* should be directed to the Marketing Consultant. For more information, see www.gem-a.com/index.php/news-publications/publications/journal-of-gemmology/advertising.

## Database Coverage

*The Journal of Gemmology* is covered by the following abstracting and indexing services: Australian Research Council academic journal list, British Library Document Supply Service, Chemical Abstracts (CA Plus), Copyright Clearance Center's RightFind application, CrossRef, EBSCO (Academic Search International, Discovery Service and TOC Premier), Gale/Cengage Learning Academic OneFile, GeoRef, Mineralogical Abstracts, ProQuest, Scopus and the Thomson Reuters' Emerging Sources Citation Index (in the Web of Science).

## Copyright and Reprint Permission

For full details of copyright and reprint permission contact the Editor-in-Chief.

*The Journal of Gemmology* is published quarterly by Gem-A, The Gemmological Association of Great Britain. Any opinions expressed in *The Journal* are understood to be the views of the contributors and not necessarily of the publisher.

Printed by DG3 (Europe) Ltd.
© 2016 The Gemmological Association of Great Britain
ISSN: 1355-4565

Mixed Sources
Product group from well-managed forests and other controlled sources
www.fsc.org Cert no. TT-COC-002454
© 1996 Forest Stewardship Council
FSC

Gem-A
THE GEMMOLOGICAL ASSOCIATION
OF GREAT BRITAIN

21 Ely Place
London EC1N 6TD
UK

t: +44 (0)20 7404 3334
f: +44 (0)20 7404 8843
e: information@gem-a.com
w: www.gem-a.com

Registered Charity No. 1109555
A company limited by guarantee and
registered in England No. 1945780
Registered office: Palladium House,
1–4 Argyll Street, London W1F 7LD

**President**
Maggie Campbell Pedersen

**Vice Presidents**
David J. Callaghan
Alan T. Collins
Noel W. Deeks
E. Alan Jobbins,
Andrew H. Rankin

**Honorary Fellows**
Gaetano Cavalieri
Terrence S. Coldham
Emmanuel Fritsch

**Honorary Diamond Member**
Martin Rapaport

**Chief Executive Officer**
Alan D. Hart

**Council**
Justine L. Carmody – Chair
Kathryn L. Bonanno
Paul F. Greer
Kerry H. Gregory
J. Alan W. Hodgkinson
Nigel B. Israel
Jack M. Ogden
Richard M. Slater
Christopher P. Smith

**Branch Chairmen**
Midlands – Georgina E. Kettle
North East – Mark W. Houghton
South East – Veronica Wetten
South West – Richard M. Slater

*Understanding Gems™*

# What's New

## INSTRUMENTATION

### DiaPix Jewelry Imaging System

In March 2016, OGI Systems Ltd. (Ramat Gan, Israel) released DiaPix Jewelry, an "all in one video imaging machine" that captures high-definition images and 360° videos of loose gemstones as well as jewellery of any size. The unit measures 42 × 24 × 37 cm, and the system includes video editing tools that allow the user to rapidly upload interactive videos to the internet. Visit www.ogisystems.com/diapixjewel.html. *CMS*

### DiaTrue Diamond Screening System

Released by OGI Systems Ltd. in September 2016, the DiaTrue is designed to screen colourless natural diamonds, HPHT synthetic diamonds and HPHT-treated CVD synthetic diamonds. Both mounted and unmounted samples can be tested, the latter including parcels and individual gems from 0.01 to ~20 ct. The system reportedly operates by detecting weak phosphorescence of catalyst residues from the HPHT process, and suspect gems must be confirmed by additional laboratory testing. The unit weighs approximately 8.5 kg and measures 28 × 25 × 50 cm. Visit www.ogisystems.com/diatrue.html. *CMS*

### GemTrue Experior Tester

The GemTrue Multi Experior DK9000, released by DiKai Industrial (Shenzhen, China) in April 2016, is a pen-style thermoelectric probe that reportedly can identify diamond, synthetic moissanite and cubic zirconia, as well as help distinguish natural from synthetic ruby and sapphire. Both mounted and loose gems can be tested. Measuring 150 × 33 × 23 mm and weighing 42 g, it is highly portable. Visit www.dikaitools.com/en/Diamond_Testers_Moissanite_Testers/20160404/432.html. *CMS*

### GLIS-3000 GEM Luminous Imaging System

Released in October 2015 by Biaoqi Guangzhou Electronic Science Technology Co. Ltd. (Guangzhou, China), the GLIS-3000 GEM Luminous Imaging System is designed to quickly test batches of loose diamonds (rough or cut, including melee), as well as mounted stones. The instrument contains a UV spectrometer and excites diamond luminescence to produce fluorescence and phosphorescence images that allow the user to refer certain samples for further testing to confirm natural or synthetic (HPHT and CVD) origin. Visit www.gzbiaoqi.com/ProductShow.asp?ArticleID=393. *CMS*

### J-Secure Synthetic Diamond Detector

As a follow-up to the D-Secure instrument (see What's New section, **35**(2), 91), J-Secure was released by DRC Techno (Gujarat, India) in October 2016 to identify synthetic dia-

monds in jewellery. The instrument is available in two versions: the J-Secure, which is for use only with jewellery, and the J-Secure Plus, which can be used with both mounted and loose diamonds. For details, including video demonstrations, visit www.jsecure.in. *CMS*

### Solico Diamond-Cutting Machine

Announced in June 2016, the Solico Diamond Robotics Process from OGI Systems Ltd. is a fully automated system for cutting diamonds. The machine first analyses the rough (including CVD synthetic diamond shapes) to determine which of nine shapes will yield maximum profit. It will then block, brute, table-saw and polish to within 90% of the finished product. Visit www.ogisystems.com/solico.html. *CMS*

### Synova Diamond-Cutting Machines

Synova Advanced Laser Systems (Synova SA, Lausanne, Switzerland) announced in May 2016 the release of three models of diamond-cutting machines. The different units are optimized for cutting specific size ranges, and all of them use Synova's Laser MicroJet technology that combines a 532 nm laser with a thin water jet. Three-axis and five-axis versions are available for a range of capabilities. Information about each model is available at www.synova.ch/products/diamond-cutting-systems.html. *CMS*

## NEWS AND PUBLICATIONS

### CIBJO Congress 2016 Presentations and Special Reports

Five of the presentations from this year's CIBJO Congress, held 26–28 October in Yerevan, Armenia, are available at www.cibjo.org/congress2016/presentations. They include talks by Andrew Bone about the Responsible Jewellery Council; Eduardo Escobedo on the Responsible Ecosystems Sourcing Platform; Ian Harebottle about Gemfields as a coloured stone supplier; and Dr Michael Krzemnicki on laboratory standards for the coloration of 'pigeon-blood' ruby and 'royal blue' sapphire. Special Reports released prior to the Congress from the commissions on pearls, gemmology, precious metals, coloured stones, diamonds, ethics, and marketing and education are also available for download at www.cibjo.org/congress2016/special-reports-2. *CMS*

### GIT Lab Updates

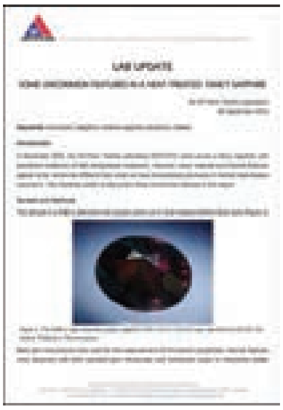

In September 2016, the Gem and Jewelry Institute of Thailand released two Lab Updates: 'Cymrite: An unusual jade imitation' and 'Some uncommon features in a heat-treated fancy sapphire'. To download these and other reports, including some GIT-authored abstracts from the GIT 2016 conference, visit www.git.or.th/2014/articles_technic_en.html. *CMS*

### USA Lifts Ban on Burmese Ruby and Jadeite

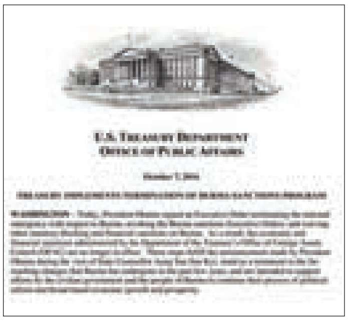

On 7 October 2016, President Obama signed an Executive Order terminating the Burma Sanctions programme that for more than a decade has banned the importation into the USA of Burmese ruby and jadeite (rough, cut and mounted). For in-depth information and related

resources, visit www.treasury.gov/resource-center/sanctions/programs/pages/burma.aspx. *CMS*

### *Margaritologia* Pearl Newsletter No. 5/6

*Margaritologia* No. 5/6 was released in August 2016 and includes reports on the history of the pearling trade as presented at the International Maritime Economic History Association's 7th International Congress of Maritime History; 'The Art and Science of Gems' exhibition at the ArtScience Musum in Singapore; and pearling icon Bill Reed's autobiographical book *The Long Road to Broome*. To subscribe to the newsletter, visit www.gemmologisches-institut-hamburg.de. *CMS*

## MISCELLANEOUS

### David Friend Hall at the Yale Peabody Museum

October 2016 marked the opening of the David Friend Hall, to coincide with the 150th anniversary of the Yale Peabody Museum (New Haven, Connecticut, USA). This new gallery displays more than 150 gem and mineral specimens in dramatic fashion, including many notable specimens (e.g. a large tanzanite crystal, a 77 ct yellow diamond and a 75 ct sapphire). Some are permanent exhibits, while others are on loan from private collections. Under development is an accompanying mobile app that visitors can download to their smartphone or tablet to enhance their visit. To learn more, read this pre-opening article: http://news.yale.edu/2016/10/17/peabody-museum-s-new-mineral-gallery-will-knock-your-socks. *CMS*

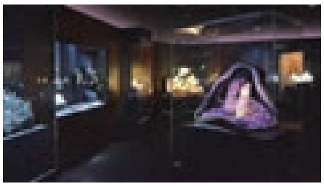

### Harvard Museum Virtual Tour

Take a virtual tour of some of the gems and minerals at Harvard University's Mineralogical and Geological Museum (Cambridge, Massachusetts, USA) through Google Arts & Culture, which presents images from more than 1,000 partner museums and archives. At the time of writing, three Harvard exhibits were available: 'Opals', 'Albert Burrage and His Rare Golds' and 'The Hamlin Collection' (featuring tourmaline from Mount Mica, Maine, USA). These online exhibits include high-resolution photos of notable pieces along with descriptive text and historical material. Also pictured are various additional specimen photos and a profile of the museum, which is headed by Dr Raquel Alonso-Perez FGA. Take the tour at www.google.com/culturalinstitute/beta/partner/mineralogical-and-geological-museum-harvard-university. *CMS*

### Jades for Life and Death Online

In October 2016, the Smithsonian's Freer Gallery of Art and Arthur M. Sackler Gallery (Washington DC, USA) launched the first part of their five-volume online digital catalogue, 'Jades for Life and Death'. It features more than 250 ancient Chinese jades from the extensive Freer and Sackler collections dating from the Chinese Stone Age (ca. 5000–1700 BC) through the Han Dynasty (206 BC–220 AD), along with essays on the history of the collection, related scientific studies and an archaeological survey of the Neolithic Liangzhu culture. The searchable catalogue is available at www.asia.si.edu/publications/jades/default.php. *CMS*

---

**What's New** provides announcements of new instruments/technology, publications, online resources and more. Inclusion in What's New does not imply recommendation or endorsement by Gem-A. Entries were prepared by Carol M. Stockton (CMS) or Brendan M. Laurs (BML), unless otherwise noted.

# Anomalous Behaviour of a Sumitomo Synthetic Diamond on the Reflectance Meter

*Alan Hodgkinson*

Gemmological surprises sometimes come when least expected. At the September 2016 Registered Valuer conference in Loughborough, I ran three 'Yellow Gemstone' workshops. Thirty-four gems were available for 'hands-on' access, accompanied by a list of the instruments that were available to probe further into their identity.

A fine 'canary' diamond (Bruton, 1970; Cunningham, 2011) was included among the study samples (Figure 1, left) along with its definition: no absorption features are visible with a hand-held spectroscope, and the identity of such a type Ib diamond is further clinched by bright yellow fluorescence to long- and short-wave UV radiation, with the long-wave UV producing the stronger fluorescence. The yellow colour of 'canary' diamonds is due to dispersed single (unaggregated) nitrogen atoms. This contrasts with the majority (98%) of natural yellow diamonds, which are type Ia with the nitrogen in aggregated form, and with a characteristic 415 nm absorption system commonly seen (referred to as the *cape series*) with a hand-held spectroscope.

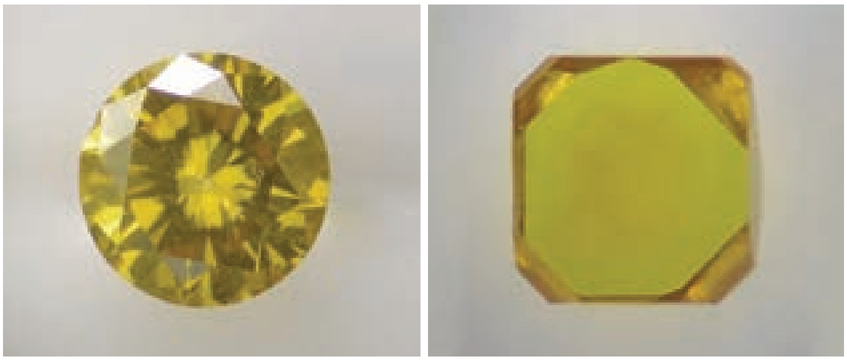

*Figure 1: The natural 'canary' diamond on the left weighs 0.50 ct, and the Sumitomo crystal on the right is 5 mm in dimension. Photos by A. Hodgkinson.*

Also available to the delegates was a yellow synthetic diamond grown by Sumitomo in Japan (Figure 1, right); such crystals were first introduced in 1985. Yellow synthetic diamonds are type Ib with no absorption seen in the visible range, like their natural type Ib equivalent. However, the yellow UV fluorescence of the Sumitomo product is stronger to short-wave than to long-wave UV. This behaviour is often observed in synthetic diamonds but is most unusual in their natural counterparts. Another interesting feature of the Sumitomo synthetic diamonds is their distorted cross-shaped pattern of strain birefringence seen between crossed polarizers (Figure 2). Bear in mind that samples cut from larger crystals (Sumitomo synthetics over 10 ct have been reported) may only yield a portion of such a pattern, which would not be so obviously diagnostic.

Among the tools available to the delegates were some Hanneman Diamond Eye reflectance meters (Figure 3). Also called

*Figure 2: A distorted cross-shaped strain pattern is seen between crossed polarizers in the 5 mm Sumitomo synthetic diamond crystal. Photomicrograph by A. Hodgkinson; magnified 10x.*

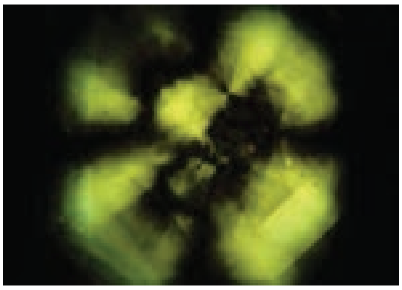

*Figure 3: The Hanneman Diamond Eye reflectance meter is a useful tool for checking the comparative RIs of diamond and its various simulants. Photo by A. Hodgkinson.*

'lustre meters', such instruments are quite useful to the gemmologist, as they require no contact liquid and can record reflection (and its comparative sequence level of refraction) to cope with any level of RI. Before measuring an unknown specimen, it is essential to set the instrument against a control sample. One of the delegates, Rupert Huddy, duly did this with a control cubic zirconia. However, on testing the Sumitomo synthetic diamond, the indicator needle raced across the scale beyond 'diamond' to the extremity of the instrument. He drew my attention to this, and I proceeded to check his finding. Care was taken to set the meter twice against a control sample of natural diamond, but each time the erratic behaviour was repeated by the Sumitomo specimen. The results were further checked using three other Hanneman reflectance meters, including a desk model that gives a more controlled reflection response across a wide 5-inch screen.

Gemmologists should be aware of the possibility for such anomalous behaviour when testing Sumitomo synthetic diamonds. It would be interesting to have readers with access to Sumitomo specimens repeat this procedure on any reflectance meter.

### *References*

Bruton E., 1970. *Diamonds*. N.A.G. Press, London (see pp. 315, 328).

Cunningham D., 2011. *The Diamond Compendium*. N.A.G. Press, London (see p. 340).

---

*Alan Hodgkinson FGA DGA is a gemmology tutor and lecturer from Ayrshire, Scotland. Email: alanhodgkinson@talktalk.net*

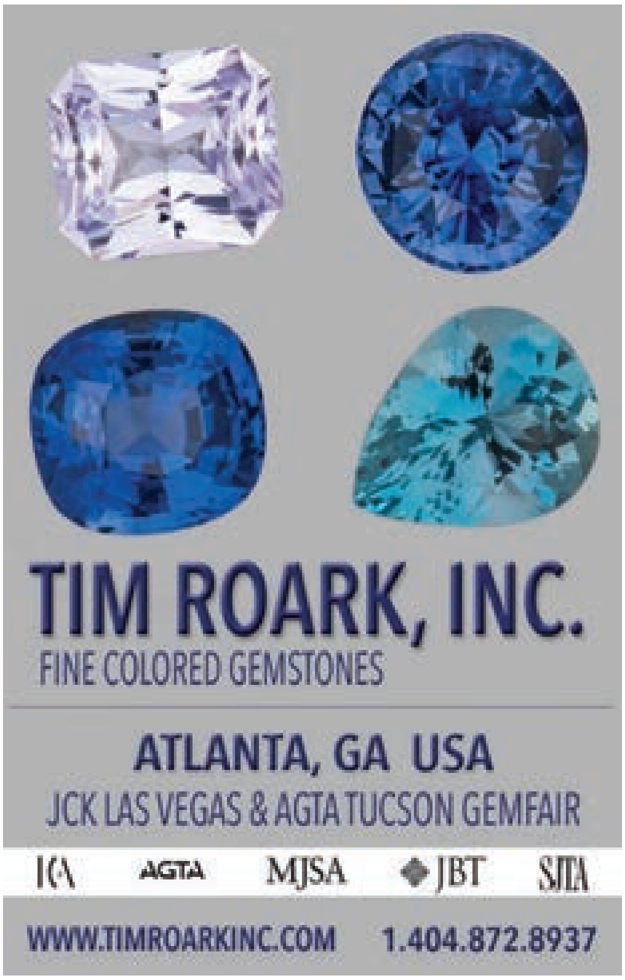

# Gem Notes

## COLOURED STONES

### Antigorite Serpentine from North-West Pakistan

During the 2015 Tucson gem shows in Arizona, USA, one of the authors (BML) was informed about some recently produced translucent green gem materials from north-west Pakistan by two different dealers. Syed Iftikhar Hussain (Syed Trading Co., Peshawar, Pakistan) donated to Gem-A a weakly chatoyant cabochon (16.77 ct) and a piece of rough material that were thought to be actinolite, as well as a cobble that was sold to him as nephrite, while Anzor Douman (Arzawa Mineralogical Inc., Winchester, Virginia, USA) had a sample of chatoyant material that resembled nephrite upon initial inspection. Later, during the following year's Tucson gem shows, Sir Ahmad (Farooq) Hashmi of Intimate Gems (Glen Cove, New York, USA) loaned one faceted stone (3.71 ct) and three oval cabochons (6.29–8.59 ct) consisting of an unidentified green material that was reportedly mined from north-west Pakistan. The overall appearance of all the samples (i.e. the semi-transparent to translucent diaphaneity and the 'olive' green colour; e.g. Figure 1) were typical of some nephrite showing good transparency.

The 'actinolite' samples from Hussain and the 'unknowns' from Hashmi were examined by authors CW and BW, and analysis with a GemmoRaman-532SG spectrometer identified all of them as antigorite serpentine, $Mg_3(Si_2O_5)(OH)_4$. Fourier-transform infrared (FTIR) spectroscopy with a PerkinElmer Spectrum100 unit revealed the expected high amounts of OH and $H_2O$ associated with serpentine minerals, and none of the samples showed any indications of polymer-type treatment.

Further testing of the polished stones revealed spot RI values of approximately 1.56, and hydrostatic SG measurements ranged from 2.59 to 2.60, typical of serpentine. The lustre of the gems ranged from sub-vitreous to silky, which is consistent with the variable low Mohs hardness of antigorite (2½–4, rarely up to 6; Gaines et al., 1997). The samples were inert to long- and short-wave UV radiation, and visible-to-near-infrared (Vis-NIR) spectra with an Ocean Optics USB4000 spectrometer showed a strong absorption peak at 460 nm, a weak 493 nm feature and a broad band centred at 715 nm that extended from the red region into the infrared. Energy-dispersive X-ray fluorescence (EDXRF) spectroscopy showed a chemical composition that was consistent with antigorite for the elements detectable by our Amptek X123-SDD instrument (i.e. Si), as well as significant Ni, minor Cr and Mn, and traces of V and Zn. All samples contained numerous parallel, near-colourless linear features (e.g. Figure 2) that showed a fibrous, feathery effect in some cases. The weak chatoyancy exhibited by the 16.77 ct cabochon was caused by a relatively large amount of these inclusions. Also present in some samples were opaque black dendritic and crumb-like masses (Figure 3).

*Figure 1: These green gems (3.71–16.77 ct), reportedly from a relatively new deposit in Pakistan, proved to be antigorite serpentine. The largest stone shows a faint cat's-eye effect. Photo by B. Williams.*

The antigorite described in this report shows some similarities to a cat's-eye serpentine from an unspecified origin documented by Choudhary (2009), except that stone fluoresced weak yellow

*Figure 2: Abundant parallel linear inclusions are present in this 6.29 ct antigorite cabochon. Photo by C. Williams.*

to long-wave UV radiation, and the desk-model spectroscope recorded only weak bands in the green and blue regions of the spectrum. Also, it contained fewer trace elements (Cr, Fe and Ni) than the material described here. Although this antigorite may be offered in the market as actinolite or nephrite, it can easily be identified by its lower RI and SG values. It also has a lower hardness, and the parallel linear features present in the samples examined for this report are not seen in nephrite, although antigorite does not always contain such inclusions.

*Cara Williams FGA and Bear Williams FGA*
*(info@stonegrouplabs.com)*
*Stone Group Laboratories*
*Jefferson City, Missouri, USA*

*Brendan M. Laurs*

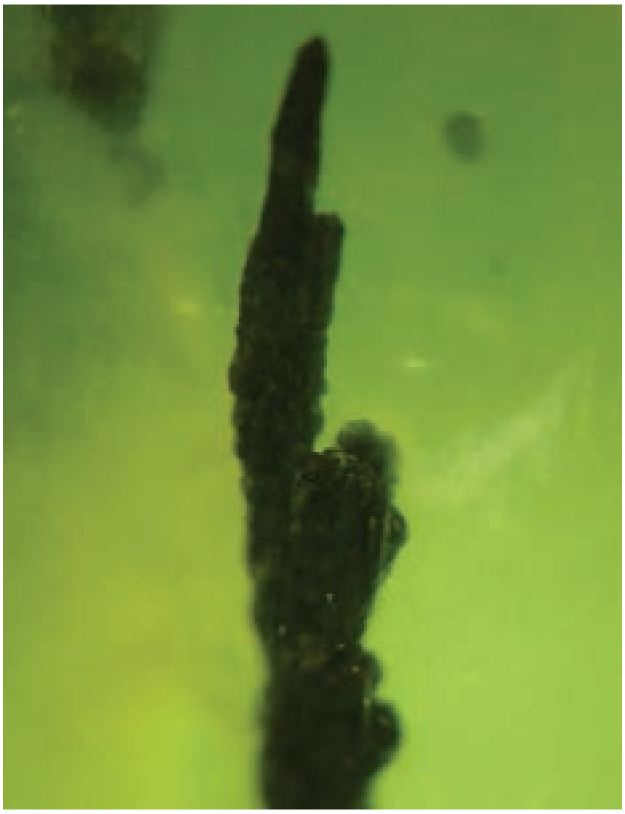

*Figure 3: Some of the antigorite samples contained opaque black dendritic inclusions, such as those seen here. Photomicrograph by C. Williams; magnified 30×.*

### References

Choudhary G., 2009. Gem News International: Serpentine cat's-eye. *Gems & Gemology*, **45**(2), 151–152.

Gaines R.V., Skinner H.C.W., Foord E.E., Mason B. and Rosenzweig A., 1997. *Dana's New Mineralogy*, 8th edn. John Wiley & Sons, New York, New York, USA, 1872 pp. (see pp. 1415–1417).

## 'Black' Axinite

Axinite is a rather unusual gem material that is most commonly encountered as the species axinite-(Fe), $Ca_2Fe^{2+}Al_2BSi_4O_{15}OH$, which typically shows an overall dark purplish brown coloration. However, at the February 2015 Tucson gem shows, some faceted examples of 'black' axinite were displayed by Mauro Pantò (The Beauty in the Rocks, Sassari, Italy). Pantò cut approximately 10 stones from a single large axinite crystal of unknown origin that his supplier suspected to be from Russia. The dark colour and translucent diaphaneity of the gems both appeared to be caused by abundant inclusions (Figure 4). Pantò mentioned that

*Figure 4: These samples of 'black' axinite (5.04–12.87 ct) are coloured by abundant clinochlore inclusions. Photo by Mauro Pantò.*

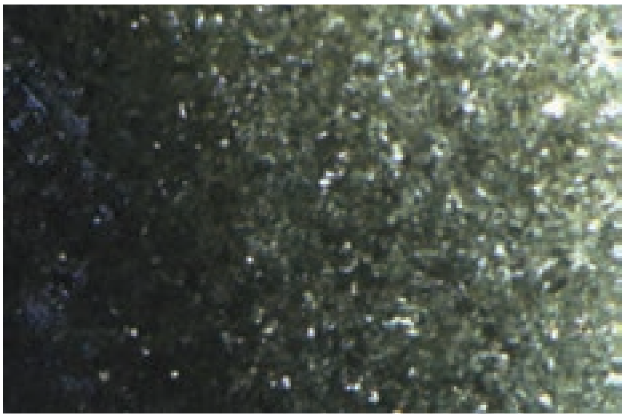

*Figure 5: Clinochlore forms randomly oriented flakes in the 'black' axinite. Photomicrograph by N. Renfro, © GIA; image width 1.8 mm.*

in an area of one stone containing a lower density of inclusions, the axinite appeared reddish purple.

Pantò kindly donated a 4.03 ct sample to Gem-A, which was examined by author NR. Viewed with the microscope, the sample contained a dense aggregation of randomly oriented greenish grey flakes (Figure 5); the abundant inclusions absorbed light and made the axinite appear black. Raman analysis of the inclusions with a Renishaw InVia instrument identified them as clinochlore. Gaines et al. (1997) reported that axinite-(Fe) may rarely be replaced by clinochlore-chamosite, but in this case the inclusions were syngenetic with the host.

Similar-appearing 'black' axinite crystals are known from Dal'negorsk, Primorskiy Kray, Far-Eastern Region, Russia, and also from Medel Valley, Grischun, Switzerland (www.mindat.org/gm/29239).

*Brendan M. Laurs*

*Nathan Renfro*
*Gemological Institute of America (GIA)*
*Carlsbad, California, USA*

### Reference

Gaines R.V., Skinner H.C.W., Foord E.E., Mason B. and Rosenzweig A., 1997. *Dana's New Mineralogy*, 8th edn. John Wiley & Sons, New York, New York, USA, 1872 pp. (see p. 1154).

## Beryl from Tanzania with Phenakite Inclusions

Gemmologists typically associate phenakite inclusions in beryl with so-called nail-head spicules in hydrothermal- and flux-grown synthetic emerald (e.g. Choudhary and Golecha, 2007). These synthetics may host elongate spindle-shaped two-phase (liquid and gas) inclusions that appear to have formed when a tiny crystalline inclusion (such as synthetic phenakite) locally interrupted the growth of the host synthetic emerald.

*Figure 6: These 14.05 and 11.02 ct samples of beryl from Tanzania contain abundant colourless mineral inclusions that proved to be phenakite. Photo by Robison McMurtry, © GIA.*

We were therefore interested to encounter inclusions of phenakite in two natural beryls. The tumble-polished 11.02 and 14.05 ct colourless beryls (goshenite; Figure 6) were donated to Gem-A by gem and mineral dealer Werner Radl (Mawingu Gems, Niederwörresbach, Germany) during the 2015 Tucson gem shows. According to his Tanzanian supplier, the beryl was mined from a claim owned by a Mr Madinga in the Haneti area of the Dodoma region in central Tanzania. All of the beryl showed diminished transparency due to abundant colourless inclusions.

Microscopic examination of both stones by one of us (NR) revealed numerous low-relief, colourless, blocky inclusions (Figure 7). Raman micro-spectroscopy with a Renishaw InVia instrument identified them as phenakite. Some of the phenakite inclusions were associated with tiny black grains that were too small to be identified with Raman analysis.

Phenakite has been reported previously in emerald from Madagascar (Gübelin and Koivula, 2008), but this is the first time to these authors' knowledge that it has been documented in any other beryl va-

Figure 7: The phenakite inclusions in the Tanzanian beryl occur as colourless euhedral-to-subhedral crystals. Photomicrograph by N. Renfro, © GIA; image width 2.6 mm.

riety. Although the Dodoma area is not known as a source of beryl, there are reports of Li-bearing pegmatites in this region (e.g. www.aspecthuntley.com.au/asxdata/20160819/pdf/01768945.pdf). The potential for additional production of this goshenite is not known at this time.

*Brendan M. Laurs and Nathan Renfro*

### References

Choudhary G. and Golecha C., 2007. A study of nail-head spicule inclusions in natural gemstones. *Gems & Gemology*, **43**(3), 228–235, http://dx.doi.org/10.5741/gems.43.3.228.

Gübelin E.J. and Koivula J.I., 2008. *Photoatlas of Inclusions in Gemstones*, Vol. 3. Opinio Publishers, Basel, Switzerland, 672 pp. (see p. 400).

## Clinohumite from Vietnam

The Cổng Trời mine in northern Vietnam is a well-known producer of various colours of spinels that are occasionally associated with orange clinohumite (e.g. Huong et al., 2012). This marble-hosted deposit is located ~3 km from An Phú in the Lục Yên District of Yên Bái Province. On separate buying trips to Lục Yên in 2013 and 2014, gem dealer Dudley Blauwet (Dudley Blauwet Gems, Louisville, Colorado, USA) obtained a single piece of facetable clinohumite (both of which were presented to him as chondrodite) from one of his regular suppliers of spinel crystals from Cổng Trời. One of the two pieces was cut into a single gem weighing >1 ct and the other one was faceted into five stones totalling 1.05 carats. The latter faceted pieces were received from the cutting factory in November 2014, and during the February 2016 Tucson gem shows, Blauwet loaned two of them for examination (Figure 8).

Figure 8: These samples of clinohumite from Vietnam (0.32 and 0.54 ct) were studied for this report. Photo by Dirk van der Marel.

The stones consisted of a round brilliant and a cushion modified brilliant that weighed 0.32 and 0.54 ct, and measured 4.37–4.38 × 2.76 mm and 5.72 × 4.26 × 3.05 mm, respectively. RI readings of the two gems gave 1.635–1.670 and 1.639–1.670, yielding birefringence values of 0.035 and 0.031, respectively. Both were biaxial positive, and for the 0.32 ct stone, the RI of the β vibration direction could be seen as 1.640. Average hydrostatic SG values of 3.19 and 3.20 were obtained for the 0.32 and 0.54 ct samples, respectively. Strong orange and yellow pleochroism was observed in both stones using a calcite dichroscope. The gems were inert to long-wave UV radiation, but they fluoresced weak orange to the short-wave UV lamp.

The RIs were consistent with clinohumite, which has values between 1.623 and 1.674, and $n_\beta$ = 1.636–1.643 (i.e. for a low-Fe composition; cf. Dedeyne and Quintens, 2007; Deer et al., 1982). By contrast, the RIs were higher than those reported for chondrodite (another mineral of the humite group), which typically are between 1.592 and 1.646 ($n_\beta$ = 1.602–1.627). Also, the stones' reaction to short-wave UV radiation was typical for clinohumite, whereas chondrodite would remain inert (e.g. Fryer, 1986; Zwaan and Zoysa, 2002; Dedeyne and Quintens, 2007).

Both gems were only slightly included. Apart from partially healed fissures that consisted of minute voids, they contained rounded-to-euhedral transparent crystals (Figure 9) that were identified as apatite by Raman spectroscopy (with the closest match to fluorapatite).

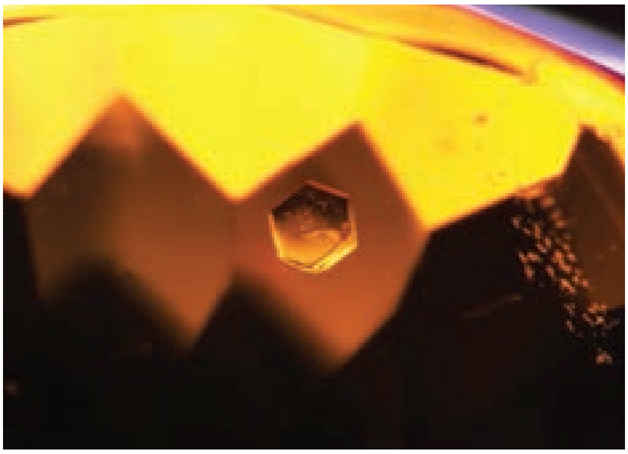

*Figure 9: Both of the clinohumite study samples contained transparent apatite inclusions, which were mostly rounded. This particular apatite displays a hexagonal outline when viewed along the c-axis. Photomicrograph by J. C. Zwaan; image width 2.1 mm.*

Chemical analyses were obtained by EDXRF spectroscopy with an EDAX Orbis Micro-XRF Analyzer on the tables of the two stones, using a spot size of 300 µm. Apart from the main elements Mg and Si, the analyses showed low Fe (0.20–0.25 wt.% FeO) and considerable Ti (1.8–2.0 wt.% $TiO_2$).

As expected, both samples showed identical Raman spectra, which were collected with a Thermo Scientific DXR Raman microscope using 532 nm laser excitation. The spectra gave an excellent match with those for clinohumite in the RRUFF database (http://rruff.info)—and differed significantly from the spectra of chondrodite in the RRUFF database and those published by Frost et al. (2007), especially in the 1000–350 $cm^{-1}$ region (Figure 10). Humite-group minerals are composed of silicate layers with the structure of olivine ($Mg_2SiO_4$) and brucite ($Mg[OH]_2$). The number of silicate layers varies depending on the mineral. The Raman spectra in the 1000–800 $cm^{-1}$ region show a characteristic pattern that is attributed to stretching vibrations of the layered olivine $(SiO_4)^{4-}$ structural units. The Raman spectrum of chondrodite (a two-silicate-layered mineral) shows two or three bands depending on the chemical composition, while the spectra for clinohumite (a four-silicate-layered mineral) shows increased complexity in this region. The bands in the 750–500 $cm^{-1}$ region correspond to the bending vibrations of the $(SiO_4)^{4-}$ units. A number of bands between 790 and 740 $cm^{-1}$ are ascribed to MgOH and other $M^{2+}OH$ ($M^{2+}$ = Mg, Ca, Mn, Fe, Co) deformations (Frost et al., 2007).

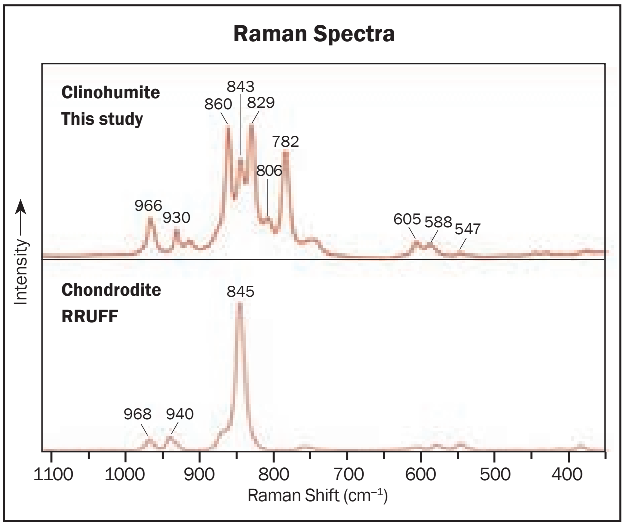

*Figure 10: Raman spectra of the analysed samples (here, the 0.32 ct stone) show an excellent match with those of clinohumite, but differ greatly from chondrodite spectra in the RRUFF database.*

Vietnamese clinohumite will likely remain a rarity in the marketplace. According to Blauwet, it is typically poorly crystallized and heavily fractured, and only rarely are there clean areas suitable for cutting small gemstones. Although the orange material from Cổng Trời is commonly sold as chondrodite in Vietnam, this study confirms information from the literature that it is clinohumite.

*Dr J. C. (Hanco) Zwaan (hanco.zwaan@naturalis.nl)*
*Netherlands Gemmological Laboratory*
*National Museum of Natural History 'Naturalis'*
*Leiden, The Netherlands*

## References

Dedeyne R. and Quintens I., 2007. *Tables of Gemstone Identification*. Glirico-Gent, Belgium, 309 pp.

Deer W.A., Howie R.A. and Zussman J., 1982. *Rock-Forming Minerals—Orthosilicates*, Vol. 1A, 2nd edn. Longman, London, 919 pp.

Frost R., Palmer S., Bouzaid J. and Reddy J., 2007. A Raman spectroscopic study of humite minerals. *Journal of Raman Spectroscopy*, **38**(1), 68–77, https://doi.org/10.1002/jrs.1601.

Fryer C.W., Ed., 1986. Gem Trade Lab Notes: Faceted clinohumite. *Gems & Gemology*, **22**(4), 236.

Huong L.T.-T., Häger T., Hofmeister W., Hauzenberger C., Schwarz D., Van Long P., Wehrmeister U., Khoi N.N. and Nhung N.T., 2012. Gemstones from Vietnam: An update. *Gems & Gemology*, **48**(3), 158–176, http://dx.doi.org/10.5741/gems.48.3.158.

Zwaan J.C. and Zoysa E.G., 2002. Gem-quality chondrodite from Balangoda, Sri Lanka. *Journal of Gemmology*, **28**(3), 162–168, https://doi.org/10.15506/jog.2002.28.3.162.

## Lace Opal from Utah

The western USA is a source of both 'common' and play-of-colour varieties of opal. Recently these authors had the opportunity to examine some colourful banded samples marketed as 'Utah Lace Opal' (e.g. Figure 11). They were submitted to two of the authors (CW and BW) for identification and analysis by Larry and Joyce Wright of Aspen Rock and Gem, Cedaredge, Colorado, USA. They have been mining this material since 2008 in Milford County, south-central Utah, but it has yet to be gemmologically characterized.

Three pieces of rough, four polished slabs and three cabochons were examined. Most areas of the samples were opaque to slightly translucent, although some transparent bands were present that were colourless with a crackled appearance. Overall, white-to-grey areas were most common in the samples, and these alternated with purple to orangey red bands, as well as pink and 'mustard'-yellow layers (see Figures 11 and 12). A few of the specimens contained bluish grey bands. According to Mr Wright, the colour range of the material changes every few feet along the vein.

Several areas of each sample were analysed by FTIR spectroscopy (with a PerkinElmer Spectrum100 instrument) and Raman spectroscopy (GemmoRaman-532SG), which revealed that they consisted primarily of opal. Some of the colourless areas showed a 500 cm$^{-1}$ Raman peak indicative of moganite. On two polished samples, spot

*Figure 11: Left: These rough (up to ~11 × 7 cm) and cut (58.72 ct cabochon) samples of Utah Lace Opal show a range of colours and patterns. Right: These cabochons of Utah Lace Opal measure 41.4 × 28.61 × 7.14 mm (44.63 ct) and 31.7 × 23.73 × 7.15 mm (29.67 ct). Photos by B. Williams.*

*Figure 12: Left: Bands consisting mostly of colourless, white, purple and orangey red form well-defined layers in this Utah Lace Opal. Right: The purple band contains clusters of Fe-oxide inclusions within the colourless opal matrix. Photomicrographs by A. U. Falster; image width 3 mm (left) and 0.8 mm (right).*

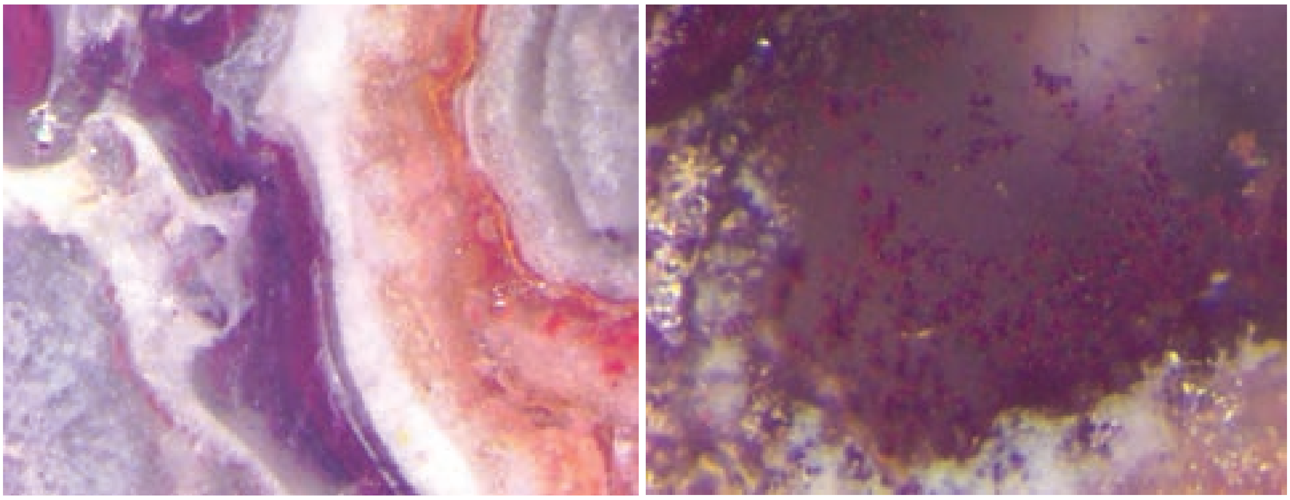

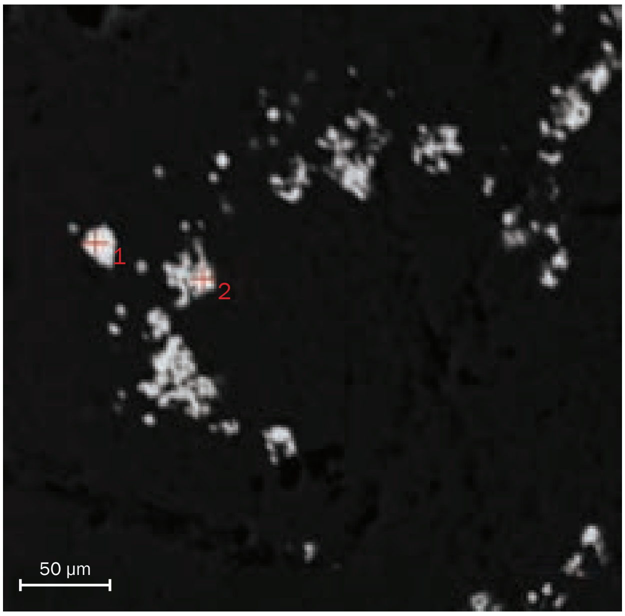

*Figure 13: Backscattered-electron imaging of a polished surface of Utah Lace Opal shows bright-appearing sulfide inclusions. Approximately 20% of them consisted of an unidentified antimony thallium sulfide (e.g. spots 1 and 2), and the remainder were pyrite or marcasite. Image by A. U. Falster.*

RI readings of 1.43 and 1.44 were obtained, and hydrostatic SG was measured as 2.08. Chemical analysis with an Amptek X123-SDD EDXRF spectrometer indicated the main impurities consisted of Fe, Mn, Ti, Ca and K. Iron was present in the red and yellow areas, and Mn in the black areas. The Ca and K are presumed to be present in the form of feldspar inclusions (see below). Trace amounts of Ni, Zn and Cu also were present.

A JEOL JSM-6400 scanning electron microscope was used to further investigate the composition of one piece of rough and two polished slabs by authors AUF and WBS. Backscattered-electron imaging and energy-dispersive spectroscopy (EDS) were used to analyse various inclusions, including Fe oxides (Figure 12, right), Fe sulphides (pyrite or marcasite; Figure 13) and alkali feldspar. Perhaps the most interesting were blebs of an antimony thallium sulphide (Figure 13). The only mineral species known with this combination of elements is weissbergite, $TlSbS_2$. However, the EDS spectrum indicated that Tl was not present in sufficient amounts, and more work is needed to confirm the identity of these inclusions. Nevertheless, Sb- and Tl-sulfide mineralization is common in a low-temperature hydrothermal environment, consistent with the formation of opal.

Areas of porosity were evident in some of the rough pieces, and the polished samples were brittle and easily broken along their edges. For these reasons, Wright stated that some of the cut material is treated by polymer stabilization, but none of the submitted samples showed indications of any treatment.

The name ‘Utah Lace Opal’ seems appropriate for this material, as it closely resembles the colourful, intricate, banded appearance seen in so-called lace agates, but tests primarily as common opal.

*Cara Williams FGA*

*Alexander U. Falster and*
*Dr William B. (Skip) Simmons*
*Maine Mineral & Gem Museum*
*Bethel, Maine, USA*

*Bear Williams FGA*

## Pollucite from Pakistan with Polylithionite Inclusions

Pollucite, $(Cs,Na)_2(Al_2Si_4O_{12})\cdot 2H_2O$, is an uncommon cesium mineral that is typically colourless or white. It has a Mohs hardness of 6½ but is rarely faceted as a collector’s stone since it is very brittle and typically not very transparent. For approximately two decades, the granitic pegmatites in northern Pakistan—particularly in the Shengus area (Blauwet et al., 1997)—have been a source of fine pollucite crystals that are highly valued by mineral collectors.

At the 2015 Tucson gem shows, Dr Marco Campos Venuti (Gems in Gems, Seville, Spain) had faceted pollucite from northern Pakistan that contained interesting clusters of colourless inclusions (e.g. Figure 14). Approximately 0.5 kg of the rough material was obtained in early 2013, and 300–400 carats of stones were faceted that weighed up to ~60 ct (the largest stone present in Tucson weighed 14.31 ct). In November 2014, the inclusions in two samples were analysed by Raman micro-spectroscopy at Geospectra Scientific Solutions (Torrejón del Rey, Spain) and identified as polylithionite, $KLi_2Al(Si_4O_{10})(F,OH)_2$, a lithium-rich mica. The association of Li-rich mi-

Figure 14: This 1.20 ct pollucite from Pakistan contains inclusions of polylithionite. Photo by Robison McMurtry, © GIA.

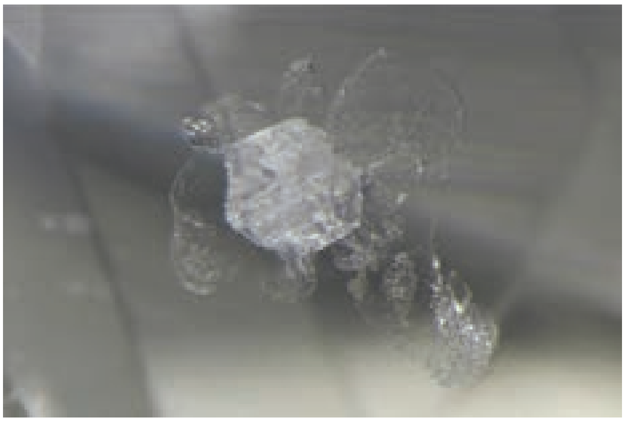

Figure 15: The polylithionite inclusions form clusters of subhedral crystals in the pollucite host. Photomicrograph by N. Renfro, © GIA; image width 2.0 mm.

cas with pollucite is known to occur in highly evolved granites and pegmatites (e.g. Wang et al., 2004), in which such micas are commonly called 'lepidolite', a discredited species that falls near or within the polylithionite-trilithionite series.

Dr Campos Venuti kindly donated a 1.20 ct oval cut to Gem-A, and microscopic examination by author NR showed the polylithionite inclusions forming in platy groups that were colourless to white and were mostly subhedral (Figure 15). As expected, Raman analysis (with a Renishaw InVia Raman instrument instrument) gave a close match to polylithionite in the RRUFF database. Interestingly, the inclusions displayed pale yellow fluorescence to short-wave UV radiation.

Gem-quality pollucite is quite rare, and these polylithionite inclusions make these gemstones even more interesting for collectors.

*Brendan M. Laurs and Nathan Renfro*

### References

Blauwet D., Smith B. and Smith C., 1997. A guide to the mineral localities of the Northern Areas, Pakistan. *Mineralogical Record*, **28**(3), 183–200.

Wang R.C., Hu H., Zhang A.C., Huang X.L. and Ni P., 2004. Pollucite and the cesium-dominant analogue of polylithionite as expressions of extreme Cs enrichment in the Yichun topaz lepidolite granite, southern China. *Canadian Mineralogist*, **42**(3), 883–896, http://dx.doi.org/10.2113/gscanmin.42.3.883.

## Large Ruby Matrix Specimen from Lục Yên, Vietnam

In the Lục Yên region of northern Vietnam, gem mining activity—mainly for ruby and sapphire—boomed in the mid-1990s, but since the late 2000s facet-grade gem corundum has become rare (Huong et al., 2012). This is apparently due to the lack of access to appropriate technology and expertise, and mining is now typically restricted to small-scale diggings at easily worked secondary deposits near the surface. One of the main primary sources for ruby and sapphire in the area is marble, and only a few such hard-rock deposits have been exploited so far. The production from these mines typically consists of small matrix pieces of ruby/sapphire in marble that are commonly offered as collectors' samples in the local market.

Occasionally quite large matrix specimens are produced, and during a field excursion to the Lục Yên area that took place after the International Gemmological Conference in October 2013, a two-tonne marble specimen containing purple/violet corundum crystals was shown to participants by a local miner. The corundum crystals in that specimen ranged up to 20 cm long. It reportedly was recovered in spring 2013 from the Mây Thượng mine in the An Phú area. Interestingly, on the opposite side of the mountain from Mây Thượng is a well-known source of spinel, the Cổng Trời mine.

More recently, during a subsequent excursion to Lục Yên in March 2015, this author was shown by another local miner (Van Khiem Vu) several

*Figure 16: This 400 kg specimen of ruby-bearing marble was recovered from the Mây Thượng mine in 2014 by Van Khiem Vu (pictured), who has worked the deposit for more than a decade. Photo by L. T.-T. Huong.*

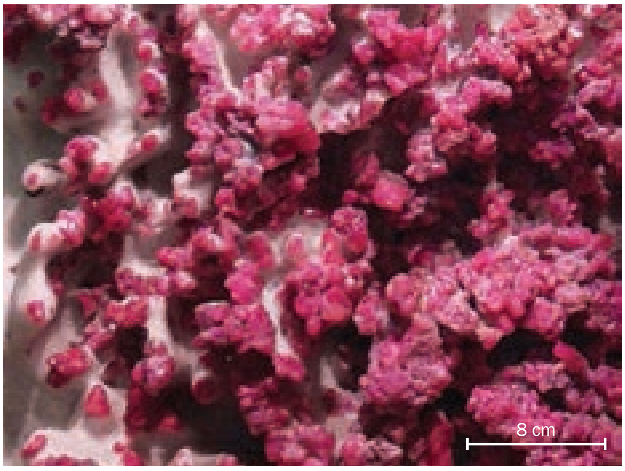

*Figure 17: A closer view of the specimen in Figure 16 shows dense clusters of ruby crystals that have been carefully exposed from the marble. Photo by Lutz Nasdala.*

large marble specimens containing ruby crystals that also were extracted from Mây Thượng. The most impressive specimen (Figure 16) weighed about 400 kg, and was carved from a two-tonne block of marble that was found in 2014. It contained dense clusters of ruby crystals, several of which possessed good transparency and were up to 4–5 cm long (Figure 17). According to Vu, he and his two brothers have worked the mine for approximately 10 years, and several tonnes of corundum-bearing marble have been extracted during that time. The quarrying is done by drilling and blasting, and then the corundum crystals are carefully exposed from the marble using simple tools such as a hammer, chisel and rasp. It took more than two months to prepare the specimen shown in Figure 16. Other large pieces that Vu and his team have produced weighed 300–700 kg after processing. Such specimens are prepared for sale as a single piece rather than being broken down into gem rough, because the price for such impressive mineral specimens is higher than the gem value they contain.

*Dr Le Thi-Thu Huong (letth@vnu.edu.vn)*
*Vietnam National University, Hanoi*

### Reference

Huong L.T.-T., Häger T., Hofmeister W., Hauzenberger C., Schwarz D., Van Long P., Wehrmeister U., Khoi N.N. and Nhung N.T., 2012. Gemstones from Vietnam: An update. *Gems & Gemology*, **48**(3), 158–176, http://dx.doi.org/10.5741/gems.48.3.158.

## Scapolite from Badakhshan, Afghanistan

While on a buying trip to Pakistan in June 2015, gem dealer Dudley Blauwet obtained a parcel of colourless-to-grey rough material that was represented as zoisite. According to his regular Afghan supplier, the stones came from Lajuar Madan, Kokcha Valley, Badakhshan, Afghanistan. The etched crystals showed a strong resemblance to the zoisite from the well-known Alchuri deposit in northern Pakistan, and some of them contained parallel inclusion features that would likely produce chatoyancy. Blauwet selected 80 pieces totalling 27.6 g for cutting, and in September 2015 he received from his factory 60 faceted stones weighing a total of 18.57 carats, as well as 18 cat's-eye cabochons weighing 8.94 carats.

During the 2016 Tucson gem shows, Blauwet loaned two samples to this author for examina-

*Figure 18: Afghanistan is the source of these samples of colourless transparent and dark grey cat's-eye scapolite (0.76 and 1.06 ct, respectively). Photo by Dirk van der Marel.*

tion: a colourless transparent emerald cut (6.76 × 4.77 × 3.70 mm) that weighed 0.76 ct, and a dark grey translucent cabochon (6.22–6.28 × 3.73 mm) that weighed 1.06 ct and showed a sharp cat's-eye (Figure 18). The cabochon's dark grey colour and translucency were caused by abundant inclusions; it was otherwise transparent and colourless, like the emerald-cut sample.

The RI values of the faceted stone were 1.548–1.570, yielding a birefringence of 0.022, and it was uniaxial negative. The cabochon gave a spot-RI reading of around 1.55. Average hydrostatic SG values of 2.70 and 2.68 were obtained for the faceted stone and the cabochon, respectively. The emerald-cut gem was practically inert to long-wave UV radiation, but under completely dark conditions it showed a very weak yellowish fluorescence, whereas the cabochon remained inert. Both stones showed weak red fluorescence to short-wave UV radiation.

The analysed properties are consistent with those of scapolite (cf. Deer et al., 2004; Dedeyne and Quintens, 2007); zoisite would show significantly higher RI and SG values. Raman analysis with a Thermo Scientific DXR Raman microscope, using 532 nm laser excitation, showed a closest match with the spectra of marialite (the Na-rich scapolite end member) in the RRUFF database. However, the RI and SG values indicated an intermediate composition between marialite, $Na_4Al_3Si_9O_{24}Cl$, and meionite, $Ca_4Al_6Si_6O_{24}CO_3$ (cf. Deer et al., 2004). EDXRF analysis (performed with an EDAX Orbis Micro-XRF Analyzer, using a spot size of 300 μm) confirmed an intermediate composition, with approximately equal amounts of Na and Ca (~7 wt.% oxide).

Both stones showed parallel-oriented growth tubes that were partially filled with opaque material and/or dendritic opaque minerals (Figure 19). The high abundance of these inclusions in the cabochon created the cat's-eye effect under pinpoint lighting. The many opaque inclusions also caused the overall dark grey colour of the stone. The faceted sample additionally hosted some multiphase inclusions that contained a gas bubble with opaque and transparent phases (Figure 20). Raman analysis of the inclusions was hampered by the rather strong fluorescence of the host scapolite. Attempts to analyse the opaque phases along the growth tubes and within the multiphase inclusions consistently yielded the spectrum of scapolite with an additional band at ~660 $cm^{-1}$. This position corresponds to the main vibration band of pyrolusite, suggesting the presence of manganese oxide(s). In addition, calcite was identified in a multiphase inclusion.

This scapolite is much different from the colourless material reported previously from the Lajuar Madan area in Afghanistan, which showed yellow UV fluorescence, had lower RI and SG

*Figure 19: Parallel growth tubes containing opaque material are present in both the faceted stone (left) and the chatoyant cabochon (right) of scapolite. Photomicrographs by J. C. Zwaan; image width 1.4 mm.*

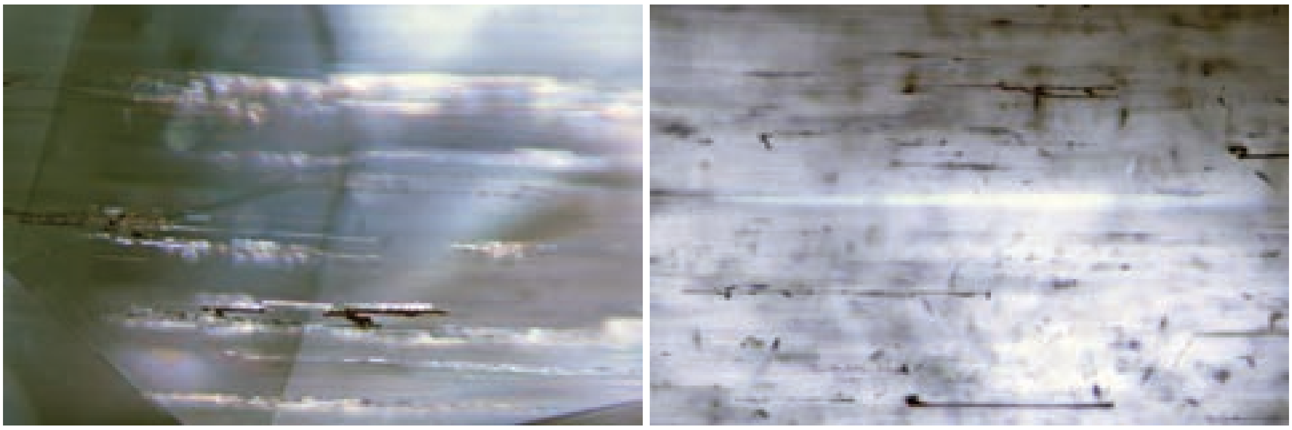

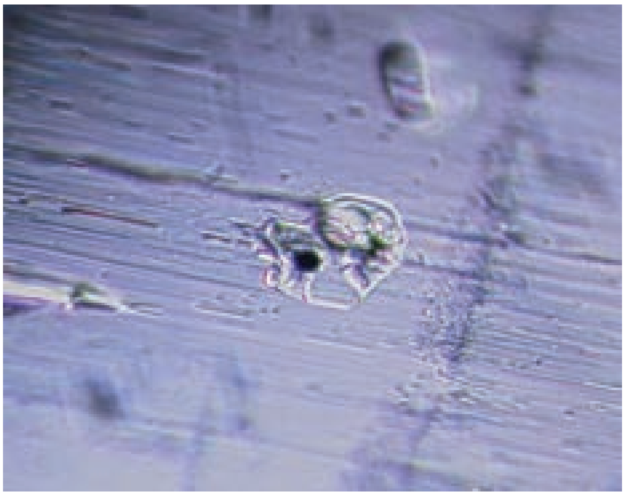

Figure 20: The faceted scapolite also contained multiphase inclusions, here consisting of a bubble in the upper part with an opaque grain (probably Mn oxide) and some colourless crystals. The crystal below the opaque mineral was identified as calcite; the other phases could not be identified. Photomicrograph by J. C. Zwaan; image width 0.3 mm.

values (corresponding to marialite), and contained inclusions of lazurite and apatite (Shen, 2011). In addition, it is distinct from the violet cat's-eye scapolite that has been documented from near the Papra (or Paprok) tourmaline mine in Afghanistan (Milisenda and Wehr, 2009).

*Dr J. C. (Hanco) Zwaan*

### References

Dedeyne R. and Quintens I., 2007. *Tables of Gemstone Identification*. Glirico, Gent, Belgium, 309 pp.

Deer W.A., Howie R.A. and Zussman J., 2004. *Rock-Forming Minerals—Framework Silicates: Silica Minerals, Feldspathoids and the Zeolites*, Vol. 4B, 2nd edn., Longman, London, 982 pp.

Milisenda C.C. and Wehr K., 2009. Gemmologie Aktuell: Skapolite cat's eyes from Afghanistan. *Gemmologie: Zeitschrift der Deutschen Gemmologischen Gesellschaft,* **58**(3–4), 86.

Shen A., 2011. Gem News International: Scapolite from Afghanistan. *Gems & Gemology*, **47**(1), 65–66.

## Tourmaline from Ife, Osun State, Nigeria

For approximately the past three decades, Oyo State in south-west Nigeria has been known as a source of gem-quality pink, green and bicoloured tourmaline. In 2015, a new gem tourmaline occurrence was discovered in neighbouring Osun State, near the town of Ife (or Ilé-Ifẹ̀). Alluvial deposits of tourmaline and aquamarine in Osun State were reported by Ajeigbe et al. (2014), and the new tourmaline mine near Ife was briefly mentioned by Nwadique (2015).

During the 2016 Tucson gem shows, gem dealer Dudley Blauwet obtained approximately 35 bicoloured pink-green tourmaline crystals (total weight ~350 g) from Ife that showed good colour saturation, as well as sharp crystal faces with no evidence of alluvial transport. Most were sold as mineral specimens, although Blauwet had some broken pieces polished into cabochons (e.g. Figure 21). He loaned two stones to this author for examination that weighed 14.30 and 23.00 ct, and both of them displayed chatoyancy in their green portions. The most conspicuous inclusions consisted of partially healed fractures composed of typical 'trichite' fluid inclusions, which were particularly abundant in the pink portions of the stones, and elongate growth tubes oriented parallel to the c-axis (mostly in the green portions; Figure 22). Tiny birefringent colourless mineral inclusions were visible at the ends

Figure 21: This crystal (4.2 cm long) and cabochon (14.30 ct) of bicoloured tourmaline are from a new deposit in Osun State, Nigeria. The cabochon displays chatoyancy in its green portion. Photo by Orasa Weldon.

of some of the tubes. The tubes were responsible for the cat's-eye effect exhibited by the green portion of the cabochons.

It remains to be seen whether Osun State will become a significant source of gem-quality tourmaline in the future.

*Brendan M. Laurs*

### References

Ajeigbe O.M., Adeniran O.J. and Babalola O.A., 2014. Mineral prospecting potentials of Osun State. *European Journal of Business and Management*, **6**(2), 115–123. www.iiste.org/Journals/index.php/EJBM/article/download/10393/10591.

Nwadique G.U., 2015. Nigeria gemstone supplies: A brief overview. International Colored Gemstone Association, 14 October, http://tinyurl.com/z6vr5xg (accessed 30 November 2016; link to be redirected to new ICA website in the future).

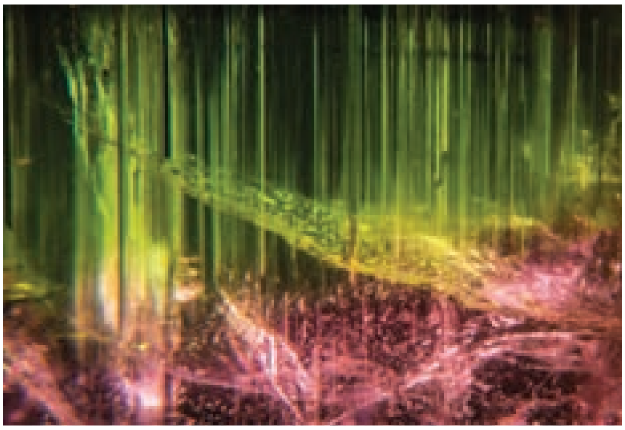

*Figure 22: Parallel growth tubes are responsible for the chatoyancy of the green side of the Nigerian tourmaline cabochon in Figure 21, while the pink portion contains abundant partially healed fractures. Photomicrograph by Orasa Weldon; magnified ~45×.*

## Cat's-eye Väyrynenite from Pakistan

Väyrynenite, $MnBe(PO_4)(OH,F)$, is a rare phosphate mineral that is known in gem quality only from granitic pegmatites in Pakistan and Afghanistan (Laurs and Fritz, 2006a,b). During a buying trip to Skardu, Pakistan, in June 2014, gem dealer Dudley Blauwet obtained a small parcel of väyrynenite, with some pieces having a silky appearance. The parcel was sourced from a miner who was active in the Sabsar and Khargulook areas, located ~10 km east of Shengus in northern Pakistan. Blauwet sent 11 pieces weighing 3.8 g to his cutting factory, and when the order was returned in 2015, he found that one of the silky pieces was polished into a 0.62 ct cabochon that showed chatoyancy.

*Figure 23: This 0.62 ct väyrynenite from northern Pakistan shows a weak cat's-eye, making it an extremely rare example of this unusual mineral. Photo by Dirk van der Marel.*

The sample was transparent, slightly orangey pink, and had a weak cat's-eye (Figure 23). It measured 4.53–4.60 × 3.55 mm and weighed 0.62 ct. A spot-RI reading of ~1.64 and an average hydrostatic SG value of 3.22 were obtained. These data are consistent with those reported previously for faceted väyrynenite (Laurs and Fritz, 2006a,b) and correspond to the known values for the mineral: RIs of 1.638–1.667 (birefringence 0.026–0.028; biaxial negative) and SG of 3.23 (cf. Dedeyne and Quintens, 2007).

The stone showed distinct pleochroism in pink and 'straw' yellow, and was inert to both long- and short-wave UV radiation. The most notable inclusions were partially healed fissures that contained two-phase inclusions (Figure 24). Also present were some parallel-oriented very fine tubes or needles, although not in the abundance that normally would be expected in a chatoyant gem. However, many elongated voids in the partially healed fissures lined up parallel to these needles, possibly adding to the reflection of light, and thus contributing to the rather weak cat's-eye.

Raman analysis was carried out with a Thermo Scientific DXR Raman microscope using 532 nm laser excitation. The obtained spectrum showed an excellent match with a reference spectrum in the RRUFF database for väyrynenite, also from

*Figure 24: Partially healed fissures containing two-phase inclusions are prominent features in the cat's-eye väyrynenite. Photomicrograph by J. C. Zwaan; image width 1.4 mm.*

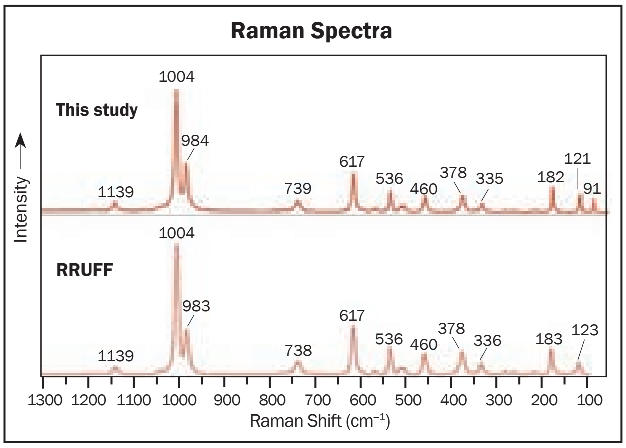

*Figure 25: The Raman spectrum of the cat's-eye stone provides a good match to väyrynenite in the RRUFF database that is from Shengus in northern Pakistan.*

northern Pakistan (Figure 25). The main peak at 1004 cm$^{-1}$ and the strong band at 984 cm$^{-1}$ are attributed to the $PO_4^{3-}$ $\nu_1$ symmetric stretching mode, while peaks between 800 and 300 cm$^{-1}$ are due to $PO_4^{3-}$ bending modes and vibrations of POH units (Frost et al., 2014). Additionally, in the 3800–2600 cm$^{-1}$ region (not shown in Figure 25), a strong band was present at 3219 cm$^{-1}$ that is assigned to the OH stretching vibration (Frost et al., 2014). Note that Raman spectra of väyrynenite from different localities (e.g. from Finland and Pakistan) may show significant differences, and these appear to be related to variations in chemical composition (Frost et al., 2014).

EDXRF analyses were performed with an EDAX Orbis Micro-XRF Analyzer, using a spot size of 300 µm. As expected, the main elements Mn and P were found (Be cannot be detected with this technique). Minor Fe and traces of Ca also were present, and these are consistent with electron microprobe analyses of väyrynenite reportedly from Gilgit, Pakistan (Falster et al., 2012).

This cat's-eye väyrynenite is extremely rare, and is the only example of this stone that Blauwet has seen after decades of dealing in gem material from Pakistan and Afghanistan.

*Dr J. C. (Hanco) Zwaan*

## References

Dedeyne R. and Quintens I., 2007. *Tables of Gemstone Identification*. Glirico, Gent, Belgium, 309 pp.

Falster A.U., Nizamoff J.W., Bearss G. and Simmons W.B., 2012. 38th Rochester Mineralogical Symposium—Contributed Papers in Specimen Mineralogy: Part 2: A second U.S. location for väyrynenite—The Estes quarry, West Baldwin, Maine, and new data on väyrynenite from Wisconsin and Pakistan. *Rocks & Minerals*, **87**(3), 281–282, http://doi.org/10.1080/00357529.2012.681982.

Frost R.L., López A., Xi Y., Gobac Ž. and Scholz R., 2014. The molecular structure of the phosphate mineral väyrynenite: A vibrational spectroscopic study. *Spectroscopy Letters*, **47**(4), 253–260, https://doi.org/10.1080/00387010.2013.795174.

Laurs B.M. and Fritz E.A., 2006a. Gem News International: Väyrynenite from Afghanistan. *Gems & Gemology*, **42**(2), 184–185.

Laurs B.M. and Fritz E.A., 2006b. Gem News International: Väyrynenite from Pakistan. *Gems & Gemology*, **42**(1), 75.

# SIMULANTS

## Quartzite and Calcite Bangles, Resembling Jadeite

Recently submitted by an appraiser for identification were five bangle bracelets that were all represented as jade when sold to their client. Among them were obvious examples of agate and typical B-jade (bleached and polymer impregnated), but also some unexpected imitations.

One bangle appeared near-colourless but was actually very pale yellowish green (seen

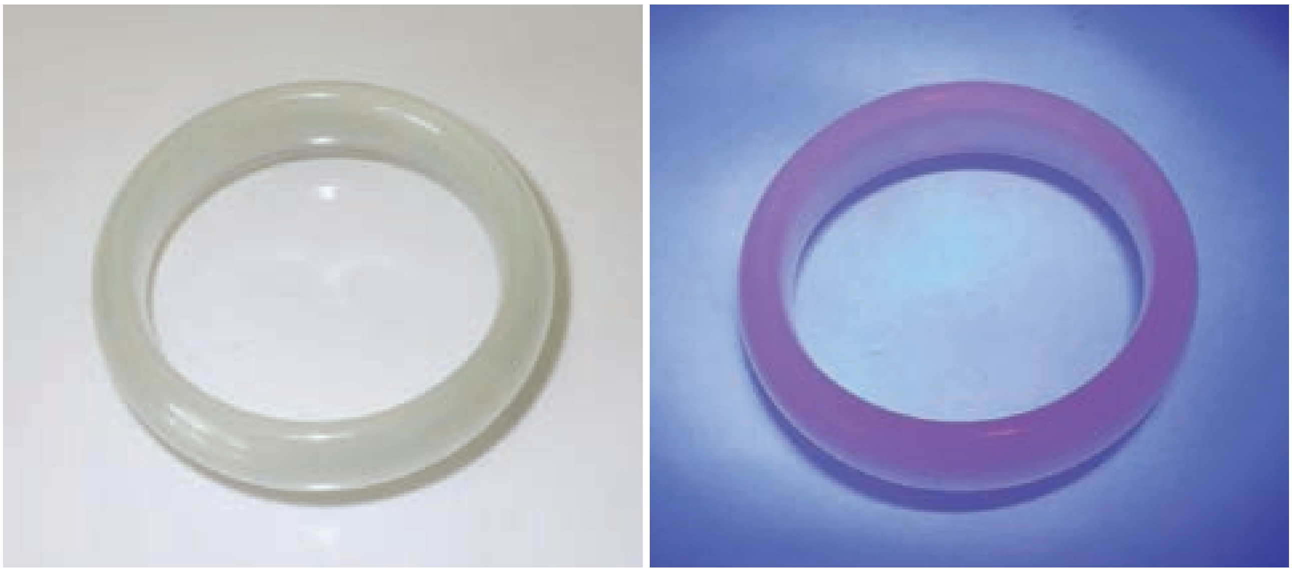

*Figure 26: This 16.5-mm-diameter bangle resembling 'ice jade' proved to consist of calcite (left). It displays pink fluorescence to long-wave UV radiation (right). Photos by B. Williams.*

only when placed on a white background). It exhibited the watery translucency typical of finer 'ice jade' (Figure 26, left), but Raman analysis with a GemmoRaman-532SG instrument identified it as calcite. Weighing 63.79 g, it was 16.5 mm in diameter and had an average thickness of 9.1 mm—which was somewhat thicker than a typical stone bangle. Close examination with a 10× loupe revealed an even pattern of colourless parallel banding throughout the piece, which created a weak, billowy cat's-eye effect along the entire circumference of the bangle. Viewed with the microscope, the banding was resolved as lamellar twinning together with numerous microscopic incipient cleavage cracks. Due to the twinning, the polariscope showed no 'blink' (i.e. the bangle remained light when it was rotated between crossed polarizers). No polymers or dyes were detected, either by microscopic observation or by FTIR spectroscopy with a PerkinElmer Spectrum100 unit. EDXRF chemical analysis with an Amptek X123-SDD spectrometer revealed a relatively high Mn content, and the bangle showed a uniform moderate pink fluorescence to long-wave UV radiation (Figure 26, right).

Another bangle appeared to be an imitation of 'moss-on-snow' jadeite (Figure 27, left), a variety that exhibits small areas of vivid green coloration in a white base. The bangle weighed 66.27 g and was 16.9 mm in diameter with an average thickness of 8.6 mm. It was highly trans-

*Figure 27: Although appearing like 'moss-on-snow' jadeite, this 16.9-mm-diameter bangle consists of dyed quartzite (left). The green areas of the bangle exhibit strong green fluorescence to long-wave UV radiation (right). Photos by B. Williams.*

lucent and mostly milky white, with three areas that were mottled in deep bluish green. Microscopic observation revealed the typical translucent graininess of quartzite, and the coloured areas showed green dye concentrations along grain boundaries. Raman analysis identified the bangle as quartz, confirming that it was quartzite. FTIR spectroscopy revealed the presence of a polymer in the coloured areas, which is the presumed method of delivering the dye. The green areas fluoresced a strong green under long-wave UV radiation (Figure 27, right).

While B-jade continues to be prevalent in the market, gemmologists should also be wary of other convincing jadeite imitations such as these.

*Cara Williams FGA and Bear Williams FGA*

## TREATMENTS

### Large Pink Sapphire with Diffusion-Induced Star

In August 2016, a large, semi-transparent to translucent, oval pink star cabochon mounted in a white metal ring with several diamonds was submitted for testing to the American Gemological Laboratories in New York (Figure 28). The client indicated that the cabochon weighed 56.47 ct before it was set in the ring. Measuring approximately 25.10 × 22.07 × 9.68 mm, the stone was quite impressive for its size, and visible-range spectroscopy using an S.I. Photonics CCD (charged coupled device)-array UV-Vis spectrophotometer showed that its attractive pink colour was caused by $Cr^{3+}$.

*Figure 28: Measuring approximately 25 × 22 mm, the oval pink cabochon in this ring proved to be a heat-treated pink sapphire with a Ti-diffusion-induced star. Photo by Kelly Kramer.*

Mid-infrared spectroscopy of the cabochon using a Thermo Nicolet 6700 FTIR spectrometer identified it as a sapphire. It also showed extremely weak lines at 3309 and 3232 cm$^{-1}$, which are part of a series of absorptions (3309, 3232 and 3185 cm$^{-1}$) that are indicative of heat treatment in metamorphic-related sapphires (Smith, 2010). Microscopic examination revealed numerous thermally-altered 'fingerprints' (partially healed fissures) that had a melted and drippy appearance. Coupled with sheets of heating residues that also were prevalent in the stone, heat treatment was evident. Fibre-optic lighting revealed an extremely shallow, sub-surface milky sheen/layer all over the stone (Figure 29). At 60× magnification, extremely minute needles could be discerned in this layer. In the absence of

*Figure 29: The thin, sub-surface milky sheen/layer seen in the sapphire using fibre-optic lighting is an indication that the star is the result of a diffusion process. As shown here at 60× magnification, minute needles can be discerned. A thermally altered partially-healed fissure with a melted/drippy appearance can be seen at the lower left. The three prominent straight lines are parting planes. Photomicrograph by Christopher P. Smith.*

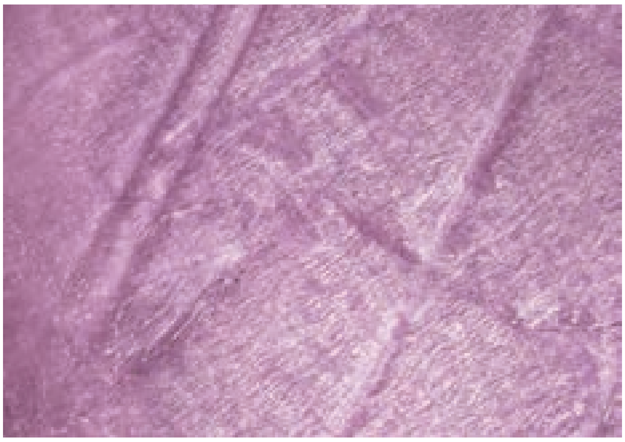

the typical three directions of rutile 'silk', it was evident that the stone's asterism was caused by this sub-surface layer. Semi-quantitative chemical analysis using a Thermo Scientific ARL Quant'X EDXRF spectrometer showed a relatively high amount of Ti (0.2 wt.%), which proved the star was not natural, but rather induced, by the diffusion of Ti.

Gemmologists should always be wary of a star stone that is missing the asterism-causing oriented needles. In sapphire, these needles consist of rutile ($TiO_2$) and they are resorbed into the corundum during the standard heating process, so a heated sapphire showing a star should arouse suspicion. For this particular pink sapphire, the absence of 'silk' combined with the sub-surface sheen provided telling evidence that the star is the result of a diffusion treatment process.

*Wendi M. Mayerson (wmayerson@aglgemlab.com)*
*American Gemological Laboratories*
*New York, New York, USA*

### Reference

Smith C.P., 2010. Inside sapphires. *Rapaport Diamond Report*, **33**(7), 123–132.

## MISCELLANEOUS

### Mid-Year 2016 Myanma Jade & Gems Emporium

*Figure 30: This is one of several warehouses containing jade lots at the recent Mid-Year 2016 Emporium. Photo by T. Hlaing.*

On 20–29 November 2016, the Mid-Year 2016 Myanma Jade & Gems Emporium took place in Nay Pyi Taw, Myanmar. The opening day was marked by a visit from Myanmar's vice president, U Henry Van Thio, and this author also attended the Emporium on the same day. Some of the gem merchants there were seen with interpreters, and those buyers reportedly came from Guangdong, China, to attend the event. On offer were nearly 6,000 jade lots and 439 'gems' lots (e.g. rough or faceted ruby, sapphire, peridot, danburite, etc.). In addition to the main building, there were 15 warehouses containing various 'jade' lots (e.g. Figure 30), including those labelled as bowenite, amphibole, quartzite, albite and idocrase (e.g. Figure 31).

The Emporium was attended by 1,796 foreign and 1,746 local merchants. A total of €327.9 million were obtained from the sale of 4,041 jade lots, and €1.6 million came from 44 'gems' lots. Revenues were down compared to the previous Emporium, in which jade lots sold for €527.08 million and 'gems' lots brought in €3.15 million (see Gem Notes section, **35**(3), 210).

At next year's Emporium, scheduled for November 2017, sales are planned to take place in dollars rather than euros, since the USA's sanctions against Burmese jadeite and ruby from Myanmar have been lifted.

*Dr U Tin Hlaing (p.tinhlaing@gmail.com)*
*Dept. of Geology (retired)*
*Panglong University, Myanmar*

*Figure 31: The 'jade' lots at the Emporium included boulders of various materials, such as those labelled amphibole, quartzite and idocrase. Photos by T. Hlaing.*

# Ruby and Pink Sapphire from Aappaluttoq, Greenland

*Christopher P. Smith, Andrew J. Fagan and Bryan Clark*

Since 1966, rubies and pink sapphires have been recovered from the southwest coastal region of Greenland. Until recently, only minor amounts of gem material were produced by local people using small-scale artisanal mining techniques. In 2014, True North Gems Inc. (Vancouver, British Columbia, Canada) completed mine permitting, and an exploitation licence for the extraction of gem corundum was issued for the area around the Aappaluttoq deposit. The property changed ownership in November 2016, and the first sale of its rubies and pink sapphires is expected to take place in 2017. The mineralization is hosted by the Fiskenæsset Anorthosite Complex, primarily within a phlogopite-bearing metasomatic rock. Standard gemmological properties are consistent with metamorphic-metasomatic-type rubies and pink sapphires from other world deposits. Typical inclusion features consist of coarse particles and fine needles of rutile, as well as inclusions of mica, talc, pargasite, cordierite, sillimanite, plagioclase and boehmite. The chemical composition of the Greenland rubies and pink sapphires is characterized by relatively high Fe contents and comparatively low concentrations of Ti, V and Ga.

*The Journal of Gemmology*, **35**(4), 2016, pp. 294–306, http://dx.doi.org/10.15506/JoG.2016.35.4.294

## Introduction

Little attention has been paid to the gem corundum localities of Greenland since their discovery in the 1960s. However, during the past several years, True North Gems Inc. applied detailed geological mapping, geophysics, drilling (more than 6,000 m of core), geochemical and heavy mineral concentrate sampling, and mini-bulk and bulk sampling techniques to characterize and define a minable reserve at their Aappaluttoq deposit (Weston, 2009; Reggin and Horan, 2015). In 2014, True North received an exploitation licence after undergoing strict environmental and social permitting that accompanied extensive baseline surveys of the local ecology and villages. However, in September 2016, True North Gems Greenland, the operating subsidiary of True North Gems Inc., was unable to raise sufficient working capital to put the mine into production, and the project was taken over by LNS Group of Norway, which continues to work towards production and sales in 2017.

With the development of the Aappaluttoq deposit, Greenland is poised to become a significant producer of ruby and pink sapphire (e.g. Figure 1). The deposit has the potential to make an important contribution to the global supply of ruby and pink sapphire for many years. This article provides an update on the geology of the Aappaluttoq deposit and gives a comprehensive gemmological description of its rubies and pink sapphires.

Figure 1: A range of colour and clarity is shown by these rubies and pink sapphires (0.61–2.37 ct) from Greenland's Aappaluttoq deposit. Photo by Bilal Mahmood.

## Location and Access

The gem corundum deposits of south-west Greenland are located approximately 200 km south of Greenland's capital city, Nuuk (Figure 2). From there, the mine is accessible by either a 45 minute helicopter flight or a five hour speedboat trip; there are no roads nearby. The area receives significant snowfall during the winter, when the average temperatures range from −10°C to +10°C (Statistics Greenland, 2016). Compared to the climate of the diamond mines in northern Canada, it is easier to conduct a mining operation in the more temperate environment of south-west Greenland.

The coast of western Greenland is mountainous with deeply incised fjords that run from the Davis Straight (between Canada and Greenland) inland toward the permanent ice sheet. At Aappaluttoq, only the local fjords (and not the open sea) freeze during the winter, so the mine is considered to have year-round sea access—a major logistical advantage. The vast majority of the labour required for the mine can be sourced from local towns and villages; this ensures that staff is well accustomed to working through the winter and also throughout the long days of summer.

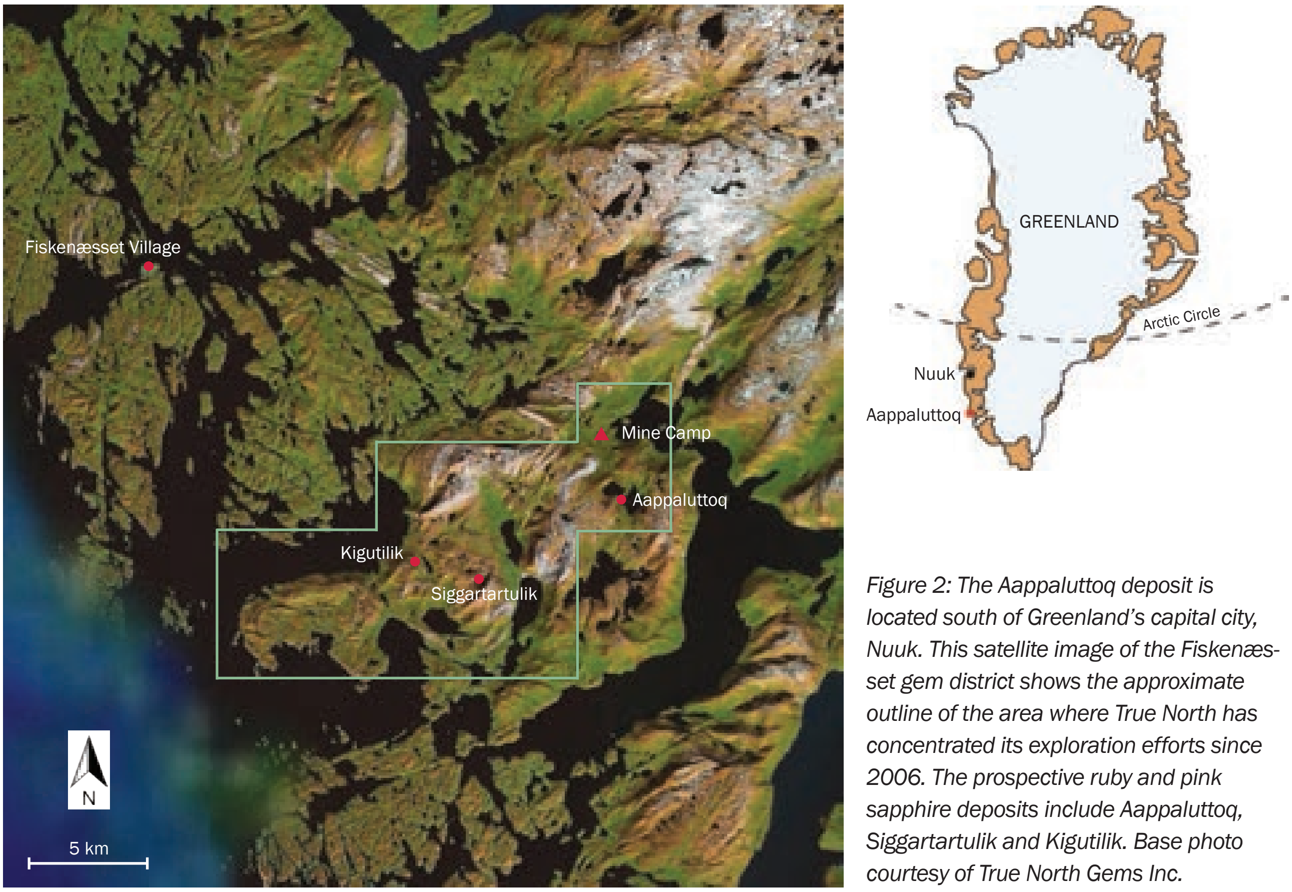

Figure 2: The Aappaluttoq deposit is located south of Greenland's capital city, Nuuk. This satellite image of the Fiskenæsset gem district shows the approximate outline of the area where True North has concentrated its exploration efforts since 2006. The prospective ruby and pink sapphire deposits include Aappaluttoq, Siggartartulik and Kigutilik. Base photo courtesy of True North Gems Inc.

## Geology and Gem Formation

The geology of the Aappaluttoq deposit has been summarized in several papers and conference abstracts (Appel, 1995; Weston, 2009; Reggin and Chow, 2011; Fagan and Groat, 2014a,b; Giuliani et al., 2014; Fagan, 2015; Reggin and Horan, 2015), and is still being actively researched by a team of company and academic geologists.

The rocks at Aappaluttoq have been subjected to high-pressure, high-temperature metamorphism and are very old (Mesoarchean); recent research suggests an age of approximately 2.9 billion years (Polat et al., 2010). Research is ongoing to define the actual age of the gem mineralization; the gems probably are significantly younger than their host rocks, related to later regional metamorphism and metasomatism. Nevertheless, Aappaluttoq still may be one of the oldest coloured stone deposits in the world (Krebs et al., 2016).

Greenland's gem corundum deposits are hosted by the Fiskenæsset Anorthosite Complex (FAC; see, e.g., Herd et al., 1969; Myers, 1975, 1985). The mineralization at Aappaluttoq is hosted by a reaction zone that formed from metasomatic interactions between ultramafic rock (peridotite) and mafic rock (leucogabbro). The peridotite forms a small lens or layer within the FAC and is composed of olivine, clinopyroxene, orthopyroxene, green spinel, amphibole and ilmenite, with minor apatite, magnesite, pyrrhotite and chalcopyrite. This ultramafic rock has low $SiO_2$ (<45 wt.%) and contains various chromophore elements (particularly Cr, and also V, Fe and Ti) that are important for the formation of an economically significant gem corundum deposit. The leucogabbro is a large and well-defined layer within the FAC. It has an Al-rich composition and comprises varying amounts of plagioclase, amphiboles (mostly hornblende and pargasite) and micas (biotite and phlogopite) with minor quartz. Although both the peridotite and leucogabbro have been regionally metamorphosed, most of their original igneous layering and textures are preserved.

In the metasomatized reaction zone, the ultramafic rock is rich in phlogopite (and is therefore called a *phlogopitite*; Figure 3) and consists of a steeply dipping layer approximately 2–5 m thick that extends to a depth of more than 90 m. It is composed of phlogopite-biotite (~80%), corundum (~10%), plagioclase (~5%) and oxide minerals (~5%) with minor amounts of amphiboles (pargasite, hornblende and gedrite). Adjacent to the phlogopitite reaction zone, the peridotite has been altered to a sapphirine-gedrite-hornblende assemblage. The metasomatized leucogabbro hosts some corundum mineralization, but since it does not contain as much Cr as the peridotite, it contains pink sapphire rather than ruby.

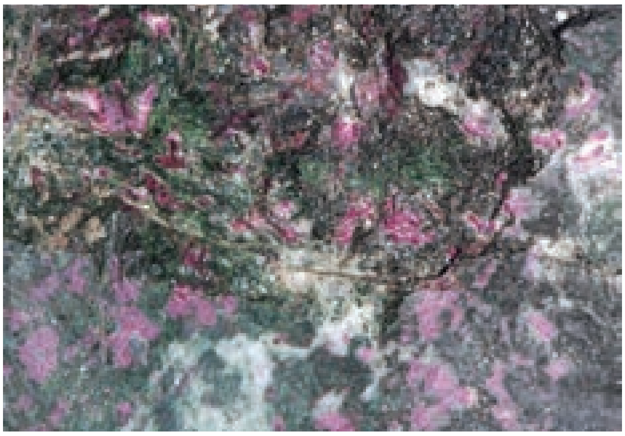

*Figure 3: This unusually coarse-grained and high-grade corundum ore from Aappaluttoq consists of a phlogopitite rock that contains brown phlogopite-biotite, white plagioclase, dark green pargasite and pink-to-red corundum crystals up to 4 cm long. The lower part of the sample has been sawn, while the top part is a broken surface. Photo courtesy of True North Gems Inc.*

Geochemical interactions between the differing rocks are thought to be responsible for forming the gem corundum. Although the general mechanism was suggested decades ago (Herd et al., 1969), new ideas regarding the geochemistry and timing have only recently been presented (Fagan and Groat, 2014a,b; Fagan et al., 2014; Krebs et al., 2016). According to these models, during regional metamorphism, fluid interactions between the two differing rock types created a metasomatic reaction zone encompassing part of the peridotite, the leucogabbro and the contact zone between the two units. Within this zone, silica was leached from the leucogabbro and the chromophoric elements were removed from the peridotite (Fagan and Groat, 2014). Upon regional cooling, the reaction zone formed significant volumes of stable phlogopite with corundum. Alumina ($Al_2O_3$), the main component of corundum, is believed to have remained stable in the residue of the altered leucogabbro. The concentration of Al in the reaction zone was high, and the availability of Cr from the adjacent peridotite

*Figure 4: This aerial photo shows the construction of the processing plant and main workshop at the Aappaluttoq deposit, well underway. The processing plant will employ dense media and magnetic separation, as well as advanced optical sorting technology to extract the corundum. Since this image was taken in October 2015, the plant building has been completed. Photo courtesy of True North Gems Inc.*

allowed the substitution of $Cr^{3+}$ for $Al^{3+}$ in the corundum, producing its pink-to-red coloration.

An examination of rough gem corundum derived from the 200 tonnes of rock extracted by True North from Aappaluttoq since 2006 reveals several crystal morphologies. The primary form for both ruby and pink sapphire is the hexagonal tablet, with crystals commonly ranging from 1.7 to 20 mm in dimension. These tablets formed between the layers of mica (phlogopite and biotite) in the main phlogopitite host rock. The morphology is not linked to coloration, with the tablets exhibiting all colours from deep red to 'lilac' pink. Within the altered leucogabbro, the dominant morphology consists of hexagonal prisms with pinacoidal terminations, in slightly larger sizes than those observed within the phlogopitite ore. In addition, hexagonal dipyramidal crystals up to 4 cm long rarely have been recovered from exploration samples.

*Figure 5: Processing of ore from Aappaluttoq resulted in this rough concentrate of <4.6 mm-sized material. The pink-to-red corundum in this material will then be further separated with an optical sorter. Photo courtesy of True North Gems Inc.*

## Mining and Recovery

The Aappaluttoq deposit is being developed into one of the most advanced coloured stone mines in the world (Figure 4). Modern mining techniques are planned to maximize production, minimize cost and limit the opportunity for theft.

The extraction process is planned to begin with blocks of ore being quarried with large commercial wire saws—a technique borrowed from the dimension stone industry. These blocks will weigh approximately 20 tonnes each, and 5–8 of them will be produced each day. Each block will be transported to a processing facility, where it will be crushed into small pieces (initially 20 mm and processed down to 1.7 mm). Iterative crushing and recovery will ensure that the largest corundum stones are liberated rather than crushed. The material will be transported on closed conveyor belts to the Aappaluttoq Gem Recovery plant for further processing using dense media and magnetic separation followed by optical sorting technology to produce a corundum concentrate (e.g. Figure 5). This material will be sent to a separate facility in Greenland where the remaining host rock (approximately 25–30%) will be removed using a 24-hour hydrofluoric acid wash. The corundum will then be graded according to a customized sort matrix. After the opaque material is removed, the gem corundum (Figure 6) will be prepared for valuation and export. More

*Figure 6: Initial sorting experiments of the rough gem corundum yielded these categories (from left to right) of 'medium pink', 'red' and 'lilac pink'. Photo courtesy of True North Gems Inc.*

details on the ore processing and corundum recovery procedures are provided by Reggin and Horan (2015).

## Production, Quality and Size

The use of modern exploration techniques at Aappaluttoq allows for a high degree of predictability in the grade and volume of gem corundum recovered from each mined block over the entire life-of-mine. This is unusual for a coloured gemstone deposit and should enable a dependable supply of rough material to the market.

From the outset, True North Gems modelled the mine economics using only melee-sized (<4 mm) rough gem material. Although geological sampling has shown that larger stones are present within the deposit, their recovery is highly difficult to predict. The focus on melee-sized material will enable a steady supply of rough to partners in the marketplace, rather than relying on auctions that take place a few times per year. This improves mine cash flow and avoids 'peaks and surges' of gem corundum production. Although this strategy has led some to believe that Aappaluttoq will only produce small stones, this actually is not the case. Numerous faceted gemstones of >1 ct are held by the company in inventory recovered from exploration bulk samples; some of those gems were made available for this study (e.g. see the cover of this issue and Figure 7). The largest piece of corundum recovered to date is the carved opaque 440 ct Kitaa Ruby (see www.diamonds.net/News/NewsItem.aspx?ArticleID=15699).

The exploration bulk samples obtained during the early phases of the project have been processed for 'test-polishing' exercises, in which several kilograms of rough material were faceted to assess the quality of the material. The resulting sample inventory includes approximately 15,000 carats of polished material, ranging from cabochon-quality to extra-fine faceted material, in various colours, sizes and shapes. Pink sapphire makes up approximately 60–80% of this production, with ruby making up the balance. This colour proportion is in line with other deposits of this type, such as the Montepuez ruby mine in Mozambique (Roberts and Beare, 2015). For the highest quality polished stones from Aappaluttoq, valuations reached US$3,200/ct for intense pink sapphires and US$6,000/ct for deep red rubies.

Production from Aappaluttoq is expected to last for a minimum of nine years, and the deposit currently has defined minable reserves of 59.2 million grams of corundum, with an additional 21.8 million grams as inferred resources (i.e. exploration targets that could prolong the life-of-mine once they have been investigated further; see Reggin and Horan, 2015). Approximately 70% of the corundum is allocated to the non-gem 'opaque' category, 20–25% is 'near-gem' and 5–10% is 'gem'. These percentages are consist-

*Figure 7: These sapphires from Greenland range from light to intense pink; some also exhibit a subtle purplish colour modifier. The stones are eye-clean to moderately included and weigh 0.42–1.43 ct. Photo by Bilal Mahmood.*

ent with other large gem corundum deposits (e.g. Roberts and Beare, 2015).

## Materials and Methods

Nineteen faceted samples were provided by True North Gems to American Gemological Laboratories for this study. These consisted of 10 rubies (0.29–2.53 ct; see cover of this issue) and nine pink sapphires (0.42–1.43 ct; Figure 7).

Standard gemmological instrumentation was used to record pleochroism, RI, birefringence, optic character, hydrostatic SG, UV fluorescence (with a 4 W combination 365 nm long-wave and 254 nm short-wave lamp) and optical absorption spectra (with a prism-type desk-model spectroscope) for all samples. A binocular microscope, incorporating fibre-optic and other lighting techniques, was used to document internal features in the stones.

Identification of mineral inclusions was performed using a Renishaw 2000 Raman microscope. Additionally, we utilized a Thermo Scientific Nicolet 6700 Fourier-transform infrared (FTIR) spectrometer to record the absorption of all samples in the near- to mid-IR region of the spectrum (7000–400 $cm^{-1}$). Polarized ultraviolet-visible-near infrared (UV-Vis-NIR) spectra in the range of 250–850 nm were recorded on four of the stones with a PerkinElmer Lambda 950 spectrometer. A Thermo Scientific ARL Quant’X energy-dispersive X-ray fluorescence spectrometer (EDXRF) was used to determine the semi-quantitative chemical composition of all samples.

## Results and Discussion

### *Gemmological Characteristics*

**Colour and Visual Appearance:** Ten of the samples possessed a richly saturated, pure red coloration that classified them as ruby (see, e.g., the cover of this issue). The remaining nine pink sapphires ranged from a light pastel pink to an intense pink face-up appearance (Figure 7). Several of the pink sapphires displayed a subtle purplish colour modifier. No eye-visible colour zoning was observed. The majority of the samples were transparent, while several trended towards semi-transparent due to the nature and number of their inclusions.

All samples exhibited moderate-to-strong dichroism when viewed perpendicular to the c-axis with a dichroscope. Yellowish orange to orangey red or pink coloration was seen parallel to the c-axis, and reddish purple to purple-red (for rubies) or purplish pink to purple-pink (for pink sapphires) was observed perpendicular to the c-axis.

**Gemmological Properties:** The standard gemmological properties were consistent with corundum in general, and also with past research on rubies and pink sapphires from Greenland (Thirangoon, 2009): RI—$n_{\omega}$ = 1.769–1.700 and $n_{\varepsilon}$ = 1.760–1.762, birefringence—0.008–0.009, optic character—uniaxial negative and SG—3.98–4.01. In general, the ruby samples displayed moderate-to-strong red fluorescence when exposed to long-wave UV radiation, whereas the pink sapphires displayed a weak-to-moderate red reaction. All samples showed weaker red fluorescence to short-wave radiation, ranging from weak to none. Four of the samples contained unidentifiable inclusions that fluoresced bright orange when exposed to both long-wave and short-wave UV radiation.

**Internal Features:** A rich diversity of features were noted in the rubies and pink sapphires from Greenland. In addition to twinning (see below), the most commonly observed internal features were clouds of minute rutile particles (i.e. ‘silk’, see Figure 8), as well as some fine rutile needles and arrowhead-shaped platelets (Figure 9). Generally speaking, few additional mineral inclusions were observed. Of these, we identified whitish inclusions of talc (Figure 10), whitish to

*Figure 8: Clouds of fine rutile particles are one of the most common inclusion features observed in the rubies and pink sapphires from Greenland. Photomicrograph by C. P. Smith; magnified 55×.*

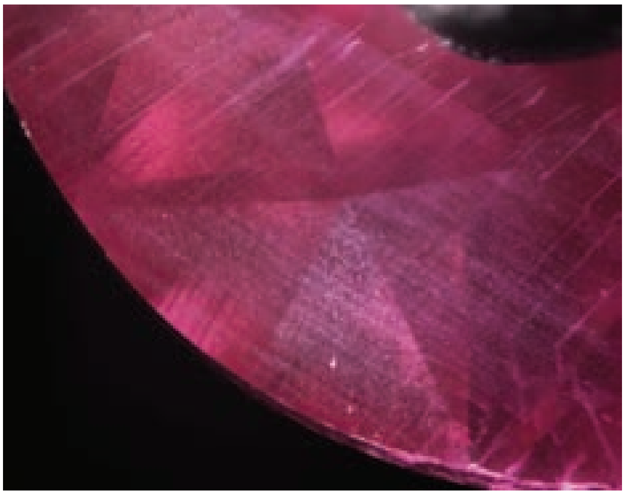

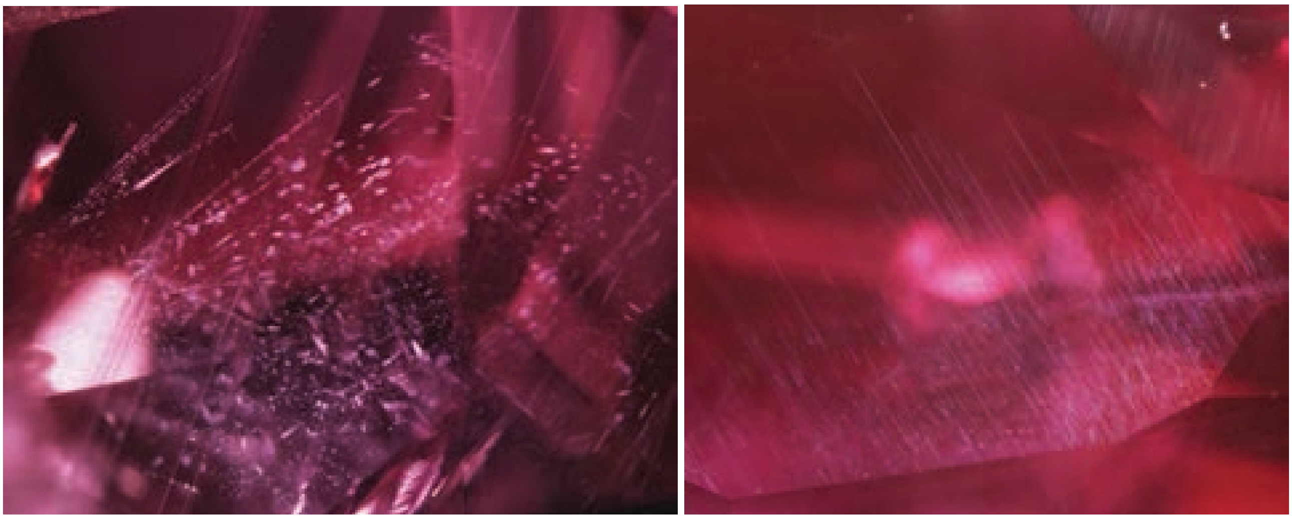

Figure 9: Fine exsolutions of rutile needles and platelets (sometimes arrowhead shaped) also are commonly encountered in Greenland gem corundum. Photomicrographs by C. P. Smith; magnified 58× (left) and 75× (right).

brownish crystals of mica (Figure 11), as well as cordierite, sillimanite, plagioclase and columnar crystals of pargasite (Figure 12). Additionally, we observed several rounded-to-oblong, colourless crystals that could not be identified with Raman spectroscopy (because Cr luminescence from the host gemstone swamped the Raman detector and resulted in a poor analysis); their appearance resembled apatite and zircon (Figure 13). Also present at the polished surface of some samples were inclusion assemblages composed of a variety of minerals, including talc, plagioclase, sillimanite and others.

We noted various patterns of partially healed fissures that were composed primarily of isolated (not interconnected) negative crystals (Figure 14).

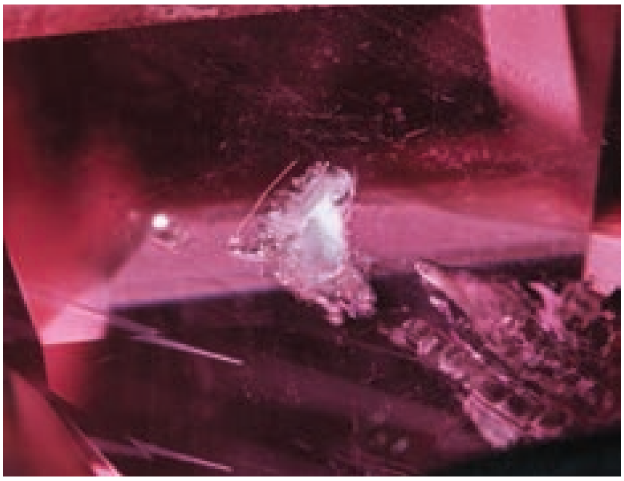

Figure 10: Of the various mineral inclusions identified, translucent, whitish inclusions of talc were the most commonly observed in the rubies and pink sapphires from Greenland. Photomicrograph by C. P. Smith; magnified 58×.

Figure 11: Mica is another of the more common mineral inclusions identified in Greenland rubies and pink sapphires. Photomicrograph by C. P. Smith; magnified 60×.

Figure 12: Pargasite is not commonly found in rubies and sapphires, although a few samples in this study possessed columnar euhedral crystals of this amphibole-group mineral. Photomicrograph by C. P. Smith; magnified 62×.

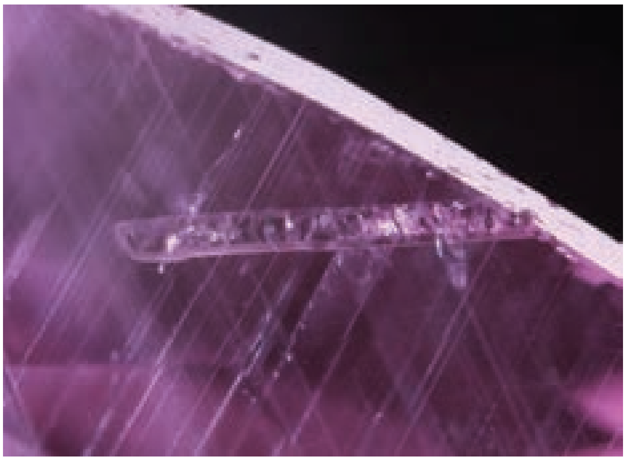

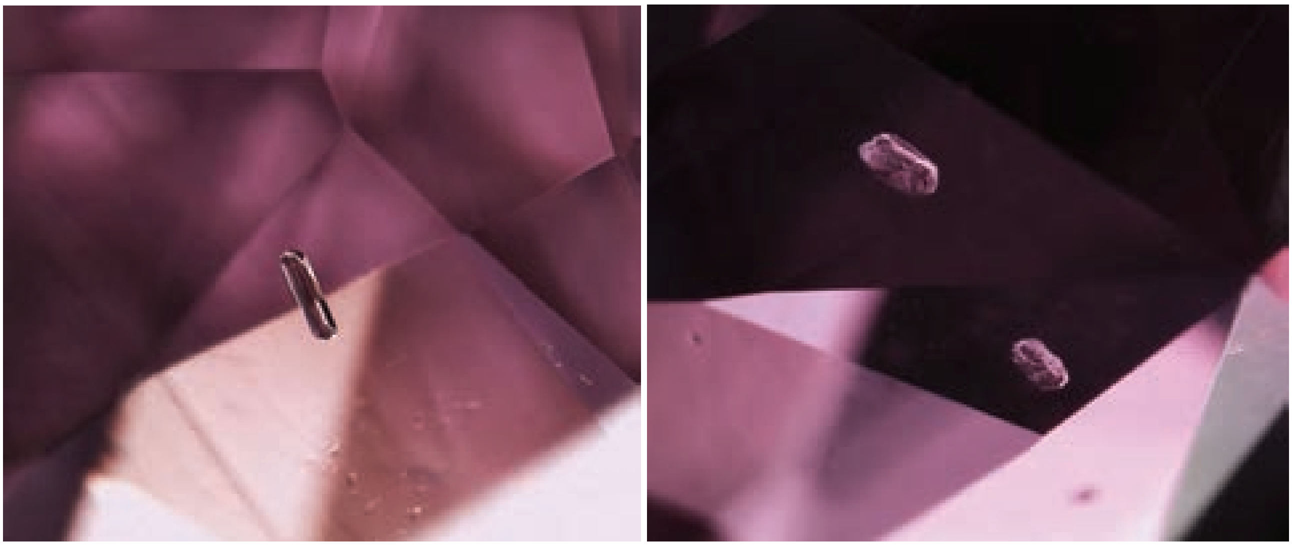

Figure 13: These inclusions could not be identified in this study, although they resemble zircon and/or apatite. Photomicrographs by C. P. Smith; magnified 60×.

In addition, one sample possessed basal-oriented thin films associated with negative crystals (Figure 15). The partially healed fissures and negative crystals seen in these samples interestingly did not trap any fluid phase. Also, the necking-down process of fissure healing typical of rubies and pink sapphires from most other deposits was not observed in these samples, and only tiny negative crystals were seen. It is possible that fluid may be present in these minute negative crystals but was too small to be recognized. It is also possible that there was not much fluid present under the high temperature and pressure conditions that the gems formed (i.e. near granulite metamorphic conditions).

Boehmite (identified by mid-IR spectroscopy) commonly formed an alteration product along a series of coarse, whitish intersection tubules occurring at the intersection of two or three twinning/parting planes (Figure 16). Open fissures also were commonly observed, and often they were lined by epigenetic minerals such as boehmite, kaolinite, goethite and other weathering minerals.

Additional mineral inclusions of catapleiite, chlorite, cosalite, dolomite, magnesite, margarite, pyroxene and sapphirine have been identified in

Figure 14: Partially healed fissures composed of groups of isolated negative crystals are a common feature in Greenland rubies and pink sapphires. Photomicrograph by C. P. Smith; magnified 55×.

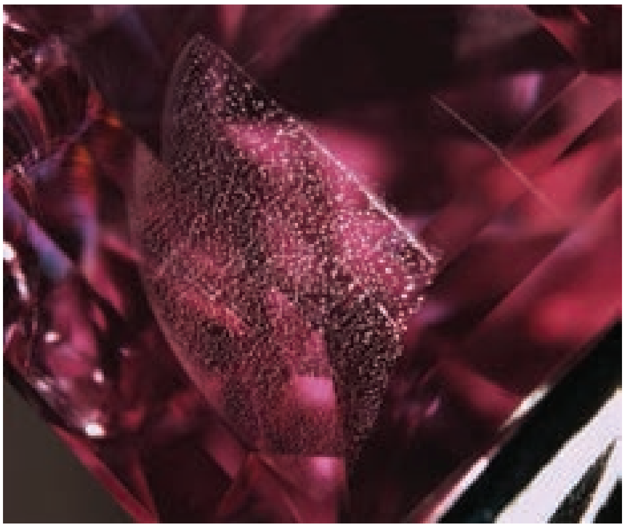

Figure 15: A series of fine, platy negative crystals and thin films are oriented along the basal growth planes in this pink sapphire. Photomicrograph by C. P. Smith; magnified 50×.

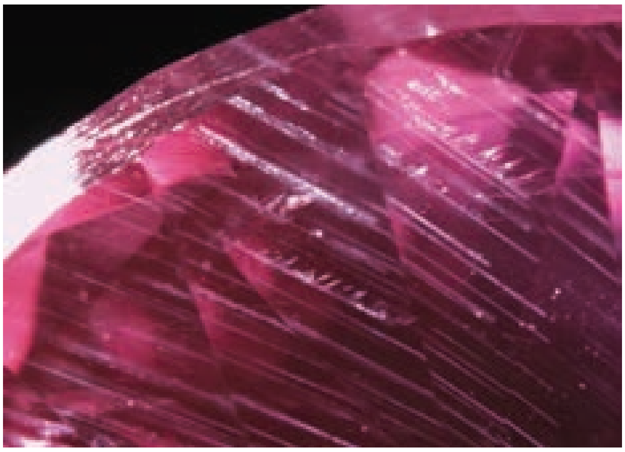

*Figure 16: Boehmite is found along intersection tubules that commonly occurred at the crossing of twinning (and sometimes parting) planes in the rubies and pink sapphires. Also visible are a series of stress fractures along the length of some of the tubules. Photomicrograph by C. P. Smith; magnified 60×.*

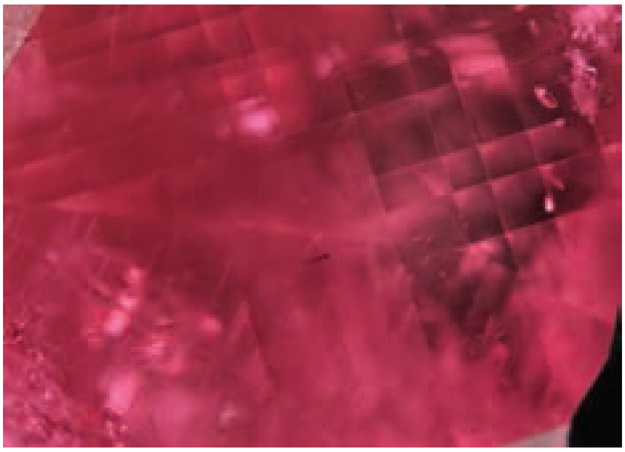

*Figure 17: Intersecting twinning along different directions of the positive rhombohedron* r *{10$\bar{1}$1} create a checkerboard pattern in this ruby. Photomicrograph by C. P. Smith; magnified 42×.*

Greenland rubies and pink sapphires by other researchers (e.g. Thirangoon, 2009).

**Internal Growth Structures, Colour Zoning and Twinning:** Generally, the samples contained rare-to-no internal growth structures, and their colour was homogeneous. A few showed subtle planar growth structures, and weak-to-distinct pink-to-red colour zones were rarely noted.

Several of the stones displayed twinning parallel to the positive rhombohedron *r* {10$\bar{1}$1}. Typically we noted only one direction of laminated twinning, parallel to a single series of *r* planes. Occasionally, however, there were as many as three directions of twinning parallel to additional *r* planes. Parting parallel to *r* also was prominent in a few samples. The intersections of twinning and/or parting planes created a checkerboard pattern (Figure 17).

### *Visible and UV-Vis-NIR Spectroscopy*

All spectra were dominated by chromium absorption features. The strength of the absorption bands varied with the intensity of the pink-to-red colour of the gems.

**Desk-model Spectroscope:** In the visible range, a general absorption to approximately 450 nm was apparent, along with weak-to-distinct lines at 468 nm and at 475/476 nm (doublet). A broad absorption band was observed from approximately 525 to 585 nm; its width depended on the saturation of pink-to-red colour. We also noted faint lines at 659 and 668 nm, plus two strong lines at 692 and 694 nm (which appeared as a bright emission line at 693 nm).

**UV-Vis-NIR Polarized Spectroscopy:** Two broad bands, centred at approximately 405 and 550 nm, as well as weak-to-distinct sharp peaks recorded at 468, 475, 476, 659, 668, 692 and 694 nm, are

*Table I: Semi-quantitative EDXRF chemical analyses of rubies and pink sapphires from Greenland.**

| Variety | Ruby (sample no.) | | | | | | | | | |
|---|---|---|---|---|---|---|---|---|---|---|
| **Element** | **1681** | **1889** | **1945** | **1952** | **2165** | **2236** | **2309** | **2311** | **3403** | **3426** |
| Al | 99.27 | 99.43 | 99.33 | 99.24 | 99.09 | 99.30 | 99.46 | 99.39 | 98.88 | 99.44 |
| Ti | 228 | 1227 | 141 | 95 | 112 | 124 | 81 | 139 | 128 | 156 |
| V | 72 | 46 | 64 | 67 | 62 | 72 | 83 | 36 | 38 | 44 |
| Cr | 4552 | 2701 | 4353 | 5242 | 6860 | 5084 | 3358 | 3086 | 8387 | 2754 |
| Fe | 2261 | 2686 | 1999 | 2058 | 1837 | 1624 | 1728 | 2706 | 2435 | 2507 |
| Ga | 49 | 49 | 55 | 54 | 53 | 54 | 56 | 41 | 52 | 42 |

* Data are in wt.% for Al and in parts per million by weight (ppmw) for all other elements. Approximate detection limits are Ti = 22, V = 20, Cr = 18, Fe = 11 and Ga = 7 ppmw.

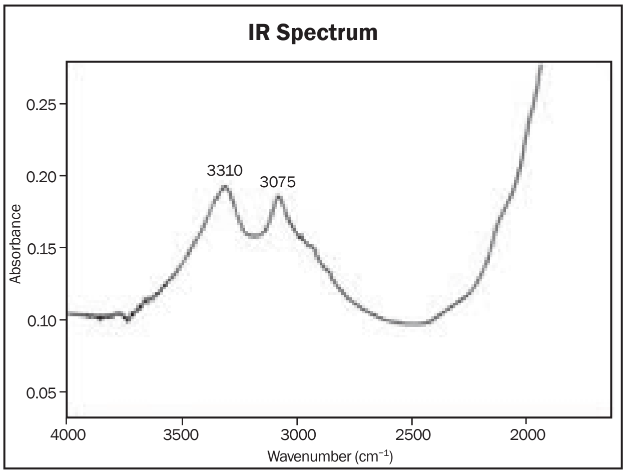

*Figure 18: In the mid-infrared region of the spectrum, some rubies and pink sapphires from Greenland showed distinct bands at approximately 3310 and 3075 cm$^{-1}$ (and weak bands at approximately 2100 and 1980 cm$^{-1}$). These features indicate the presence of boehmite, which was mostly concentrated along intersection tubules related to twinning and/or parting planes. Such absorption characteristics are helpful not only for identifying the presence of foreign mineral phases, but also for proving that a gem has not been heated.*

all ascribed to Cr$^{3+}$. A weak band was also occasionally observed at 450 nm, attributed to Fe$^{3+}$ pair transition.

## FTIR Spectroscopy

In addition to the dominant IR absorption characteristics of corundum between 1000 and 400 cm$^{-1}$ (i.e. approximately 760, 642, 602 and 450 cm$^{-1}$: Wefers and Bell, 1972), the rubies and pink sapphires in this study commonly had weak-to-very strong absorptions related to structurally bonded OH groups and foreign minerals. A nominal, sharp band was recorded at 3310 cm$^{-1}$ in several samples. Additionally, a weak series of absorptions with the dominant feature at 3161 cm$^{-1}$ was found in one stone. These are all associated with structurally bonded OH groups (Smith and van der Bogert, 2006). Also common were two dominant bands positioned at approximately 3310 and 3075 cm$^{-1}$ (Figure 18), with an additional pair of weak bands at approximately 2100 and 1980 cm$^{-1}$. These features are related to OH-stretching frequencies associated with boehmite, an aluminium hydroxide mineral (Farmer, 1974; Wefers and Misra, 1987; Smith et al., 1997). Several samples had additional absorptions in this region that further signalled the presence of kaolinite, goethite and other weathering minerals (cf. Smith and van der Bogert, 2006). The specific mineral phase could not be identified in all instances.

The presence of boehmite was generally traced to locations along parting planes, interpenetrating intersection tubules and open fissures, whereas the presence of kaolinite, goethite, etc. was generally attributed to epigenetic staining present in surface-reaching fissures.

## Chemical Analyses

The most significant minor- to trace-element variations were recorded in Cr concentrations, which again correlated to the intensity of the red-to-pink colour. Ti and Fe were the next most significant trace elements, followed by very small amounts of V and Ga (Table I). Although higher Ti contents were recorded previously by Thirangoon (2009), other elements (Cr, V, Fe and Ga) were consistent with that study. Mg was below the detection limit of EDXRF spectroscopy in all samples. Although Keulen and Kalvig (2013) also analysed corundum from Greenland, a direct comparison to their dataset is impossible due to their use of normalized data and the absence of any verifiably comparable gem-quality

| **Pink Sapphire (sample no.)** | | | | | | | | |
|---|---|---|---|---|---|---|---|---|
| **1512** | **1519** | **1849** | **1888** | **1891** | **1894** | **1895** | **1896** | **1897** |
| 99.73 | 99.80 | 99.71 | 99.56 | 99.64 | 99.63 | 99.69 | 99.74 | 99.74 |
| 141 | 149 | 128 | 81 | 56 | 130 | 143 | 108 | 139 |
| 94 | 42 | 32 | 69 | 82 | 38 | 40 | 37 | 67 |
| 561 | 869 | 750 | 2269 | 1524 | 1070 | 1058 | 775 | 298 |
| 1784 | 886 | 1919 | 1895 | 1788 | 2407 | 1705 | 1580 | 1997 |
| 40 | 31 | 57 | 50 | 63 | 58 | 63 | 42 | 60 |

*Figure 19: (a) The concentrations of Fe, Ti and Ga are plotted for the rubies and pink sapphires from Greenland as compared to some other major world sources, including marble-type deposits from Afghanistan (Jegdalek) and Myanmar (Mogok and Mong Hsu), mafic metamorphic-metasomatic rocks from Mozambique (Montepuez) and alkali basalts from Thailand (Chanthaburi and Trat). The relatively higher Fe contents of the mafic-ultramafic-derived gems from Greenland, Mozambique and Thailand readily separate these sources from marble-type deposits. (b) Further correlations of these and other elements such as V help to separate the relatively higher-Fe sources from those of Greenland, although there is some overlap—particularly with stones from Mozambique.*

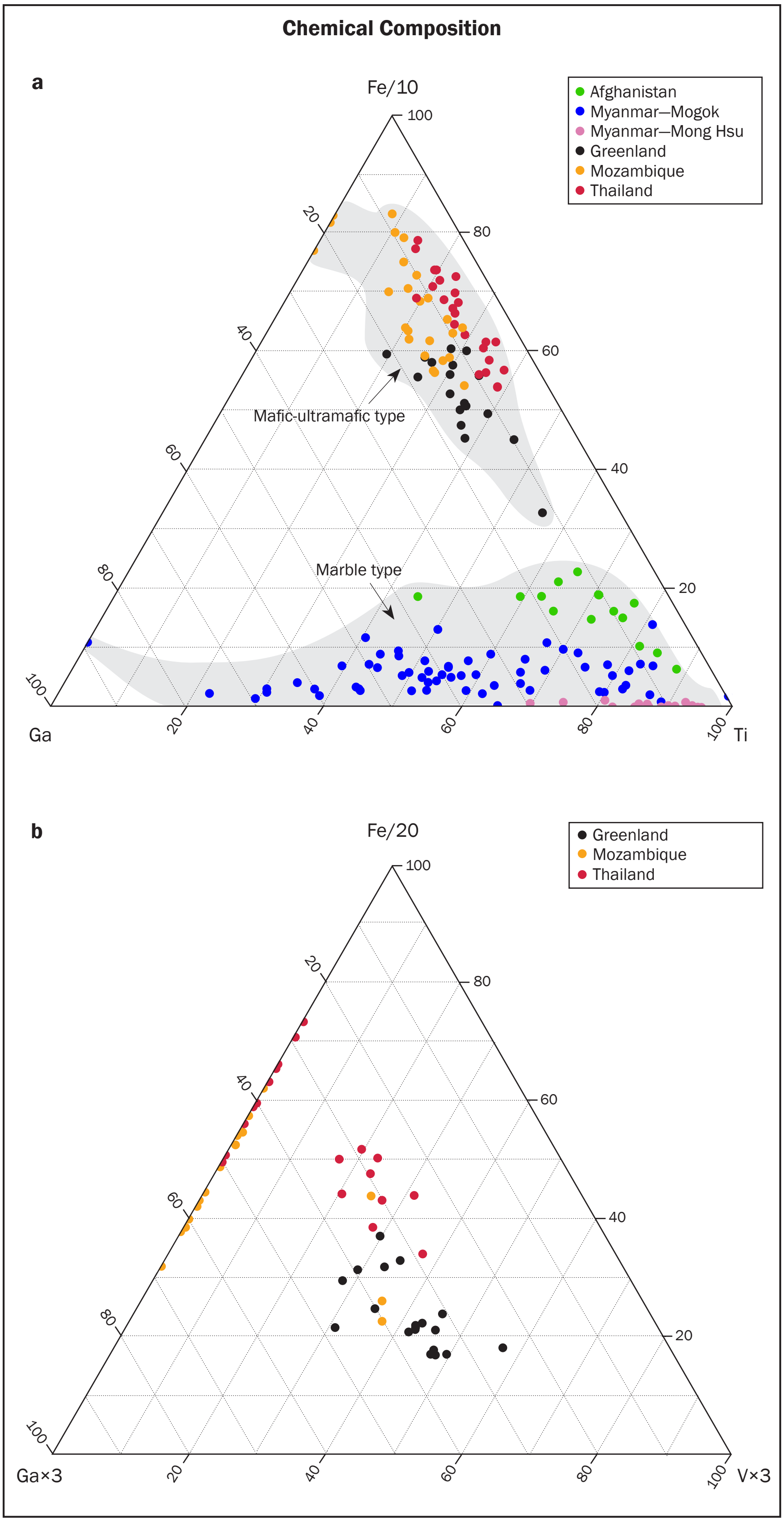

samples from the same deposit. In the present authors' opinion, the analyses of opaque material in a geographic origin study do not normally compare well to those of the high-quality stones that are routinely submitted to gemmological laboratories.

Figure 19 illustrates how the composition of the rubies from Greenland compares to that of rubies from some other major deposits. Further geochemical and isotopic work is ongoing in association with the University of Alberta (Krebs et al., 2016) and the University of British Columbia.

## Geographic Origin Determination

There are a number of features that may help gemmologists recognize a ruby or pink sapphire from Greenland. Their relatively high Fe content separates them from the majority of stones from marble-type deposits, such as those in Afghanistan, Myanmar, Nepal, Pakistan and Vietnam, as well as plumasites (i.e. Mangare, Kenya) and metasomatized mafic dykes in marble (i.e. Mahenge and Matombo in Tanzania). For pink sapphires, this also includes the placer deposits of Sri Lanka and Madagascar (Ilakaka).

Rubies and pink sapphires from basalt-related deposits also contain relatively high Fe, although correlations between other trace elements can help to separate them from those of Greenland (again, see Figure 19). In addition, the typical inclusion features of thin films oriented along basal growth zoning and associated with doubly truncated negative crystals, such as those found in the basalt-related deposits of Thailand, Cambodia and Kenya (Lake Baringo), were not encountered in our Greenland samples. The Fe content of our Greenland stones was similar to that of some rubies and pink sapphires from East Africa (Madagascar, Mozambique, Tanzania and Malawi). Further work on the trace-element and isotopic composition of the Greenlandic material is ongoing and should prove helpful for origin fingerprinting (Fagan and Groat, 2014a,b; Krebs et. al., 2016).

Some typical microscopic properties of Greenland gem corundum include the relative fineness of the rutile silk as compared to the typically coarser rutile particles observed in a number of the East African deposits. In addition, certain mineral inclusions such as cordierite, cosalite and catapleiite that have been identified in previous studies (Thirangoon, 2009) may also point to a Greenland origin.

It should be noted that none of the rubies and pink sapphires included in this study were heat treated, and this is one of the current marketing points of the Greenland gem corundum. However, and the majority of the rubies and pink sapphires sold in the market have been heat treated, it should be expected that heated Greenland gems will also become available (directly or indirectly) at some point. Once a stone has been heated, geographic origin determination becomes more difficult, as key identification features such as rutile patterns and other mineral inclusions become altered.

## Conclusions

In the near future, it is expected that rubies and pink sapphires from Greenland will become a significant new addition to the gem and jewellery market. Although gem corundum was first discovered there in the 1960s, a full mineral exploration study was not completed until 2011. Since then, the Aappaluttoq deposit has gone through the mine permitting process, and an exploitation licence was issued in 2014. Once fully financed and constructed, large-scale mining activities will commence.

Mineral inclusions in these rubies and pink sapphires are consistent with the metamorphosed and metasomatized mafic-ultramafic host rocks. Inclusions of mica (mostly brown phlogopite-biotite), feldspar (plagioclase) and pargasite are typical minerals of the phlogopitite and leucogabbro host rocks. Inclusions of talc are consistent with the alteration of ultramafic rocks, and boehmite also may be attributed to a retrograde metamorphic alteration of the host corundum. The presence of sillimanite and cordierite inclusions is consistent with the pressure-temperature conditions expected for the Aappaluttoq stones. Other researchers have also identified catapleiite, chlorite, cosalite, dolomite, magnesite, margarite, pyroxene and sapphirine inclusions in rough ruby and pink sapphire samples from Greenland (Thirangoon, 2009). The minor-to-trace-element composition of the Greenland gem corundum revealed relatively high Fe with comparatively low Ti, V and Ga.

By taking into account the complete array of gemmological characteristics and chemical data, we found that it is possible to separate the gem-quality Greenland rubies and pink sapphires from those of the more commercially important deposits in Myanmar, Thailand, Madagascar, Mozambique, Kenya, Vietnam and elsewhere.

Despite the poor mining finance climate that currently exists, it is likely that Aappaluttoq will go into production in 2017. Thus the gem and jewellery trade should expect an influx of Greenland rubies and pink sapphires in the near future.

## References

Appel P.W.U., 1995. *Ruby Occurrences in the Fiskenæsset Area, West Greenland*. Grønlands Geologiske Undersøgelse Open File Report 95/11, Copenhagen, Denmark, 26 pp.

Fagan A.J., 2015. True North Gems Greenland mining – The final lap. *InColor*, Issue 29, 36–49.

Fagan A.J. and Groat L.A., 2014a. The Fiskenæsset gem district SW Greenland – A new source of ruby and pink sapphire. *21st General Meeting of the International Mineralogical Association*, Johannesburg, South Africa, 1–5 September, 279.

Fagan A.J. and Groat L.A., 2014b. The geology of the Aappaluttoq ruby and pink sapphire deposit, SW Greenland. *Geological Society of America Abstracts with Programs*, **46**(6), Vancouver, British Columbia, Canada, 19–22 October, 417.

Fagan A.J., Groat L.A. and Boyce A., 2014. Initial thoughts on the geology of the Aappaluttoq ruby deposit. *North Atlantic Craton Conference 2014*, St Andrews, 20–21 March, 27.

Farmer V.C., Ed., 1974. *The Infrared Spectra of Minerals*. Mineralogical Society of Great Britain and Ireland, London, Monograph 4, http://dx.doi.org/10.1180/mono-4.

Giuliani G., Ohnenstetter D., Fallick A.E., Groat L.A. and Fagan A., 2014. The geology and genesis of gem corundum deposits. In L.A. Groat, Ed., *The Geology of Gem Deposits*, 2nd edn., Mineralogical Association of Canada Short Course Series, **44**, Québec City, Québec, 29–112.

Herd R.K., Windley B.F. and Ghisler M., 1969. *The Mode of Occurrence and Petrogenesis of the Sapphirine-bearing and Associated Rocks of West Greenland*. Rapport Grønlands Geologiske Undersøgelse, No. 24, Copenhagen, Denmark, 44 pp.

Keulen N. and Kalvig P., 2013. Fingerprinting of corundum (ruby) from Fiskenæsset, West Greenland. *Geological Survey of Denmark and Greenland Bulletin*, No. 28, 53–56.

Krebs M.Y., Pearson D.G. and Fagan A.J., 2016. Trace element and Sr isotope characteristics of ruby. *Goldschmidt Conference*, Yokohama, Japan, 26 June–1 July, 1,608.

Myers J.S., 1975. *Igneous Stratigraphy of Anorthosite, SW Greenland*. Rapport Grønlands Geologiske Undersøgelse, No. 74, Copenhagen, Denmark, 27 pp.

Myers J.S., 1985. *Stratigraphy and Structure of the Fiskenæsset Complex, Southern West Greenland*. Bulletin Grønlands Geologiske Undersøgelse, No. 150, Copenhagen, Denmark, 72 pp.

Polat A., Frei R., Scherstén A. and Appel P.W.U., 2010. New age (ca. 2970 Ma), mantle source composition and geodynamic constraints on the Archean Fiskenæsset anorthosite complex, SW Greenland. *Chemical Geology*, **277**(1–2), 1–20, http://dx.doi.org/10.1016/j.chemgeo.2010.06.016.

Reggin L. and Chow J., 2011. Pre-Feasibility Report on the Aappaluttoq Ruby Project, Greenland. True North Gems, Vancouver, British Columbia, Canada, 164 pp., www.truenorthgems.com/wp-content/uploads/2015/05/True_North_Gems_2011_PFS_Report_2.pdf.

Reggin L. and Horan M., 2015. An Updated Pre-Feasibility Report on the Aappaluttoq Ruby Project, Greenland—National Instrument 43-101 Technical Report. True North Gems, Vancouver, British Columbia, Canada, 170 pp., www.truenorthgems.com/wp-content/uploads/2015/05/Aappaluttoq-PFS-report-2015.pdf.

Roberts L. and Beare M., 2015. A Competent Persons Report on the Montepuez Ruby Project, Mozambique. SRK Consulting (UK) Limited, Cardiff, 195 pp., https://xmbl.files.wordpress.com/2015/07/u6362_mrm_cpr_mining_report_final_v3a_clean.pdf.

Smith C.P. and van der Bogert C., 2006. Infrared spectra of gem corundum. *Gems & Gemology*, **42**(3), 92–93.

Smith C.P., Gübelin E.J., Bassett A.M. and Manandhar M.N., 1997. Rubies and fancy-color sapphires from Nepal. *Gems & Gemology*, **33**(1), 24–41, http://dx.doi.org/10.5741/gems.33.1.24.

Statistics Greenland, 2016. Greenland in Figures. Statistics Greenland, 40 pp., www.stat.gl/publ/en/GF/2016/pdf/Greenland in Figures 2016.pdf.

Thirangoon K., 2009. Ruby and Pink Sapphire from Aappaluttoq, Greenland: Status of On-Going Research. Gemological Institute of America, Bangkok, Thailand, 18 pp., www.giathai.net/pdf/Greenland_Ruby_March_2009.pdf.

Wefers K. and Bell G.M., 1972. *Oxides and Hydroxides of Aluminum*. Technical Paper 19, Alcoa Laboratories, St Louis, Missouri, USA, 51 pp.

Wefers K. and Misra C., 1987. *Oxides and Hydroxides of Aluminum*. Technical Paper 19, Revised, Alcoa Laboratories, St Louis, Missouri, USA, 92 pp., www.alcoa.com/global/en/innovation/papers_patents/pdf/TP19_Wefers.pdf.

Weston B.C., 2009. 2008 Report on Field Activities for the Fiskenæsset Ruby Project, Greenland. True North Gems, Vancouver, British Columbia, Canada, 76 pp.

## The Authors

**Christopher P. Smith FGA and Bryan Clark**
American Gemmological Laboratories (AGL)
580 5th Avenue, Suite 706, New York,
New York, USA
Email: chsmith@aglgemlab.com

**Andrew J. Fagan**
True North Gems Inc., 700–1055 West Georgia
Street, Vancouver, British Columbia, Canada

## Acknowledgements

Author AJF acknowledges Bonnie Weston (True North Gems Inc.) for assistance with drafting figures and for geological discussions, as well as John Mattinson (True North Gems Inc.) for comments that aided an early draft of this manuscript. AJF also acknowledges funding and field support from True North Gems Inc. Four anonymous reviewers contributed to a clearer article.


The Prestige Report™
Gemological Analysis
AGL
AGL
American Gemological Laboratories™
Grading

# Geology, Gemmological Properties and Preliminary Heat Treatment of Gem-Quality Zircon from the Central Highlands of Vietnam

*Le Thi-Thu Huong, Bui Sinh Vuong, Nguyen Thi Minh Thuyet, Nguyen Ngoc Khoi, Somruedee Satitkune, Bhuwadol Wanthanachaisaeng, Wolfgang Hofmeister, Tobias Häger and Christoph Hauzenberger*

Gem-quality brown zircon occurs in alluvial deposits derived from Neogene–Quaternary alkali basalts in the Central Highlands of Vietnam. Rough and cut samples were characterized using standard gemmological methods, chemical analysis (electron microprobe and LA-ICP-MS), and Raman, FTIR and UV-Vis-NIR spectroscopy. Among the internal features observed were colour zoning and various mineral inclusions, such as apatite, ilmenite, hematite and iron hydroxide. The analysed samples contained up to 1.14 wt.% $HfO_2$ and 0.08 wt.% total REE oxides. Darker brown stones contained greater amounts of Hf than the lighter-coloured ones. Raman and FTIR spectroscopy showed that the zircon is high-type (i.e. has high crystallinity). As with the famous Ratanakiri zircon of neighbouring Cambodia, heat treatments can be applied to dark-coloured samples to lighten the coloration in an oxidizing atmosphere or induce blue colour in reducing conditions.

*The Journal of Gemmology*, **35**(4), 2016, pp. 308–318, http://dx.doi.org/10.15506/JoG.2016.35.4.308

## Introduction

Zircon ($ZrSiO_4$) crystallizes in the tetragonal system and is a common and widely distributed accessory mineral in most types of igneous and metamorphic rocks. Zircon of gem quality has been reported from various localities, including Australia, Cambodia, Thailand, Myanmar, Sri Lanka, China and Tanzania (Shigley et al., 2010; Yu et al., 2010; Chen et al., 2011; Sutherland et al., 2016). In the Central Highlands of Vietnam, gem-quality brown zircon (e.g. Figure 1) has been exploited—usually together with sapphire—in basalt-related alluvial deposits (Garnier et al., 2005; Huong et al., 2012).

In general, zircon comes in a variety of colours, and most gem material falls into one of two colour series (Gastil et al., 1967): (1) a common pink series that is highly metamict (radiation damaged) and ranges from pink to 'rose', red, purple ('hyacinth') and green to black; and (2) a

*Figure 1: Vietnamese zircon commonly ranges from reddish to orangey brown, as shown by these 3.25–6.70 ct gemstones. Photo by N. T. M. Thuyet.*

less-common yellow series of highly crystalline to moderately radiation-damaged zircon that ranges from pale yellow to 'straw' or 'honey' yellow to brown. In general, the coloration of zircon is affected by its trace-element composition (i.e. transition metals and rare-earth elements [REEs]) and also by radiation damage (i.e. radiation-induced colour centres; Wanthanachaisaeng et al., 2014).

Typically, traces of REEs are incorporated into zircon through the substitution $REE^{3+} + P^{5+} \rightarrow Si^{4+} + Zr^{4+}$ (Hanchar et al., 2001). Other trivalent elements can substitute in $Zr^{4+}$ sites in the form $M^{3+} + H^+ \rightarrow Zr^{4+}$, accompanied by $H^+$ as well as $OH^-$, where $H^+$ may bond with a nearby oxygen atom (Woodhead et al., 1991b). Hafnium as well as radioactive elements such as $U^{4+}$ and $Th^{4+}$ can substitute for $Zr^{4+}$ in dodecahedral coordination; the resulting radiation damage to the structure results in metamict zircon (Finch et al., 2001). In extreme cases, the radiation damage increases the distance between atoms and decreases the degree of lattice ordering, forming amorphous zircon as a final end-product of metamictization. Vibration frequencies corresponding to lattice ordering and bond length in the zircon structure can be characterized by Fourier-transform infrared (FTIR) and Raman spectroscopy. Both FTIR and Raman modes of the $[SiO_4]^{4-}$ group show intense and sharp bands in crystalline zircon, weakened bands in radiation-damaged samples and the absence of these bands in highly metamict zircon (Woodhead et al., 1991a; Nasdala et al., 1995).

This article presents the gemmological and physical properties of brown zircon from the Central Highlands of Vietnam, together with its chemical composition (major and trace elements, including total REE and the radioactive elements Th and U), as well as Raman, FTIR and ultraviolet-visible-near infrared (UV-Vis-NIR) spectroscopic features. Also described are preliminary heat-treatment experiments. The results show that zircon from the Central Highlands has similar properties and heat-treatment behaviours to those of zircon from Ratanakiri, Cambodia (cf. Khoi et al., 2012; Huong et al., 2012, 2014).

## Geology and Occurrence

In Southeast Asia and the adjacent Pacific region, gem-quality zircon has been brought to the earth's surface in basalts that formed as a result of diffused mantle magmatic activity. Particularly important are alkali basalts that commonly contain mantle xenoliths as well as sapphire and zircon xenocrysts, such as those in the Central Highlands of Vietnam (Hoang and Flower, 1998; Sutherland et al., 2016). These zircon occurrences are hosted by the Kon Tum (or Kontum) block, one of five structural terranes of Vietnam (Nam, 1995; see Figure 2). This block forms the earliest continental part of Vietnam, as the first granitization process took place 2.3 billion years ago. The Kon Tum massif has been stable since the Late Proterozoic, with only thin platform cover formation and virtually no Paleozoic rocks (Nam, 1995). In the Neogene–Quaternary Periods, mantle melting took place under a vast region of Southeast Asia, including central and southern Vietnam as well as adjacent Cambodia and Laos. This resulted in a large basalt plateau that formed during the age range of 0.8–17.6 million years (see Rangin et al., 1995; Hoang et al., 1998; Garnier et al., 2005; Sutherland et al., 2016). Two distinct basaltic suites are recognized in the region: tholeiitic (without xenocrysts) and alkaline (containing mantle and lower-crustal xenocrysts, including gems such as sapphire, zircon and olivine; Hoang and Flower, 1998; Garnier et al., 2005; Izokh et al., 2010; Thuyet et al., 2016). Several zircon occurrences related to these basalts have been discovered, among them the famous Ratanakiri deposit in Cambodia (e.g. Payette and Pearson, 2011). Significant zircon deposits also are located in Vietnam, including the Kon Tum, Gia Lai, Đắk Lắk, Đắk Nông, Lâm Đồng and Bình

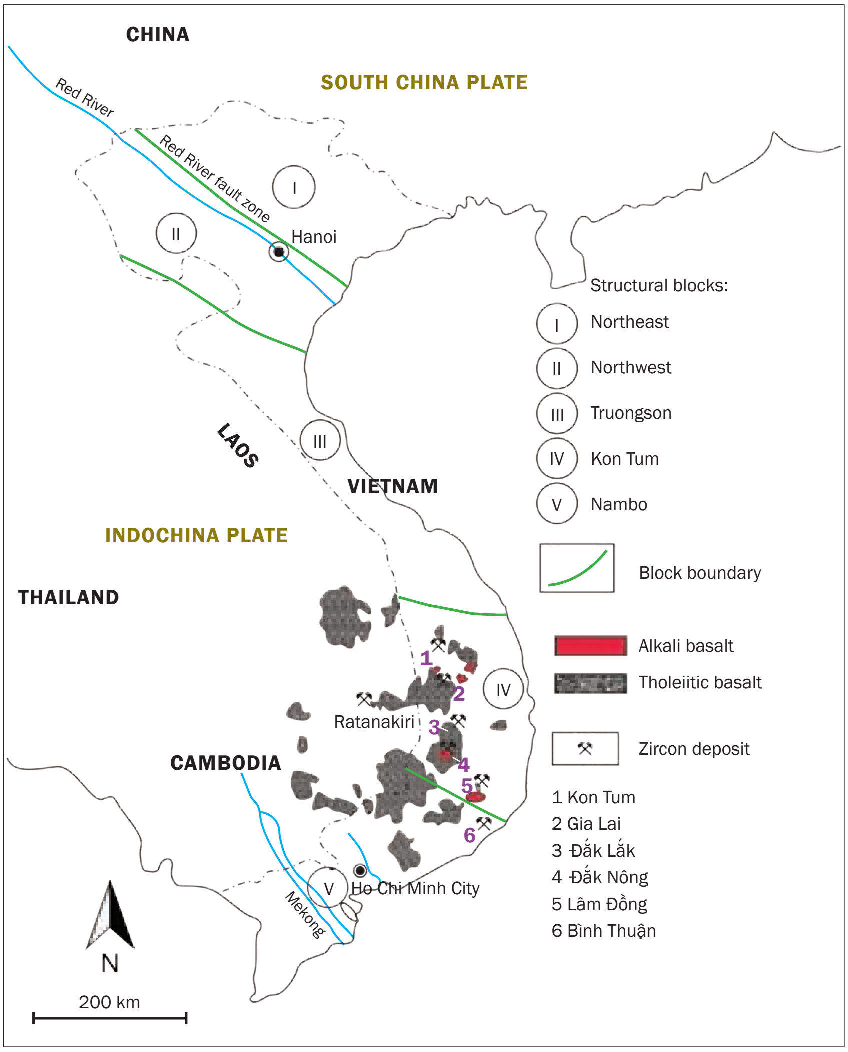

*Figure 2: Alluvial deposits of brown zircon in Southeast Asia are related to basaltic magmatism. Most of the zircon mines in Vietnam are located within the Kon Tum block. The famous zircon deposit of Ratanakiri, Cambodia, is located about 150 km from the closest zircon mine in Vietnam (in Gia Lai Province).*

Thuận Provinces. The formation ages of basalts containing gem zircon are in the range of 0.8–1.6 million years (Ma) at Ratanakiri, which is comparable with the ages of the Gia Lai (0.8–4.3 Ma), Đắk Nông (1.1–7.1 Ma) and Đắk Lắk basalts (1.1–5.8 Ma; Hoang and Flower, 1998; Garnier et al., 2005; Sutherland et al., 2016).

The Vietnamese zircon deposits have been known since the late 1980s, and during the past two decades sporadic mining activities have taken place at numerous small workings. All deposits have been exploited by informal surface digging by local people, who extract the gems by hand after washing the alluvial material. As reported by local miners, monthly production from each site varies from 200 kg to some hundreds of kilograms (Huong et al., 2012). Although widespread in its occurrence in the region, the zircon commonly shows a similar reddish brown coloration (e.g. Figure 3) from the various deposits, including Ratanakiri. Overall, the colour ranges from very light brown (near-colourless) to orangey or yellowish brown to very dark reddish brown (Figure 4). Zircon samples from various locations in the Central Highlands were briefly described by Khoi et al. (2012) and Huong et al. (2014).

## Samples and Methods

For this article, we investigated the gemmological, chemical and spectroscopic features of 20 rough zircon samples (up to 1 cm in dimension; again, see Figure 4) from the Gia Lai and Đắk Nông deposits, and six faceted samples (3.25–6.70 ct; see, e.g., Figure 1) from unspecified localities in the Central Highlands. The rough samples were collected by the authors from the field or bought from miners after they finished washing the soil; they ranged from very light brown (near-colourless) to orangey, reddish and dark reddish brown. The faceted stones, purchased from a

*Figure 3: Vietnamese zircon typically consists of short, stubby or elongated prismatic crystals and fragments ranging from very light brown to orangey, reddish and dark reddish brown. Photo by L. T.-T. Huong.*

trusted local dealer in Đắk Lắk, were dark reddish brown (4), reddish brown (1) and orangey brown (1). All samples were tested with a dichroscope, a hydrostatic Shimadzu balance (for specific gravity), a UV lamp, a desk-model prism-type spectroscope and a Schneider immersion microscope with Zeiss optics. Eight rough samples representing the four different colour categories—very light brown (near-colourless) and orangey, reddish and dark reddish brown (two samples per category)—were selected for quantitative chemical analysis by electron microprobe and laser ablation inductively coupled plasma mass spectrometry (LA-ICP-MS) and also for Raman, FTIR and UV-Vis-NIR spectroscopy.

Electron microprobe analysis was performed with a JEOL JXA-8900RL instrument equipped with wavelength-dispersive spectrometers, using 20 kV acceleration voltage and 20 nA filament current. Only the Si content of the samples was analysed by microprobe, and wollastonite was used as a standard. The trace elements were measured with an LA-ICP-MS system (ESI NWR193 laser ablation unit and Agilent 7500 ICP-MS) at the Central Lab for Water, Minerals and Rocks, NAWI Graz Geocentre, Graz, Austria. The samples were ablated using a 193 nm laser pulsed at 9 Hz, with a 75 µm spot size and an energy of ~8 J/cm$^2$. Helium was used as the carrier gas (flow of ~0.7 l/min), and data were acquired in time-resolved mode. For each analysis, a gas blank was obtained for background correction. The laser was active for 60 seconds followed by 30 seconds of washout time. The glasses

*Figure 4: These rough samples of Vietnamese zircon were studied for this report. They are divided into four different colour groups: very light brown, orangey brown, reddish brown and dark reddish brown. Photo by N. T. M. Thuyet.*

NIST610 or NIST612 were routinely analysed for standardization and drift correction, while zircon standard 91500 and basalt standard BCR-2 were analysed as unknowns to monitor the accuracy of the measurements. Both standards could be reproduced to within ±10% of the certified values. Silicon was used as an internal standard.

Raman spectra were collected with a Horiba Jobin Yvon LabRAM HR800 spectrometer coupled with an Olympus BX41 optical microscope and a Si-based charge-coupled device (CCD) detector; samples were excited by a 633 nm red He-Ne laser. Raman micro-spectroscopy of inclusions was performed in confocal mode, facilitating analysis at the micron scale (2–5 μm). Infrared spectra were collected in the 4000–400 cm$^{-1}$ range with 64 scans and 4 cm$^{-1}$ resolution, using a Thermo Scientific Nicolet 6700 FTIR spectrometer equipped with an optimized beam condenser. The analyses were done on powder ground from inclusion-free areas of the zircon samples. The measurements were carried out in transmittance mode, and the spectra were converted from transmittance to absorbance (so that bands in the 3800–3400 cm$^{-1}$ range were more obvious). UV-Vis-NIR absorption spectra were recorded in the 200–1600 nm range with 20 scans using a Zeiss Axio Imager.A2m microscope that was connected to two spectrometers from J&M Analytik AG: a TIDAS S with a diode-array CCD detector (200–980 nm range with 0.75 nm resolution) and a TIDAS S 900 with an InGaAs detector (900–1600 nm range with 2.8 nm resolution).

Heat-treatment experiments were done with a Nabertherm L9/SH furnace, under both oxidizing (one faceted and 20 rough samples) and reducing (24 pieces of rough) conditions. After annealing at the target temperature (200–1,000°C for two hours), the furnace was slowly cooled to room temperature before the samples were removed. After heat treatment, the samples were analysed with Raman spectroscopy to check their structural state.

## Results and Discussion

### Visual Appearance and Physical Properties

The rough zircon samples consisted of short, stubby or elongated prismatic crystals (again, see Figures 3 and 4). Irregularly shaped fragments were common, but some well-formed tetragonal prisms also were present. Diaphaneity varied from translucent to transparent. The samples ranged from almost colourless to orangey brown to dark reddish brown. Viewed with the dichroscope, they showed weak-to-distinct pleochroism in purplish brown and brownish yellow. Hydrostatic SG ranged from 4.10 to 4.60; transparent samples usually had higher SG values than translucent ones. All samples were inert to long- and short-wave UV radiation. Absorption spectra could be observed only for the transparent, near-colourless to light-coloured samples, which showed typical REE-related features.

### Internal Features

Microscopic observation revealed straight and angular growth zoning consisting of different shades of yellow, orange or brown (e.g. Figure 5a). Tension cracks and partially healed fissures also were quite common. In some samples, dark, elongated, euhedral inclusions identified by Raman micro-spectroscopy as apatite were observed (Figure 5b). We also identified hematite, red iron hydroxide (Figure 5c) and ilmenite (Figure 5d). Rare inclusions of baddeleyite, tourmaline and jadeite were reported in another study (Izokh et al., 2010).

### Chemical Composition

The average chemical composition of the different-coloured zircon groups is presented in Table I. The results show generally low contents of non-formula elements. The most abundant chemical substitution was Hf, with an oxide concentration of 0.60–1.14 wt.%. The concentration of Hf was significantly higher in the darker samples than in the lighter ones. The total REE-oxide concentrations were 0.03–0.08 wt.%. (For more specific data on REEs in Vietnamese zircon, see Khoi et al., 2012, which included REE plots of samples from Ma Lâm, Đá Bàn [Bình Thuận] and Đắk Ton [Đắk Nông].) The concentrations of Th and U were low (average 10–85 ppm and 24–105 ppm, respectively), and varied among sample groups and even within a group. The Th:U ratio was >0.2 for all samples, which is typical for zircon of magmatic origin (Williams and Claesson, 1987; Rubatto and Gebauer, 2000). Other significant trace elements included Y, P, Al and Ca; the average Y concentration ranged up to 469 ppm in reddish brown samples.

The chemical properties of our Vietnamese zircon samples were similar to those from Ra-

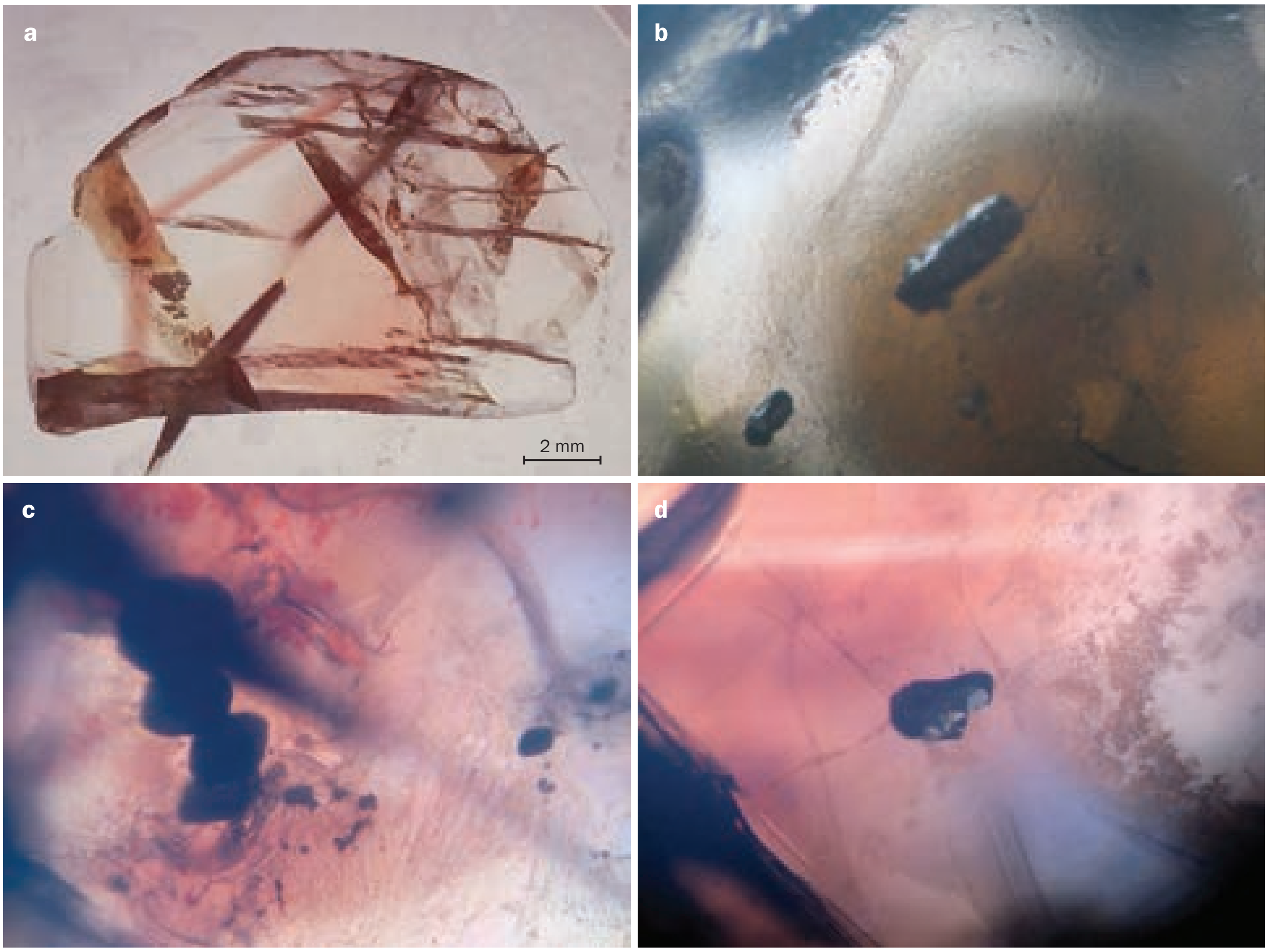

*Figure 5: Typical internal features observed in Vietnamese zircon include (a) colour zoning (seen here in a fragment that has been mounted in epoxy and polished), (b) apatite crystals (magnified 20×), (c) masses of opaque hematite and red iron hydroxide (magnified 20×) and (d) ilmenite crystals (magnified 10×). Photomicrographs by N. T. M. Thuyet and L. T.-T. Huong.*

tanakiri, which also contain low trace-element contents (i.e. an average of 0.7 wt.% $HfO_2$, and 40–240 ppm U and 10–270 ppm Th; see Wittwer et al., 2013).

### *Raman Spectroscopy*

Raman spectra of all sample categories showed similar patterns and band values. The dominant peaks were at 1008, 975, 437, 392, 355, 225, 214 and 202 $cm^{-1}$ (Figure 6). According to Dawson et al. (1971), the bands in the 230–200 $cm^{-1}$ range are generated by intense external lattice (inter-tetrahedral) vibrations, while the strongest bands in the 450–350 $cm^{-1}$ range and around 1000 $cm^{-1}$ are due to internal (intra-tetrahedral) vibrations of $SiO_4$ tetrahedra. Metamictization increases the distance between the atoms in the zircon structure, resulting in decreased vibration frequency of inter-tetrahedra and intra-tetrahedra (Nasdala et al., 1995). The width of the Raman bands broadens, and the peaks shift toward lower wavenumbers. Nasdala et al. (1995) reported that in medium-to-high-degree metamict zircon, the three vibrational bands of inter-tetrahedra in the range 230–200 $cm^{-1}$ broaden and shift to form a single broad, weak band at 200 $cm^{-1}$. In completely metamict samples, the zircon structure is mostly destroyed and these bands can be absent. Special attention should be paid to the most intense intra-tetrahedral vibrational band at 1008 $cm^{-1}$, which Nasdala et al. (1995) showed is best suited to quantify the degree of metamictization. Crystalline (high-type) zircon shows a full width at half maximum (FWHM) value of $\leq 5$ $cm^{-1}$ for this peak, while amorphous (low-type) samples have the values $>30$ $cm^{-1}$. The Raman data of Vietnamese zircon have FWHM values in the 2–3 $cm^{-1}$ range, which show a good match to those of Ratanakiri zircon (cf. Wittwer et al., 2013).

*Table I: Average chemical composition of Vietnamese zircon.**

| **Chemical composition** | **Very light brown** | | **Orangey brown** | | **Reddish brown** | | **Dark reddish brown** | |
|---|---|---|---|---|---|---|---|---|
| | **Average** | **SD** | **Average** | **SD** | **Average** | **SD** | **Average** | **SD** |
| Oxides (wt.%) | | | | | | | | |
| $SiO_2$ | 31.91 | 0.11 | 32.08 | 0.09 | 32.32 | 0.16 | 32.36 | 0.20 |
| $ZrO_2$ | 65.91 | 0.43 | 65.68 | 0.18 | 65.87 | 0.37 | 65.75 | 0.27 |
| $HfO_2$ | 0.60 | 0.02 | 0.61 | 0.01 | 1.02 | 0.09 | 1.14 | 0.01 |
| $REE_2O_3$ | 0.03 | 0.02 | 0.08 | 0.01 | 0.05 | 0.03 | 0.07 | 0.02 |
| Total | 98.45 | -- | 98.45 | -- | 99.26 | -- | 99.32 | -- |
| Trace elements (ppm) | | | | | | | | |
| Li | <0.05 | -- | 0.10 | 0.04 | 0.45 | 0.31 | 0.10 | 0.03 |
| Be | <0.05 | -- | 0.68 | 0.02 | 0.15 | 0.08 | 0.23 | 0.04 |
| Al | 41.9 | 4.35 | 11.8 | 1.26 | 22.1 | 10.2 | 32.2 | 2.99 |
| P | 77.8 | 2.32 | 72.1 | 16.4 | 44.4 | 13.0 | 71.1 | 8.85 |
| Ca | 7.79 | 3.88 | 8.24 | 2.52 | 39.4 | 10.5 | 14.0 | 3.67 |
| Ti | 1.27 | 0.07 | 4.28 | 0.31 | 5.31 | 1.49 | 6.96 | 0.51 |
| Cr | 0.42 | 0.03 | 0.45 | 0.08 | 0.50 | 0.05 | 0.42 | 0.09 |
| Mn | 0.06 | 0.01 | 0.77 | 0.10 | 1.31 | 0.50 | <0.06 | -- |
| Ni | 0.57 | 0.09 | 0.19 | 0.04 | 1.44 | 1.08 | <0.05 | -- |
| Cu | <0.01 | -- | <0.01 | -- | 0.54 | 0.40 | <0.01 | -- |
| As | 0.16 | 0.01 | 0.18 | 0.02 | 0.20 | 0.07 | 0.20 | 0.05 |
| Rb | 0.03 | 0.01 | 0.08 | 0.03 | 0.11 | 0.04 | 0.09 | 0.03 |
| Sr | 0.06 | 0.01 | 0.11 | 0.04 | 0.55 | 0.34 | 0.13 | 0.02 |
| Y | 107 | 23.9 | 444 | 126 | 469 | 120 | 333 | 88.5 |
| Nb | 0.69 | 0.19 | 3.14 | 1.10 | 5.45 | 2.12 | 3.29 | 1.00 |
| Mo | 0.56 | 0.17 | 0.48 | 0.04 | 0.49 | 0.03 | 0.46 | 0.04 |
| Sn | 0.07 | 0.01 | 0.12 | 0.04 | 0.11 | 0.02 | 0.09 | 0.02 |
| Ta | 0.57 | 0.15 | 1.55 | 0.49 | 4.48 | 2.17 | 5.99 | 1.35 |
| W | 0.05 | 0.02 | 0.16 | 0.07 | 0.17 | 0.04 | 0.13 | 0.05 |
| Th | 10.6 | 3.34 | 36.6 | 18.3 | 79.5 | 37.6 | 84.5 | 70.2 |
| U | 24.0 | 2.53 | 78.7 | 28.5 | 105 | 80.2 | 101 | 76.3 |

* Concentrations of V, Co, Zn and $^{208}$Pb were below the detection limits (0.05, 0.01, 0.01 and 0.10 ppm, respectively) in all samples. $SiO_2$ was analysed by electron microprobe (five spots per sample) and other elements by LA-ICP-MS (three spots per sample); $ZrO_2$, $HfO_2$ and $REE_2O_3$ values were calculated from LA-ICP-MS data. Abbreviation: SD = standard deviation.

### *FTIR Spectroscopy*

FTIR spectra displayed three sharp, intense bands in the 1100–400 cm$^{-1}$ range at 854, 609 and 430 cm$^{-1}$ (Figure 7). The intense band around 854 cm$^{-1}$ (and shoulder at 970 cm$^{-1}$) is due to internal stretching vibrations of $SiO_4$ tetrahedra; this band weakens and broadens in metamict zircon. The band at 609 cm$^{-1}$ (due to internal bending vibrations of $SiO_4$ tetrahedra) and the band at 430 cm$^{-1}$ (due to the external or lattice vibration mode) may also weaken and broaden with metamictization, and they are nearly absent from highly metamict samples (Woodhead et al., 1991a).

FTIR spectroscopy of the Vietnamese zircon confirms the results of the Raman spectra showing that the samples are well crystallized. In addition to the $SiO_4$-related bands, other weak bands were observed between 3800 and 3400 cm$^{-1}$ that correspond to hydrous components ($OH^-$ and/or $H_2O$). The broadening of the bands in this range can be explained by the band overlap of $OH^-$ in different sites of the zircon structure, as well as the $(SiO_4)^{4-}$ internal vibrations. The presence of $OH^-$ in crystalline zircon has been explained by the substitutions $M^{3+} + H^+ \rightarrow Zr^{4+}$ and/or $4(OH)^- \rightarrow (SiO_4)^{4-}$ (Woodhead et al., 1991b).

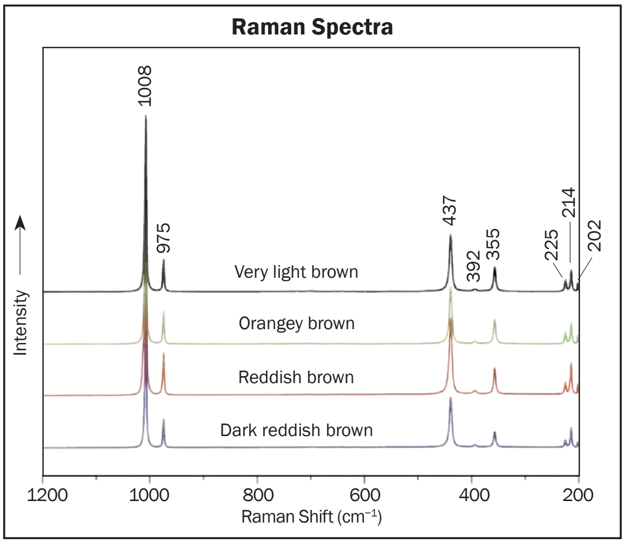

*Figure 6: Raman spectra of representative samples from the four colour groups of Vietnamese zircon all show bands in the 230–200 cm$^{-1}$ range generated by intense external lattice (inter-tetrahedral) vibrations, as well as bands in the 450–350 cm$^{-1}$ range and at around 1000 cm$^{-1}$ due to internal (intra-tetrahedral) vibrations of $SiO_4$ tetrahedra. Spectra are offset vertically for clarity.*

### UV-Vis-NIR Spectroscopy

UV-Vis-NIR absorption spectra for the zircon samples of the four colour categories are shown in Figure 8. The spectra of the two reddish brown categories show a similar continuous increase in absorption toward the UV region, in particular between 400 and 600 nm with a shoulder at around 500 nm, giving an absorption window toward the red end of the spectrum. As a result, those samples show red-orange-yellow colour components. The spectra of the very light brown and orangey brown categories have a shoulder of very low intensity. Similar absorption patterns have been reported for reddish brown and brownish red zircon from other localities, including Ratanakiri and Muling (China). Those samples are believed to owe their colour to radiation damage (Chen et al., 2011).

### Heat Treatment

Under oxidizing conditions, most brown Vietnamese zircon becomes lighter coloured with heat treatment. Figure 9 shows a dark reddish brown sample before and after being heated to 200–600°C under oxidizing conditions. From 200°C to 500°C, the stone became lighter with a more obvious orangey red component. However, the treated colour was unstable and reverted to its original appearance after less than one hour of exposure to light (i.e. in a combination of reflected sunlight and fluorescent lighting). Only when heated to 600°C did the resulting colour stabilize, after much of the orange and red components disappeared, resulting in a pale brown coloration after heat treatment.

Under reducing conditions, the brown Vietnamese zircon began turning light blue at 800°C. The blue colour intensified upon heating the zircon to 1,000°C (Figure 10). The treated blue colour was stable, and its intensity depended on the shade of the original brown colour: the browner the sample, the deeper blue after treatment.

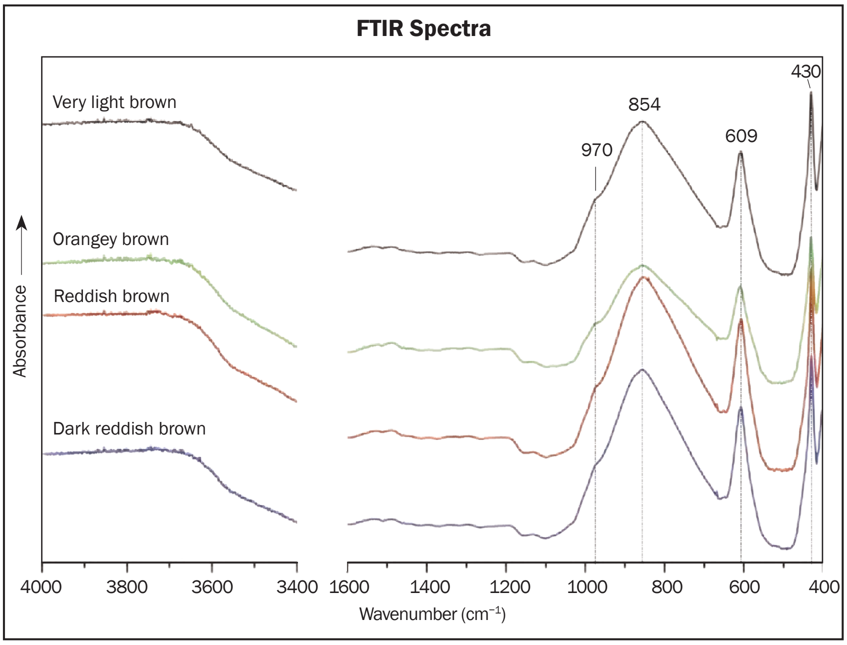

*Figure 7: FTIR spectra for the four colour groups of Vietnamese zircon all display intense bands at around 854 and 609 cm$^{-1}$ due to internal vibrations of $SiO_4$ tetrahedra. The band at 430 cm$^{-1}$ belongs to external (lattice) vibrations. Other weak bands between 3800 and 3400 cm$^{-1}$ are due to hydrous components. Spectra are offset vertically for clarity.*

The colour of blue zircon that is grown synthetically is apparently due to U$^{4+}$ (cf. Richman et al., 1967), whereas the blue colour in heat-treated natural zircon may be due to a composite of features including the transition of U$^{5+}$ to U$^{4+}$ (Satitkune et al., 2013) and others of unknown origin (Wittwer et al., 2013). Interestingly, not every brown zircon—even from the same mine—turns blue after heat treatment at the same conditions.

Raman spectroscopy of the heat-treated zircon in this study showed no change in structural state; the FWHM value of the 1008 cm$^{-1}$ peak remained the same.

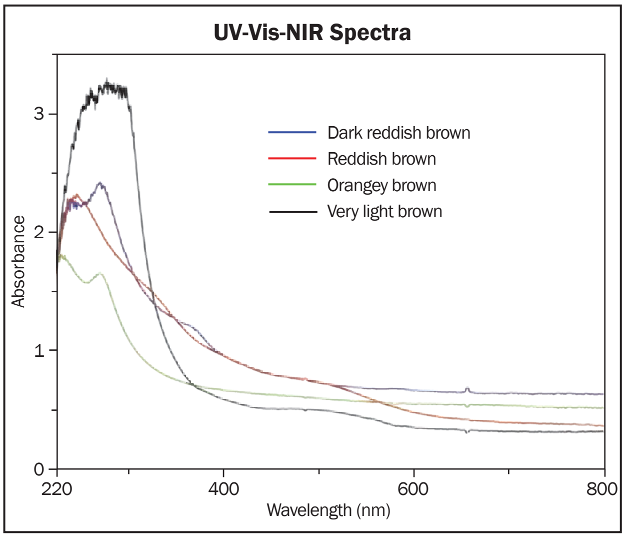

*Figure 8: The UV-Vis-NIR absorption spectra of dark brown and reddish brown samples of Vietnamese zircon show a similar continuous increase in absorption toward the UV region (see text for discussion).*

## Conclusions

Alluvial deposits in the Central Highlands of Vietnam host gem-quality zircon ranging from very light brown to orangey or reddish brown to dark reddish brown. Common internal features include straight and angular growth zoning as well as inclusions of apatite and iron-oxide and iron-titanium-oxide minerals. The main chemical difference between the dark and light brown zircon is the Hf concentration, which is higher in the darker stones. All the samples contained low amounts of Th and U, and the Th:U ratios are consistent with a magmatic origin (and subsequent transport to the earth's surface in alkali basalts). Raman and FTIR spectroscopy indicate that the zircons are high type (highly crystalline). Heat treatment under oxidizing conditions produced a lighter but unstable brownish orange colour in the range of 200–500°C and a stable pale brown colour after heating to 600°C, whereas treatment under reducing conditions yielded a stable blue colour after heating to 800–1,000°C.

*Figure 9: Heat treatment of a 6.70 ct dark reddish brown zircon (a) in an oxidizing atmosphere produced an unstable lighter brownish orange coloration after exposure to 200 °C (b), 400 °C (c) and 500 °C (d), and a stable pale brown colour after heating to 600 °C (e). Photos by L. T.-T. Huong.*

*Figure 10: Reddish brown Vietnamese zircon is shown before (top) and after (bottom) heat treatment under reducing conditions at 1,000 °C, resulting in a stable blue colour. Photo by L. T.-T. Huong.*

## References

Chen T., Ai H., Yang M., Zheng S. and Liu Y., 2011. Brownish red zircon from Muling, China. *Gems & Gemology*, **47**(1), 36–41, http://dx.doi.org/10.5741/gems.47.1.36.

Dawson P., Hargreave M.M. and Wilkinson G.R., 1971. The vibrational spectrum of zircon ($ZrSiO_4$). *Journal of Physics C: Solid State Physics*, **4**(2), 240–256, http://dx.doi.org/10.1088/0022-3719/4/2/014.

Finch R.J., Hanchar J.M., Hoskin P.W.O. and Burns P.C., 2001. Rare-earth elements in synthetic zircon: Part 2. A single-crystal X-ray study of xenotime substitution. *American Mineralogist*, **86**(5–6), 681–689, http://dx.doi.org/10.2138/am-2001-5-608.

Garnier V., Ohnenstetter D., Giuliani G., Fallick A.E., Phan Trong T., Hoáng Quang V., Pham Van L. and Schwarz D., 2005. Basalt petrology, zircon ages and sapphire genesis from Dak Nong, southern Vietnam. *Mineralogical Magazine*, **69**(1), 21–38, http://dx.doi.org/10.1180/0026461056910233.

Gastil R.G., DeLisle M. and Morgan J.R., 1967. Some effects of progressive metamorphism on zircons. *Geological Society of America Bulletin*, **78**(7), 879–906, http://dx.doi.org/10.1130/0016-7606(1967)78[879:SEOPMO]2.0.CO;2.

Hanchar J.M., Finch R.J., Hoskin P.W.O., Watson E.B., Cherniak D.J. and Mariano A.N., 2001. Rare earth elements in synthetic zircon: Part 1. Synthesis, and rare earth element and phosphorus doping. *American Mineralogist*, **86**(5–6), 667–680, http://dx.doi.org/10.2138/am-2001-5-607.

Hoang N. and Flower M., 1998. Petrogenesis of Cenozoic basalts from Vietnam: Implication for origins of a 'diffuse igneous province'. *Journal of Petrology*, **39**(3), 369–395, http://dx.doi.org/10.1093/petroj/39.3.369.

Huong L.T.-T., Häger T., Hofmeister W., Hauzenberger C., Schwarz D., Van Long P., Wehrmeister U., Khoi N.N. and Nhung N.T., 2012. Gemstones from Vietnam: An update. *Gems & Gemology*, **48**(3), 158–176, http://dx.doi.org/10.5741/gems.48.3.158.

Huong L.T.-T., Vuong B.S., Satitkune S. and Wathanachaiseng B., 2014. Chemical and spectroscopic study of zircon from Dak Lak, Central Highlands of Vietnam. *The 4th International Gem and Jewelry Conference—GIT 2014*, Chiang Mai, Thailand, 8–9 December, 172–176.

Izokh A.E., Smirnov S.Z., Egorova V.V., Anh T.T., Kovyazin S.V., Phuong N.T. and Kalinina V.V., 2010. The conditions of formation of sapphire and zircon in the areas of alkali-basaltoid volcanism in central Vietnam. *Russian Geology and Geophysics*, **51**(7), 719–733, http://dx.doi.org/10.1016/j.rgg.2010.06.001.

Khoi N.N., Hauzenberger C., Tuan D.A. and Thuyet N.T.M., 2012. Zircon from Vietnam, some gemological aspects. *The 3rd International Gem and Jewelry Conference—GIT 2012*, Bangkok, Thailand, 12–13 December, 135–138.

Nam T.N., 1995. The Geology of Vietnam: A brief summary and problems. *Geoscience Reports of Shikuoka University*, **22**, 1–9, http://doi.org/10.14945/00000334.

Nasdala L., Irmer G. and Wolf D., 1995. The degree of metamictization in zircon: A Raman spectroscopic study. *European Journal of Mineralogy*, **7**(3), 471–478, http://dx.doi.org/10.1127/ejm/7/3/0471.

Payette F. and Pearson G., 2011. The 'hill of the precious stones', Rattanak Kiri, Cambodia. *Australian Gemmologist*, **24**(6), 148–153.

Rangin C., Huchon P., Le Pichon X., Bellon H., Lepvrier C., Roques D., Hoe N.D. and Van Quynh P., 1995. Cenozoic deformation of central and south Vietnam. *Tectonophysics*, **251**(1–4), 179–196, http://dx.doi.org/10.1016/0040-1951(95)00006-2.

Richman I., Kisliuk P. and Wong E.Y., 1967. Absorption spectrum of $U^{4+}$ in zircon ($ZrSiO_4$). *Physical Review*, **155**(2), 262–267, http://dx.doi.org/10.1103/physrev.155.262.

Rubatto D. and Gebauer D., 2000. Use of cathodoluminescence for U-Pb zircon dating by ion microprobe: Some examples from the Western Alps. In M. Pagel, V. Barbin, P. Blanc and D. Ohnenstetter, Eds., *Cathodoluminescence in Geosciences*, Springer, Berlin, Germany, 373–400, https://doi.org/10.1007/978-3-662-04086-7_15.

Satitkune S., Wanthanachaisaeng B., Won-in K., Wongkokau W., Chantararat P., Leelawattanasuk T. and Wathanakul P., 2013. Heat treatment of zircon samples from Kanchanaburi, Thailand and Ratanakiri, Cambodia. *33rd International Gemmological Conference*, Hanoi, Vietnam, 12–16 October, 158–160.

Shigley J.E., Laurs B.M., Janse A.J.A., Elen S. and Dirlam D.M., 2010. Gem localities of the 2000s. *Gems & Gemology*, **46**(3), 188–216, http://dx.doi.org/10.5741/gems.46.3.188.

Sutherland L., Graham I., Yaxley G., Armstrong R., Giuliani G., Hoskin P., Nechaev V. and Woodhead J., 2016. Major zircon megacryst suites of the Indo-Pacific lithospheric margin (ZIP) and their petrogenetic and regional implications. *Mineralogy and Petrology*, **110**(2), 399–420, http://dx.doi.org/10.1007/s00710-015-0421-3.

Thuyet N.T.M., Hauzenberger C., Khoi N.N., Diep C.T., Lam C.V., Minh N.T., Hoang N. and Häger T., 2016. Peridot from the Central Highlands of Vietnam: Properties, origin, and formation. *Gems & Gemology*, **52**(3), 276–287, http://dx.doi.org/10.5741/GEMS.52.3.276.

Wanthanachaisaeng B., Bunnag N., Satitkune S., Ounorn P., Sutthirat C. and Pisutha-Arnond V., 2014. Influence of irradiation and heating on Ratanakiri zircon structure. *The 4th International Gem and Jewellery Conference—GIT 2014*, Chiang Mai, Thailand, 8–9 December, 101–103.

Williams I.S. and Claesson S., 1987. Isotopic evidence for the Precambrian provenance and Caledonian metamorphism of high grade paragneisses from the Seve nappes, Scandinavian Caledonides. II. Ion microprobe zircon U-Th-Pb. *Contributions to Mineralogy and Petrology*, **97**(2), 205–217, http://dx.doi.org/10.1007/bf00371240.

Wittwer A., Nasdala L., Wanthanachaisaeng B., Bunnag N., Škoda R., Balmer W.A., Giester G. and Zeug M., 2013. Mineralogical characterisation of gem zircon from Ratanakiri, Cambodia. *Conference on Raman and Luminescence Spectroscopy in the Earth Sciences—CORALS–2013*, Vienna, Austria, 3–6 July, 115–116.

Woodhead J.A., Rossman G.R. and Silver L.T., 1991a. The metamictization of zircon: Radiation dose-dependent structural characteristics. *American Mineralogist*, **76**(1–2), 74–82.

Woodhead J.A., Rossman G.R. and Thomas A.P., 1991b. Hydrous species in zircon. *American Mineralogist*, **76**(9–10), 1533–1546.

Yu Y., Xu X. and Chen X., 2010. Genesis of zircon megacrysts in Cenozoic alkali basalts and the heterogeneity of subcontinental lithospheric mantle, eastern China. *Mineralogy and Petrology*, **100**(1), 75–94, http://dx.doi.org/10.1007/s00710-010-0120-z.

## The Authors

**Dr Le Thi-Thu Huong, Bui Sinh Vuong, Dr Nguyen Thi Minh Thuyet and Dr Nguyen Ngoc Khoi**
Faculty of Geology, Hanoi University of Science
Vietnam National University, 334 Nguyen Trai,
Hanoi, Vietnam. Email: letth80@gmail.com

**Dr Somruedee Satitkune FGA**
Faculty of Science, Kasetsart University
50 Ngamwongwan Road, Bangkok 10900,
Thailand

**Dr Bhuwadol Wanthanachaisaeng**
Faculty of Science, Srinakharinwirot University
114 Sukhumvit 23, Bangkok 10110, Thailand

**Prof. Dr Wolfgang Hofmeister DSc hc (VAST) and Dr Tobias Häger**
Institute for Geosciences, Johannes Gutenberg-University, Saarstraße 21, Mainz 55122,
Germany

**Prof. Dr Christoph Hauzenberger**
NAWI Graz Geocentre, University of Graz
Graz A8010, Austria

## Acknowledgements

This research was supported by the Asia Research Center, Vietnam National University, Hanoi. Research facilities were provided by the Institute of Earth Sciences (Mineralogy and Petrology) at the University of Graz (Austria), the Institute of Geosciences (Gemstone Research Centre) at Johannes Gutenberg-University of Mainz (Germany) and the Hanoi University of Science (Vietnam National University, Hanoi). We also thank the ASEAN-European Academic University Network, the Austrian Federal Ministry of Science, Research and Economy, and the Austrian Agency for International Cooperation in Education and Research for financial support.

# Identification of Reconstructed Amber from Different Periods

*Haibo Li, Jie Liang, Taijin Lu, Jun Zhang and Jun Zhou*

Recently, reconstructed amber has been more commonly encountered in the Chinese jewellery market. Some of the newer (post-2009) material presents a serious identification challenge for gemmological laboratories. This article divides reconstructed ambers into two categories—early and current—corresponding to their properties and the approximate time period that they were manufactured. By comparing the structure of reconstructed amber from either category with that of natural amber, it is generally possible to differentiate it using microscopic features. In addition, the distinctive structure of reconstructed amber can sometimes be seen using cross-polarized light and UV fluorescence imaging with a standard UV lamp or with the Diamond-View instrument.

*The Journal of Gemmology*, **35**(4), 2016, pp. 320–328, http://dx.doi.org/10.15506/JoG.2016.35.4.320

## Introduction

Reconstructed amber (also known as 'pressed amber'; Zhang, 2006, 2010a) consists of small amber fragments or scraps that have been reformed into larger amber pieces under heat and pressure (e.g. Figure 1). In this article, we classify reconstructed amber into two categories: early (pre-2009) and current (i.e. from ~2009–2010 to the present time). Most previous studies on identifying reconstructed amber were limited to early-stage material. Those samples are relatively easy to identify—even distinguishable with the unaided eye in some cases —as they have obvious structural characteristics. Current reconstructed amber is more difficult to identify, and the authors are not aware of any previous systematic research being done on it.

Based on the documentation of reconstructed amber in the literature (Koivula et al., 1993; Hänni, 2005; Qi et al., 2005; Ma, 2007; Zhu and Xing, 2008; Campbell Pedersen and Williams, 2011; Zhou and Yang, 2011; Wang et al., 2012), along with the present authors' examination using multiple instruments and lighting techniques to analyse reconstructed amber from various periods of time, this article summarizes the identification criteria for early and current reconstructed ambers. Our initial observations were published (in Chinese) in Li et al. (2012).

## Materials and Methods

The study is based on ~100,000 documented samples that were encountered in the National Gemstone Testing Center's Beijing laboratory during approximately the past decade. We summarized all those records and classified a selection of typical cases for this article. The samples included various loose beads, strung beads, cabochons, rough material, carved pieces and more.

Standard gemmological testing was carried out on all the samples, including examination with a microscope, polariscope and UV lamp. Observations were made with brightfield and darkfield

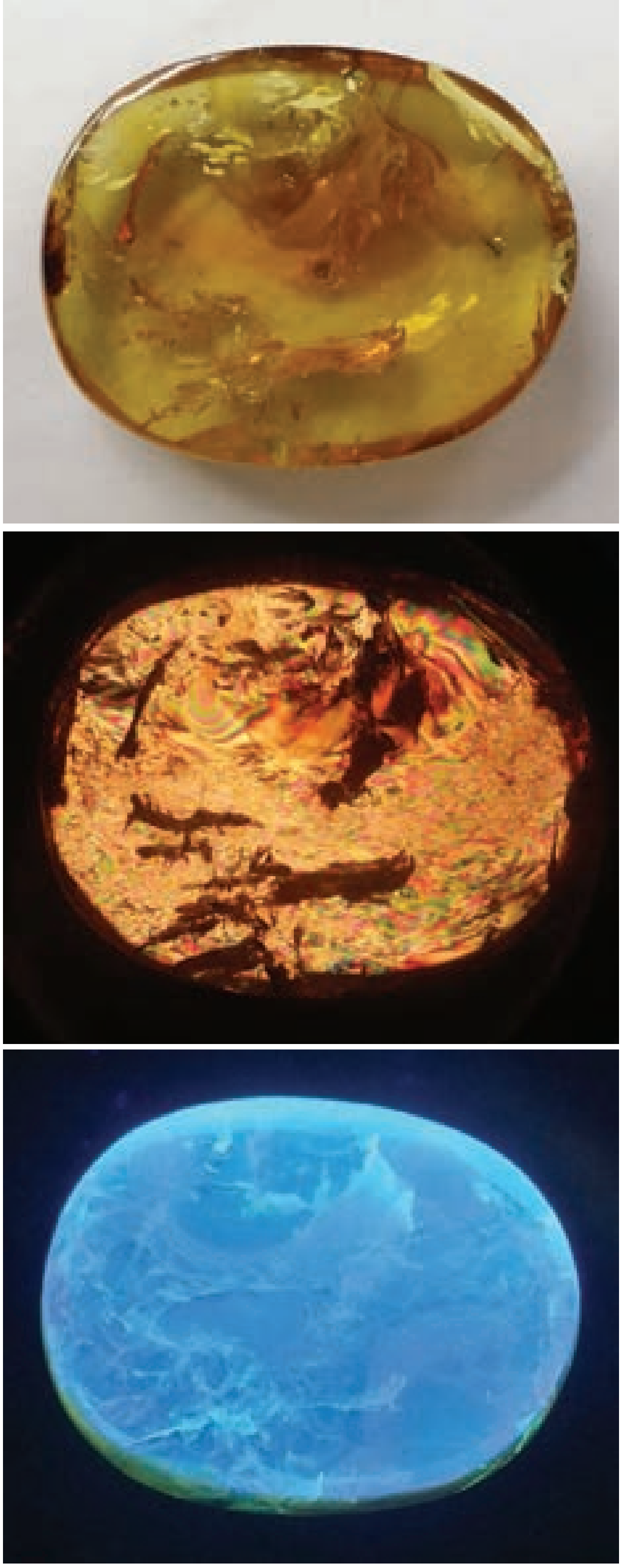

*Figure 1: This cabochon of current-stage reconstructed amber (6 × 4 mm) does not show an obvious fragmental or 'blood streak' structure to the unaided eye (top), but examination with a polariscope (in cross-polarized light) reveals a mylonitic pattern of extinction accompanied by interference colours (centre), and long-wave UV fluorescence shows a mosaic texture (bottom) indicative of its reconstructed origin. Photos by H. Li.*

illumination, as well as with additional lighting such as a fibre-optic illuminator. In addition, a DiamondView instrument was used to observe details of the samples' ultra-short-wave UV fluorescence. Fourier-transform infrared (FTIR) spectra of all samples were recorded with a Nicolet 6700 spectrometer in the 4000–400 $cm^{-1}$ region, at a resolution of 4.0 $cm^{-1}$ and 8–64 scans. Several points were analysed on some samples to confirm the identity of the constituent material(s). All FTIR analyses were performed non-destructively by specular reflection, and a Kramers-Kronig transformation was performed to remove distortions in the spectra (e.g. Zhang, 2006, pp. 120–121).

## Constituents of Reconstructed Amber

As Baltic material is the main amber variety sold in the market, reconstructed amber is commonly manufactured from pieces of this material. The samples submitted to the authors' laboratory were therefore suspected as being made from Baltic amber, and this origin was confirmed by the presence of a 'Baltic shoulder' (e.g. Beck et al., 1964) in most of their FTIR spectra.

According to the process used, there are two main types of reconstructed amber typically seen in the market. Type 1 is made without the addition of any substances to the amber fragments, while type 2 contains foreign substances (e.g. natural or artificial resins) that are added to make the material more solid and durable. If the artificial material is too abundant, then the resulting sample may no longer be called 'amber', but rather an amber imitation. For cases where FTIR spectroscopy can easily detect different areas of a reconstructed sample consisting of amber and a foreign substance, then more tests are needed to assess the proportion of the constituents and determine the proper nomenclature (i.e. reconstructed amber or imitation amber).

On the other hand, when there is little or no foreign substance present, the FTIR spectra of reconstructed amber may look quite similar to that of natural amber, and additional examinations using a microscope, polariscope and UV lamp should be performed to make the proper identification.

In the authors' experience, both types 1 and 2 can be found from various time periods (i.e. early and current). However, most samples encountered in our laboratory have been type 1.

*Figure 2: Left: These 13-mm-diameter beads, sold as 'African amber', proved to be early reconstructed amber that also contains foreign substances. Right: The beads show uneven fluorescence to long-wave UV radiation, with an obvious fragmental structure. The cementing agents surrounding the amber fragments exhibit two different fluorescence reactions: blue and inert (the latter appearing dark/black in contrast with the adjacent amber luminescence). Photos by H. Li.*

## Identification of Early Reconstructed Amber

### *Microscopic Features*

Processing of early reconstructed amber involved the use of relatively high temperature and pressure conditions in air (i.e. the amber fragments being fully in contact with oxygen). The resulting material often displays a relatively dark body colour, poor transparency with a muddy-looking interior, and a diagnostic fragmental or mosaic structure (e.g. Figure 2). It can be identified by visual observation; the boundaries between fragments have darker (oxidized) edges that appear translucent brown or red (Figure 3). The boundaries show various three-dimensional patterns corresponding to the different shapes and sizes of the amber fragments used in the reconstruction process. This fragmental or mosaic structure in reconstructed amber is also known as 'blood streak' in Chinese because it may resemble blood vessels in colour and distribution. In addition, some early-stage reconstructed amber may display uneven surface lustre due to different hardness characteristics of the partially melted amber fragments (Figure 4).

In early reconstructed amber, the 'blood streak' structure is usually obvious, making it easy to distinguish from natural amber, although an inexperienced gemmologist could confuse it with heat-enhanced amber (Zhang, 2010a,b) contain-

*Figure 3: These samples of early reconstructed amber contain some unmelted amber fragments that show dark oxidized boundaries. Photomicrograph by H. Li; magnified 10×.*

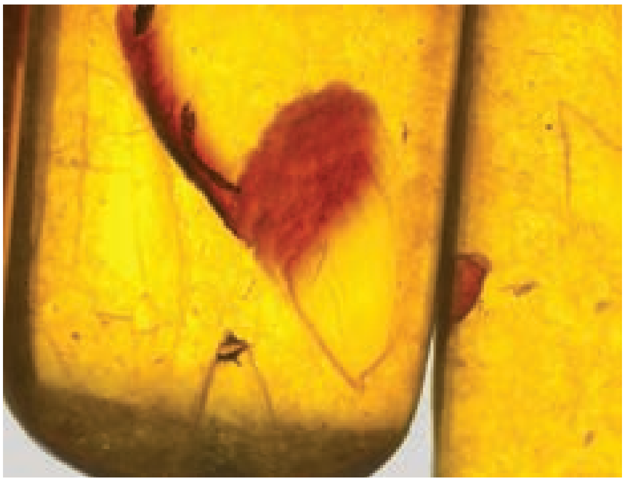

*Figure 4: Viewed in reflected light, the surface of this early reconstructed amber sample shows uneven polish lustre due to the different hardnesses of the constituent amber fragments. Photomicrograph by H. Li; magnified 10×.*

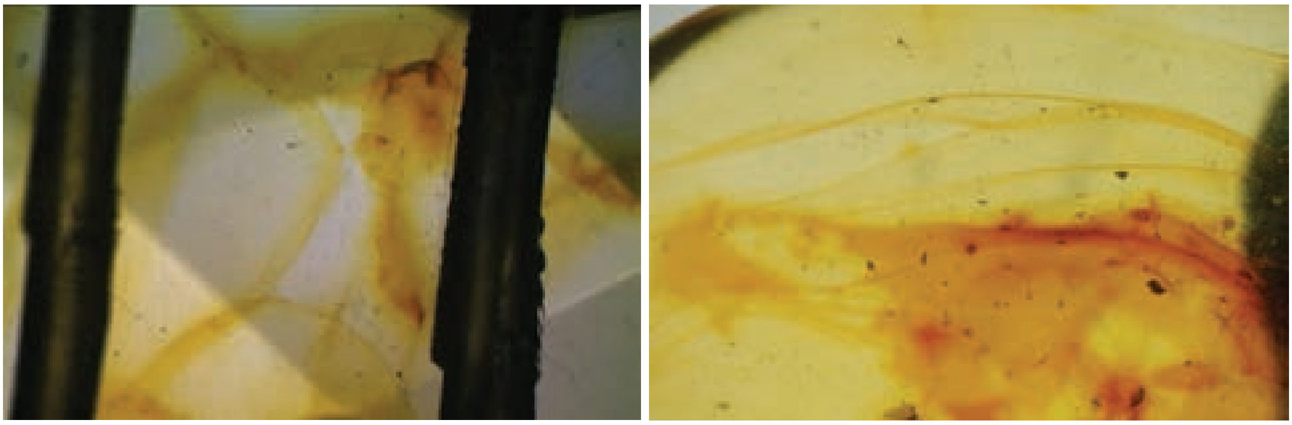

*Figure 5: Left: A three-dimensional mosaic (or 'blood streak') structure in early reconstructed amber shows a network of angular boundaries that completely enclose the fragments. Right: By contrast, heat-enhanced amber displays brownish red flow lines that do not interconnect. Photomicrographs by H. Li; magnified 10×.*

ing brownish flow lines. These flow lines result from the oxidation of pre-existing cracks that are healed during enhancement at low temperature and pressure to solidify the raw material and help avoid future cracking. (Because raw amber commonly has a layered structure that is accompanied by cracks, it can be difficult to carve and manufacture without this enhancement. According to the Chinese standard for amber, since this process does not change the basic component of the amber raw material, it should be recorded as an 'enhancement' rather than a treatment. By contrast, reconstructed amber is an artificial product, although it is produced using fragments of natural material [Zhang, 2010a].) In reconstructed amber, the coloured boundaries defining the fragmental structure of the material form interconnected networks that completely enclose the grains, while in heat-enhanced natural amber the flow lines are not commonly interconnected (Figure 5).

*Figure 6: Viewed between crossed polarizers in a polariscope, this 7-mm-long carved piece of natural amber shows anomalous double refraction with snake-like and wavy extinction patterns. Photo by H. Li.*

### *Appearance in the Polariscope*

Natural amber is amorphous and often shows anomalous double refraction in the polariscope, sometimes displaying snake-like, wavy or patchy extinction patterns (Figure 6). By contrast, early-stage reconstructed amber shows patchy grainy extinction with clear grain boundaries and often exhibits interference colours. If the fragments in the sample are small, then it may show distorted mylonitic patterns (Figure 7, left), while samples with larger unmelted fragments commonly show snake-like extinction and interference colours within the individual pieces (Figure 7, right).

### *Fluorescence*

Natural amber usually displays even fluorescence, regardless of whether it is viewed with a UV lamp (long- and short-wave) or in the DiamondView instrument. While darker-coloured early-stage reconstructed amber may not show diagnostic fluorescence, pale-coloured material commonly shows uneven luminescence with a fragmental or granular structure (Figures 8 and 9). Depending on the size of the fragments in the sample, it may be necessary to adjust the magnification of the DiamondView to properly observe the grain boundaries. However, it is not always possible to examine amber samples in the DiamondView due to the size limitations of the instrument.

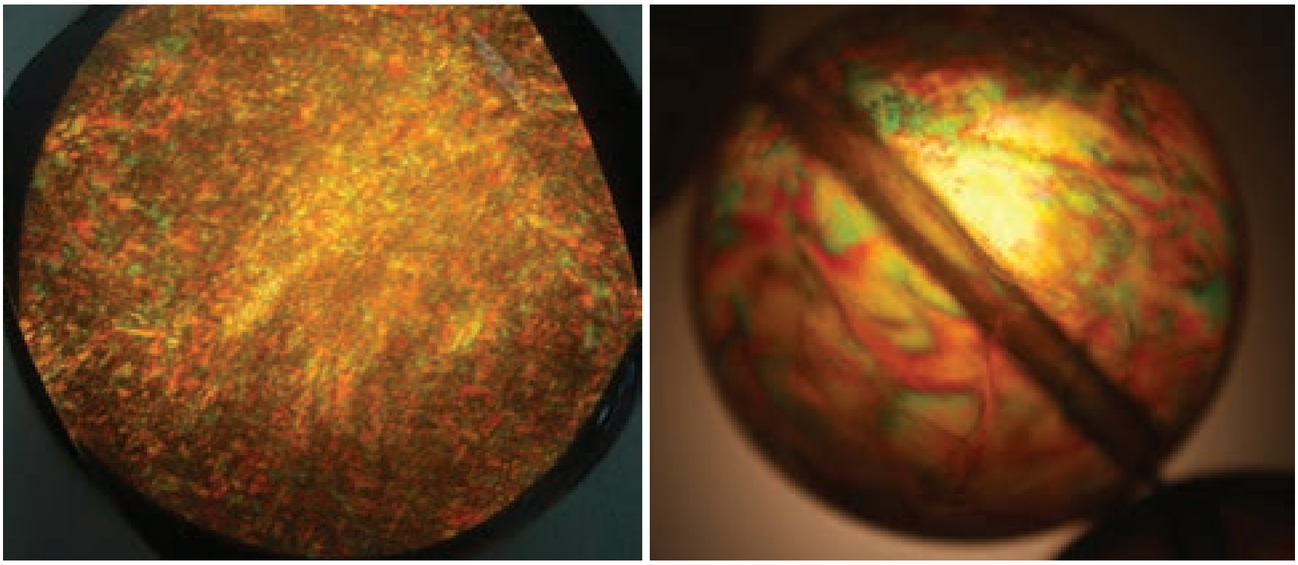

*Figure 7: Left: Distorted mylonitic extinction patterns accompanied by interference colours are seen with the polariscope in this reconstructed amber that was manufactured from tiny grains of raw material (magnified 10×). Right: A coarse pattern of wavy extinction and bright interference colours is visible with the polariscope in this 12-mm-diameter bead of reconstructed amber that was made from larger fragments of raw material. Photomicrographs by H. Li.*

## Identification of Current Reconstructed Amber

As the techniques for reconstructing amber have evolved, the characteristics used for identifying this material also have needed refinement. Compared to early reconstructed amber, the authors believe that current-stage reconstructed amber is manufactured under relatively higher temperatures and pressures in an oxygen-free environment. Also, current reconstructed amber is often subjected to post-processing treatments that are designed to conceal any identifying features. These include inducing internal and surface cracks (by heating and cooling), polishing with coarse grit to create a matt appearance (usually represented as an unpolished surface), darkening the surface colour (by baking), carving complex patterns and applying coloured coatings. Although these processes make identification more difficult, they do not completely hide the internal evidence of the reconstruction process.

*Figure 8: Long-wave UV fluorescence reveals various fragmental patterns in these early reconstructed amber samples consisting of larger (left) and smaller (right) amber fragments. The carving on the left is 8 cm tall and the piece on the right is 13 cm wide. Photos by H. Li.*

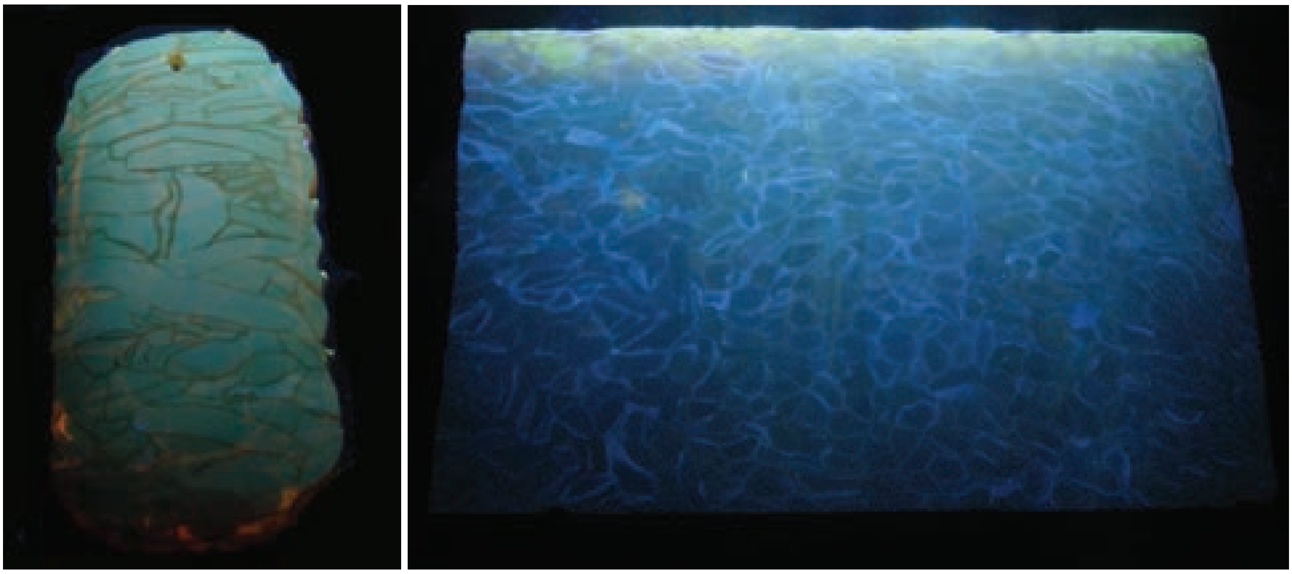

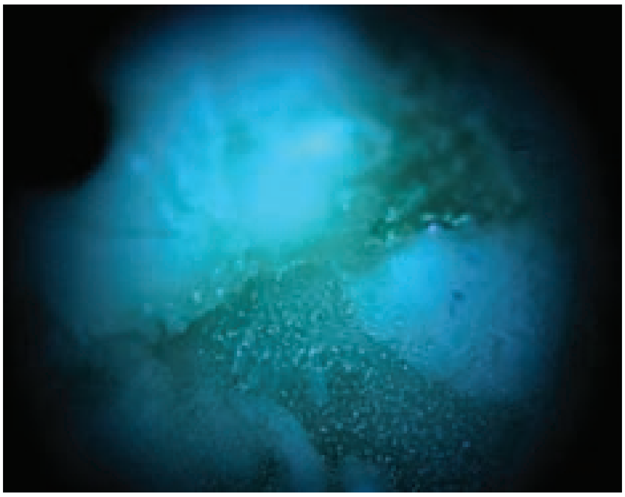

Figure 9: With the DiamondView, an early reconstructed amber bead shows angular grain boundaries. Photomicrograph by H. Li; magnified ~8×.

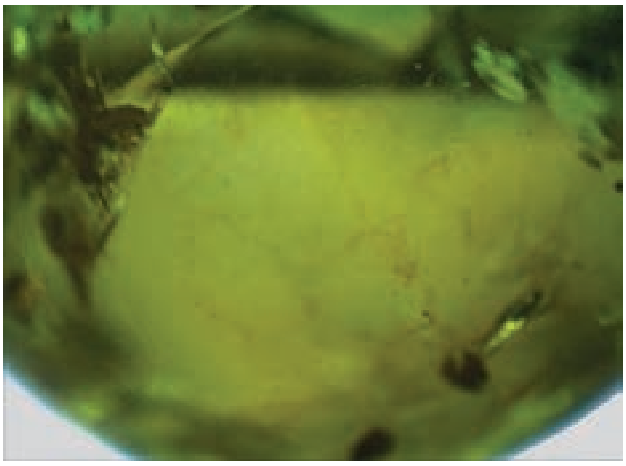

Figure 10: The fragmental structure of current reconstructed amber commonly shows subtle boundaries between grains. Here, the boundaries are pale reddish brown with a dot-like appearance. Photomicrograph by H. Li; magnified 16×.

### *Microscopic Features*

Current reconstructed amber can often be identified by carefully observing the sample with the microscope using a strong light source. Rather than coarse amber fragments, finer grains are typically used as the raw material for current reconstructed amber. As a result, it usually shows a more subtle and fine-grained fragmental structure consisting of areas with pale colour that are enclosed by dot-like edges (Figure 10). However, in some current reconstructed amber, the dark-coloured grain boundaries are nearly absent, or are quite fuzzy and only can be seen with careful observation; thus the 'blood streak' structure is not apparent (Figure 11). In addition, current reconstructed ambers made from tiny grains of raw material may not show an apparent fragmental structure, although they sometimes exhibit a granulated sugar-like texture, with or without a flowed appearance (Figure 12).

Careful examination of samples with transmitted illumination using a strong light source is helpful for revealing the interconnected mosaic pattern or angular grain boundaries in current reconstructed amber subjected to various post-processing treatments. Heat treatment (followed by abrupt cooling)

Figure 11: Left: Viewed with a strong transmitted light source, this opaque reconstructed amber bead exhibits no 'blood streak' structure, although the angular fragments are still quite apparent. Right: Two beads in an amber bracelet consist of natural amber (left side) and current reconstructed amber (right side) that displays fuzzy grain boundaries with no 'blood streak' structure. The presence of small grains with angular boundaries is the key identification factor for the reconstructed amber bead. Photomicrographs by H. Li; magnified 16× (left) and 12.5× (right).

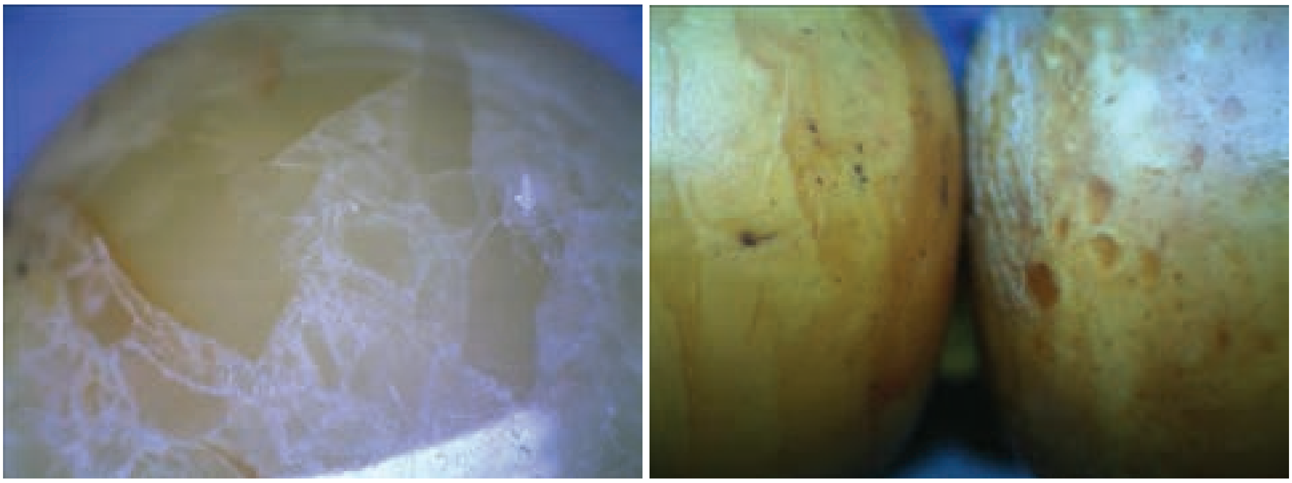

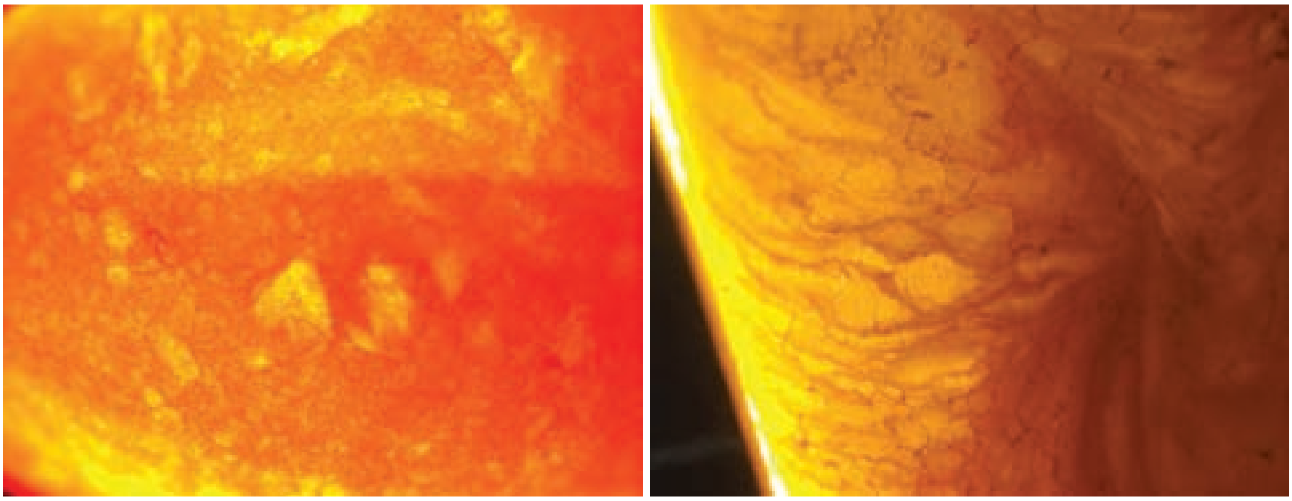

Figure 12: Left: A grainy 'sugar-like' texture is seen with strong transmitted light in a colour-coated sample of current reconstructed amber. Right: Current reconstructed amber made from somewhat larger grains exhibits a granulated structure with a flowed appearance when viewed with strong transmitted light. Photomicrographs by H. Li; magnified 32× (left) and 8× (right).

of reconstructed amber may create scattered flaky internal fractures or a network of surface cracks, which can obscure the diagnostic mosaic structure (Figure 13). Care must also be exercised when identifying reconstructed amber submitted to other post-processing treatments (e.g. Figures 14 and 15).

### *Polariscope and UV Fluorescence*

The post-processing treatments mentioned above often obscure the diagnostic features of current reconstructed amber in the polariscope and when observed for fluorescence with a UV lamp or the DiamondView. Therefore, these tests frequently cannot be used to reliably separate current reconstructed amber from natural amber.

## Discussion and Conclusions

Previous research on reconstructed amber has shown that variations in RI readings and the height of infrared absorption peaks at ~2930 and ~1735 cm$^{-1}$ can confirm that a sample has been heat treated and, further, suggest that it might be reconstructed (Zhu et al., 2009; Wang et al., 2012). During the heating process, the surface of the amber becomes oxidized, which also changes the RI and infrared spectral readings. The higher the temperature used, the higher the RI value will be, up to a maximum of 1.60 (distant-vision or 'spot' reading). Exposure to greater temperatures may cause the FTIR features to change: the ~1735

Figure 13: Left: Evidence of post-processing heat treatment in current reconstructed amber can be seen in the flaky internal cracks that are partially distributed along the fragmental structure. Right: Heating also may induce surface cracking, partially obscuring the fragmental structure of the reconstructed amber. Photomicrographs by H. Li; magnified 10× (left) and 12.5× (right).

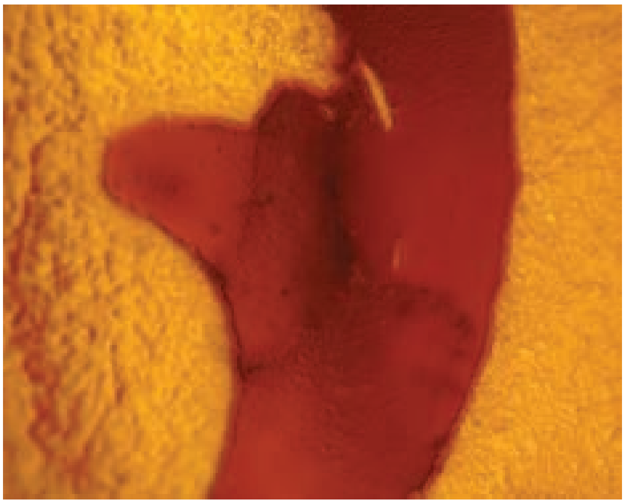

*Figure 14: This current reconstructed amber sample was baked to develop a much deeper brown-red surface colour, and then carved into a complex pattern that was finished with a matte surface. These features conceal the internal structure and makes identification difficult. Viewed with a strong transmitted light source, an unusual pattern can be seen under the smooth, transparent part of the surface—a pattern similar to the Chinese character '人' (meaning people)—corresponding to be the junction of three pieces of the amber raw material. Photomicrograph H. Li; magnified 20×.*

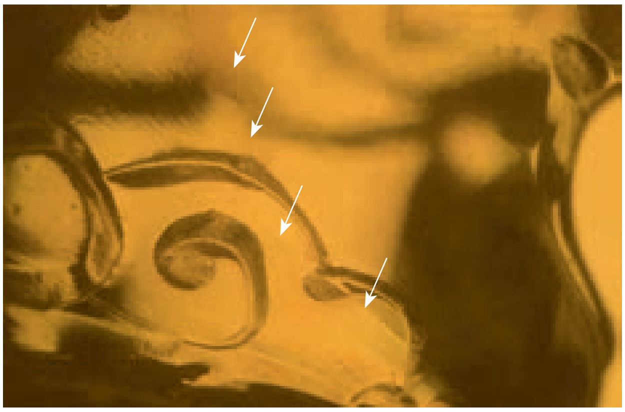

*Figure 15: This transparent hand-carved sample of current reconstructed amber shows subtle angular boundaries intersecting at an angle of about 145 ° (see arrows). The carved surface decorations make the internal texture details very easy to overlook. Photomicrograph by H. Li; magnified 20×.*

cm$^{-1}$ absorption band shifts to lower wavenumbers (down to 1716 cm$^{-1}$), and the ~1157 cm$^{-1}$ absorption band moves to higher wavenumbers (up to 1175 cm$^{-1}$). In addition, the intensity of the ~2930 cm$^{-1}$ feature decreases and the ~1735 cm$^{-1}$ band increases (Figure 16). These variations in RI and infrared spectra indicate that an amber specimen has been heated, but they do not provide conclusive evidence of reconstruction. While it is normal for the infrared spectra of reconstructed amber to show indications of heating, this does not prove that a sample has been reconstructed. For example, most of the 'blood amber' (named for its brownish red to red surface colour) currently on the market is the result of heating light yellow or yellow starting material. Variations in the RI values and infrared spectral characteristics of these ambers are similar to those seen in reconstructed ambers. However, 'blood amber' does not show the distinctive internal structures exhibited by reconstructed amber, and no other evidence points to these ambers having been reconstructed. Moreover, some reconstructed ambers have the same RI and infrared spectral features as natural untreated amber, so these are not reliable distinguishing characteristics (e.g. Figure 17). However, such samples can be revealed as reconstructed by careful microscopic observation of the internal fragmental/grainy textures.

In summary, the most effective method for identifying reconstructed amber is microscopy with the use of various lighting techniques to observe the internal microstructure. Observations with the polariscope and the UV lamp or DiamondView are useful auxiliary methods for the identification of reconstructed amber. Despite

*Figure 16: Infrared spectra (after Kramers-Kronig transformation) are shown for natural Baltic amber, reconstructed amber and heated natural amber that was enhanced to produce a darker surface appearance. Analysis of the intensity of the absorption bands at ~2930 and 1735 cm$^{-1}$ reveals that the temperature used for creating a darker surface colour was much higher than that used to produce reconstructed amber. Therefore, it is problematic to use infrared spectroscopy for determining whether or not an amber sample is reconstructed.*

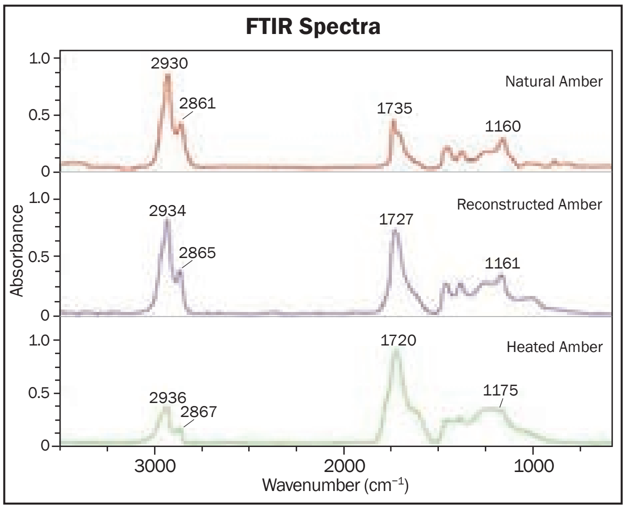

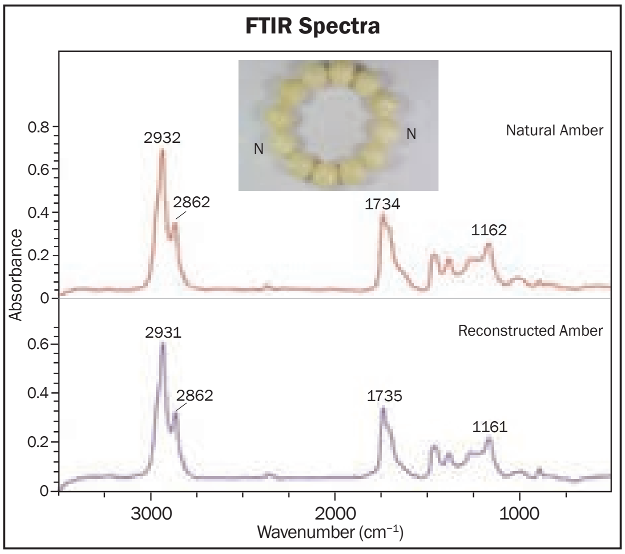

*Figure 17: Gemmological examination of a bead bracelet submitted by a client (see inset; photo by H. Li) showed that two of the beads were natural amber ('N'), while the rest were reconstructed amber. Infrared spectra (after Kramers-Kronig transformation) of all beads in the sample presented the same absorption features, consistent with their identity as Baltic amber, regardless of natural or reconstructed origin.*

recent improvements in amber reconstruction manufacturing techniques and post-processing treatments, in almost all cases there are clues remaining that allow reconstructed amber to be distinguished from natural amber.

## References

Beck C., Wilbur E. and Meret S., 1964. Infra-red spectra and the origin of amber. *Nature*, **201**(4916), 256–257, http://dx.doi.org/10.1038/201256a0.

Campbell Pedersen M. and Williams B., 2011. Copal vs. amber. *Gems&Jewellery*, **20**(2), 20–24.

Hänni H., 2005. Gem News International: Lizard in amber? *Gems & Gemology*, **42**(4), 361–362.

Koivula J.I., Kammerling R.C., Fritsch E., Eds., 1993. Gem News: Reconstructed amber. *Gems & Gemology*, **29**(1), 63.

Li H., Lu T., Shen M. and Zhou J., 2012. Comparison and identification of reconstructed ambers produced in different periods based on micro-structures. *Journal of Gems & Gemmology*, **15**(2), 36–39, 43 [in Chinese with English abstract].

Ma J., 2007. Identification characteristics of amber and its imitations. *Superhard Material Engineering*, **19**(5), 54–59 [in Chinese with English abstract].

Qi L., Yuan X., Peng G. and Wang Y., 2005. Three dimensional fluorescence spectra representation of natural and treated amber. *Journal of Gems & Gemmology*, **7**(1), 10–16 [in Chinese with English abstract].

Wang Y., Yang M. and You Z., 2012. Latest progress of pressed amber. *Journal of Gems & Gemmology*, **14**(1), 38–45 [in Chinese with English abstract].

Zhang B., 2006. *Systematic Gemmology*, 2nd edn. Geology Publishing, Beijing, China [see pp. 120-121, 542–547; in Chinese].

Zhang B., Gao Y., Wang M. and Shen M., 2010a. *Gems—Nomenclature*. General Administration of Quality Supervision, Inspection and Quarantine of the People's Republic of China [in Chinese; see p. 2].

Zhang B., Li J., Shen M., Zhang J., Su J. and Li H., 2010b. *Gems—Testing*. General Administration of Quality Supervision, Inspection and Quarantine of the People's Republic of China [in Chinese; see p. 60].

Zhou P. and Yang Z., 2011. *Organic Gemmology*. China Geological University Publishing, Wuhan, China [in Chinese; see pp. 140–158].

Zhu L. and Xing Y., 2008. Infrared absorption spectrum representation of amber and its imitation. *Journal of Gems & Gemmology*, **10**(1), 33–36, 39 [in Chinese with English abstract].

Zhu L., Wang X. and Luo L., 2009. Gemological characteristics of reconstructed amber. *Superhard Material Engineering*, **21**(6), 48–53 [in Chinese with English abstract].

## The Authors

**Haibo Li, Jie Liang FGA, Dr Taijin Lu, Jun Zhang and Jun Zhou***
National Gemstone Testing Center (NGTC) Laboratory, 22 F, Building C, Global Trade Center, North 3rd Ring East Road, Beijing 100013, China
Emails: 1978lihb@163.com and 921174302@qq.com

## Acknowledgements

All tests and examinations for this study were performed at the NGTC Beijing laboratory, and the authors thank all of the clients and suppliers who cooperated and supported this work. The authors also are grateful for support from NGTC Beijing lab personnel.

* Haibo Li and Jie Liang contributed equally to this article.

# Violet-to-Blue 'Nuummite' from Simiuttat, Greenland: Origin of Colour Appearance and Conditions of Formation

*Leander Franz, Tay Thye Sun, Richard Wirth, Christian de Capitani and Loke Hui Ying*

Iridescent orthoamphibole rock ('Nuummite') from the Nuuk District in south-west Greenland is an unusual gem material known in the trade since 1983. Unlike most Nuummite that shows a 'golden' brown iridescence, some specimens from Simiuttat in the Buksefjorden Archipelago display a violet-to-blue colour similar to that seen in some labradorite. The rock is a biotite-cordierite-anthophyllite granofels that formed in the Late Archean and subsequently experienced a polymetamorphic overprint, with peak metamorphism at amphibolite-facies conditions. While electron microprobe analyses and Raman spectroscopy classify the orthoamphibole as an Al-rich anthophyllite without any inhomogeneities on a micrometre scale, transmission electron microscopy revealed sub-microscopic exsolution lamellae of anthophyllite and gedrite parallel to (010). The periodic lamellae have an average spacing of 124–133 nm, which generates the violet-to-blue diffraction coloration. This study shows that the colour appearance of Nuummite is not due to chemical variations from grain to grain, but to the spacing of exsolution lamellae in orthoamphibole.

*The Journal of Gemmology*, **35**(4), 2016, pp. 330–339, http://dx.doi.org/10.15506/JoG.2016.35.4.330

## Introduction

Iridescent orthoamphibole (anthophyllite-gedrite) has been reported from New Hampshire and Massachusetts in the USA (Robinson et al., 1971), south-west Greenland (Appel and Jensen, 1987; Rodgers et al., 1996; Champness and Rodgers, 2000) and Mauritania (Kobayashi, 2009; Renfro, 2011); the gem-quality material from Greenland is commonly marketed as 'Nuummite'. In most cases, a golden brown iridescence colour is observed (Bøggild, 1905, 1924; Appel and Jensen, 1987), although yellow-green and blue colours also occur (Champness and Rodgers, 2000; Renfro, 2011).

This study focuses on violet-to-blue-appearing orthoamphibole from Greenland (e.g. Figure 1). (Note that although the body colour of this material is dark grey, in this article the 'violet-to-blue' description refers to the coloration shown by the diffraction of light from suitably-oriented cleavages in the amphiboles constituting the rock.) According to geologists at the Geological Survey of Denmark and Greenland (N. Keulen, K. Secher and P. Appel, pers. comm., 2016), this material is known to occur on Simiuttat Island in the Buksefjorden Archipelago near Nuuk, the capital of Greenland (Figure 2). The Nuummite is hosted by a sequence of Precambrian polymetamorphic rocks (mainly quartz-cordierite gneisses) called the Malene supracrustals (McGregor, 1969; Dymek and Smith, 1990) with an average age of 2,732 ± 10 million years old (Rodgers et al., 1996). Nuummite occurs as thin bands and lenses up to 1 m wide along the strike of the rock sequence (Appel and Jensen, 1987). It consists almost exclusively of orthoamphibole with minor amounts of gahnite, magnetite, pyrrhotite, chalcopyrite and molybdenite. The orthoamphiboles form a solid-solution series between the end members anthophyllite $(Mg,Fe^{2+})_7[Si_8O_{22}](OH)_2$ and gedrite $(Mg,Fe^{2+})_5Al_2[Al_2Si_6O_{22}](OH)_2$ (Robinson et al., 1971; Spear, 1980).

The iridescence of Nuummite is due to the interference of light reflected from sub-microscopic, alternating gedrite and anthophyllite exsolution lamellae (Rodgers et al., 1996; Champness and Rodgers, 2000). While golden brown iridescence is typical, subordinate occurrences showing violet-to-blue coloration also are found (Ap-

*Figure 1: This checkerboard-cut Nuummite gemstone (57.73 ct; 47.04 × 28.62 × 4.86 mm) shows long, thin, violet-to-blue prisms. Photo by Tay Thye Sun.*

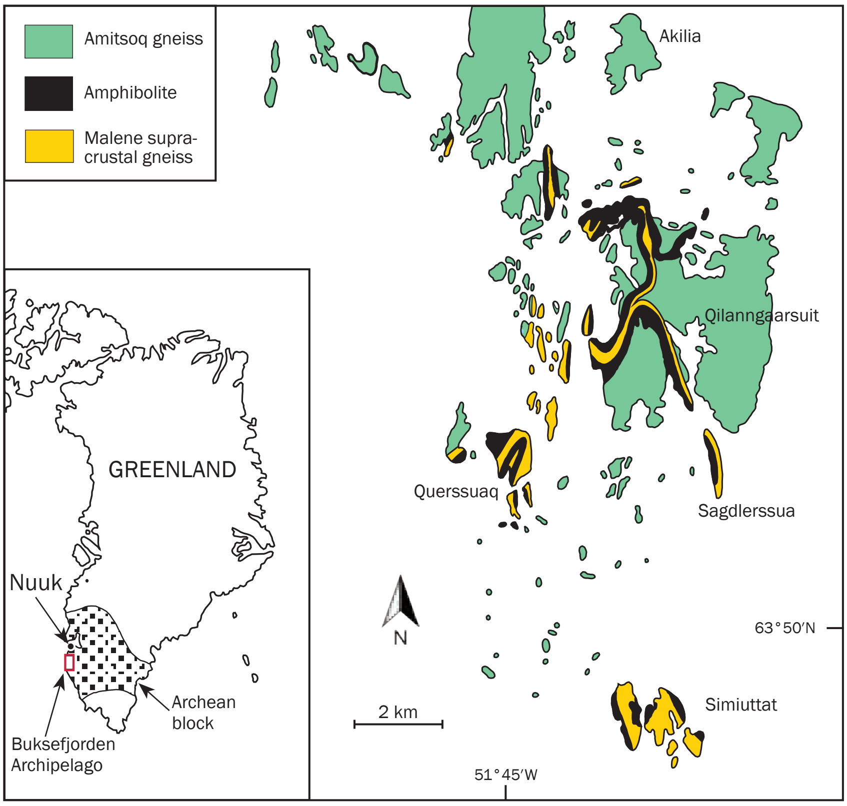

*Figure 2: The Nuummite investigated in this study came from Simiuttat Island in Greenland's Buksefjorden Archipelago, where it is hosted by Precambrian Malene supracrustal gneiss. The inset shows the capital Nuuk and the position of the Buksefjorden region in the Archean block of Greenland. Modified after Beech and Chadwick (1980).*

*Figure 3: These Nuummite slabs (5.1 and 4.7 g) show rather subtle violet-to-blue coloration because they are only roughly polished. Photo by Tay Thye Sun.*

pel, 1983; Appel and Jensen, 1987). This study investigates the mechanism for the violet-to-blue diffraction coloration of the Simiuttat Nuummite, provides a petrological description of the rock and highlights the metamorphic pressure-temperature (PT) conditions of its formation.

## Materials and Methods

A sizable rough sample of Nuummite showing violet-to-blue coloration was provided by author TTS's client Rex Guo. In addition, Guo supplied two triangular slabs that were cut and partially polished from the same piece of rough; one of them weighed 5.1 g (42.00 × 15.76 × 5.57 mm) and the other was 4.7 g (30.73 × 19.24 × 5.69 mm; Figure 3). From these two samples, a polished slice and a polished thin section were prepared for further analysis.

Mineral abbreviations used in this article are after Spear (1993).

### Gemmological and Petrographic Methods

The polished slice was visually examined with a Keyence VHX-1000 digital microscope, and its RI values were determined with a Gem-A refractometer. The slice also was used for hydrostatic SG measurements and was examined with a UV lamp and a desk-model prism spectroscope. The mineralogy and micro-texture of the thin section were studied using a Leica DMRX polarized-light microscope.

### Electron Microprobe Analysis (EMPA)

The composition of rock-forming minerals in the thin section was quantitatively measured by EMPA using a JEOL JXA-8600 instrument at the University of Basel, Switzerland. The instrument was equipped with an UltraDry silicon energy-dispersive X-ray detector (Noran System 7 spectral imaging system by Thermo Scientific). The accelerating voltage was 15 kV and beam current was 20 nA, and we used a peak counting time of 30 seconds for all elements. Data correction was performed using the Proza (ϕρZ) method. To avoid volatilization of Na we chose a spot size of 10 μm. As the analyses were performed without the use of standards, an overall error of 2% is assumed. Backscattered electron (BSE) imaging was done at a relatively low magnification in the microprobe to investigate the mineralogical composition of the phases.

### Raman Spectroscopy

Confocal Raman micro-spectroscopy was used to non-destructively identify the minerals and especially to characterize the composition of the orthoamphiboles in the polished slice. We used a dispersive Bruker Senterra Raman microscope equipped with a 532 nm laser. The high spatial resolution of this method (measurement of spots with diameters of 1–3 μm is possible) may even allow the identification of complex mineral intergrowths, zoning and exsolution lamellae. Measurements were performed at 20 mW (on the sample) with a 50 second counting time; we used objective lenses with 50× and 100× magnification and an aperture of 25 μm. Spectral matching was performed using the RRUFF database (Downs, 2006) and our own Raman database at the Mineralogical Institute in Basel.

### Transmission Electron Microscopy (TEM) and Analytical Electron Microscopy (AEM)

Two slices taken from the {210} cleavage surface of orthoamphibole showing violet-to-blue coloration were investigated. Both TEM and AEM were carried out using a FEI Tecnai F20 X-Twin transmission electron microscope with a Schottky field emitter as an electron source. The accelerating voltage was 200 kV. The TEM was equipped with a Gatan imaging filter, a Fischione high-angle annular dark field detector for Z-contrast imaging, and an EDAX X-ray analyser. Electron diffraction patterns were acquired on image plates.

### Calculated PT Conditions

Phase diagram calculations for the PT formation conditions of Nuummite were performed with

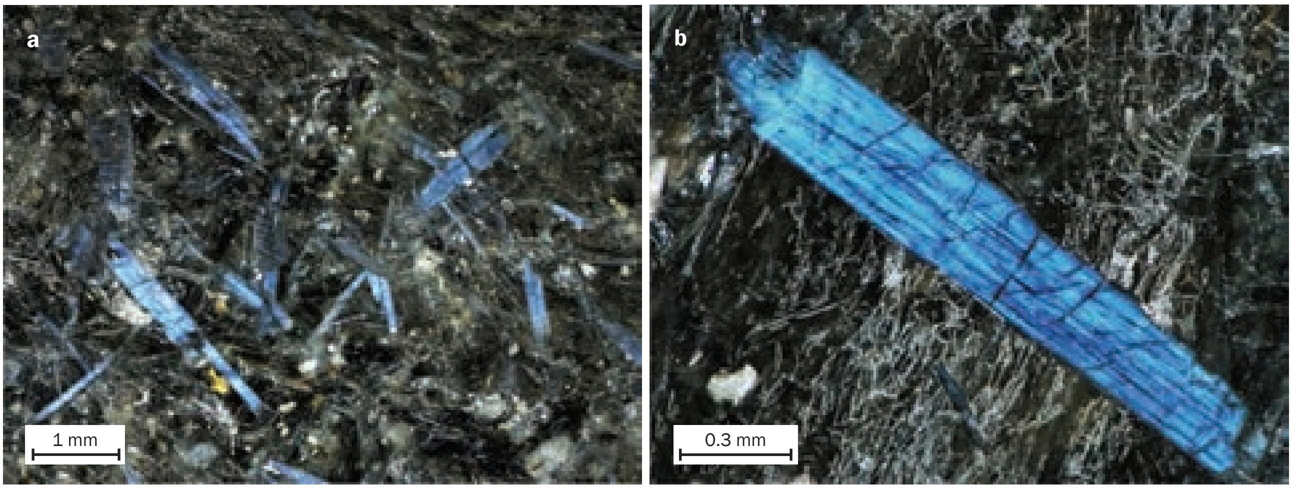

*Figure 4: Keyence digital microscope photos (in reflected light) of a polished slice of Nuummite show (a) criss-crossing orthoamphibole prisms in a dark matrix of cordierite and biotite, and (b) an orthoamphibole prism displaying violet-to-blue coloration. Photomicrographs by L. Franz.*

the Theriak/Domino program of de Capitani and Brown (1987; see also de Capitani and Petrakakis, 2010) in the model system $TiO_2$-CaO-$K_2O$-FeO-MgO-$Al_2O_3$-$SiO_2$-$H_2O$ using the JUN92.bs dataset of Berman (1988) with an ideal model for anthophyllite (JUN92ANTH). A synthetic bulk-rock composition was derived from EMPA data for the equilibrium mineral assemblage and from the modal proportions of the individual phases.

## Results and Discussion

### *Gemmological and Petrological Properties*

While the rough sample was uniformly dark and hardly revealed any coloration, the roughly polished samples showed a few subtle bluish shimmers (Figure 3). By contrast, the highly polished gemstone in Figure 1 (seen previously by author TTS) displayed distinct violet-to-blue colour from mm-sized prisms over a dark grey body colour. The RIs of the polished slice were 1.650–1.660, with a second shadow edge at approximately 1.54. Hydrostatic SG measurements were 3.09 ± 0.01, and the material was inert to long- and short-wave UV radiation. No absorption features were seen with the spectroscope.

Observation of the polished slice with the Keyence digital microscope showed laths of orthoamphiboles criss-crossing one another (Figure 4a). The crystals displayed blue-to-violet flashes, which were only visible on {210} cleavages (e.g. Figure 4b). The colours vanished when the crystal was tilted to an angle of 5–15° depending on the tilting axis, indicating a strong geometric control on the colouring phenomenon. The blue-to-violet coloration was not evident on fractures and on other cleavage planes.

Polarized microscopy of the thin section revealed a close intergrowth of prismatic orthoamphibole, granular cordierite (with weak pinitization) and brown, strongly pleochroic biotite flakes (Figure 5). All minerals displayed a random orientation, although biotite may have had a weak foliation. With the use of a point counter, the mineral content of the thin section was estimated at 60 vol.% orthoamphibole, 31 vol.% cordierite, 8 vol.% biotite and 1 vol.% accessory minerals (mainly ilmenite with tiny inclusions of relic rutile and subordinate apatite and chlorite). The presence of amphibole-, biotite- and cordierite-rich areas explains the different refractometer readings, with values of about 1.66 being typical for orthoamphibole while the additional shadow edge of 1.54 originated from cordierite. Due to the lack of any significant foliation or banding, and considering the abundance of the observed minerals, the petrographic name of the rock was determined as biotite-cordierite-anthophyllite granofels. A granofels is a metamorphic rock with prevailing granular-textured minerals lacking any alignment (Schmid et al., 2007).

Orthoamphibole prisms in the thin section showed a weak pleochroism from pale yellow ($\alpha$) to brownish yellow ($\beta$) to greyish brown ($\gamma$), and displayed no violet-to-blue coloration with either crossed or parallel polarizers. The prisms

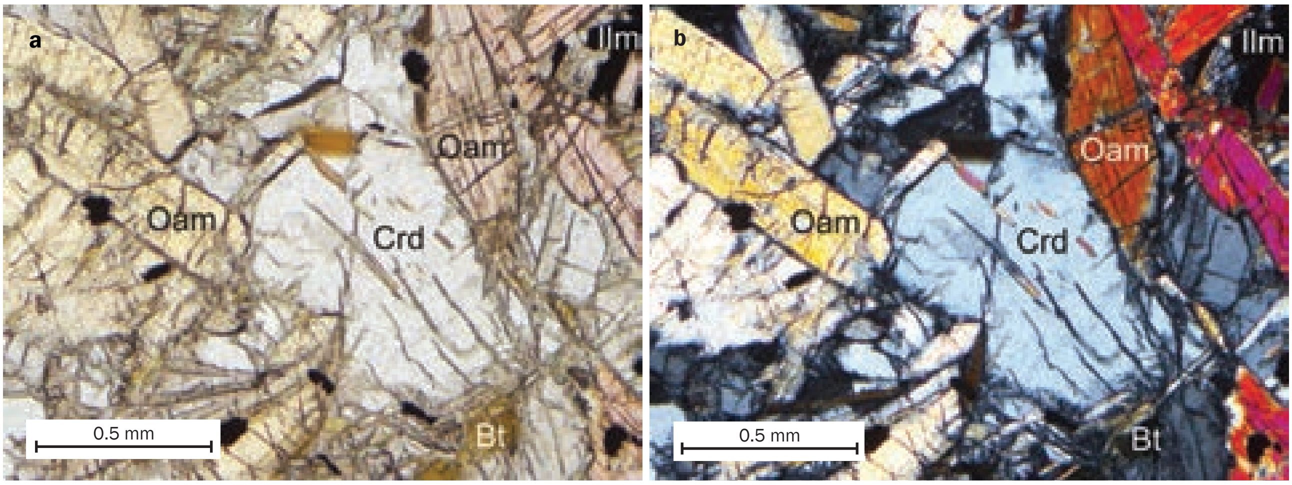

*Figure 5: The mineral composition in a thin section of Nuummite is shown with (a) parallel and (b) crossed polarizers, revealing randomly oriented orthoamphibole (Oam), cordierite (Crd), biotite (Bt) and accessory ilmenite (Ilm). Photomicrographs by L. Franz.*

were up to 4 mm long and had a length-to-width ratio ranging from 4:1 to 20:1. Raman spectroscopy of the orthoamphibole showed great similarities to gedrite in the RRUFF database (Downs, 2006) and to anthophyllite 75296E in our own database (Figure 6).

Selected EMPA data are shown in Table I, and all of the analyses can be found in Tables DD-1–DD-5 of the *Journal*'s data depository. The data indicated that the orthoamphibole is Al-rich anthophyllite using the classification of Hawthorne et al. (2012). All of the minerals in the rock were unzoned and had similar composition throughout the thin section. Backscattered-electron imaging, EMPA, and Raman profiles across the orthoamphibole crystals did not reveal any evidence of zonation or exsolution lamellae in the micrometre or larger scale; the same applied to the other rock-forming minerals. The cordierite was Mg-rich with $X_{Mg}$ values [Mg/(Mg+Fe$^{2+}$)] of 0.80–0.83, while biotite had $X_{Mg}$ values of 0.70–0.75 with $TiO_2$ contents of 1.0–1.7 wt.%. Biotite and cordierite were intergrown with pale green chlorite (ripidolite/sheridanite with $X_{Mg}$ values of 0.79–0.81).

*Figure 6: Raman spectra of the violet-to-blue orthoamphibole from the Simiuttat Nuummite (a) had many similarities to the spectra of the gedrite and anthophyllite reference standards (b and c).*

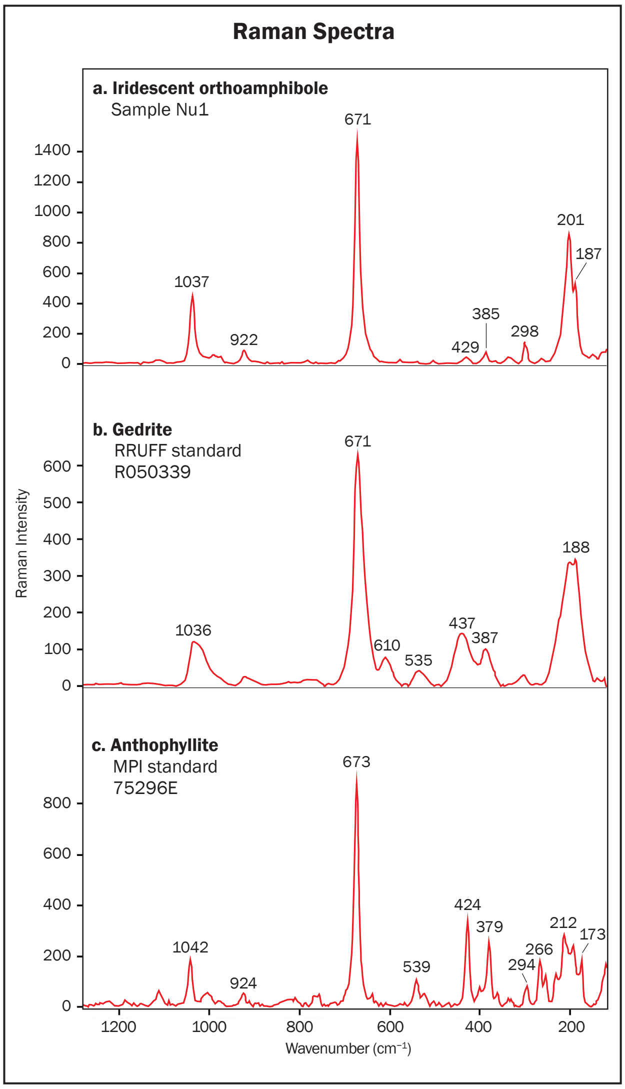

## *TEM and AEM*

TEM images (e.g. Figure 7a) showed a continuous succession of alternating exsolution lamellae of anthophyllite (wide, dark grey bands) and gedrite (narrow, light grey lamellae), which also were revealed by AEM chemical analyses (Table I). The electron diffraction pattern (Figure 7b) of the orthoamphibole showed that the exsolu-

*Table I: EMPA and AEM data of rock-forming minerals in iridescent violet-to-blue Nuummite from Simiuttat, Greenland.**

| Mineral | Orthoamphibole | | | | | | Cordierite | Biotite | Chlorite |
|---|---|---|---|---|---|---|---|---|---|
| Technique | EMPA | EMPA | EMPA | EMPA | AEM | AEM | EMPA | EMPA | EMPA |
| Point | F1 core | F1 rim | F5 core | F5 rim | A2 Ged | A2 Ath | Average | Average | Average |
| Oxides (wt.%) | | | | | | | | | |
| $SiO_2$ | 53.02 | 52.49 | 51.49 | 52.95 | 43.14 | 52.44 | 50.22 | 38.81 | 28.15 |
| $TiO_2$ | 0.16 | bdl | bdl | 0.04 | bdl | bdl | bdl | 1.25 | bdl |
| $Al_2O_3$ | 6.11 | 6.91 | 6.78 | 5.65 | 17.84 | 1.95 | 33.18 | 17.76 | 22.58 |
| $Fe_2O_3$ | 1.27 | 1.70 | 2.47 | 1.19 | bdl | bdl | nd | nd | 0.38 |
| $Cr_2O_3$ | bdl | bdl | bdl | bdl | bdl | bdl | nd | bdl | nd |
| MgO | 19.96 | 19.99 | 19.69 | 20.49 | 24.88 | 31.61 | 11.61 | 18.08 | 25.24 |
| CaO | 0.43 | 0.42 | 0.46 | 0.52 | 0.53 | 0.21 | bdl | bdl | bdl |
| MnO | 0.26 | bdl | 0.11 | 0.33 | bdl | bdl | 0.13 | 0.22 | 0.40 |
| FeO | 16.13 | 15.86 | 16.66 | 16.54 | 13.58 | 13.78 | 4.60 | 11.57 | 11.29 |
| $Na_2O$ | 0.78 | 0.80 | 0.59 | 0.40 | nd | nd | 0.26 | 0.39 | bdl |
| $K_2O$ | bdl | bdl | bdl | bdl | bdl | bdl | bdl | 7.75 | bdl |
| Total | 98.13 | 98.17 | 98.25 | 98.12 | 99.97 | 99.99 | 100.00 | 95.83 | 88.05 |
| Cations | per 23 oxygens | | | | | | per 18 oxygens | per 12 oxygens | per 28 oxygens |
| Si | 7.472 | 7.388 | 7.301 | 7.476 | 5.947 | 7.214 | 5.005 | 2.790 | 5.471 |
| Ti | 0.017 | bdl | bdl | 0.004 | bdl | bdl | bdl | 0.067 | bdl |
| Al | 1.014 | 1.146 | 1.133 | 0.941 | 2.899 | 0.316 | 3.897 | 1.505 | 5.172 |
| $Fe^{3+}$ | 0.135 | 0.180 | 0.264 | 0.127 | bdl | bdl | nd | nd | 0.056 |
| Cr | bdl | bdl | bdl | bdl | bdl | bdl | nd | bdl | nd |
| Mg | 4.194 | 4.195 | 4.162 | 4.313 | 5.113 | 6.482 | 1.725 | 1.937 | 7.313 |
| Ca | 0.065 | 0.064 | 0.070 | 0.079 | 0.078 | 0.031 | bdl | bdl | bdl |
| Mn | 0.032 | bdl | 0.013 | 0.040 | bdl | bdl | 0.011 | 0.014 | 0.066 |
| $Fe^{2+}$ | 1.901 | 1.867 | 1.976 | 1.953 | 1.566 | 1.585 | 0.383 | 0.695 | 1.836 |
| Na | 0.214 | 0.219 | 0.162 | 0.110 | nd | nd | 0.050 | 0.054 | bdl |
| K | bdl | bdl | bdl | bdl | bdl | bdl | bdl | bdl | bdl |
| Total | 15.044 | 15.059 | 15.081 | 15.041 | 15.603 | 15.628 | 11.072 | 7.773 | 19.915 |

* Estimates of $Fe^{3+}$ in the EMPA data of orthoamphibole were done with the min-max method of Leake et al. (1997) using the intermediate value of $Fe^{3+}$. Na could not be determined with AEM due to an overlap of the Na($K\alpha$) line with the Ga($L\alpha$) line; consequently, an estimate of $Fe^{3+}$ for those analyses was not performed. $Fe^{3+}$ in chlorite was estimated using the method of Laird and Albee (1981). Abbreviations: bdl = below detection limit; nd = not determined.

tion of the lamellae occurred parallel to (010)—that is, (010) anthophyllite || (010) gedrite—as previously observed by Gittos et al. (1976). Our images showed close correspondence with the observations of Champness and Rodgers (2000) and with atomic force microscopy images of Rodgers et al. (1996) on golden brown iridescent orthoamphibole. The main difference between our results and those previous studies is a variation in the thickness of the gedrite-anthophyllite lamellae pairs. While the mean thickness of the lamellar pairs in our sample was 124–133 nm, Champness and Rodgers (2000) observed a mean of ~180 nm, while Rodgers et al. (1996) found 190–350 nm.

Due to the difference in RI values between the anthophyllite and gedrite lamellae (0.035 for $n_z$), the wavelength of the observed colour for incident light on the lamellar interfaces can be calculated with the Bragg equation, $\lambda = 2nd\sin\Theta$, where n is the mean RI of the two phases, d is the mean thickness of the lamellar pairs and $\Theta$ is the angle of incidence of the light on the lamellar interface (cf. Laves et al., 1965). Assuming an RI value of 1.66 (average for the anthophyllite-gedrite solid solution; cf. Champness and Rodgers, 2000) and an angle of 80° for $\Theta$, the Bragg equation yields a wavelength of 405–435 nm (i.e. violet-to-blue light). This shows that the observed lamellar spacing of 124–133 nm is consistent with

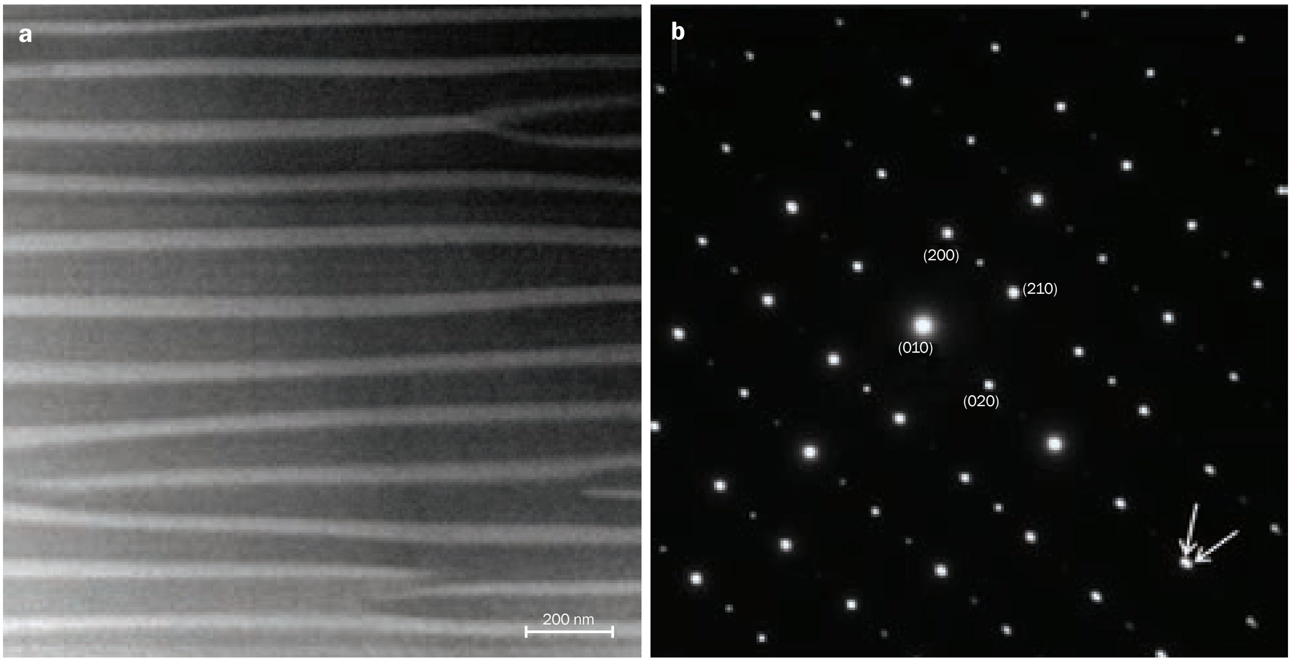

*Figure 7: (a) The TEM image of violet-to-blue orthoamphibole shows alternating lamellae of anthophyllite (dark grey; major phase) and gedrite (light grey; minor phase) with a spacing of ~133 nm, seen parallel to (010). (b) In the electron diffraction pattern from the orthoamphibole in (a), each spot along the crystallographic b-direction is split (e.g. see arrows). The splitting is due to different lattice parameters and is very small. It is only visible at higher-order reflections such as those from (020) to (080), and indicates that there are two contiguous phases with analogous structures visible at higher-order reflections of {0k0}. Images by R. Wirth.*

the violet-to-blue diffraction coloration observed in this Nuummite.

### PT Formation Conditions

Phase diagram calculations with the Theriak/Domino program (Figure 8) clearly show the stability field for the mineral assemblage anthophyllite-cordierite-biotite-chlorite-ilmenite-$H_2O$ at temperatures of 505–660°C and pressures below 6.4 kbar, corresponding to upper greenschist to amphibolite-facies conditions at low-to-moderate pressures (see yellow field in Figure 8). The EMPA data of the orthoamphibole crystals from our Nuummite samples plot at 590–600°C (±25°C) in the T–$Al^{IV}$ solvus diagram of Spear (1980; see Figure 9), constraining the minimum metamorphic temperature experienced by the rock. Due to the polymetamorphic history of the Nuummite, however, it is not possible to infer the timing of the exsolution in the orthoamphibole.

Figure DD-1 in *The Journal's* data depository shows a phase diagram including mineral reactions and activity models used, and all mineral reactions are listed in Table DD-6 of the data depository.

## Conclusions

Iridescent orthoamphibole has been reported from various locations, such as New Hampshire and Massachusetts (Robinson et al., 1971), south-west Greenland (Appel and Jensen, 1987; Rodgers et al. 1996; Champness and Rodgers, 2000) and Mauritania (Kobayashi, 2009; Renfro, 2011). In most cases, these orthoamphiboles show a golden brown iridescence with greenish and bluish colours being subordinate (Rodgers et al., 1996; Renfro, 2011). As shown by Rodgers et al. (1996) and Champness and Rodgers (2000), the iridescence of Nuummite results from sub-microscopic, alternating lamellar exsolution of gedrite and anthophyllite. Champness and Rodgers (2000) proved that the periodic lamellae had an average spacing of ~180 nm, which gives rise to a yellow iridescence. For our samples from Simiuttat, we found distinctly smaller spacings of 124–133 nm, resulting in violet-to-blue coloration. By comparison, Nuummite from Mauritania contains blades of orthoamphibole showing bluish coloration in the outer zones shifting to a yellowish green in the centre, which was ascribed to possible chemical

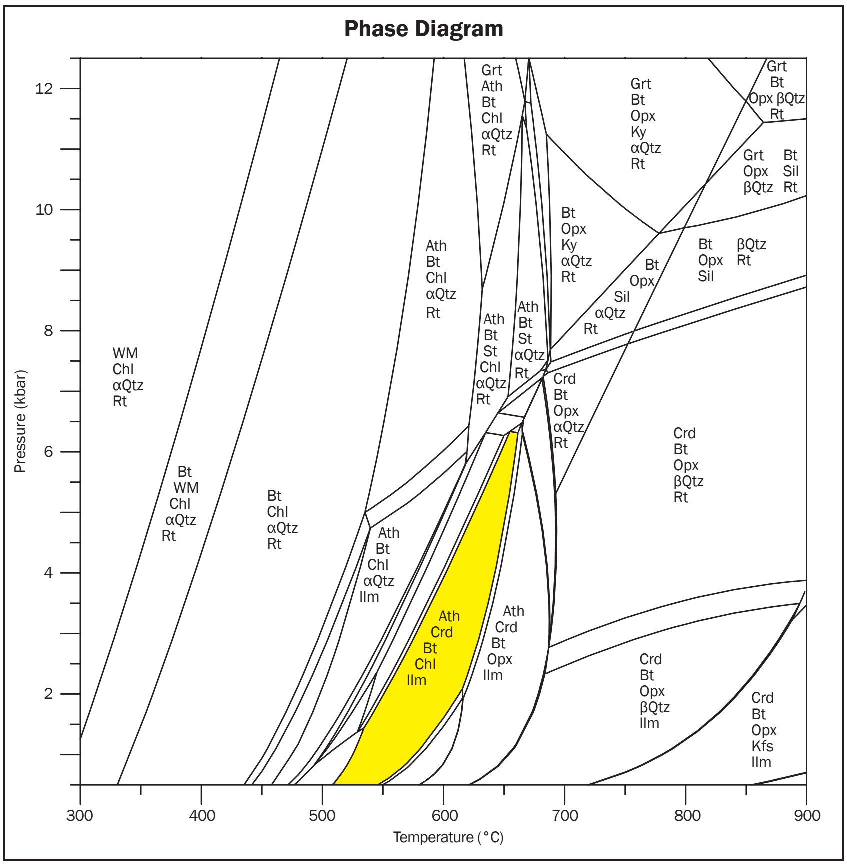

*Figure 8: This equilibrium phase diagram for the Simiuttat Nuummite was calculated with the Theriak/Domino program of de Capitani and Brown (1987) and the JUN92ANTH dataset for the most important mineral assemblages and $H_2O$ in excess. The molar bulk-rock composition is 3.612 Si, 0.04 Ti, 1.228 Al, 0.853 Fe, 1.872 Mg, 0.054 K, 50 H and 36.898 O. The stability field of the observed assemblage anthophyllite-cordierite-biotite-chlorite-ilmenite is shaded in yellow, and corresponds to temperatures of 505–660 °C and pressures below 6.4 kbar.*

variation within the crystals (Renfro, 2011). The present study, as well as former investigations (see Rodgers et al., 1996; Champness and Rodgers, 2000), prove that such differences in the colour are not due to chemical variations from grain to grain but rather are due to the spacing of the exsolution lamellae in the orthoamphibole. While Appel and Jensen (1987) ascribed Nuummite iridescence to internal reflections from alternating gedrite and anthophyllite exsolution lamellae (see also Champness and Rodgers, 2000), Rodgers et al. (1996) postulated that the surface topography of the {210} cleavages (as an expression of the underlying lamellae) might act as a diffraction grating that could contribute to the iridescence. To definitively assign the iridescence to one of these phenomena, further investigations (including ultraviolet-visible reflectance spectroscopy) would need to be performed, but these are beyond the scope of the present investigation.

Polarized microscopy showed that the correct petrographic name of the investigated Nuummite is biotite-cordierite-anthophyllite granofels, following the suggestions of Schmid et al. (2007). This investigation also confirmed that the second RI shadow edge at approximately 1.54 is due to cordierite. As shown by phase diagram calculations using the Theriak/Domino program of de Capitani and Brown (1987), the rock experienced a metamorphic overprint at low-to-moderate pressures and upper greenschist to amphibolite-facies conditions. Minimum metamorphic temperatures of 590–600°C (±25°C) were estimated using the T–$Al^{IV}$ solvus diagram for orthoamphibole of Spear (1980), constraining amphibolite-facies conditions. According to Rodgers et al.

*Figure 9: EMPA data for the orthoamphiboles in this study are plotted on the T–$Al^{IV}$ solvus diagram of Spear (1980), indicating minimum temperatures of formation of 590–600 °C. The error of the diagram is ±25 °C.*

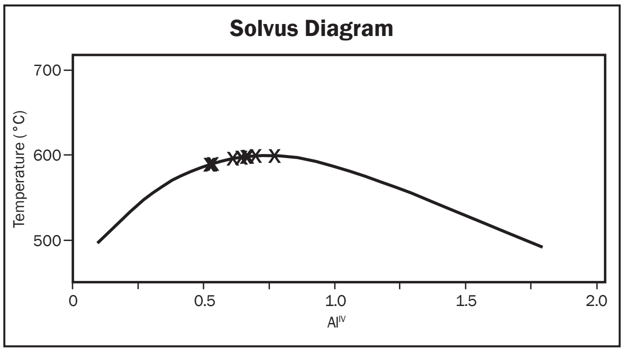

(1996), the average age range for this metamorphic overprint (using $^{207}Pb/^{206}Pb$ ages of monazite and zircon) is 2,707–2,732 (±10–12) million years. The exsolution lamellae in the orthoamphibole may have formed during cooling after peak metamorphism, during reheating processes in the course of the intrusion of the Qôrqut granite complex (~2,500 million years ago) or during a later Proterozoic metamorphic overprint (Rodgers et al., 1996).

Small amounts of violet-to-blue Nuummite from Greenland will likely continue to be available on the market in the future.

## References

Appel P., 1983. Nuukit – Grønlands nye symkkesten. *Grønland*, **31**(6), 157–159.

Appel P.W.U. and Jensen A., 1987. A new gem material from Greenland: Iridescent orthoamphibole. *Gems & Gemology*, **23**(1), 36–42, http://dx.doi.org/10.5741/gems.23.1.36.

Beech E.M. and Chadwick B., 1980. The Malene supracrustal gneisses of northwest Buksefjorden: Their origin and significance in the Archaean crustal evolution of southern West Greenland. *Precambrian Research*, **11**(3–4), 329–355, http://dx.doi.org/10.1016/0301-9268(80)90071-6.

Berman R.G., 1988. Internally-consistent thermodynamic data for minerals in the system $Na_2O$-$K_2O$-$Ca$-$MgO$-$FeO$-$Fe_2O_3$-$Al_2O_3$-$SiO_2$-$TiO_2$-$H_2O$-$CO_2$. *Journal of Petrology*, **29**(2), 445–522, https://doi.org/10.1093/petrology/29.2.445.

Bøggild O.B., 1905. Mineralogica Groenlandica. *Meddelelser om Grønland*, **32**, 1–623 [in Danish].

Bøggild O.B., 1924. On the labradorization of the feldspars. *Det Kongelige Danske Videnskabers Selskab Mathematiskfsiske Meddelelser*, **6**(3), 1–79.

Champness P.E. and Rodgers K.A., 2000. The origin of iridescence in anthophyllite-gedrite from Simiuttat, Nuuk District, southern West Greenland. *Mineralogical Magazine*, **64**(5), 885–889, http://dx.doi.org/10.1180/002646100549715.

de Capitani C. and Brown T.H., 1987. The computation of chemical equilibrium in complex systems containing non-ideal solutions. *Geochimica et Cosmochimica Acta*, **51**(10), 2639–2652, http://dx.doi.org/10.1016/0016-7037(87)90145-1.

de Capitani C. and Petrakakis K., 2010. The computation of equilibrium assemblage diagrams with Theriak/Domino software. *American Mineralogist*, **95**(7), 1006–1016, http://dx.doi.org/10.2138/am.2010.3354.

Downs R.T., 2006. The RRUFF Project: An integrated study of the chemistry, crystallography, Raman and infrared spectroscopy of minerals. *19th General Meeting of the International Mineralogical Association*, Kobe, Japan, 23–28 July, 117.

Dymek R.F. and Smith M., 1990. Geochemistry and the origin of Archean quartz-cordierite gneisses from the Gothåbsfjord region, West Greenland. *Contributions to Mineralogy and Petrology*, **105**, 715–730, https://doi.org/10.1007/bf00306536.

Gittos M.F., Lorimer G.W. and Champness P.E., 1976. The phase distributions in some exsolved amphiboles. In H.-R. Wenk, P.E. Champness, J.M. Christie, J.M. Cowley, A.H. Heuer, G. Thomas and N.J. Tighe, Eds., *Electron Microscopy in Mineralogy*, Springer-Verlag, Berlin·Heidelberg, Germany, 238–247, http://dx.doi.org/10.1007/978-3-642-66196-9_16.

Hawthorne F.C., Oberti R., Harlow G.E., Maresch W.V., Martin R.F., Schumacher J.C. and Welch M.D., 2012. Nomenclature of the amphibole supergroup. *American Mineralogist*, **97**(11–12), 2031–2048, http://dx.doi.org/10.2138/am.2012.4276.

Kobayashi T., 2009. Iridescent nuummite. *Gemmology*, **41**, 14–15 [in Japanese].

Laird J. and Albee A.L., 1981. High-pressure metamorphism in mafic schist from northern Vermont. *American Journal of Science*, **281**(2), 97–126, http://dx.doi.org/10.2475/ajs.281.2.97.

Laves F., Nissen H.U. and Bollmann W., 1965. On schiller and submicroscopical lamellae of labradorite, (Na, Ca) $(Si, Al)_3O_8$. *Die Naturwissenschaften*, **52**(14), 427–428, http://dx.doi.org/10.1007/bf00589680.

Leake B.E., Woolley A.R., Arps C.E.S., Birch W.D., Gilbert M.C., Grice J.D., Hawthorne F.C., Kato A., Kisch H.J., Krivovichev V.G., Linthout K., Laird J., Mandarino J., Maresch W.V., Nickel E.H. and Rock N.M.S., 1997. Nomenclature of amphiboles. Report of the Subcommittee on Amphiboles of the International Mineralogical Association Commission on New Minerals and Mineral Names. *European Journal of Mineralogy*, **9**(3), 623–651, http://dx.doi.org/10.1127/ejm/9/3/0623.

McGregor V.R., 1969. Early Precambrian geology of the Godthåb area. *Rapport Grønlands Geologiske Undersøgelse*, **19**, 28–30.

Renfro N., 2011. Gem News International: Nuummite from Mauritania. *Gems & Gemology*, **47**(3), 242–243.

Robinson P., Ross M. and Jaffe H.W., 1971. Composition of the anthophyllite-gedrite series, comparisons of gedrite and hornblende, and the anthophyllite-gedrite solvus. *American Mineralogist*, **56**(5–6), 1005–1041.

Rodgers K.A., Kinny P.D., McGregor V.R., Clark G.R. and Henderson G.S., 1996. Iridescent anthophyllite-gedrite from Simiuttat, Nuuk District, southern West Greenland: Composition, exsolution, age. *Mineralogical Magazine*, **60**(403), 937–947, http://dx.doi.org/10.1180/minmag.1996.060.403.08.

Schmid R., Fettes D., Harte B., Davis E. and Desmons J., 2007. How to name a metamorphic rock. Recommendations by the IUGS Subcommission on the Systematics of Metamorphic Rocks. In D. Fettes and J. Desmons, Eds., *Metamorphic Rocks: A Classification and Glossary of Terms*, Cambridge University Press, Cambridge, 3–15.

Spear F.S., 1980. The gedrite-anthophyllite solvus and the compositional limits of orthoamphiboles from the Post Pond Volcanics, Vermont. *American Mineralogist*, **65**(11–12), 1103–1118.

Spear F.S., 1993. *Metamorphic Phase Equilibria and Pressure-Temperature-Time Paths*. Mineralogical Society of America Monograph, Washington DC, USA, 799 pp.

## The Authors

**Prof. Dr Leander Franz and Prof. Dr Christian de Capitani**
Mineralogisch-Petrographisches Institut
Universität Basel, Bernoullistrasse 30,
CH-4056 Basel, Switzerland
E-mail: leander.franz@unibas.ch

**Tay Thye Sun FGA and Loke Hui Ying FGA**
Far East Gemological Laboratory
12 Arumugam Road #04-02, LTC Building B,
Singapore 409958

**Dr Richard Wirth**
Sektion 4.3: Chemie und Physik der
Geomaterialien, Helmholtz-Zentrum Potsdam,
Deutsches GeoForschungsZentrum GFZ,
Telegrafenberg, D-14473 Potsdam, Germany

## Acknowledgements

We sincerely thank Rex Guo for donating material for this research. We owe great thanks to Dr Nynke Keulen, Karsten Secher and Peter Appel of the Geological Survey of Denmark and Greenland (Copenhagen, Denmark) for providing information on the occurrence of Nuummite in Greenland. Thanks also to Willi Tschudin (Universität Basel) for preparing the thin section and polishing the slice of Nuummite. Finally, thanks to Anja Schreiber (GFZ Potsdam) for the careful preparation of the TEM slices. The manuscript was considerably improved by the suggestions of three anonymous reviewers.

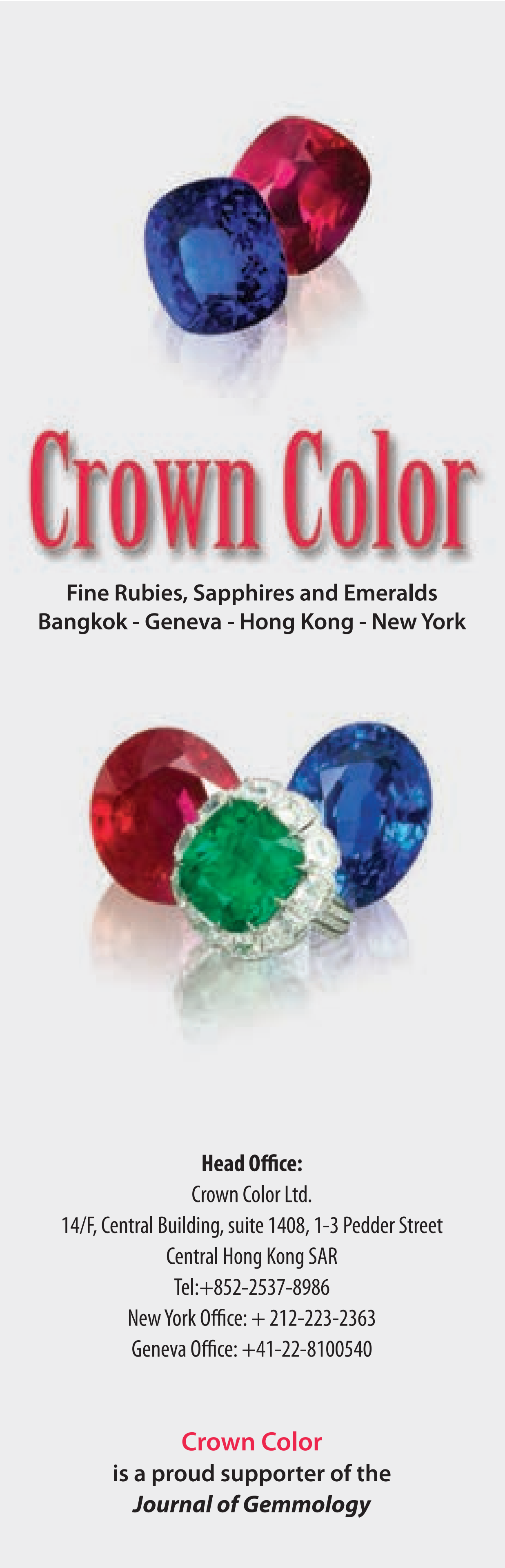

THE TUCSON GEM AND MINERAL SOCIETY PROUDLY PRESENTS:

# THE 63RD ANNUAL
# TUCSON GEM AND MINERAL SHOW®

# Mineral Treasures OF THE MIDWEST

"Cut Fluorite" by [illegible]

"Blue Fluorite" by Orasa Weldon

TUCSON
CONVENTION CENTER
FEBRUARY 9 - 12, 2017

"Cut Stone" by Mark Mauthner

FEATURING:

- RETAIL DEALERS
- SPECIAL & GUEST EXHIBITS
- EDUCATIONAL AREA
- FREE LECTURE SERIES

FOR MORE INFORMATION, VISIT: WWW.TGMS.ORG

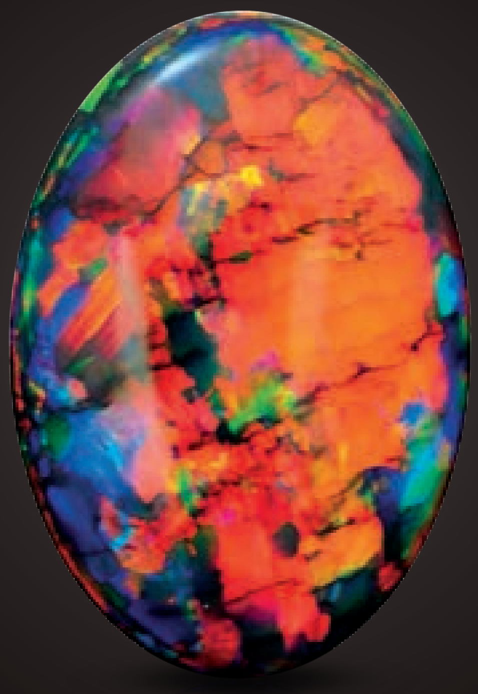

# Conferences

## 2nd European Mineralogical Conference (emc2016)

This relatively new conference took place in Rimini, on the north-east coast of Italy, on 11–15 September 2016 and attracted approximately 700 attendees. A session titled 'Gem Materials' offered 23 contributions (15 talks and eight posters), and the conference also included sessions on 'Diamonds: Open Windows to the Earth's Mantle' and 'Inclusions in Minerals as Record of Geological Processes'. Gemmologically relevant talks and posters that were seen by these authors in the Gem Materials and the Diamonds sessions are summarized below.

The session on Gem Materials opened with keynote speaker **Dr Dan Marshall** (Simon Fraser University, Burnaby, British Columbia, Canada), who revisited the convoluted topic of emerald deposit models and classifications. He reviewed various past efforts and approaches, emphasizing how specific localities can be hard to put into only one deposit type. He proposed a simplified classification with just three types: magmatic (pegmatites without schist), metamorphic (schist without pegmatite) and sedimentary (black shales with veins and breccias).

**Dr Emmanuel Fritsch** (University of Nantes, France) presented the growth factors involved in obtaining gem-quality crystals. A small number of nuclei ensure that only a few crystals will form, which generally grow via spiral dislocations to generate gem-quality crystals (e.g. Figure 1). A small number of gems grow much faster in fibres or dendrites (e.g. *gota de aceite* emeralds and some tourmalines and diamonds). Surface instability during growth induces the capture of inclusions, so optimum growth conditions must be maintained for a relatively short period of time, from a few weeks to a few months at most.

**Dr Peter Bacik** (Comenius University, Bratislava, Slovakia) followed with an overview of selected Cr- and V-bearing gem minerals and materials and their spectroscopic properties in the visible range. He reviewed the influence of bond strength on absorptions related to crystal field transitions of these important colour-causing elements. Differences in crystal structures lead to variations in positions and intensities of the absorptions, and therefore different colours perceived by the human eye.

**Dr Isabella Pignatelli** (CRPG, Vandoeuvre-lès-Nancy, France) presented her investigations of the trapiche-like growth textures in euclase from Colombia. She systematically showed through various avenues of investigation (including X-ray tomography) that although there are similarities in the origins of these textures for emerald and euclase, the term *trapiche* should not be applied to euclase.

*Figure 1: The reflection from a face of this natural topaz crystal (~2 × 2 × 1 cm) from Pakistan highlights a spiral-shaped growth hillock. Most gems grow via such a spiral dislocation mechanism, visible on their crystal faces. Photo by Benjamin Rondeau.*

**Dr Dan Marshall** presented again on emeralds, with new information on mineralization at Poona in Western Australia. Particular attention was given to fluid inclusions and stable isotopes to show that the distinctly zoned crystals have origins that can be tied to alternating crystallization in igneous and metamorphic hydrothermal fluids.

**Dr Gaston Giuliani** (CRPG, Vandoeuvre-lès-Nancy) enthusiastically reviewed his team's ongoing work on marble-hosted pink and red spinel. In particular, he presented oxygen isotope data of spinel from many localities, showing a wide range in values but with three main clusters based on the current dataset. This isotopic data, combined with trace- and minor-element composition (e.g. V, Cr, Fe and Zn), form the beginnings of a database for determining the geographic origin of gem-quality spinel.

**Dr Stefanos Karampelas** (GRS Gemresearch Swisslab AG, Lucerne, Switzerland) provided new data on the detection of heat treatment in tanzanite. Previous criteria have been refined, and attention is being paid to several absorptions in the ultraviolet-visible region that are not attributable to any specific ion or defect presently known.

**Dr Aaron Palke** (Gemological Institute of America [GIA], Carlsbad, California) presented his research on melt inclusions within sapphire from Yogo Gulch, Montana, USA. The melt inclusions are postulated to be the medium from which the sapphires crystallized; however, their bulk chemistry is distinctly different from the ouachitite dyke that hosts the sapphires and is more akin to remnant leucocratic ocelli that are also found in the dyke. This evidence supports the hypothesis by Dahy (1991) in which the lamprophyre has entrained the sapphires as xenocrysts.

**Dr David Turner** (University of British Columbia, Vancouver, Canada) discussed the application of near-field hyperspectral imaging to gem corundum exploration, using the marble-hosted Beluga sapphire occurrence at Nunavut, Canada, as an example. Indicator minerals for corundum mineralization were shown to be detectable by this technique, and the work also revealed additional spectrally active minerals that are genetically related to corundum mineralization. Potential exists to conduct airborne exploration surveys by drone in areas with decent outcrop exposure.

**Dr Benjamin Rondeau** (University of Nantes, France) presented the discovery of a probable new phosphate mineral species as inclusions in quartzite from Mt Ibity, Madagascar. Often referred to as 'blue quartz', it contains the largest-known diversity of inclusions in quartz (over 20 different species), among which lazulite dominates and causes its blue colour. The apparently new mineral is very light pinkish brown and could have a formula corresponding to $Mg_3(Ca,Sr)_2(Al,Fe^{3+})_3(PO_4)_6F$. Only five crystals were found, and the material is awaiting final characterization by X-ray diffraction analysis.

**Dr Ilaria Adamo** (International Gemological Institute, Milan, Italy) discussed the characterization of purplish blue banded chalcedony from Yozgat Province, Turkey. The presence of moganite, a rare variety of silica, is inferred from Raman spectroscopy, and scanning electron microscopy showed an uneven, somewhat porous structure. Both could contribute to light scattering, to which the blue component of the colour is attributed. As Fe is the only impurity found at concentrations above 10 ppm in this material, the authors wonder if it may cause a minor amethyst colour component.

**Dr Boris Chauviré** (University of Nantes, France) developed a model for the formation of opal at Wegel Tena, Ethiopia, now a major producer of this gem. New evidence from field research (16 mines documented) and laboratory studies reinforces the view that the opal formed in a soil. All fossils found in the opal are roots, rather than any other part of plants or other organisms. Oxygen isotope measurements also favour a low-temperature precipitation. Finally, the zoning often seen in the opal—showing a cloudy white rim and a transparent orange centre—has been reproduced in the laboratory. When gem fire opal was soaked in oxalic acid (a reasonable proxy to complex humic acids found in soils) for a few weeks, the same zoning was produced.

**Dr William 'Skip' Simmons** (University of New Orleans, Louisiana, USA) enthusiastically described the new Maine Mineral and Gem Museum in Bethel, Maine, USA. This museum is devoted to the preservation of Maine minerals, gems and historical mining material from this renowned gem pegmatite region. Two major contributors helped assemble the collection with old and newly mined material, sometimes negotiated from other museums and collections outside Maine. Many spectacular gems and mineral specimens are on display, including vividly coloured tourmalines. As an aside, some remarkable meteorite specimens are also on display.

**Ann Pizzorusso** (New York, New York, USA) delved into the historical aspect of gemstones. She took the audience through a series of examples of how gems were represented in ancient texts and what that could reveal about societal values of the time. For example, Dante was shown to have weaved both the mythology and physical properties of gems into some of his texts through both allusions and direct references.

**Dr Valeria Diella** (CNR-IDPA, Milan, Italy) studied massive pink epidote ('clinothulite') from the Val Malenco region in northern Italy (Figure 2). There are two occurrences: the main one at Pizzo Tremoge and

*Figure 2: This pink massive epidote, also known as 'clinothulite', comes from the famous Val Malenco area in northern Italy. The beads in the necklace on the right have a diameter of ~1 cm. Photo by Pietro Nana.*

one of lesser-quality material at Pra Isio, Valtellina, about 10 km away. Both are at high altitude and difficult to reach, but prospecting suggests good potential. The stone occurs in various shades of pink. Its RI is about 1.69, SG is 3.10–3.52, and it is inert to UV radiation. Its pink colour is attributed to traces of manganese.

**M. G. Reid** and **Dr Alan Anderson** (St Francis Xavier University, Antigonish, Nova Scotia, Canada) investigated melting and crystallization in the system $LiAlSi_4O_{10}$–$H_2O$ to provide insights into the crystallization of gem-bearing cavities in granitic pegmatites, which are generally believed to have formed from a volatile-saturated melt in the late stages of pegmatite crystallization. Using video footage from their experiments, they showed *in situ* crystallization in the silicate melt, the aqueous fluid or in both. Some of the crystals that initially grew in the silicate melt continued to grow beyond the melt-fluid interface by the transfer of melt material in the aqueous fluid. Thus they propose that the cavity minerals form in a low-density fluid by rapid diffusion of ions from the residual silicate melt to the growing crystal faces.

In the Diamond session, several communications were of interest to gemmologists. **Dr Hélène Bureau** (Paris-Sorbonne University, France) proposed that the presence of small discrete or isolated volumes of water in carbonate-rich fluids are necessary to grow fibrous, cloudy and coated diamonds in peridotitic or eclogitic environments. She conducted synthetic diamond growth experiments employing mixtures of carbonates, graphite and silicates together with diamond seeds, in the presence of water or saline fluids ($H_2O$-NaCl) between 6–7 GPa at 1,300–1,675°C, for 6 to 30 hours. Water promoted faster diamond growth, which is favourable for the formation of inclusions, as seen in nature. Diamond isotopic signatures near the inclusions corresponded with those of the starting carbonates, indicating that the carbon source for such diamond growth must be carbonates.

**Dr Ingrid Chinn** (De Beers Group Exploration, Johannesburg, South Africa) pointed out two major shortcomings of previous isotopic studies of diamond. Based on a detailed documentation of 198 microdiamonds from Orapa, Botswana, she demonstrated considerable zoning within a single stone: from –24.03‰ in the core to –6.21‰ $\delta^{13}C$ in the rim, and from 40 to 3,196 atomic ppm N in another crystal. Hence, the bulk analyses that comprise the majority of the global isotopic datasets are inappropriate. Furthermore, she established that the carbon isotopic data from inclusion-bearing diamonds is quite different from that of inclusion-free crystals. However, most carbon isotope data come from inclusion-bearing stones and are thus not representative of the entire diamond populations. Clearly, detailed and spatially controlled stable isotopic analyses and fully representative samples are required if the complex origins of diamonds in the mantle are to be understood.

**Dr Paolo Nimis** (University of Padova, Italy) provided the first direct evidence of the common presence of a hydrous silicic fluid surrounding typical eclogitic and peridotitic mineral inclusions (e.g. olivine) in gem-quality diamonds. The fluid film (up to 1.5 μm thick) contains $Si_2O(OH)_6$, $Si(OH)_4$ and molecular $H_2O$. This observation strongly suggests that gem-quality lithospheric diamonds grow in the presence of a water-rich fluid, an idea echoed by several other presentations.

**J. Rudloff-Grund**, a PhD student from the Goethe University Frankfurt, Germany, presented an ongoing study of the inclusions in milky diamonds from Juina, Brazil. The milky areas are filled with octahedral nanoinclusions, appearing optically empty. However, infrared spectroscopy suggests that these voids are actually filled with ammonia.

*Reference*

Dahy J.P., 1991. Geology and igneous rocks of the Yogo Sapphire deposit, Little Belt mountains, Montana. In D.W. Baker and R.B. Berg, Eds., *Central Montana Alkalic Province*, Montana Bureau of Mines and Geology, Special Publication 100, Butte, Montana, USA, 45–54.

*Dr Emmanuel Fritsch (emmanuel.fritsch@cnrs-imn.fr)*
*Institut des Matériaux Jean Rouxel*
*CNRS, Team 6502, University of Nantes, France*

*Dr David Turner*
*University of British Columbia, Vancouver, Canada*

## HRD Antwerp Symposium

The annual HRD Antwerp Symposium was held on 26 September 2016 at Elzenveld in Antwerp, Belgium. About 90 people attended the conference, which was themed 'Inspired by Nature'. **Dr Katrien De Corte**, chief officer of Education & Industry at HRD Antwerp, chaired the event. HRD Antwerp acknowledged the contributions of **Sergey Panchekhin**, managing director of Arcos Belgium, by awarding him the 2016 Certificate of Appreciation. Also, HRD Antwerp celebrates 35 years of education this year, and **Mark Van Bockstael** and **Eddy Vleeschdrager** were honoured for being its founders.

*Figure 3: Dr Ewa Wagner-Wysiecka discusses Baltic amber at the HRD Antwerp Symposium. Photo by Stijn Beckers.*

**Prof. Pierre Cartigny** (CNRS, Institut de Physique du Globe de Paris, France) analysed the 'DNA' of diamonds by using stable isotopes. He illustrated how C and N isotopes can be used to help fingerprint the geological origin of diamond.

**Frederik Degryse** (Dominion Diamond Corp., Toronto, Ontario, Canada) documented the challenges of mining diamonds in Canada's Northwest Territories, and described the sustainable mining practices in use there. He also indicated that the CanadaMark hallmark programme can be used as a verification of Canadian-origin diamonds.

**Dr Ewa Wagner-Wysiecka** (Gdańsk University of Technology, Gdańsk, Poland) summarized the origin, deposits and properties of Baltic amber (Figure 3). She also pointed out the differences between amber (succinite), copal and other resins. In addition, she classified the different types of Baltic amber and mentioned various amber imitations in today's market.

**Thanh Nhan Bui** (Louvain School of Engineering, Université catholique de Louvain, Belgium) described 'gold sheen' sapphire from East Africa. He outlined the exsolution of hematite and ilmenite inclusions to form the sheen in these sapphires and compared them with similar black star sapphires.

**Hans Smellinckx** (Artoos|Hayez, Antwerp) discussed changes in the high-end jewellery industry as a result of the accelerating pace of life that is shaking up the way of doing business and influencing marketing strategies and branding.

**Elke De Greef** (Ibriz, Bellingen, Belgium) explained how to choose the right shape and style of jewellery according to the outline of one's face and the effect the designer aims to achieve.

*Katerina Deliousi (katerina.deliousi@hrdantwerp.com)*
*HRD Antwerp, Belgium*

## Geological Society of America Annual Meeting

This large geoscience conference took place in Denver, Colorado, USA, on 26–28 September 2016. Approximately 7,100 people attended from 48 countries. A session of interest to gemmologists was titled 'Gemological Research in the 21st Century: Characterization, Exploration, and Geological Significance of Diamonds and other Gem Minerals', and was organized/advocated by Dr James Shigley, Dona Dirlam, Dr Wuyi Wang, Dr Barbara Dutrow, Dr Jeffrey Post, Dr Steven Shirey, Dr William 'Skip' Simmons and Dr John Valley. The session was attended by about 220 people, and abstracts are available at https://gsa.confex.com/gsa/2016AM/webprogram/Session40327.html (oral presentations) and at https://gsa.confex.com/gsa/2016AM/webprogram/Session41331.html (posters).

**Dr Jeffrey Post** (National Museum of Natural History, Smithsonian Institution, Washington DC, USA) and co-authors reviewed investigations into the luminescence properties and composition of coloured diamonds. Post emphasized the importance of having access to these rare samples for research via museum collections, such as at the Smithsonian Institution. Some of the notable coloured diamonds that his team has studied include the Hope, the Wittelsbach-Graff, the DeYoung Pink and those in the Cullinan Blue Diamond Necklace.

In a well-illustrated talk, **Dr Christopher 'Mike' Breeding** (GIA, Carlsbad, California, USA) examined the artistic and scientific aspects of diamond fluorescence using DiamondView images. In addition to often being quite attractive in their patterns and colours, such images also reveal the growth history, morphology, defect distribution, and migration of these defects in natural and synthetic diamonds.

**Dr Karen Smit** (GIA, New York, New York, USA) and co-authors described the unusual geologic history of rare bright yellow type Ib diamonds from Sierra Leone. Their research suggests that these diamonds formed via closed-system growth from methane-rich fluids approximately 650 million years ago, and that the presence of unaggregated single nitrogen atoms (the cause of their yellow colour) points to rapid exhumation rates after an extended residence time at temperatures below 700°C.

**D. Graham Pearson** (University of Alberta, Edmonton, Canada) and his co-author studied the composition of fluids trapped as inclusions in diamonds from the Ekati and Diavik mines in Canada, and postulated that saline fluids were key to the enrichment of the base of the lithosphere and the formation of those peridotitic diamonds. The source of the saline fluids appears to be the subducting plate under western North America, prior to the Mesozoic kimberlite eruptions that brought the diamonds to the surface.

**Dr Evan Smith** (GIA, New York) and co-authors characterized the mineral inclusions that rarely occur in a special subgroup of type II diamonds that they termed 'CLIPPIR' (Cullinan-like, large, inclusion-poor, pure [type II], irregular-shaped, resorbed). From a sample set of 73 type IIa diamonds (faceted gemstones and offcuts), they categorized 52 as CLIPPIR stones, and of those, 37 contained metallic inclusions. The most common inclusions consisted of a multiphase assemblage of Fe-carbonate, an Fe-Ni alloy and sulphide segregations. They also identified inclusions of perovskite and majoritic garnet, which suggest ultra-deep formation depths for these diamonds of >360 km, within the mantle transition zone.

**Dr Emmanuel Fritsch** (University of Nantes, France) highlighted the rising number of near-colourless synthetic diamonds in today's market (as melee and larger stones) and also noted that the reliability of melee-sorting machines for separating synthetic diamonds is not well known. He then reviewed various methods that may be helpful toward identifying near-colourless synthetic diamonds, including UV transparency (to separate type IIa samples), short-wave UV phosphorescence (more typical of synthetics), anomalous double refraction (natural diamonds show more strain than synthetics), luminescence patterns (although the differences between natural and synthetic diamonds are becoming more subtle) and photoluminescence spectroscopy (although ultrapure diamonds—whether natural or synthetic—may show no PL features).

**Jullieta Enone Lum** (University of Johannesburg, South Africa) and co-authors geochemically characterized aquamarine from the Erongo Mountains in Namibia and emerald from the Gravelotte-Leydsdorp area in South Africa. Compared to the aquamarines, the emeralds contained greater amounts of Ti, Cr, Sc, Mg and Na.

**Yury Klyukin** and his co-author (Virginia Tech, Blacksburg, USA) reviewed the occurrence of fluid and melt inclusions in gem minerals. Using examples from emerald, diamond, ruby and sapphire, they showed how such inclusions may be useful for identifying natural vs. synthetic origin, indicating heat treatment, differentiating genetic type and giving provenance information.

**Dr Peter Heaney** (Penn State University, University Park, Pennsylvania, USA) and co-authors reported on their study of iridescent specular hematite aggregates from the Andrade mine in Minas Gerais, Brazil (frequently marketed as 'rainbow hematite'). Using a combination of microanalytical techniques, they found that spindle-shaped nanocrystals of hematite comprise a highly porous framework with distances between adjacent crystals of 280–400 nm. This creates a diffraction grating that causes the iridescence.

**Mandy Krebs** (University of Alberta, Edmonton, Canada) and co-authors characterized rubies from Mozambique and Greenland (e.g. Figure 4). They used a new offline LA-ICP-MS technique to obtain a wider range of quantitative trace-element data, and found that rubies from the two deposits showed systematic differences in composition (i.e. plots of Th/Yb vs. Nb/Yb and Zr vs. Ti; see Figure 4). In addition, Sr isotopic values of rubies from the two deposits were distinct, and Pb-Pb age dating of the Green-

*Figure 4: Rubies from Mozambique and Greenland have a similar regional metamorphic-metasomatic origin, but these plots reveal significant variations in some of their trace elements. The dashed lines separate the geochemical fields for each locality, although there is minor overlap in the data.*

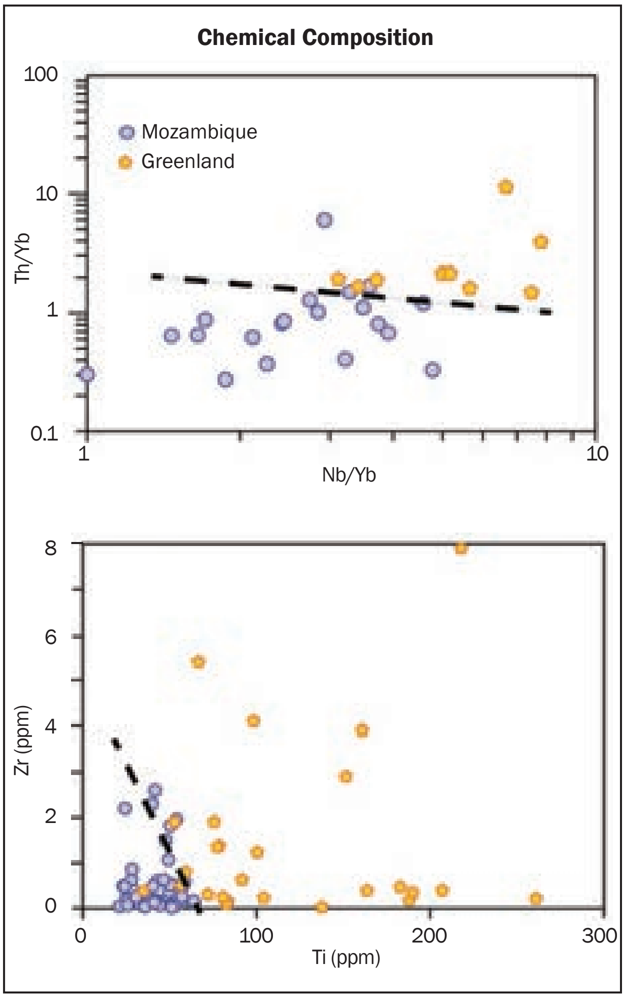

land rubies yielded 2,676 ± 40 million years, which is much older than the Pan-African age assumed for Mozambique rubies.

**Dr Raquel Alonso-Perez** (Harvard University, Cambridge, Massachusetts, USA) and her co-author studied a cabochon-quality emerald deposit (Gilles mine) at Irondro in the Mananjary area of Madagascar. Field and analytical studies show that the emeralds formed in a 'blackwall' alteration zone (amphibolite-phlogopite-rich rocks) situated between a felsic gneiss and a talc-serpentine schist.

**Dr David London** and co-authors (University of Oklahoma, Norman, Oklahoma, USA) reviewed the nature and origins of internal zonation within granitic pegmatites. Understanding the formation of such zonation may aid in the exploration for gem minerals that are hosted by cavities or 'pockets' within such pegmatites. *Brendan M. Laurs*

## Gem-A Conference

The annual Gem-A Conference took place 5–6 November 2016 at the Royal Institute of British Architects in London and was attended by approximately 200 people from 27 countries.

The event was introduced by Gem-A's CEO **Alan Hart**. Then **Ian Harebottle** (Gemfields, London) gave a provocative presentation on the evolution of coloured stones in jewellery design. Although coloured stones are among the first recorded luxury goods, he indicated that they have been trapped in a sector that has shown little meaningful growth in more than 500 years. Using Gemfields' mining projects for emerald, ruby and amethyst as examples, he described efforts to enhance demand for coloured stones through marketing and providing a stable and large enough supply to meet the needs of the industry.

**Jim Clanin** (JC Mining, Bethel, Maine, USA) described his experiences with mining coloured gemstones and mineral specimens at various world localities. He emphasized that each deposit is different and successful exploitation depends on customizing the mining methods for each situation (e.g. surface or underground workings, type of machinery and blasting techniques used). An exciting new development in blasting technology recently became available. Called Autostem, when detonated it causes less damage to the surrounding area (including nearby gem and mineral specimens) and it does not produce any hazardous gases.

**Dr David Fisher** (De Beers Group of Companies, Maidenhead) reviewed the detection of diamond treatments. The need to solve more complex problems has prompted the use of more advanced instrumentation. De Beers is currently investigating a new technique called confocal luminescence depth profiling to scan the intensity of luminescence through the entire thickness of a diamond sample to help with detecting natural irradiation vs laboratory irradiation.

**John Dyer** (John Dyer & Co., Edina, Minnesota, USA) examined the art and science of gem cutting, using photos and video footage to illustrate case studies of successful and unsuccessful outcomes. When evaluating the cut quality of coloured stones, one should beware of rounded or misshapen facets; a girdle that is wavy, too sharp or of variable thickness; lack of facet symmetry or shape; poor polish; and windowed stones. A well-cut gem should show lots of brilliance, but also an attractive contrast pattern that displays a pleasing balance of light and dark areas along with good colour saturation.

**Robert Weldon** (GIA, Carlsbad, California, USA) took the audience on a virtual journey to the Chivor emerald mine, in the footsteps of Peter W. Rainier. Author of the book *Green Fire*, Rainier managed operations at the Chivor mine during some of its most productive times from 1926 to 1931. Some of the famous stones that were produced during Chivor's long history include the Angel of the Andes (987 ct crystal) and the Patricia emerald (632 ct crystal).

**Helen Molesworth** (Gübelin Academy, Lucerne, Switzerland) explored the history of gemstones using various sources of information, including textual (written records), visual (paintings and other pictorial evidence) and physical (artefacts). The earliest use of gems can be traced back to 100,000 BC (shells), while fakes were first used around 400 BC. Later, from the 3rd century BC to the 3rd century AD, there was an increase in the availability and diversity of gem materials that corresponded with the rise of Alexander the Great's empire and the establishment of the Silk Road network of trade routes.

**Dr Michael Wise** (National Museum of Natural History, Smithsonian Institution, Washington DC, USA) described the hiddenite and emerald deposits of North Carolina. At the North American Emerald mine in Hiddenite, both gems occur within hydrothermal veins in the same mining area, but they are never found together in the same cavity. Exploration guides for emerald mineralization include cavities containing limonite (altered siderite) and red (not black) rutile, as well as more complex mineral assemblages than in the hiddenite-bearing cavities.

*Figure 5: Danny Sanchez discusses inclusion photomicrography at the Gem-A Conference. Photo by B. M. Laurs.*

In a multimedia presentation, **Danny Sanchez** (Los Angeles, California) described how he takes dramatic photomicrographs of inclusions in gem materials (e.g. Figure 5). Using a Wild microscope on a vibration reduction table, he employs various lighting accessories (e.g. black foil, reflectors and diffusers) together with fibre-optic lamps that are positioned with the help of friction arms. He generally shoots photos with a 3-mm-wide field of view, and uses image-stacking software to obtain sharp details despite the sometimes large depth of field.

**Pat Daly** (Gem-A, London) described various techniques that are useful for identifying gems and detecting treatments. For example, using a loupe within a polariscope can aid in seeing inclusions and extinction patterns in gems. In addition, a polariscope can be set on the stage of a microscope to help reveal inclusions and even to check their pleochroism.

**Bill Larson** (Palagems.com, Fallbrook, California) chronicled his extensive experience with mining and collecting gems and minerals from pegmatites in San Diego County, California, USA. Within this region, he has worked 14 mines and driven over 36,000 feet (10,970 m) of tunnels for various minerals such as tourmaline, beryl, spodumene and garnet, but he considered only three of the projects successful (i.e. no money lost). Several of these, including the Himalaya mine in Mesa Grande, had been operated since the early 1900s. The Himalaya mine is the largest producer of tourmaline in North America, and of the ~90 tonnes extracted from there, Larson mined ~2.5 tonnes from more than 1,000 pockets in the period 1980–1998.

At the end of the conference, Gem-A president **Maggie Campbell Pedersen** provided an insightful recap of the extensive information presented during the two days.

On 7 November, two workshops were held at Gem-A's headquarters, one on coloured stone grading and pricing (hosted by **Richard Drucker**, Gemworld International Inc., Glenview, Illinois, USA) and the other on visual optics (presented by **Alan Hodgkinson**, Ayrshire, Scotland). That evening marked Gem-A's graduation ceremony and presentation of awards at The Royal College of Surgeons in London.

On 8 November, two separate field trips took attendees for private viewings of the British Crown Jewels and of the Natural History Museum's mineral collection.

*Brendan M. Laurs*

# Gem-A Notices

## GEM-A CONFERENCE

The 2016 Gem-A Conference was held again at Royal Institute of British Architects in Portland Place, London, on 5 and 6 November. A full report of the Conference and events was published in the November/December 2016 issue of *Gems&Jewellery*. Highlights of the presentations are given in the Conferences section of this issue of *The Journal of Gemmology*, pages 347–348.

Seminars and workshops were presented on 7 November at the Gem-A headquarters. Visits were arranged on 8 November to the Mineral Gallery at the Natural History Museum for a guided tour by Gem-A Chief Executive Officer Alan Hart, and to the Tower of London for a private viewing of the Crown Jewels.

### Conference Sponsors

The Association is most grateful to the following for their support:

### Platinum Sponsor

**Jewelry Television (JTV)**
www.jtv.com

### Silver Sponsors

**American Gemological Laboratories (AGL)**
www.aglgemlab.com

**Canadian Gemmological Association**
www.canadiangemmological.com

**École de Gemmologie de Montréal**
http://ecoledegemmologie.com

**Gemfields**
https://gemfields.co.uk

**Gemworld International Inc.**
www.gemguide.com

**Marcus McCallum FGA**
www.marcusmccallum.com

### Bronze Sponsors

**Accredited Gemologists Association**
https://accreditedgemologists.org

**The Rock Hound**
www.therockhound.com

We would also like to thank
**DG3 Diversified Global Graphics Group** for sponsoring conference materials.
www.dg3.com

## GRADUATION CEREMONY

The Graduation Ceremony, sponsored by Gemfields, was held at the Royal College of Surgeons, Lincolns Inn Fields, London, on 7 November.

Alan Hart, CEO of Gem-A, opened the ceremony by welcoming those present. Maggie Campbell Pedersen, President of the Association, gave graduates an inspiring talk before presenting the Gem-A diplomas. Richard Lake, Chair of the Examiners, then announced the winners of the special prizes and awards.

Jack Cunningham, Sustainability Manager of Gemfields, addressed the graduates.

Alan Hart gave the closing remarks before graduates and guests enjoyed a reception in the Hunterian Museum and Surgeons Library at the Royal College of Surgeons.

*Prize winners Héloïse Collin-Randoux, Peter Sandberg, Daisy Welford-Ranson, Kate Flitcroft and Emma Testill, in the Hunterian Museum.*

## GIFTS TO THE ASSOCIATION

The Association is most grateful to the following for their gifts for research and teaching purposes:

**John Bradshaw**, Coast-to-Coast Rare Stones, Nashua, New Hampshire, USA, for rough and offcut samples of adamite from Mexico; amber; anhydrite from Balmat, New York, USA; purple apatite from Karibib, Namibia; aquamarine from Mozambique; axinite from Plumas Co., California, USA, and from Baja California, Mexico; baryte from Silverbond mine, Westmoreland, Stoneham, Colorado, USA, and Namibia; bastnaesite from Pakistan; celestite from Ontario, Canada; cobaltocalcite; datolite from Lanes quarry, Westfield, Massachusetts, USA; hemimorphite from Santa Eulalia, Mexico; hexagonite from New York, USA; hodgkinsonite; kyanite from Brazil; legrandite from Mexico; leucite from Italy; morganite from Nigeria; powellite from Inca de Oro, Chile; prehnite from Australia, Mali and unspecified localities; preobrazhenskite from Kazakhstan; probertite from Germany; sanbornite from Esquire No. 1 mine, Rush Creek, California, USA; senarmontite from Algeria; shomiokite-(Y); siderite; smithsonite from Namibia; sphalerite from Spain; spodumene; tourmaline from Afghanistan and unspecified localities; vesuvianite from Magadi, Kenya; and willemite/leucophoenicite. Faceted samples included purple apatite from Karibib, Namibia; chrome diopside from Russia; oval kornerupine from Tanzania; sapphire in a range of colours from Montana, USA; and xenotime from Zagi Mountain, Pakistan. Also donated were a broken piece of apatite from Madagascar, a cerussite preform from Namibia, diaspore crystal slices from Turkey, as well as synthetic samples of a flux-grown GGG crystal, black moissanite, willemite (hydrothermal) and zincite.

**Jim Clanin**, JC Mining, Bethel, Maine, USA, for a copy of his book *The Fundamentals of Mining for Gemstones and Mineral Specimens*.

**Charles Evans FGA DGA**, London, for three examples of vegetable ivory from *Hyphaene petersiana* (lala palm) from Shingwedzi River, Limpopo Province, South Africa.

**Institut de Gemmologie de Madagascar**, Antananarivo, Madagascar, for a large specimen of epidote crystals on calcite matrix from Andapa, Madagascar.

**Mark Joias**, Joias, Shepton Mallet, Somerset, for 11 jadeite cabochons and one piece of maw-sit-sit.

**Brett Kosnar**, Kosnar Gem Co., Black Hawk, Colorado, USA, for 19 samples of gem rhodochrosite from various localities including rough from N'Chwaning mines, Kuruman, Northern Cape, South Africa; Sweet Home mine, Mount Bross, Colorado, USA; Sunnyside mine group, Gladstone, Colorado, USA; Uchucchacua mine, Oyon, Peru; and Pederneira mine, São José da Safira, Minas Gerais, Brazil. The samples also include cabochons from Capillitas mine, Andalgalá Department, Catamarca, Argentina, and faceted stones from Wutong mine, Guangxi, Zhuang, China.

**Antonio Silva**, London, for a copy of *Emeralds Around the World* by Jules Roger Sauer.

**Anne van der Meulen Cunningham FGA DGA**, Chicago, Illinois, USA, for faceted samples consisting of an amethyst, 13 emeralds, two bicoloured quartzes (smoky–rock crystal), a ruby, a sapphire, a greenish blue spinel, a pale blue synthetic spinel and three blue topazes. Also donated were a pink tourmaline carving, a ruby cabochon and a rough white opal showing play-of-colour, as well as fragments of aquamarine, malaya garnet, rhodolite, blue and yellow sapphire, heated and unheated tanzanite, tourmaline and chrome tourmaline, and tsavorite.

**Beth West**, Bucklebury Common, Berkshire, for a collection of 32 ivory beads and four bone beads.

## GEM-A AWARDS

In the Gem-A examinations held in January and June 2016, 487 students qualified in the Gemmology Diploma examination, including 41 with Distinction and 52 with Merit, and 590 qualified in the Foundation Certificate in Gemmology examination. In the Gem Diamond examination 126 qualified, including 16 with Distinction and 25 with Merit.

The **Tully Medal** is awarded to the candidate who submits the best set of answers in the Gemmology Diploma examinations which, in the opinion of the examiners, are of sufficiently high standard. **Héloïse Collin-Randoux** of Garches, France, was awarded the **Tully Medal**, the **Christie's Prize for Gemmology** for the best candidate of the year, and the **Anderson Bank Prize** for the best set of theory papers.

The **Read Practical Prize** for excellence in the practical examination was awarded to **Daisy Welford-Ranson** of Tadley, Hampshire.

In the Foundation Certificate in Gemmology examination, the **Anderson Medal** for the candidate who submitted the best set of answers which, in the opinion of the examiners, were of sufficiently high standard, was awarded to **Kate Flitcroft** of London.

In the **Diamond Diploma** examination, the **Bruton Medal** for the best set of answers which, in the opinion of the examiners, were of sufficiently high standard, was awarded to **Rachel Bailey** of Edinburgh.

The **Deeks Diamond Prize** for the best set of theory answer papers of the year was awarded to **Emma Testill** of Cannock, Staffordshire.

The **Mok Diamond Practical Prize** for excellence in the Diamond Practical examination, sponsored by Dominic Mok of AGIL, Hong Kong, was awarded to **Peter Sandberg** of Stockholm, Sweden.

The names of the successful candidates are listed below.

## Examinations in Gemmology

### *Gemmology Diploma*

#### Qualified with Distinction

Beauséjour, Joanie, *Longueuil, Quebec, Canada*
Bu Di, *Beijing, P.R. China*
Chedid, Karine, *Paris, France*
Chen Wanzhu, *Beijing, P.R. China*
Collin-Randoux, Héloïse, *Garches, France*
Du Jie, *Beijing, P.R. China*
Du Mingyue, *Beijing, P.R. China*
Dzikowski, Tashia, *Freiburg, Germany*
Fung Chun Yan, *New Territories, Hong Kong*
Hou Yitong, *Beijing, P.R. China*
Hu Zhe, *Beijing, P.R. China*
Khoudian, Christina, *Luton, Bedfordshire*
Li Zi Tian, *Beijing, P.R. China*
Liang Huan, *Beijing, P.R. China*
Liang Lin, *Beijing, P.R. China*
Liu Congyi, *Beijing, P.R. China*
Liu Hao, *Beijing, P.R. China*
Liu Mingyue, *Beijing, P.R. China*
Man Ka Yi, *Wong Tai Sin, Hong Kong*
Peng Jingxin, *Beijing, P.R. China*
Shi Jingzhe, *Beijing, P.R. China*
Thomas, Isaac Matthew David, *Bristol*
Tian Lu, *Beijing, P.R. China*
Viala, Martin, *Montreal, Quebec, Canada*
Vicente, Elisabeth, *Paris, France*
Viguier, Murielle, *Pontault-Combault, France*
Wainer, Stephane, *Singapore*
Wang Ying Ying, *Shanghai, P.R. China*
Wang Yuwei, *Beijing, P.R. China*
Wei Jiarong, *Tangshan, Hebei, P.R. China*
Wu Muyun, *Beijing, P.R. China*
Xu Chang, *Beijing, P.R. China*
Yang Chiyu, *Beijing, P.R. China*
Zhang Cheng, *Beijing, P.R. China*
Zhang Shangqi, *Beijing, P.R. China*
Zhang Zheng, *Beijing, P.R. China*
Zhong Yuanyuan, *Beijing, P.R. China*
Zhou Yan, *Shanghai, P.R. China*
Zhu Jingran, Beijing, P.R. China
Zhu Mengchen, Beijing, P.R. China
Zhu Yun You, *Taoyuan, Taiwan, R.O. China*

#### Qualified with Merit

Chan Wing Chi, *Tsuen Wan, Hong Kong*
Chen Suni, *Fuzhou, Fujian, P.R. China*
Chen Yanran, *Beijing, P.R. China*
Chin Chun-Yu, *Taipei City, Taiwan, R.O. China*
Ding Dong, *Beijing, P.R. China*
Feng Jie, *Beijing, P.R. China*
Fujii, Yuko, *Tokyo, Japan*
Haddad, Zena, *London*
Haniel, Louisa, *London*
Hao Yue, *Beijing, P.R. China*
Hu Wai Ping, *Tin Shui Wai, Hong Kong*
Huang Ying-Yun, *Kaohsiung City, Taiwan, R.O. China*
Lavoie Ste-Marie, Bénédicte, *Montreal, Quebec, Canada*
Lebrun, Amelie, *Bagnolet, France*
Li Dianhui, *Beijing, P.R. China*
Li Jingting, *Beijing, P.R. China*
Li Ying, *Beijing, P.R. China*
Lin Yian-Ting, *Kaohsiung City, Taiwan, R.O. China*
Lin Yucheng, *New Taipei City, Taiwan, R.O. China*
Liu Dan, *Guangzhou, Guangdong, P.R. China*
Liu Di, *Beijing, P.R. China*
Liu Meiying, *Beijing, P.R. China*
Liu Shengpeng, *Beijing, P.R. China*
Nijem, Karmel, *Lézignan-Corbières, France*
Ning Zhenhua, *Beijing, P.R. China*
Pavula, Nathalie, *Châtillon, France*
Petit, Fabienne, *Versailles, France*
Qu Hongting, *Beijing, P.R. China*
Ren Baichen, *Beijing, P.R. China*
Ruan Chentao, *Beijing, P.R. China*
Schintu, Emanuele, *Bologna, Italy*
Somsa-Ard, Nanthaporn, *Bangkok, Thailand*
Sun Ying, *Beijing, P.R. China*
Tai Tianjiao, *Beijing, P.R. China*
Taiclet, Alexia, *Paris, France*
Toche, Claire, *Aubagne, France*
Tsai Tzu-Yin, *New Taipei City, Taiwan, R.O. China*
Villaret Deprez, Christine, *Paris, France*
Wang Han, *Shanghai, P.R. China*
Wu Linjie, *Beijing, P.R. China*
Xu Nan, *Shanghai, P.R. China*
Xu Nijie, *Beijing, P.R. China*

Xu Su, *Chengdu, Sichuan, P.R. China*
Xue Ru, *Shijiazhuang, Hebei, P.R. China*
Yam Man Hung, *Tseung Kwan O, Hong Kong*
Yan Qiu Li, *Beijing, P.R. China*
Yang Jiwen, *Wuhan, Hubei, P.R. China*
Yang Yujiao, *Beijing, P.R. China*
Yuan Zelu, *Beijing, P.R. China*
Yuen Angel, *Tsuen Wan, Hong Kong*
Zhang Chuanzheng, *Liaocheng, Shandong, P.R. China*
Zheng Shuyuan, *Beijing, P.R. China*
Zhou Jin, *Beijing, P.R. China*

### Qualified

Addeo, Juanita, *Heathrow, Florida, USA*
Ahmed, Fazlul, *Kandy, Sri Lanka*
Aiken, Juliette, *London*
Akiyama, Kayo, *Fukuoka, Japan*
Alonso-Perez, Raquel, *Arlington, Massachusetts, USA*
Armengaud, Anne Florence, *Carcassonne, France*
Arredondo, Gabriel, *Geneva, Switzerland*
Arrive, Raphael, *Annecy, France*
Ashri, Atul, *Reading, Berkshire*
Balmer, Isabel, *Derby, Derbyshire*
Barrault, Mathilde, *Angers, France*
Bastien, Ellyn, *Palaiseau, France*
Beardmore, Lindsay Ann, *Walsall, West Midlands*
Bejarano Prieto, Fernando Jose, *Lima, Peru*
Bergamin, Irene, *Zurich, Switzerland*
Bhattarai, Amikar, *Yangon, Myanmar*
Brown, Gareth, *Bristol*
Bu Zhao, *Beijing, P.R. China*
Bullock, Emily, *Birmingham, West Midlands*
Cai Haoyu, *Beijing, P.R. China*
Cai Yiming, *Beijing, P.R. China*
Caldicott, Gary, *Rowley Regis, West Midlands*
Cani Mazin, Sandra, *London*
Cao Han, *Beijing, P.R. China*
Cao Yunyu, *Beijing, P.R. China*
Chan Ching Ching, Hilary, *New Territories, Hong Kong*
Chan Shih, Sally, *Flushing, New York, USA*
Chang Chia-Yu, *Taichung City, Taiwan, R.O. China*
Chang Hui Min, *Taipei City, Taiwan, R.O. China*
Chang Shu-Hua, *New Taipei City, Taiwan, R.O. China*
Chang Siwen, *Beijing, P.R. China*
Chang Yu-Chin, *New Taipei City, Taiwan, R.O. China*
Chao Yan, *Hangzhou, Zhejiang, P.R. China*
Chauveron, Alain, *Bordeaux, France*
Chen Chaoyang, *Dongying, Shandong, P.R. China*
Chen Jing, *Beijing, P.R. China*
Chen Lin-En, *New Taipei City, Taiwan, R.O. China*
Chen Peng-Yu, *Taichung City, Taiwan, R.O. China*
Chen Po Kai, *Kaohsiung City, Taiwan, R.O. China*
Chen Qianyu, *Guangzhou, Guangdong, P.R. China*
Chen Shaohua, *Beijing, P.R. China*
Chen Si, *University Park, Pennsylvania, USA*
Chen Silei, *Shanghai, P.R. China*
Chen Wei-Ting, *Taipei City, Taiwan, R.O. China*
Chen Yu Lu, *Shanghai, P.R. China*
Chen Yuxin, *Beijing, P.R. China*
Chen YuXin, *Guilin, Guangxi, P.R. China*
Chen Zechao, *Shanghai, P.R. China*
Chen Zhiying, *Linhai, Taizhou, Zhejiang, P.R. China*
Cheng Kwok Hoo, Henry, *Quarry Bay, Hong Kong*
Chinotaikul, Chanaporn, *Bangkok, Thailand*
Choi Tsz Ling, *Mongkok, Hong Kong*
Chow Wai Yin, *Central, Hong Kong*
Chu Jiyuan, *Hangzhou, Zhejiang, P.R. China*
Chui Kwan Fung, *Sau Mau Ping, Hong Kong*
Chung Yueh Chi, *Kaohsiung City, Taiwan, R.O. China*
Cong Zhong, *Beijing, P.R. China*
Cossard, Pierre-Edouard, *Paris, France*
Cousins, Julian, *Faversham, Kent*
Cupillard, Bruno, *Besançon, France*
Dai Jialin, *Sanmenxia, Henan, P.R. China*
Dai Jiamin, *Beijing, P.R. China*
Dai Yushan, *Beijing, P.R. China*
Davis, Ruth, *Edinburgh, Midlothian*
Davison, Alexander, *Southend-on-Sea, Essex*
Deng Changjie, *Guangzhou, Guangdong, P.R. China*
Deng Xia, *Shanghai, P.R. China*
Ding Hai Ju, Emily, *Tseung Kwan O, Hong Kong*
Ding Ke, *Beijing, P.R. China*
Dong Huiliang, *Beijing, P.R. China*
Dong Xiaozhen, *Foshan, Guangdong, P.R. China*
Doyle, Robert Charles, *Laval, Quebec, Canada*
Eichler, Alexandre, *Limoges, France*
Evans, Charlotte Louise, *Leeds, West Yorkshire*
Faber, Lily, *London*
Fang Hsing Wen, *Yunlin County, Taiwan, R.O. China*
Farrow, Rachel May, *Saffron Walden, Essex*
Feng Yuning, *Beijing, P.R. China*
Frisnes, Marte, *Bridgnorth, Shropshire*
Fu Yizhu, *Beijing, P.R. China*
Fyzee Farhan, Mohamed, *Tsim Sha Tsui, Hong Kong*
Gao Fang, *Beijing, P.R. China*
Gao Ke, *Sihui, Guangdong, P.R. China*
Gao Lichao, *Beijing, P.R. China*
Gao Nana, *Xuzhou, Jiangsu, P.R. China*
Gao Yubo, *Wuhan, Hubei, P.R. China*
Garcia-Carballido, Carmen, *Tarves, Aberdeenshire*
Geng Huijuan, *Sanmenxia, Henan, P.R. China*
Girardot, Caroline, *Marseille, France*
Gu Shining, *Xiamen, Fujian, P.R. China*
Guilin Yang, *Guilin, Guangxi, P.R. China*
Guljé, Maxime Elise, *Ouderkerk aan de Amstel, The Netherlands*
Guo Dandan, *Beijing, P.R. China*
Guo Han, *Ruili, Yunnan Province, P.R. China*
Guo Wenting, *Beijing, P.R. China*
Guo Zehang, *Shantou, Guangdong, P.R. China*
Haensel, Sebastian, *Basel, Switzerland*
Han Dongdong, *Beijing, P.R. China*
Han Xue, *Beijing, P.R. China*
Hanaki, Yu, *Beppu City, Oita, Japan*
He Huizhen, *Shanghai, P.R. China*
He Min, *Shanghai, P.R. China*
He Tianshu, *Beijing, P.R. China*

Henghui Zhan, *Guilin, Guangxi, P.R. China*
Hirao, Keiko, *Osaka, Japan*
Hou Juncan, *Beijing, P.R. China*
Hou Peng, *Tai'an, Shandong, P.R. China*
Hou Yun Tien, *Kaohsiung City, Taiwan, R.O. China*
Hsieh Meng-Chun, *Taipei, Taiwan, R.O. China*
Huang Han, *Dazhou, Sichuan, P.R. China*
Huang Hongchuan, *Zhejiang Province, P.R. China*
Huang Hsiao-Chuan, *New Taipei City, Taiwan, R.O. China*
Huang Mianzhi, *Traben-Trarbach, Rheinland-Palatinate, Germany*
Huang Shana, *Guilin, Guangxi, P.R. China*
Huang Yang Ting, *Kaohsiung City, Taiwan, R.O. China*
Huang Yi-Chen, *Kaohsiung City, Taiwan, R.O. China*
Huang Yuan, *Shenzhen, Guangdong, P.R. China*
Huang Yudan, *Longyan, Fujian, P.R. China*
Huang Yuzhang, *Guilin, Guangxi, P.R. China*
Hui Yee Mei, *Homantin, Hong Kong*
Hung Erh-Nu, *New Taipei City, Taiwan, R.O. China*
Ichikawa, Yurie, *Chuo-ku, Tokyo, Japan*
Iezaki, Kei, *Nishi, Tokyo, Japan*
Ivanov, Andra Raluca, *London*
Jao, Andy, *Taipei City, Taiwan, R.O. China*
Jayarathne, Ruwini, *Ratmalana, Sri Lanka*
Jia Ru, *Beijing, P.R. China*
Jian Qiu, *Guilin, Guangxi, P.R. China*
Jiang Chenglei, *Beijing, P.R. China*
Jiang Haijing, *Sai Ying Pun, Hong Kong*
Jiang Tao, *Dazhou, Sichuan, P.R. China*
Jie Chen, *Shanghai, P.R. China*
Jing Chen, *Guilin, Guangxi, P.R. China*
Jing Jie, *Tangshan, Hebei, P.R. China*
Kakati, Sushmita, *West Byfleet, Surrey*
Kao Wei Chen, *New Taipei City, Taiwan, R.O. China*
Kenouche, Naguib, *Neuilly-sur-Seine, France*
Khowpong, Charuwan, *Bangkok, Thailand*
Kiilu, Kyalo, *Birmingham, West Midlands*
Klumb, Alexander, *Baden-Württemberg, Germany*
Koosathian, Kanate, *Nonthaburi, Thailand*
Kuo Chia-Ying, *New Taipei City, Taiwan, R.O. China*
Kwan Chi Fai, *Cheung Sha Wan, Hong Kong*
Kwong Chin-Ting, *Chai Wan, Hong Kong*
Kyi, Nan Khine Thazin, *Yangon, Myanmar*
Lai Pin-Miao, *Taipei, Taiwan, R.O. China*
Lai Wenbo, *Guangzhou, Guangdong, P.R. China*
Lai Wing Lam, *Sai Kung, Hong Kong*
Lam Shuk Yi, *Kowloon, Hong Kong*
Lao Qionghui, *Beijing, P.R. China*
Lee, Fiola, *Zurich, Switzerland*
Lee Li-Hsiang, *Douliu City, Taiwan, R.O. China*
Lee Tak Yan, *Tsing Yi, Hong Kong*
Leung Wai Kai, Alexander, *Macau SAR*
Leung Car Ni, *Quarry Bay, Hong Kong*
Leung Ching Han, Estella, *Sheung Shui, Hong Kong*
L'Huillier, Patrice, *Paris, France*
Li Anlong, *Lüliang, Shanxi, P.R. China*
Li Chunyu, *Zhangjiakou, Hebei, P.R. China*
Li Dongyang, *Beijing, P.R. China*
Li Fengyi, *Beijing, P.R. China*
Li Jinjun, *Guilin, Guangxi, P.R. China*
Li Lihui, *Shanghai, P.R. China*
Li Qian, *Beijing, P.R. China*
Li Qidi, *Beijing, P.R. China*
Li Qiong, *Shanghai, P.R. China*
Li Ruoxi, *Beijing, P.R. China*
Li Wenpeng, *Beijing, P.R. China*
Li Yaguang, *Beijing, P.R. China*
Li Yang, *Beijing, P.R. China*
Liang Xi, *Shenzhen, Guangdong, P.R. China*
Liao Guoping, *Beijing, P.R. China*
Liao Ping, *Guangzhou, Guangdong, P.R. China*
Liao Yi Chen, *Taipei City, Taiwan, R.O. China*
Lin Chang Te, *New Taipei City, Taiwan, R.O. China*
Lin Chenlu, *Beijing, P.R. China*
Lin Chih-Yin, *Taichung City, Taiwan, R.O. China*
Lin Sheng Che, *Taipei City, Taiwan, R.O. China*
Lin Ta Wei, *Taichung City, Taiwan, R.O. China*
Lin Ying, *Guilin, Guangxi, P.R. China*
Liu Bingjie, *Chifeng, Neimenggu, P.R. China*
Liu Chang, *Beijing, P.R. China*
Liu Hong Lin, *Kaohsiung City, Taiwan, R.O. China*
Liu Jung-Ting, *Taichung City, Taiwan, R.O. China*
Liu Kunquan, *Shenzhen, Guangdong, P.R. China*
Liu Li, *Zaozhuang, Shandong, P.R. China*
Liu Liyuan, *Guangzhou, Guangdong, P.R. China*
Liu Rui, *Tianjin, P.R. China*
Liu Xiang, *Beijing, P.R. China*
Liu, Yimiao, *Zibo, Shandong, P.R. China*
Liu Yujiao, *Suizhou, Hubei, P.R. China*
Lo Ying-Ting, *Shetou, Changhua, Taiwan, R.O. China*
Lodha, Rahul, *Kalwa, Thane Maharashtra, India*
Logan, Amy, *Birmingham, West Midlands*
Lognay, Lauriane, *Brossard, Quebec, Canada*
Longhurst, Stephanie, *Blandford Forum, Dorset*
Lu Dan, *Zhongwei, Ningxia, P.R. China*
Lu Hanyu, *Taizhou, Jiangsu, P.R. China*
Lu Hao Teng, *Kaohsiung City, Taiwan, R.O. China*
Lu Yina, *Hangzhou, Zhejiang, P.R. China*
Lui Wing-Tak, *New Taipei City, Taiwan, R.O. China*
Luo Shixia, *Guangzhou, Guangdong, P.R. China*
Ma Hongjing, *Beijing, P.R. China*
Ma Ke, *Beijing, P.R. China*
Ma Shuangyi, *Beijing, P.R. China*
Mackie, Annabel, *London*
Maghni, Karim Christophe, *Laval, Quebec, Canada*
Mak Fei-Fei, *Taipei City, Taiwan, R.O. China*
Mali, Batoure, *Niamey, Niger*
Man Koon Ho, *Ma Wan, Hong Kong*
Marquis, Sophie Jessica Annabelle, *Torteval, Guernsey, Channel Islands*
Massolou Mouiry, Ornella Darlaine, *Anatananarivo, Madagascar*
Merckens, Robert, *Heemstede, The Netherlands*
Mohamed Hilmy, Mohamed Fahmy, *Beruwala, Sri Lanka*
Muralidharan, Akilandaeaswari, *Tamil Nadu, India*
Muralidharan, Seshagobal, *Tamil Nadu, India*
Muskin, Sarah, *Fortis Green, London*

Ng Siu Lun, *Kwun Tong, Hong Kong*
Ng Wai Fong, *Lam Tin, Hong Kong*
Olm, Mark C., *Tucson, Arizona, USA*
Ou Minhui, *Beijing, P.R. China*
Ourny, Olivier, *Neuchâtel, Switzerland*
Pachchigar, Yash, *Surat, Gujarat, India*
Packeerally, Aqeelah, *Wattala, Sri Lanka*
Paing, Kyaw Thet, *Yangon, Myanmar*
Palthey, Katherine, *Grasse, France*
Pan Jingwen, *Beijing, P.R. China*
Pan Xin, *Lanzhou, Gansu, P.R. China*
Peng Kuo-Chen, *Zhutian, Taiwan, R.O. China*
Perera, Yasasi, *Sri Jayawardenapura Kotte, Sri Lanka*
Perren, Simon Grantley Dean, *Seven Hills, Queensland, Australia*
Piryns, Oraibi, *Hiesse, France*
Portch, Amanda Victoria, *Surbiton, Greater London*
Pu Zhenxiao, *Shanghai, P.R. China*
Qi Wen, *Beijing, P.R. China*
Qian Wenni, *Shanghai, P.R. China*
Qin Di, *Beijing, P.R. China*
Qin Shu, *Beijing, P.R. China*
Qin Yongda, *Beijing, P.R. China*
Qin Zhinan, *Beijing, P.R. China*
Qiu Ziyun, *Guilin, Guangxi, P.R. China*
Qixiu Li, *Guilin, Guangxi, P.R. China*
Qu Yi, *Qingdao, Shandong, P.R. China*
Rabemanjaka, Mammie Nantenaina Danuta, *Antsirabe, Madagascar*
Rajohson, Tantely Hasina, *Antananarivo, Madagascar*
Rakotomamonjy, Jean Rodriguez, *Antananarivo, Madagascar*
Rastogi, Kushagra, *Uttar Pradesh, India*
Ren, Manfei, *Tokyo, Japan*
Road, Lucy, *London*
Rodwell, Nathalie, *Chiswick, London*
Rueck, Julian, *Anna Paulowna, The Netherlands*
Rytel, Miroslawa, *Staten Island, New York, USA*
Saksirisamphan Rimml, Phornthip, *Näfels, Switzerland*
Sangsawong, Supharart, *Bangkok, Thailand*
Saruwatari, Kazuko, *Tokyo, Japan*
Sasaki, Mina, *Yokohama, Kanagawa, Japan*
Satou, Naoto, *Saitama, Saitama, Japan*
Seneca, Laurent, *Roquebrune, France*
Shepherd, Abby Jayne, *New Plymouth, New Zealand*
Shi Hui, *Shanghai, P.R. China*
Shih Yu Hong, *New Taipei City, Taiwan, R.O. China*
So Yuk Mei, *Tuen Mun, Hong Kong*
Song Danni, *Beijing, P.R. China*
Song Peiming, *Beijing, P.R. China*
Song Wanying, *Beijing, P.R. China*
Stadlin, Sonja Andrea, *Baar, Zug, Switzerland*
Stonley, Fiona, *Birmingham, West Midlands*
Sun Jing, *Tianjin, P.R. China*
Sun Li Chuan, *Taichung City, Taiwan, R.O. China*
Sun Mengdi, *Zaozhuang, Shandong, P.R. China*
Sun Ruizhen, *Wuhan, Hubei, P.R. China*
Sun Yutian, *Beijing, P.R. China*
Sun Yuxin, *Beijing, P.R. China*
Sunga, Mary Josephine Feliciano, *Clifton, New Jersey, USA*
Takagi, Asako, *Kamakura, Kanagawa, Japan*
Tang Haiying, *Beijing, P.R. China*
Tang Yongfang, *Weihai, Shandong, P.R. China*
Tarditi, Carlo, *Alghero, Sardinia, Italy*
Taylor, Gyunel, *London*
Thet Oo, Aung, *Yangon, Myanmar*
Tian Hanchao, *Guiyang, Guizhou, P.R. China*
Tian Jiang, *Beijing, P.R. China*
Tian Rongrong, *Shenzhen, Guangdong, P.R. China*
Tong Yanzhuang, *Xian, Shanxi, P.R. China*
Tonkin, Jennifer, *Croydon, Greater London*
Toque, Nathalie, *Bollène, France*
Triki, Alexandre, *Émerainville, France*
Trivier, Adrien Francois P., *Beloeil, Belgium*
Tsai Pei Ju, *Yuanchang, Yunlin, Taiwan, R.O. China*
Tsang Hon Man, *Tseung Kwan O, Hong Kong*
Tsang Kim Lan, *Tuen Mun, Hong Kong*
Turkman, Claudine, *Montreal, Quebec, Canada*
Venn, Andrea, *Beavercreek, Ohio, USA*
Vogt, Kai-Ludwig, *Leyton, London*
Wang Bing, *Beijing, P.R. China*
Wang Chen-Yu, *New Taipei City, Taiwan, R.O. China*
Wang Dan Dan, *Shanghai, P.R. China*
Wang Jianwei, *Beijing, P.R. China*
Wang Qi, *Qingda, Qingdao, P.R. China*
Wang Shashan, *Chengdu, Sichuan, P.R. China*
Wang Shuaiqiang, *Wulumuqi, Xinjiang, P.R. China*
Wang Tianshi, *Beijing, P.R. China*
Wang Wanxin, *Shantou, Guangdong, P.R. China*
Wang Weiwei, *Beijing, P.R. China*
Wang Xueqing, *Beijing, P.R. China*
Wang Yajue, *Beijing, P.R. China*
Wang Yilei, *Taiyuan, Shanxi, P.R. China*
Wang Zhenzhen, *Zhengzhou, Henan, P.R. China*
Wang Zitong, *Guangzhou, Guangdong, P.R. China*
Weeramong Khonlert, Vararut, *Bangkok, Thailand*
Wei Chang Hsi, *Taipei City, Taiwan, R.O. China*
Wei Guowen, *Guangzhou, Guangdong, P.R. China*
Wei Jinchao, *Beijing, P.R. China*
Welford-Ranson, Daisy, *Tadley, Hampshire*
Wen Dan, *Beijing, P.R. China*
Weng Chih-I, *New Taipei City, Taiwan, R.O. China*
Wo, Tina, *London*
Wo Yixiao, *Guilin, Guangxi, P.R. China*
Wong Hoi Ting, *Sheung Wan, Hong Kong*
Wong Tik, *Kwai Chung, Hong Kong*
Woodfine, Jennifer, *Montreal, Quebec, Canada*
Wu Chien Chi, *New Taipei City, Taiwan, R.O. China*
Wu Chun-Lin, *Taoyuan City, Taiwan, R.O. China*
Wu Jeng Long, *Kaohsiung City, Taiwan, R.O. China*
Wu Jiejun, *Guangzhou, Guangdong, P.R. China*
Wu Ruolin, *Beijing, P.R. China*
Wu Shang-En, *Tainan City, Taiwan, R.O. China*
Wu Shuai, *Beijing, P.R. China*
Xi Wei, *Xuzhou, Juangsu, P.R. China*
Xia Mingqi, *Qingzhou, Shandong, P.R. China*
Xiang Yu, *Chongqing, P.R. China*
Xie Weiyi, *Beijing, P.R. China*

Xie Ziyun, *Beijing, P.R. China*
Xin Meiying, *Dalian, Liaoning, P.R. China*
Xu Fan, *Shanghai, P.R. China*
Xu Yan, *Shanghai, P.R. China*
Xu Yun, *Chengdu, Sichuan, P.R. China*
Yan Xiaochen, *Beijing, P.R. China*
Yang Huanbin, *Guangzhou, Guangdong, P.R. China*
Yang Peiwen, *Shenzhen, Guangdong, P.R. China*
Yang Wan Cheng, *Beijing, P.R. China*
Yang Wenni, *Liuzhou, Guangxi, P.R. China*
Yang Xin, *Beijing, P.R. China*
Yang Yi, *Jinan, Shandong, P.R. China*
Yao Jijun, *Beijing, P.R. China*
Yao Yi Jun, *Shanghai, P.R. China*
Yaqi Zhuang, *Guilin, Guangxi, P.R. China*
Ye Jienan, *Guilin, Guangxi, P.R. China*
Ye Run Ling, *Shenzhen, Guangdong, P.R. China*
Yeh Shu Fen, *Kaohsiung City, Taiwan, R.O. China*
Yeh Ting-Yi, *Taoyuan City, Taiwan, R.O. China*
Yin Zhenzhu, *Poissy, France*
Ying Jian Feng, *Hangzhou, Zhejiang, P.R. China*
Yoda, Yuko, *Tokyo, Japan*
You Ting Ting, *Sydney, New South Wales, Australia*
Yu Jinding, *Suzhou, Jiangsu, P.R. China*
Yu Wen Li, *New Taipei City, Taiwan, R.O. China*
Yu Yihang, *Chibi, Hubei, P.R. China*
Yu Yinglei, *Beijing, P.R. China*
Yuan Renjun, *Yangzhong, Jiangsu, P.R. China*
Zaman, Mariyam, *Swiss Cottage, London*
Zang Bowen, *Qingdao City, Shandong Province, P.R. China*
Zhang Le, *Beijing, P.R. China*
Zhang Lijing, *Beijing, P.R. China*
Zhang Linxue, *Guilin, Guangxi, P.R. China*
Zhang Lu, *Guilin, Guangxi, P.R. China*
Zhang Luqing, *Shenyang, Liaoning, P.R. China*
Zhang Mei, *Beijing, P.R. China*
Zhang Shun, *Guilin, Guangxi, P.R. China*
Zhang Tianqiang, *Hefei, Anhui, P.R. China*
Zhang Tong, *Hengyang, Hunan, P.R. China*
Zhang Xi, *Guilin, Guangxi, P.R. China*
Zhang Xiaole, *Solihull, West Midlands*
Zhang Yi, *Shanghai, P.R. China*
Zhang Zhizheng, *Yantai, Shandong, P.R. China*
Zhao Jing, *Zaozhuang, Shandong, P.R. China*
Zhao Wei, *Guilin, Guangxi, P.R. China*
Zhao Xinyi, *Beijing, P.R. China*
Zhou Ziwei, *Beijing, P.R. China*
Zhou Baojie, *Dongying, Shandong, P.R. China*
Zhou Quan, *Beijing, P.R. China*
Zhou Xinyu, *Langfang, Hebei, P.R. China*
Zhou Yan, *Beijing, P.R. China*
Zhou Yao, *Guangzhou, Guangdong, P.R. China*
Zhou Yurui, *Tianjin, P.R. China*
Zhou Ziyang, *Guangzhou, Guangdong, P.R. China*
Zhu Di, *Beijing, P.R. China*
Zhu Shichao, *Guilin, Guangxi, P.R. China*
Zhu Yuan, *Beijing, P.R. China*
Zhu Zihui, *Beijing, P.R. China*

## *Foundation Certificate in Gemmology*

### Qualified

Adkins, Maiko, *Warabi, Saitama, Japan*
Agrawal, Rohan, *Bardonia, New York, USA*
Albronda, Jeanine, *Amsterdam, The Netherlands*
Amouhay, Fadma, *Saint-Denis, France*
Andriamaheninarivo, Nihry Lanto Colette, *Antananarivo, Madagascar*
Angus, Emily, *Petworth, West Sussex*
Anjomani, Najmeh, *Carlsbad, California, USA*
Armand, Anouck, *Paris, France*
Atikarnsakul, Ungkhana, *Bangkok, Thailand*
Aung, Thet Sandar, *Yangon, Myanmar*
Bai Liping, *Beijing, P.R. China*
Bakshi, Anisha, *Thane West, India*
Ban, Mengshu, *Epsom, Surrey*
Barrault, Mathilde, *Angers, France*
Bastien, Ellyn, *Palaiseau, France*
Becket, Alexandra, *Birmingham, West Midlands*
Beissekova, Zhanna, *London*
Bie Zhi Tao, *Shanghai, P.R. China*
Bigot, Violaine, *Versailles, France*
Boccardo, Laura, *Genova, Italy*
Botella, Rudy, *Fillinges, France*
Botros, Michael Youssef, *Cairo, Egypt*
Bouriaud, Jean Dominique, *La Grande-Motte, France*
Bowkett, Alexandra, *Stroud, Gloucestershire*
Boydell, Emma, *Solihull, West Midlands*
Bridges, Bruce, *Tucson, Arizona, USA*
Brown, Louisa Brigid, *London*
Brown, Natalie, *Burntwood, Staffordshire*
Bruneau, Phuong-Lien, *London*
Buckroyd, Sarah, *Beadle, North Yorkshire*
Buffoni, Claire, *London*
Bupparenoo, Pimtida, *Bangkok, Thailand*
Burnette, Mike, *Kennesaw, Georgia, USA*
Casdagli, Anna Miranda, *London*
Chambers-Quigley, Valerie, *Founex, Switzerland*
Chan Fai, *Tsing Yi, Hong Kong*
Chan Helen, *Tai Po, Hong Kong*
Chan Pak Ling, *Shatin, Hong Kong*
Chan Siu Chung, *Shatin, Hong Kong*
Chan Wai Ki, *Tai Wai, Hong Kong*
Chan Yuen Ling, Agnes, *Sheung Wan, Hong Kong*
Chandrasekara, Nuwan, *Rakwana, Sri Lanka*
Chang Chia-Yu, *Taichung City, Taiwan, R.O. China*
Chang Ching Hsiu, *Pingtung, Taiwan, R.O. China*
Chang Hui Min, *Taipei City, Taiwan, R.O. China*
Chang Yu-Chin, *New Taipei City, Taiwan, R.O. China*
Chanoey, Channarong, *Islington, London*
Chao Yan, *Hangzhou, Zhejiang, P.R. China*
Charles, Rebecca, *Brighton and Hove, East Sussex*
Chau Chui Ping, *Wanchai, Hong Kong*
Chauvin, Alice, *Ventabren, France*
Chemin, Frederick, *Saint-Aubin-lès-Elbeufs, France*
Chen Hao-Cheng, *Keelung, Taiwan, R.O. China*
Chen Jianhua, *Yongchuan, Chongqing, P.R. China*
Chen Jie, *Shanghai, P.R. China*

Chen Lian, *Guilin, Guangxi, P.R. China*
Chen Lu, *Danyang, Jiangsu, P.R. China*
Chen Min, *Fuzhou, Fujian, P.R. China*
Chen Peng-Yu, *Taichung City, Taiwan, R.O. China*
Chen Wei Ci, *Shanghai, P.R. China*
Chen Yao, *Yiwu, Zhejiang, P.R. China*
Chen Yen-Yu, *New Taipei City, Taiwan, R.O. China*
Chen Yu Lu, *Shanghai, P.R. China*
Chen Zechao, *Shanghai, P.R. China*
Chen Zeqi, *Hangzhou, Zhejiang, P.R. China*
Cheng Jui-Chien, *New Taipei City, Taiwan, R.O. China*
Cheng Wen Hsin, *Ksohsiung City, Taiwan, R.O. China*
Chenyang He, *Bangkok, Thailand*
Cheong Lei Mou, *Macau, SAR*
Cheong Nean Chee, *Ipoh, Malaysia*
Cheung Yo Yo, *Tai Po, Hong Kong*
Chiang Ning-En, *Kaohsiung, Taiwan, R.O. China*
Chin Chi Ming, *Taipei, Taiwan, R.O. China*
Chin Chun-Yu, *Taipei City, Taiwan, R.O. China*
Chinotaikul, Chanaporn, *Bangkok, Thailand*
Chiu Kuan-Hao, *Ping Tong Xiang, Taiwan, R.O. China*
Chiu Yi-Ju, *Pingdong County, Taiwan, R.O. China*
Choi Chung Tak, Redi, *Sheung Wan, Hong Kong*
Choi Pak Ka, *Tai Po, Hong Kong*
Choi Yi Ling, *Shatin, Hong Kong*
Chou Hung-Teng, *Taipei City, Taiwan, R.O. China*
Chow Tinyi, *Kowloon, Hong Kong*
Chu Chi Ting, *Sheung Shui, Hong Kong*
Chu Jie Wei, *Shanghai, P.R. China*
Chu Thi Song Ha Lea, *Paris, France*
Combalbert, Laure, *Saint-Cannat, France*
Cooperwaite, Hannah, *Pulborough, West Sussex*
Coquebert de Neuville, Jehan, *Boulogne-Billancourt, France*
Cossard, Pierre-Edouard, *Paris, France*
Cousteix, Raphaelle Marie, *London*
Cuney, Hélène Emilie Stephanie, *Bayern, Germany*
Dai Jingyuan, *Shanghai, P.R. China*
Dai Tiantian, *Birmingham, West Midlands*
Dai Yi Qing, *Shanghai, P.R. China*
Deen, Muhammadh Ashfaq, *Colombo, Sri Lanka*
Ding Lei, *Guilin, Guangxi, P.R. China*
Dobrzanski, Andrew Jan, *Edinburgh, Midlothian*
Dong Jin, *Shanghai, P.R. China*
Dong Xiaozhen, *Foshan, Guangdong, P.R. China*
Dong Yitan, *Dalian, Liaoning, P.R. China*
Drault-Bisaillon, Mathieu, *Longueuil, Quebec, Canada*
Dubois, Nastasia, *Brunoy, France*
Ducrot, Marie Caroline, *Grans, France*
Duerden, Claire, *Great Glen, Leicestershire*
Duffy, Alisha, *Liverpool, Merseyside*
Edmonds, Jessie May, *Witney, Oxfordshire*
Enright, Tara Alexandra, *Wrexham, Wrexham*
Eu Chew, Phang, *Shah Alam, Selangor, Malaysia*
Eyles, Vikki, *Chatham, Kent*
Fabre, Nicolas, *Morteau, France*
Facey, Lynda, *Solihull, West Midlands*
Fan Yuen Yi, *Tin Hau, Hong Kong*
Fang Ning, *Taipei City, Taiwan, R.O. China*
Farkhari, Ashkan, *London*
Fernandez, Gregory, *Marseille, France*
Fernando, Nalin, *Dehiwela, Sri Lanka*
Ferrando, Rossella, *Alessandria, Italy*
Ferrari, Stefania, *Genova, Italy*
Flitcroft, Kate McKenzie, *London*
Fork Wing Yin, *Lam Tin, Hong Kong*
Francey, Daniel, *Auckland, New Zealand*
Fridez, Catherine Marie, *Geneva, Switzerland*
Fu Shu, *Tsimshatsui, Hong Kong*
Fuchino, Izumi, *Urayasu-Shi, Chiba, Japan*
Fukuchi, Yukiko, *Tokyo, Japan*
Fung Hang Shun, Jessica, *Tai Po, Hong Kong*
Fyzee, Mohamed Farhan, *Tsim Sha Tsui, Hong Kong*
Gamlath, Wasantha, *Deraniyagala, Sri Lanka*
Gao Boqiu, *Beijing, P.R. China*
Gao Yu, *Beijing, P.R. China*
Gradwell, Amber, *Cape Town, South Africa*
Granger, Marion, *Paris, France*
Grant, Henrietta, *London*
Green, Francesca, *Exeter, Devon*
Grieve, Elaine Helen, *Hamilton, South Lanarkshire*
Grigorov, Martin, *Shabla, Bulgaria*
Gu Ying, *Shanghai, P.R. China*
Gu Yu, *Beijing, P.R. China*
Guilin Yang, *Guilin, Guangxi, P.R. China*
Guo Cong Hui, *Shanghai, P.R. China*
Guo Hongshu, *Beijing, P.R. China*
Guo Liping, *Urumqi, Xinjiang Uyghur, P.R. China*
Hagiwara, Yusuke, *Tokyo, Japan*
Haniel, Louisa, *London*
Hashizume, Hiroko, *Tokyo, Japan*
Haywood, Paul, *Birmingham, West Midlands*
Hazel, Amandine Julie, *Rochester, Kent*
He Shu, *Fanling, Hong Kong*
Henghui Zhan, *Guilin, Guangxi, P.R. China*
Herdman, Nancy Anne, *Linlithgow, West Lothian*
Hewitt, Isabella, *London*
Hilt, Claudia, *Cannes, France*
Ho Choi Mei, *Tai Po, Hong Kong*
Ho Ka Cheong, *Sham Shui Po, Hong Kong*
Hohberger, Robin, *Veraz, France*
Hong Yuan, *Guangzhou, Guangdong, P.R. China*
Hong Yuk Lin, *Tseung Kwan O, Hong Kong*
Hsieh Meng-Chun, *Taipei, Taiwan, R.O. China*
Hsieh Nga Fong, *Siu Sai Wan, Hong Kong*
Htut, Than, *Yangon, Myanmar*
Hu, Anshu, *Milan, Italy*
Hu Juan Ao, *Shanghai, P.R. China*
Hu Mei Qun, *Wuxi, Jiangsu, P.R. China*
Hu Yajie, *Beijing, P.R. China*
Huang Chun-Hui, *New Taipei City, Taiwan, R.O. China*
Huang Hsiao-Chuan, *New Taipei City, Taiwan, R.O. China*
Huang Hua, *Beijing, P.R. China*
Huang Jing-Kai, *New Taipei City, Taiwan, R.O. China*
Huang Runni, *Guilin, Guangxi, P.R. China*
Huang Siyi, Sylvia, *London*
Huang Ting, *Guilin, Guangxi, P.R. China*

Huang Wenmin, *Guilin, Guangxi, P.R. China*
Huang Yi-Chen, *Kaohsiung City, Taiwan, R.O. China*
Huang Ying-Yun, *Kaohsiung City, Taiwan, R.O. China*
Huang Ziyun, *London*
Huen Tin Yeung, *Tin Hau, Hong Kong*
Hugon, Isabelle, *Amélie-les-Bains, France*
Hui Li, *Guilin, Guangxi, P.R. China*
Hui Pui Sin, *Aberdeen, Hong Kong*
Hui Hiu Wan, *Tseung Kwan O, Hong Kong*
Humbert, Timon, *Lussas, France*
Hung Chun Man, *Kowloon, Hong Kong*
Huo Xiao Yan, *Shanghai, P.R. China*
Inoue, Yuka, *Konosu City, Saitama, Japan*
Issa, Mohamud, *Zoetermeer, The Netherlands*
Ivanov, Andra Raluca, *London*
Jacob, Antoine, *Riedsheim, France*
Ji Sutong, *Beijing, P.R. China*
Ji Yuan, *Beijing, P.R. China*
Jian Qiu, *Guilin, Guangxi, P.R. China*
Jiang Yue Lin, *Shanghai, P.R. China*
Jiao Can, *Guilin, Guangxi, P.R. China*
Jin Hong, *Shanghai, P.R. China*
Jing Chen, *Guilin, Guangxi, P.R. China*
Kabore, Yakouba Saydou, *Antananarivo, Madagascar*
Kaidbey, Samy, *Saint-Lambert, Quebec, Canada*
Kaiyuan Lin, *Guilin, Guangxi, P.R. China*
Kang Junyu, *Linfen, Shanxi, P.R. China*
Karnon, Jude, *Leighton Buzzard, Bedfordshire*
Kawasaki, Kimie, *Tokyo, Japan*
Kennedy, Lisa, *Brick, New Jersey, USA*
Kessrapong, Promlikit, *Bangkok, Thailand*
King, Victoria, *Kings Lynn, Norfolk*
Ko Ka Yin, *Yuen Long, Hong Kong*
Koda, Ayaka, *Chiba, Japan*
Koinuma, Hiroko, *Tokyo, Japan*
Kong Yaqian, *Beijing, P.R. China*
Koosathian, Kanate, *Nonthaburi, Thailand*
Koot, Andor, *Arnhem, The Netherlands*
Koroma, Barickeh Charles Kholifa, *Romford, Essex*
Kotsakou, Iakovina, *Manchester, Greater Manchester*
Kou Guanyu, *Cangzhou, Hebei, P.R. China*
Krawiec, Natalia, *Birmingham, West Midlands*
Kuo Jung-En, *Kao-Hsiung City, Taiwan, R.O. China*
Kwok Yuk Lun, *Tuen Mun, Hong Kong*
Kwong Chi Hei, *Chi Fu Fa Yuen, Hong Kong*
Lacoste, Christel, *Geneva, Switzerland*
Lai Pin-Miao, *Taipei, Taiwan, R.O. China*
Lai Shan Shan, *Kowloon City, Hong Kong*
Lai Tsz Tung, *Kowloon City, Hong Kong*
Lam Fan, *Quarry Bay, Hong Kong*
Lam Hiu Yan, *Kwai Chung, Hong Kong*
Lang Peng Ching, *Singapore*
Lao Fu Wai, *Macau, SAR*
Lasserre, Solange, *Sainte-Mesme, France*
Law How Kwong, *Kowloon, Hong Kong*
Lawanwong, Kwanreun, *Nong Ya Sai, Suphanburi, Thailand*
Le Parc, John, *Mitcham, Greater London*
Lebrun, Amelie, *Bagnolet, France*
Lee Chi Wing, *Sheung Shui, Hong Kong*
Lee Chin Pang, *Shatin, Hong Kong*
Lee, Evelyn Swee Kim, *Auckland, New Zealand*
Lee, Fiola, *Zürich, Switzerland*
Lee, Junyoung, *Seoul, South Korea*
Lee Li-Hsiang, *Douliu City, Taiwan, R.O. China*
Lee Man Hoi, *Tsuen Wan, Hong Kong*
Lee Yi-Chen, *New Taipei City, Taiwan, R.O. China*
Lee Ying Hao, *New Taipei City, Taiwan, R.O. China*
Lee Yuk Ki, *Kwai Chung, Hong Kong*
Leong Chui Fung, *Hung Hom, Hong Kong*
Lerouyer, Ingrid, *Meudon, France*
Leung Kam Wah, *Mei Foo Sun Chuen, Hong Kong*
Leung Sin Man, *Tseung Kwan O, Hong Kong*
Leung Tat Fong, *Sheung Wan, Hong Kong*
Levy, Francoise, *Paris, France*
L'Huillier, Patrice, *Paris, France*
Li Chao, *Guangzhou, Guangdong, P.R. China*
Li Da, *Beijing, P.R. China*
Li Hiu Ying, *Chai Wan, Hong Kong*
Li Junfeng, *Guilin, Guangxi, P.R. China*
Li Meijun, *Beijing, P.R. China*
Li Min, *Guangzhou, Guangdong, P.R. China*
Li Qiang, *Zhuhai, Guangdong, P.R. China*
Li Qiong, *Shanghai, P.R. China*
Li Wing Yin, Polly, *Kowloon, Hong Kong*
Li Yu Chuen, *Tseung Kwan O, Hong Kong*
Li Yuan, *Sanpokong, Hong Kong*
Liang Yiming, *Guangzhou, Guangdong, P.R. China*
Liang Ying, *Guangzhou, Guangdong, P.R. China*
Lim Kang Wei, *Holborn, London*
Lin Aung Htet, *Yangon, Myanmar*
Lin Chi-Chen, *Kaohsiung City, Taiwan, R.O. China*
Lin Chih-Yin, *Taichung City, Taiwan, R.O. China*
Lin Chin-Yen, *New Taipei City, Taiwan, R.O. China*
Lin Hsiu-Chuan, *Kaohsiung City, Taiwan, R.O. China*
Lin Jung-Hsuan, *Birmingham, West Midlands*
Lin Lainey, *Tainan, Taiwan, R.O. China*
Lin Meng-Shin, *Taoyuan City, Taiwan, R.O. China*
Lin Qin, *Shanghai, P.R. China*
Lin Wen Jing, *Mong Kok, Hong Kong*
Lin Yian-Ting, *Kaohsiung City, Taiwan, R.O. China*
Lin Yu Sheng, *Shanghai, P.R. China*
Ling Fang, *Jiaxing, Zhejiang, P.R. China*
Lio Si Wan, *Macau, SAR*
Liping Que, *Singapore*
Lister Kroening, Susan, *Leeds, West Yorkshire*
Liu Guangxin, *Tianjin, P.R. China*
Liu Haowen, *Beijing, P.R. China*
Liu Jiahui, *Guilin, Guangxi, P.R. China*
Liu Jung-Ting, *Taichung City, Taiwan, R.O. China*
Liu Kunquan, *Shenzhen, Guangdong, P.R. China*
Liu Lu, *Shanghai, P.R. China*
Liu Peng, *Beijing, P.R. China*
Liu Shihao, *Shenyang, Liaoning, P.R. China*
Liu Ting, *Shanghai, P.R. China*
Liu Xia, *Ningbo, Zhejiang, P.R. China*
Liu Xiao Ming, *Jinan, Shandong, P.R. China*
Liu Yan, *Beijing, P.R. China*

Liu Yang, *Beijing, P.R. China*
Liu Yazhu, *Changcha, Hunan, P.R. China*
Liyaudeen, Shahl, *Ratnapura, Sri Lanka*
Liyaudeen, Suhail, *Ratnapura, Sri Lanka*
Lorentz, Marc, *Les Cèdres, Quebec, Canada*
Lou Li, *Shanghai, P.R. China*
Lu Suzhu, *Beijing, P.R. China*
Luan Siyu, *Qiqiha'er, Heilongjiang, P.R. China*
Luo Shixia, *Guangzhou, Guangdong, P.R. China*
Lv Nan, *Guilin, Guangxi, P.R. China*
Lv Yan Yan, *Suzhou, Jiangsu, P.R. China*
Ma Chui Ying, *Kowloon City, Hong Kong*
Ma Yiyi, *Changsha, Hunan, P.R. China*
MacLachlan, Sammantha, *Linwood, Renfrewshire*
Mak Fei-Fei, *Taipei City, Taiwan, R.O. China*
Mak Hiu Lam, *Shatin, Hong Kong*
Mak Man Ho, *Wong Tai Sin, Hong Kong*
Mao Xue, *Dalian, Liaoning, P.R. China*
Mares, Ombeline, *Paris, France*
Massolou Mouiry, Ornella Darlaine, *Anatananarivo, Madagascar*
McCabe, Eleanor Elizabeth, *St Helens, Merseyside*
Meera Sahib, Muhammad, *Bangkok, Thailand*
Mendelevich, Nadezhda, *London*
Meng Xuemei, *Beijing, P.R. China*
Meng Ziyuan, *Beijing, P.R. China*
Mengdi Yang, *Guilin, Guangxi, P.R. China*
Millar, Megan Aindrea, *Blairgowrie, Perthshire*
Min, Tin Naing, *Yangon, Myanmar*
Miu Cheuk Yan, *Kwai Chung, Hong Kong*
Mo, May Myint, *Yangon, Myanmar*
Mohamed Nizar, Mohamed Fawasdeen, *Beruwala, Sri Lanka*
Mohamed Nizar, Mohamed Shiham, *Beruwala, Sri Lanka*
Möller, Katharina, *Toronto, Ontario, Canada*
Morath-Gibbs, Raymond, *Peckham, London*
Nakase, Ayako, *Cyuouku, Chiba, Japan*
Nassi, Joshua, *New York, New York, USA*
Nemoto, Anri, *Chiba, Chiba, Japan*
Ng Koon Hang, *Hung Hom, Hong Kong*
Ng Wing Man, *Tsuen Wan, Hong Kong*
Ng Wing Sze, *Sheung Shui, Hong Kong*
Ng Yuen Lam, *Shatin, Hong Kong*
Ng Yuk Ting, *Sham Tseng, Hong Kong*
Nicolo, Rigamonti, *Genova, Italy*
Nielsen, Agnete Dalgaard, *Skane, Sweden*
Nijem, Karmel, *Lézignan Corbières, France*
Ning Huang, *Guilin, Guangxi, P.R. China*
Nishikawa, Shizuka, *Tokyo, Japan*
Offringa, Anne Nienke, *Utrecht, The Netherlands*
Okubo, Yoshihito, *Tokyo, Japan*
Olufson, Elisa, *Corvallis, Oregon, USA*
Oo, Moe Yadanar, *Yangon, Myanmar*
Oprescu, Ashlyn, *Rancho Santa Fe, California, USA*
Oramah, Eucharia Chinelo, *Cairo, Egypt*
Orman, Stephanie Louise, *Huddersfield, West Yorkshire*
Pai, Praveen, *Mumbai, India*
Pang Min Rong, *Suzhou, Jiangsu, P.R. China*
Paramita, Sumarni, *Tsimshatsui, Hong Kong*
Patalano, Ciro Mario, *Aylesbury, Buckinghamshire*
Pate, Kirsten, *Dunoon, Argyll and Bute*
Patel, Hemma, *London*
Pavula, Nathalie, *Châtillon, France*
Pei Yu, *Shenzhen, Guangdong, P.R. China*
Peng Ancheng, *Beijing, P.R. China*
Penlington, Erin Kathryn, *London*
Pirrone, Vincenzo, *Sartirana Lomellina, Italy*
Piryns, Oraibi, *Hiesse, France*
Pla, Ambre, *Loc, Switzerland*
Pona, Oumar Kalifa, *Montreal, Quebec, Canada*
Qing Yuyao, *Beijing, P.R. China*
Qiu Taige, *Beijing, P.R. China*
Qixiu Li, *Guilin, Guangxi, P.R. China*
Quick, Kimberley, *Saltford, Somerset*
Quinn, Danielle Laura, *Lewisham, London*
Quinn, Neassa, *Penge, London*
Rabemanjaka, Mammie Nantenaina Danuta, *Antsirabe, Madagascar*
Rajohson, Tantely Hasina, *Antananarivo, Madagascar*
Rakotomamonjy, Jean Rodriguez, *Antananarivo, Madagascar*
Randall, Richard, *Egleton, Rutland*
Randrianasolo, Tsitohaina Maherinandrianina, *Antananarivo, Madagascar*
Raposo, Ashley, *Oromocto, New Brunswick, Canada*
Rasolonjatovo, Andrianirina R., *Antananarivo, Madagascar*
Ravecca, Roberto, *Genoa, Italy*
Ren An Hui, *Yantai, Shandong, P.R. China*
Ren He, *Beijing, P.R. China*
Ren Yong, *Beijing, P.R. China*
Robertson, Anna, *Sutton Valence, Kent*
Rogerson, Hannah, *Sevenoaks, Kent*
Rossi, Roberta, *Genoa, Italy*
Rowse, Tessa, *London*
Ruiz, Maria-Jose, *Putney, London*
Ruyi Zuo, *Guilin, Guangxi, P.R. China*
Saito, Midori, *Sayama, Saitama, Japan*
Sakai, Kumi, *Kasugai-shi, Aichi, Japan*
Sakai, Masumi, *Ageo, Saitama, Japan*
Salani, Anthony, *Bury St Edmunds, Suffolk*
Saltarelli, Alessandro, *Laval, Quebec, Canada*
Saori, Tsutsumi, *Tokyo, Japan*
Sargsyan, Anna, *London*
Sathyamoorthy, Parthasarathy, *Tamil Nadu, India*
Sathyamurthy, Priyanka, *Panruti, India*
Schneider, Virginia, *Austin, Texas, USA*
Schwab, Christine, *Montreal, Quebec, Canada*
Scott, Harriet, *London*
Sellors, Christopher William, *Ashbourne, Derbyshire*
Sethi, Vikas, *Bangkok, Thailand*
Shen Chia-Sheng, *London*
Shen Ke, *Shanghai, P.R. China*
Shikhare, Lakshmiprasad, *Maharashtra, India*
Shiu Ka Wai, Tazel, *Stanley, Hong Kong*
Simon, Sophie, *Marseille, France*
Siyam, Mohammedi, *Pune, India*

Skipworth, Helen, *Barnetby le Wold, Lincolnshire*
Smeaton, Emily, *London*
Soe, Kendrick Aung, *Yangon, Myanmar*
Song Jian, *Beijing, P.R. China*
Sonoda, Tetsuro, *Fukuoka, Japan*
Sorrentino, Vincenzo, *London*
Spencer, Sally Jane, *Didcot, Oxfordshire*
Stapleton, Rebecca Jane, *Chelmsford, Essex*
Su Shichao, *Guangzhou, Guangdong, P.R. China*
Su Xin Yao, *Yuhuan, Zhejiang, P.R. China*
Sumino, Akiko, *Yokohama, Kanagawa, Japan*
Sun A Nan, *Shanghai, P.R. China*
Sun Jia, *Shanghai, P.R. China*
Sun Jingyao, *Beijing, P.R. China*
Sun Li Chuan, *Taichung City, Taiwan, R.O. China*
Sun Ling, *Shanghai, P.R. China*
Sun Ziyin, *San Diego, California, USA*
Suzuki, Hiroki, *Tokorozawa, Saitama, Japan*
Suzuki, Jessica Eri, *Chichester, West Sussex*
Sz Wing, *Heng Fa Chuen, Hong Kong*
Takeda, Ami, *Namegata, Ibaraki, Japan*
Takuma, Kentaro, *Kofu, Yamanashi, Japan*
Tam Hoi San, *Macau, SAR*
Tam Suk Han, Sara, *Ma On Shan, Hong Kong*
Tanaka, Junko, *Tokyo, Japan*
Tang Jia Yun, *Shanghai, P.R. China*
Tang Lun-Yu, *New Taipei City, Taiwan, R.O. China*
Tang Yao-Jia, *Taipei, Taiwan, R.O. China*
Tarditi, Carlo, *Alghero, Sardinia, Italy*
Taylor, Emily, *London*
Taylor, Gyunel, *London*
Thamrin Ham, Dickson, *Singapore*
Thatcher, Laura, *London*
Thellabura Vithanage, Yoshani, *Baththaramulla, Sri Lanka*
Thomas, Lauren, *Birmingham, West Midlands*
Tian Rongrong, *Shenzhen, Guangdong, P.R. China*
Ting Evon, *Tsuen Wan, Hong Kong*
To Yuen Ming, Tony, *Sai Wan, Hong Kong*
Traechslin, Viviane, *Geneva, Switzerland*
Trivier, Adrien Francois P., *Beloeil, Belgium*
Tsai Cheng Tao, *Kaoshiung, Taiwan, R.O. China*
Tsai Hsin-Chen, *Kaohsiung, Taiwan, R.O. China*
Tsang, Rebecca, *San Marcos, California, USA*
Tsang Yung, *Wanchai, Hong Kong*
Tse Hoi Yan Jay, *Kowloon City, Hong Kong*
Tsen Chung-Lin, *Ksohsiung City, Taiwan, R.O. China*
Tsuboi, Mina, *Tokyo, Japan*
Tsui Yu-Yen, *Ksohsiung City, Taiwan, R.O. China*
Tucker, Rebecca, *Whitby, North Yorkshire*
Tung Chi Ming, *Tsuen Wan, Hong Kong*
Tung Chun-Hsiao, *Douliu City, Taiwan, R.O. China*
Tyser, Hugh, *West Kensington, London*
U Wai Fan, *Mong Kok, Hong Kong*
Usman, Nadia, *London*
Van Bragt-Verhage, Patricia, *Rotterdam, The Netherlands*
Van Heijningen, Tim, *Leiden, The Netherlands*
Van Maris Van Dijk, Michele, *Oxshott, Surrey*
Vane-Wright, Naomi Elizabeth, *Croydon, Greater London*
Vaughan, Emma, *Alresford, Hampshire*
Vayssier, Benedicte, *Pers-Jussy, France*
Venus, Gemma, *Maidstone, Kent*
Vertriest, Wim, *Bangkok, Thailand*
Viala, Martin, *Montreal, Quebec, Canada*
Vidal Del La Blanche, Paula, *Marseille, France*
Vinten, Lance George, *Leigh-on-Sea, Essex*
Vogt, Kai-Ludwig, *Leyton, London*
Von Baeyer, Anne, *London*
Vuillaume-Stap, Charlotte, *Birmingham, West Midlands*
Waldstaedter, Riki, *Vienna, Austria*
Wan Hang Lun, *Burton-upon-Trent, Staffordshire*
Wang Chen-Yu, *New Taipei City, Taiwan, R.O. China*
Wang, Ching-Hsing, *Taichung City, Taiwan, R.O. China*
Wang Dan Dan, *Shanghai, P.R. China*
Wang Haoyu, *Taiyuan, Shanxi, P.R. China*
Wang Jiaying, *Beijing, P.R. China*
Wang Junlan, *Beijing, P.R. China*
Wang Kexin, *Beijing, P.R. China*
Wang Mengheng, *London*
Wang Shashan, *Chengdu, Sichuan, P.R. China*
Wang Shuo, *Beijing, P.R. China*
Wang Wenyi, *Wandsworth, London*
Wang Xi, *Shanghai, P.R. China*
Wang Xiao Ying, *Shanghai, P.R. China*
Wang Xiaoze, *Beijing, P.R. China*
Wang Xueding, *Beijing, P.R. China*
Wang Yanjia, *Baotou, Inner Mongolia, P.R. China*
Wang Ying, *Shanghai, P.R. China*
Wang Ying Ying, *Shanghai, P.R. China*
Wang Yuhua, *Beijing, P.R. China*
Warden-Owen, Beverley, *Llandudno, Conwy,*
Webb, Oliver, *Holt, Norfolk*
Weerakoon, Chathura Sachith, *Ratnapura, Sri Lanka*
Wei Ying, *Qinzhou, Guangxi, P.R. China*
Weng Chih-I, *New Taipei City, Taiwan, R.O. China*
Whittock, Caroline, *Walsall, West Midlands*
Wicker, Joanne, *Ashford, Kent*
Wiesenfelder, Heidi, *Tucson, Arizona, USA*
Wilson, Rose, *Preston, Lancashire*
Win, Than Htike, *Diamond Bar, California, USA*
Win, Yin Nwe, *Yangon, Myanmar*
Wong Ching Man, *Discovery Bay, Hong Kong*
Wong Ka Yee, *Ngau Tau Kok, Hong Kong*
Wong Kwan Wai, Alison, *Kennedy Town, Hong Kong*
Wong Kwong Mei, Ice, *Mongkok, Hong Kong*
Wong Wai Yin, *Sheung Shui, Hong Kong*
Wong Wing Yan, *Kowloon, Hong Kong*
Wong Yik Ling, *Yuen Long, Hong Kong*
Wong Yung Lam, *Yau Tong, Hong Kong*
Wongrawang, Patcharee, *Bangkok, Thailand*
Wu Chun-Lin, *Taoyuan City, Taiwan, R.O. China*
Wu Hong Zheng, *Shanghai, P.R. China*
Wu Min-Hao, *Kaohsiung, Taiwan, R.O. China*
Wu Pei-Chen, *New Taipei City, Taiwan, R.O. China*
Wu Shang-En, *Tainan, Taiwan, R.O. China*
Wu Tsai-Huei, *New Taipei City, Taiwan, R.O. China*

Xi Yifeng, *Taiyuan, Shanxi, P.R. China*
Xia Wen Jing, *Shanghai, P.R. China*
Xianglian Huang, *Guilin, Guangxi, P.R. China*
Xiu Yang, *Shenyang, Liaoning, P.R. China*
Xu Huan, *Shanghai, P.R. China*
Xu Jia Yin, *Yixing, Jiangsu, P.R. China*
Xu Jinping, *Beijing, P.R. China*
Xu Jun, *Shanghai, P.R. China*
Xu Nan, *Shanghai, P.R. China*
Xu Xian, *Shanghai, P.R. China*
Xu Xinyi, *Beijing, P.R. China*
Xu Yeze, *Beijing, P.R. China*
Yamamoto, Akiko, *Tokyo, Japan*
Yan Ya Qing, *Shanghai, P.R. China*
Yan Yan, *Shanghai, P.R. China*
Yan Yufei, *Beijing, P.R. China*
Yang Fan, *Shanghai, P.R. China*
Yang Han, *Guangzhou, Guangdong, P.R. China*
Yang Hao, *Shanghai, P.R. China*
Yang He, *Xinjiang, P.R. China*
Yang Jia Hui, *Shanghai, P.R. China*
Yang Kang, *Shanghai, P.R. China*
Yang Li, *Guangzhou, Guangdong, P.R. China*
Yang Ming-Hsun, *Tainan City, Taiwan, R.O. China*
Yang Rujie, *Beijing, P.R. China*
Yao Yi Jun, *Shanghai, P.R. China*
Yaqi Zhuang, *Guilin, Guangxi, P.R. China*
Ye Qian, *Beijing, P.R. China*
Yeh Ting-Yi, *Taoyuan City, Taiwan, R.O. China*
Yeung Hiu Ying, Rosa, *Fanling, Hong Kong*
Yeung Ka Yan, *Tai Po, Hong Kong*
Yim Cheukying, *Tsing Yi, Hong Kong*
Ying Jian Feng, *Hangzhou, Zhejiang, P.R. China*
Ying Yan Ling, *Shanghai, P.R. China*
Yiu Po Yan, *Tsuen Wan, Hong Kong*
Yoneyama, Hiroki, *Tokyo, Japan*
Young Man Wah, *Central, Hong Kong*
Yu Chen, *Hefei, Anhui, P.R. China*
Yu Chun Ki, Stanley, *Tseung Kwan O, Hong Kong*
Yu Shen, *Tangshan, Hebei, P.R. China*
Yu Wen Li, *New Taipei City, Taiwan, R.O. China*
Yu Yang, *Guilin, Guangxi, P.R. China*
Yu Yi Fen, *Ksohsiung City, Taiwan, R.O. China*
Yuan Yue, *Beijing, P.R. China*
Yuanyuan Qin, *Guilin, Guangxi, P.R. China*
Yvorra, Kevin Philippe Jad, *Montreal, Quebec, Canada*
Zeng Xuexue, *Beijing, P.R. China*
Zgraja, Amy, *London*
Zhai Wen, *Shanghai, P.R. China*
Zhan Shiyu, *London*
Zhang Binyao, *Rui'an, Zhejiang, P.R. China*
Zhang Dongyu, *Beijing, P.R. China*
Zhang Han, *Harbin, Heilongjiang, P.R. China*
Zhang Jing, *Beijing, P.R. China*
Zhang Lan, *Beijing, P.R. China*
Zhang Mengxue, *Guilin, Guangxi, P.R. China*
Zhang Min, *Kunshan, Jiangsu, P.R. China*
Zhang Ming, *Yangzhou, Jiangsu, P.R. China*
Zhang Pei Qin, *Shanghai, P.R. China*
Zhang Shen, *Beijing, P.R. China*
Zhang Xiaojun, *Taiyuan, Shanxi, P.R. China*
Zhang Xiwen, *Guilin, Guangxi, P.R. China*
Zhang Yiqi, *Guangzhou, Guangdong, P.R. China*
Zhang Yutong, *Beijing, P.R. China*
Zhao Chen, *Beijing, P.R. China*
Zhao Jing, *Shanghai, P.R. China*
Zheng Hao Ru, *Shanghai, P.R. China*
Zhou Shu Hui, *Shanghai, P.R. China*
Zhou Xinying, *Beijing, P.R. China*
Zhou Yan, *Shanghai, P.R. China*
Zhou Yao, *Guangzhou, Guangdong, P.R. China*
Zhou Yixin, *New York, New York, USA*
Zhou Yu Xing, *Suzhou , Jiangsu, P.R. China*
Zijian Wang, *Guilin, Guangxi, P.R. China*
Zou Jing, *Beijing, P.R. China*
Zou Xinming, *Guangzhou, Guangdong, P.R. China*

## Diamond Diploma Examination

### Qualified with Distinction

Bailey, Rachel, *Edinburgh, Midlothian*
Browne, Carolyn, *West Ruislip, Hertfordshire*
Caldicott, Gary, *Rowley Regis, West Midlands*
Chater, Melanie Dawn, *Spratton, Northamptonshire*
Cheung Yuk Yin, *Tai Po, Hong Kong*
Elkington, Edwina, *London*
Gyde, John Mark Andrew, *Abingdon, Oxfordshire*
Knight Bruce, Vita, *London*
Landmark, Vivienne, *Maleny, Queensland, Australia*
McKinley, Karen L., *Milton Malsor, Northamptonshire*
Muralidharan, Akilandaeaswari, *Tamil Nadu, India*
Muralidharan, Seshagobal, *Tamil Nadu, India*
Ramadan, Amr Elsaid A. H., *West Hendon, London*
Wong Lai Sze, *Hong Kong*
Wright, William, *Mill Hill, London*
Zhou Hui, *London*

### Qualified with Merit

Akintayo, Olusegun, *Chatham, Kent*
Ashton-Konig, Oscar Ruben, *Hove, East Sussex*
Beissekova, Zhanna, *London*
Charavda, Sneha, *Leicester, Leicestershire*
Chik Yim Ting, *Kwai Chung, Hong Kong*
Choi Wai Hung, *Sheung Shui, Hong Kong*
Craig, Deborah Susan, *Sundbyberg, Sweden*
Evans, Charlotte Louise, *Leeds, West Yorkshire*
Hancock, Bethany, *Bristol*

Kwok Ka Man, *Mongkok, Hong Kong*
Kwok Pui Sheung, *Tsuen Wan, Hong Kong*
Lo Hoi Shan, *Yuen Long, Hong Kong*
Marcok, David, *Aylesbury, Buckinghamshire*
Megchelsen, David Albert Adriaan, *Sliedrecht, The Netherlands*
Ng Ming Chu, *Yuen Long, Hong Kong*
O'Sullivan, Ryan, *Nottingham, Nottinghamshire*
Rastogi, Kushagra, *Uttar Pradesh, India*
Richardson, Andree Joanna, *Waltham Chase, Hampshire*
So Sau Man, Bernadette, *Tsuen Wan, Hong Kong*
Testill, Emma, *Cannock, Staffordshire*
Wong Hiu Ying, *Yuen Long, Hong Kong*
Ye Haitao, *Birmingham, West Midlands*
Yung Yat Kwok, *Yuen Long, Hong Kong*
Zatikyan, Andranik, *London*
Zhang Shengnan, *Beijing, China*

### Qualified

Abbassi, Matin, *Birmingham, West Midlands*
Adamov, Alexander, *London*
Ainslie, Joshua, *Wellington, Somerset*
Akaoui Chackal, Marco, *Cairo, Egypt*
Anand, Gurleen Kaur, *London*
Au Yeung Sar Kin, *Un Chau, Hong Kong*
Bailey, Kim, *Telford, Shropshire*
Beckley, Stewart, *Bethnal Green, London*
Bell, Astrid, *London*
Benfield, Emma, *Winchester, Hampshire*
Chan Kam Yeung, *Yau Yat Chuen, Hong Kong*
Chan Sin Tung, Corliss, *Tin Shui Wai, Hong Kong*
Chan Wai Lap, *Yau Ma Tei, Hong Kong*
Chen Keming, *Beijing, P.R. China*
Chen Zeqi, *Beijing, P.R. China*
Cheung Wai Yee, *Sheung Shui, Hong Kong*
Cheung Yee Ki, Doris, *Ngau Tau Kok, Hong Kong*
Chien, Sabrina, *Central, Hong Kong*
Chin Chun-Yu, *Taipei City, Taiwan, R.O. China*
Chiu Yu Pik, *Mongkok, Hong Kong*
Cho Shuk Ping, *Hung Hom, Hong Kong*
Chow Siu Ling, Aggie, *Ting Shui Wai, Hong Kong*
Chua Belen, *North Point, Hong Kong*
Ciuche, Octavian, *London*
Clohessy-Brown, Amber, *Birmingham, West Midlands*
Cutmore, Joanne, *Faringdon, Oxfordshire*
Dai Jiamin, *Beijing, P.R. China*
Fattal, Nancy, *London*
Finnemore, Hannah, *Norwich, Norfolk*
Frandgie, Marushka Tehani Sidney, *Wandsworth, London*
Fronczak-Jabbal, Joanna Natalia, *Birmingham, West Midlands*
Geng Meng, *Beijing, P.R. China*
Herries, Jane Denise, *Castle Douglas, Kirkcudbrightshire*
Ho Chin Ching, *Tai Kok Tsui, Hong Kong*
Ivanov, Andra Raluca, *London*
Ktisti, Nicole, *Palmers Green, London*
Lam Ching Fei, *Shatin, Hong Kong*
Lam Hou Kai, *Macau SAR*
Lau Po Chi, *Tuen Mun, Hong Kong*
Law Hoi Ying, *Tai Po, Hong Kong*
Layton, Janina Sarah, *London*
Lee, Fiola, *Zürich, Switzerland*
Leung Lai Man, *Hung Hom, Hong Kong*
Liu Sui Chung, *Sheung Shui, Hong Kong*
Liu Yuqian, *Beijing, P.R. China*
Lo Shuk Ching, *Sham Shiu Po, Hong Kong*
Ma Jing, *Beijing, P.R. China*
Ma Kwan Yu, *Shatin, Hong Kong*
Ma Suk Fong, Cecilia, *Shatin, Hong Kong*
Ma Suk Yan, Suanne, *Tuen Mun, Hong Kong*
Ma Tsing Ping, *Ngau Tau Kok, Hong Kong*
Mak King Man, *Aberdeen, Hong Kong*
Man Ka Yi, *Wong Tai Sin, Hong Kong*
Morath-Gibbs, Raymond, *London*
Pan Haixia, *Beijing, P.R. China*
Parks, Guy Sonny, *Brighton, East Sussex*
Poulsom, Ben, *Farnham, Surrey*
Rice, Jennifer, *Hull, East Yorkshire*
Robino Rizet, Maria Bruna, *London*
Shevlin, Heather Jane, *Stone, Staffordshire*
Sicolo, Emma, *Bristol*
Sit Shan Na, *Tseung Kwan O, Hong Kong*
So Lok Wai, Winnie, *Kowloon, Hong Kong*
Springe, Karl, *Sollentuna, Sweden*
Springham, Melvin, *Berlin, Germany*
Sze Ching Man, Suki, *Shatin, Hong Kong*
Tan, Gabriel, *Singapore*
Tang Yeung, *Fanling, Hong Kong*
Taylor, Emily, *London*
Togores Romeu, Covadonga, *Galicia, Spain*
Tsang Hon Wah, *Hong Kong*
Tse Ying Kit, *Fanling, Hong Kong*
Tu En, *Taipei City, Taiwan, R.O. China*
Waters, Renee, *Wembley Downs, Western Australia, Australia*
Wolff, Caitlin, *Flagstaff, Arizona, USA*
Wong Hong Kit, *Yau Ma Tei, Hong Kong*
Wong Shu Hung, *Chai Wan, Hong Kong*
Wong Tsz Yan, *Shawkiwan, Hong Kong*
Wong Nga Wai, *Kwai Fong, Hong Kong*
Wu Chun-Lin, *Taoyuan City, Taiwan, R.O. China*
Wu Hiu Yan, Daisy, *Sai Ying Pun, Hong Kong*
Xue Jie, *Shatin, Hong Kong*
Yim Mei See, Maisy, *Tuen Mun, Hong Kong*
Zhan Shiyu, *London*
Zhang Le, *Beijing, P.R. China*
Zhao He, *Beijing, P.R. China*
Zisis, Vasileios, *London*

# MEMBERSHIP

At a meeting of the Council held on 7 September 2016, Justine Carmody was elected Chair of the Council. The following were elected to membership:

### *Fellowship and Diamond Membership*

Woodmansterne, Chloë Elinor, *St Albans, Hertfordshire*

### *Associate Membership*

Durand, Jennifer, *Burton upon Trent, Staffordshire*
Khourie, Kaylan, *Johannesburg, South Africa*
Pulese Aulehla, Herbert, *London*
Vasseur, Chantal, *Rixensart, Belgium*

At a meeting of the Council held on 7 November 2016, the following were elected to membership. Also Diploma graduates of the examinations held in June 2016 (included in the lists on pages 351–361) were elected or transferred to Fellowship and/or Diamond Membership as appropriate.

### *Associate Membership*

Bosack, Carol, *London*
Bubber, Karan, *Derby, Derbyshire*
Cullinan, Mark, *Monte Carlo, Monaco*
Gilbert, Denise, *Lowestoft, Suffolk*
Johnston, Wothaya Esther, *Middleton, Milton Keynes, Buckinghamshire*
Karnon, Jude, *Leighton Buzzard, Bedfordshire*
Keighley, Kimberly, *Round Rock, Texas, USA*
Kiefel, Philipp, *Sant Cugat del Vallès, Spain*
Kielbinska, Karina, *London*
Madivila, Kasun, *Beruwala, Sri Lanka*
Sun Ziyin, *San Diego, California, USA*

# OBITUARY

## Sheila O. Greatwood

### 1946–2016

*It is with deep regret that we announce the death of Sheila Greatwood FGA (D. 1982), Mitcham, Surrey, on 27 September 2016. Sheila had been a Gemmology Foundation examiner since 2004. Following are two tributes to her.*

It came as a huge shock to hear from Sheila's husband John that she had died suddenly while playing table tennis with him. They had enjoyed 49 years of an exceptionally happy marriage.

I first met Sheila and John in the early 1980s when they started coming to Alan Jobbins' Post Diploma Class at John Cass—far more a club than a class!

I (and I think everyone) was immediately struck by their huge enthusiasm for gemmology. Enthusiasm was normal for the members of the class, but they coupled it, considerably more than most of us, with the practical application of their knowledge. They both frequented gem markets, and there are many legendary tales of their extraordinary talent for spotting interesting and rare stones that the vendors had no idea about.

Sheila and John were licensed dealers and breeders of reptiles, and I think all who were part of the class with them will remember the lizards and snakes that would occasionally appear out of Sheila's handbag. I well remember being persuaded, admittedly very reluctantly, to stroke the head of a snake that Sheila was holding. To my great surprise it was cool and dry, and really quite pleasant.

They both became part of the Jobbins gemmological social scene, and came on the famous (or perhaps now infamous) trip to Idar-Oberstein arranged by Alan and Evelyne Stern.

Both Sheila and John went on to become Gem-A examiners, a role from which Sheila, with her great practical experience, will now be sorely missed. We all do hope that John will continue as an examiner for many years.

Outside gemmology, Sheila only retired last year (I am told at the third attempt) from a full-time job in NHS family planning. She continued her lifelong passion for cycling (their tandem was famous, although I never discovered which of them pedalled most), and was for very many years secretary of the local cycling association. She was a keen horse rider and owned a horse, Magic, that John gave her, who was part of the family for 20 years. Like everything she did, she took riding seriously and even competed in dressage in the hallowed arena at Hickstead. Magic was eventually succeeded by a new horse, Diamond.

In the last 15 years both Sheila and John practised freediving, an extreme sport that I will not describe, as even thinking about it makes me feel queasy.

Sheila and John had two sons, and it is a mystery how, amongst all her other activities (and there were many that I haven't mentioned) she had time to be a mother. She also leaves four much-loved grandchildren.

Sheila was truly an exceptional character, and the world will be the lesser without her, but all of us will remember her and feel privileged to have been able to call her a friend. *Nigel Israel*

Although I had known Sheila for a long time, I really only got to know her well when she became a Foundation examiner. She very rapidly took to this and, despite her own deep knowledge of practical gemmology, she could always see the questions from the point of view of the inexperienced student. She was more saddened than exasperated when students lost marks for careless mistakes. Sheila willingly gave up her only day off to attend meetings to set the questions for the next year's papers. At these meetings, which can be quite tedious, she was unfailingly cheerful and always ready with new suggestions for questions, but at the end of a long day she was always keen to get home to see her horse, and John of course.

Her fellow examiners will greatly miss her wise counsel and her friendship. Sheila was truly a delight to work with. We shall not forget her.

*Tony Allnutt*
*Chief Examiner*

## Thank You, Guest Reviewers

The following individuals served as guest reviewers during the past publication year. The editors extend their special thanks to all of them for lending their expertise to reviewing manuscripts submitted to *The Journal*. Together with the Associate Editors, these individuals have enhanced the quality of *The Journal* through their knowledge and professionalism.

**Dr Ahmadjan Abduriyim**
Gemological Institute of America, Tokyo, Japan

**Dr Christopher 'Mike' Breeding**
Gemological Institute of America, Carlsbad, California, USA

**Maggie Campbell Pedersen**
*Organic Gems*, London

**Jean-Pierre A. Chalain**
Swiss Gemmological Institute SSEF, Basel, Switzerland

**Dr Ulrika D'Haenens-Johansson**
Gemological Institute of America, New York, New York, USA

**Dr Barbara L. Dutrow**
Louisiana State University, Baton Rouge, Louisiana, USA

**Dr Ian C. Freestone**
UCL Institute of Archaeology, London

**Dr Gaston Giuliani**
Centre de Recherches Pétrographiques et Géochimiques, Vandoeuvre-lès-Nancy, France

**Dr Christoph Hauzenberger**
University of Graz, Austria

**Richard W. Hughes**
Lotus Gemology Co. Ltd., Bangkok, Thailand

**Dr Mary Johnson**
Mary Johnson Consulting, San Diego, California, USA

**Anette Juul-Nielsen**
Ministry of Mineral Resources, Nuuk, Greenland

**Dr Çiğdem Lüle**
Gemworld International Inc., Glenview, Illinois, USA

**Dr Sally Eaton-Magaña**
Gemological Institute of America, Carlsbad, California, USA

**Franck Notari**
GGTL Laboratories, Geneva, Switzerland

**Dr Benjamin Rondeau**
Centre National de la Recherche Scientific, University of Nantes, France

**Dr Andy Shen**
China University of Geosciences, Wuhan, China

**Sutas Singbamroong**
Dubai Gemstone Laboratory, United Arab Emirates

**Dr Frederick L. Sutherland**
Port Macquarie, Australia

**Dr Dedo von Kerssenbrock-Krosigk**
Glasmuseum Hentrich, Museum Kunstpalast, Düsseldorf, Germany

**Dr Markus Wälle**
ETH Zürich, Switzerland

# Learning Opportunities

## CONFERENCES AND SEMINARS

**Jewelry Industry Summit**
29–30 January 2017
Tucson, Arizona, USA
www.jewelryindustrysummit.com

**Somewhere In The Rainbow's 'A Modern Gem & Jewellery Collection'**
31 January 2017–January 2018
Tucson, Arizona, USA
Email shelly@somewhereintherainbow.com
*Note:* Contains a selection of historical gemmological instruments from Gem-A's collection.

**AGTA Gemfair**
31 January–5 February 2017
Tucson, Arizona, USA
www.agta.org/tradeshows/gft-seminars.html
*Note:* Includes a seminar programme.

**AGA Tucson Conference**
1 February 2017
Tucson, Arizona, USA
www.accreditedgemologists.org/currevent.php

**The 38th Annual Tucson Mineral Symposium: Mineral Treasures of the Midwest**
11 February 2017
Tucson, Arizona, USA
www.friendsofmineralogy.org/symposia.html

**Hasselt Diamond Workshop 2017 (SBDD XXII)**
8–10 March 2017
Hasselt, Belgium
www.uhasselt.be/sbdd

**Amberif International Fair of Amber, Jewellery and Gemstones**
22–25 March 2017
Gdańsk, Poland
www.amberif.amberexpo.pl/title,PROGRAMME,pid,3275.html
*Note:* Includes a seminar programme.

**American Gem Society International Conclave**
5–8 April 2017
Hollywood, California, USA
www.americangemsociety.org/Content/uploads/Conclave2017RFP.pdf

**14th Annual Sinkankas Symposium—Sapphire**
8 April 2017
Carlsbad, California, USA
www.sinkankassymposium.net

**Scottish Gemmological Association Conference**
28 April–1 May 2017
Stirling, Scotland
www.scottishgemmology.org/conference

**3rd Mediterranean Gemological and Jewellery Conference**
11–14 May 2017
Syracuse, Italy
www.gemconference.com
*Note:* The conference theme is coloured diamonds, and the program will include several speakers, a round table discussion, pre-conference workshops, and a poster competition.

**The 31st Annual Santa Fe Symposium**
21–24 May 2017
Albuquerque, New Mexico, USA
www.santafesymposium.org

**2017 Society of North American Goldsmiths (SNAG) Conference**
24–27 May 2017
New Orleans, Louisiana, USA
www.snagmetalsmith.org/events/nexus-2017

**11th International Conference on New Diamond and Nano Carbons**
28 May–1 June 2017
Cairns, Australia
http://ndnc2017.org

**JCK Las Vegas**
5–8 June 2017
Las Vegas, Nevada, USA
http://lasvegas.jckonline.com/Events/Education/Education
*Note:* Includes a seminar programme.

**Association for the Study of Jewelry and Related Arts (ASJRA) Annual Conference**
9–10 June 2017
Boston, Massachusetts, USA
www.jewelryconference.com

**PEG2017—8th International Symposium on Granitic Pegmatites**
13–15 June 2017
Kristiansand, Norway
www.nhm.uio.no/forskning/aktuelt/arrangementer/konferanser-seminarer/peg2017

**Scandinavian Gem Symposium 2017**
17–18 June 2017
Kisa, Sweden
http://sgs.gemology.se/#home

**Sainte-Marie-aux-Mines Mineral & Gem Show**
22–25 June 2017
St Marie, France
www.sainte-marie-mineral.com/english/modules/cultural-activities
*Note:* Includes a seminar programme.

Compiled by Angharad Kolator Baldwin and Brendan Laurs

**Tourmaline 2017**
23–28 June 2017
Nové Město na Moravě, Czech Republic
www.tourmaline2017.cz

**Swiss Gemmological Society Conference and European Gemmological Symposium 2017**
29 June–1 July 2017
Zermatt, Switzerland
www.gemmologie.ch

**Northwest Jewelry Conference**
11–13 August 2017
Seattle, Washington, USA
www.nwjcon.com

**28th International Conference on Diamond and Carbon Materials (DCM 2017)**
3–7 September 2017
Göteborg, Sweden
www.diamond-conference.elsevier.com

**Hong Kong Jewellery & Gem Fair**
13–19 September 2017
Hong Kong
http://tinyurl.com/hbn8y56
*Note:* Includes several seminar programmes.

**11th International Kimberlite Conference**
18–22 September 2017
Gaborone, Botswana
www.11ikc.com
*Note:* Pre- and post-conference field trips will visit diamond deposits in Botswana and neighbouring countries.

**World of Gems Conference V**
23–24 September 2017
Rosemont, Illinois, USA
gemguide.com/events/world-of-gems-conference
*Note:* Will include a poster session.

# EXHIBITIONS

## Europe

**The Spectacular Second Empire, 1852–1870**
[includes Mellerio dits Meller jewellery]
Until 15 January 2017
Musée d'Orsay, Paris, France
http://tinyurl.com/jxp82x5

**Eva's Beauty Case: Schmuck und Styling im Spiegel der Zeiten (Jewelry and Styling Through the Ages)**
Until 22 January 2017
LVR–LandesMuseum Bonn, Germany
www.landesmuseum-bonn.lvr.de/de/ausstellungen/evas_bauty_case/evas_beauty_case.html

**Illuminations—Earth to Jewel**
Until 1 February 2017
Musée de Minéralogie MINES ParisTech, Paris, France
www.musee.mines-paristech.fr/Events/TempExhibit/Illuminations

**Elements: From Actinium to Zirconium**
Until 26 February 2017
Ulster Museum, Belfast, Northern Ireland
nmni.com/um/What-s-on/Elements

**Across Art and Fashion**
Until 7 April 2017
Museo Salvatore Ferragamo, Florence, Italy
www.ferragamo.com/museo/en/usa/exhibitions

**Warrior Treasures: Saxon Gold from the Staffordshire Hoard**
Until 23 April 2017
Bristol Museum & Art Gallery, Bristol
www.bristolmuseums.org.uk/bristol-museum-and-art-gallery/whats-on/warrior-treasures

**Must-haves—Jewellery Created by Greats of the Craft** and **Must-Sees—Jewellery in the Arts**
21 May–10 September 2017
Schmuckmuseum, Prorzheim, Germany
www.schmuckmuseum.de/flash/SMP_en.html

**Authentically Inauthentic?—Jewellery from Pforzheim's Industrial Production**
28 May–10 September 2017
Municipal Museum, Pforzheim, Germany
www.schmuckmuseum.de/flash/SMP_en.html

**Smycken: Jewellery—From Decorative to Practical**
Ongoing
Nordiska Museet, Stockholm, Sweden
www.nordiskamuseet.se/en/utstallningar/jewellery

## North America

**Gold and the Gods: Jewels of Ancient Nubia**
Until 8 January 2017
Museum of Fine Arts, Boston, Massachusetts, USA
www.mfa.org/exhibitions/gold-and-gods

**Gold Rush!—El Dorado in British Columbia**
Until 15 January 2017
Canadian Museum of History, Gatineau, Quebec, Canada
www.historymuseum.ca/goldrush

**Giant Gems of the Smithsonian**
Until 17 January 2017
Perot Museum of Nature and Science, Dallas, Texas, USA
www.perotmuseum.org/explore-the-museum/traveling-exhibits/2016-giant-gems/index.html

**Arts of Islamic Lands: Selections from The al-Sabah Collection, Kuwait**
Until 29 January 2017
Museum of Fine Arts, Houston, Texas, USA
www.mfah.org/exhibitions/arts-islamic-lands-selections-al-sabah-collection-

**American Mineral Heritage: Harvard Collection**
Until February 2017
Flandrau Science Center & Planetarium, Tucson, Arizona, USA
flandrau.org/exhibits/harvard

**Beyond Bling: Jewelry from the Lois Boardman Collection**
Until 5 February 2017
Los Angeles County Museum of Art, California, USA
www.lacma.org/art/exhibition/beyond-bling

**Bijoux Parisiens: French Jewelry from the Petit Palais, Paris**
11 February–14 May 2017
The Taft Museum of Art, Cincinnati, Ohio, USA
www.taftmuseum.org/upcoming-exhibitions-draft

**Variations on a Theme: 25 Years of Design from the AJDC**
Until 1 March 2017
Gemological Institute of America, Carlsbad, California, USA
www.gia.edu/gia-museum-variations-theme-25-years-design-AJDC

**Spectacular! Gems and Jewelry from the Merriweather Post Collection**
10 June 2017–14 January 2018
Hillwood Estate, Museum & Gardens, Washington DC, USA
www.hillwoodmuseum.org/Spectacular-Gems-and-Jewelry

## Australia and New Zealand

**Lustre: Pearling and Australia**
Until 22 January 2017
Immigration Museum, Melbourne, Victoria, Australia
www.thatsmelbourne.com.au/Whatson/Exhibitions/HistoryandHeritage/Pages/7e193464-ada5-4a57-911c-70b792d4d5ba.aspx

**The Art of Adornment: Greek Jewellery of the 17th–19th Centuries**
Ongoing
Hellenic Museum, Melbourne, Victoria, Australia
www.hellenic.org.au/the-art-of-adornment

# OTHER EDUCATIONAL OPPORTUNITIES

**Gem-A Workshops and Courses**
Gem-A, London
www.gem-a.com/education/courses

**Gem-A Midlands Branch**
Fellows Auctioneers, Birmingham
Email georgina@fellows.co.uk

- 24 February 2017
  Gwyn Green—Treatments and Imitations of Gemstones
- 28 April 2017
  Elizabeth Goring—Suffragette Jewellery

**ASA Appraising Gems and Jewelry Courses**
6–10 March 2017
Carlsbad, California, USA
www.appraisers.org/Education/View-Class?ClassID=3688 and www.appraisers.org/Education/View-Class?ClassID=3689.

**Gemstone Safari to Tanzania**
10–27 July 2017
Morogoro, Umba, Arusha, Longido, Merelani and Lake Manyara, Tanzania
www.free-form.ch/tanzania/gemstonesafari.html
*Note:* Includes options for a lapidary class and/or a private trip to visit ruby mines near Morogoro and Mpwapwa (including Winza).

**Lectures with The Society of Jewellery Historians**
Society of Antiquaries of London, Burlington House, London
www.societyofjewelleryhistorians.ac.uk/current_lectures

- 24 January 2017
  Noël Adams—Gold and Garnet Cloisonné Jewellery: Recent Discoveries and New Perspectives
- 28 February 2017
  David Callaghan—(To be announced)
- 28 March 2017
  Marjan Unger—My Jewellery Collection: Confessions of an Art Historian
- 24 October 2017
  Lynne Bartlett—The Rise and Fall of the Chatelaine
- 28 November 2017
  Judy Rudoe—Cartier Gold Boxes: A Visionary Patron and a Bet with Ian Fleming

# New Media

## A Guide to the Spectroscope

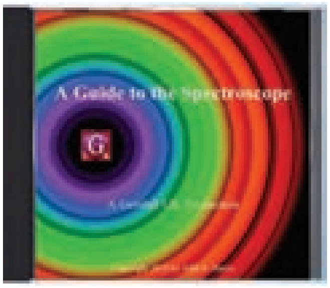

By John S. Harris, 2016. Self-published, www.gemlab.co.uk. US$25.00 CD.

This CD is formatted as an animated Microsoft PowerPoint presentation containing 23 slides that provide concise information, diagrams and photos on using the spectroscope for practical gem testing. The format allows for interactive animation with the viewer, and the slides can easily be reversed so that a sequence of the animated images may be repeated whenever necessary.

The presentation consists of three main parts: (1) the prism spectroscope, (2) the diffraction grating spectroscope and (3) observation techniques. The author starts with a review of the interaction of light with glass prisms to help the user to better understand the basic principles of this most useful and diagnostic of gem testing instruments. Then, parts 1 and 2 include comprehensive information on diffraction and prism spectroscopes, the construction of each type of instrument and also the differences in the spectra they produce. The direct visual comparison of these spectra is most informative and useful, thus enabling users to choose the best type of spectroscope for their requirements. Part 3 offers advice on observation techniques, which are of primary importance for achieving good readings. The final slides in this section (16–23) provide a comprehensive range of gem spectra that are categorized by colour. Each spectrum is accompanied by a nanometre scale and an image of the stone itself along with its colouring element, making this part of the presentation an excellent resource. Transmitted- and reflected-light techniques also are shown, with the advantages of each being described, as well as good practices for successfully viewing spectra by avoiding factors such as glare from unwanted surface reflections. The author's demonstrations of the differences between good and bad techniques are most informative.

Overall, this reviewer found this CD to be educational and intuitive to use and navigate. The information is provided in an interesting, informative and engaging way, making this CD an excellent reference/resource for tutors, students, appraisers and hobbyists or enthusiasts alike.

*Claire Mitchell FGA DGA*
*Gem-A, London*

## Ruby, Sapphire & Spinel: An Archaeological, Textual and Cultural Study

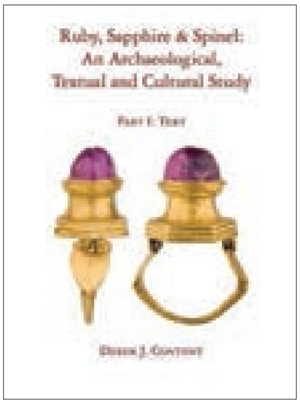

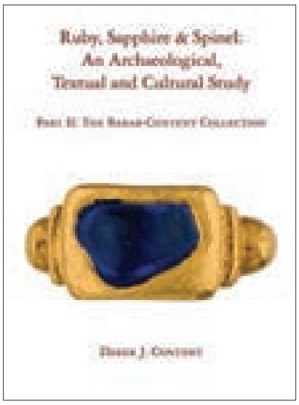

By Derek J. Content, 2016. Brepols Publishers, Turnhout, Belgium, www.brepols.net, 452 pages, illus., ISBN 978-2503568089. €150.00 hardcover.

While ruby, sapphire and spinel find occasional mention in books on engraved gems, no comprehensive text focusing on the history of these gems has been previously written. Thus the current work is welcome on that score alone. That it is the product of two true experts on antique gems—Derek Content and Riaz Babar—makes it all the more important.

*Ruby, Sapphire & Spinel: An Archaeological, Textual and Cultural Study* is split into two volumes. 'Part I: Text' is 191 pages long and gives a detailed historical description of these gems, from ancient times to the modern era. Following the Introduction are seven chapters. Chapters I and II cover the early history up through modern times (with the period after about 1830 AD being something of an afterthought). Chapter III deals with early mining technology, while Chapter IV covers fashioning methods. The remaining chapters cover usage, properties and nomenclature. Part I finishes with an epilogue, a comprehensive bibliography and a detailed index.

'Part II: The Babar-Content Collection' is 261 pages long and almost entirely composed of colour photographs (by Gonzalo Salcedo) and descriptions of 99 pieces in the combined collections of Riaz Babar and Derek Content. The photographs of each piece are excellent, and in the case of the many engraved pieces, wax replicas of the mostly Arabic inscriptions are also included, along with English translations. Approximate dates are given for each piece, increasing the value to scholars and appraisers alike.

As someone who has long been involved in researching these gems, this reviewer was extremely impressed by the high level of scholarship brought to bear on the subject. *Ruby, Sapphire & Spinel* is clearly aimed at an academic audience and is written with that in mind. Citations from the literature are both detailed and pertinent, with the original authors' words quoted rather than paraphrased. Almost every page reveals a fascinating tidbit or three, not just about these gems, but also about life, society and culture in early times. More importantly, this book gathers together an astonishing amount of information from disparate fields and sources and places it into a modern gemmological and historical context, correcting many of the errors of previous authors, who often lacked gemmological training.

This is an extremely important book on the history of gems and jewellery. If there are any flaws, they are that Part I is completely devoid of illustrations, and not a single map appears anywhere in the entire set. While scholars in the field will know the location of many of the places named in the text, adding maps and other illustrations would have enriched the reading experience for more casual readers. But these are small quibbles when one takes into account the decades of work in both collecting and research that *Ruby, Sapphire & Spinel* represents. Not only would I highly recommend this book to gemmologists, but would suggest it is a must-buy for appraisers and jewellery historians.

*Richard W. Hughes*
*Lotus Gemology, Bangkok, Thailand*

## Understanding the Gem Minerals: A Practical Guide

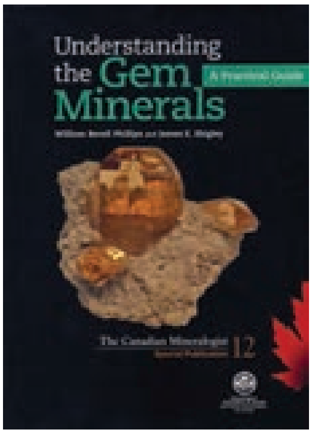

By William Revell Phillips and James E. Shigley, 2016. Canadian Mineralogist Special Publication 12, Mineralogical Association of Canada, Quebec, Canada, 259 pages, illus., ISBN 978-0921294580. US$70.00 softcover.

In the Preface to this work, the first author states: "I can only pray that this volume never falls into the hands of an expert, for he [sic] will pick it apart for its over simplification and broad generalizations…" Well, alas, this reviewer is probably what would be considered an expert; but rather than picking apart this useful guide, I will instead praise it (mostly).

Why are gems valuable? The usual criteria for a gemstone are that it be beautiful, durable and rare. After introducing the concepts of atoms, elements and crystal structures, necessary for understanding what a mineral is, the authors have arranged topics on the basis of these gem criteria.

Why is a gem beautiful? Because of the ways it interacts with light. The gem splits light into rays of different polarization; it bends light that comes in at a non-perpendicular angle, thus defining its index (or indices) of refraction; and it absorbs (and sometimes re-transmits) light, which leads to its colour. The reader is cautioned that in order to understand how light is used to distinguish among gem minerals, it will be necessary to visualize the uniaxial and biaxial indicatrices, which are, respectively, oblate and/or prolate spheroids (for uniaxial minerals), and spheroids that have been squashed or stretched in the third dimension (for biaxial minerals). Fortunately, there are many illustrations to help with this visualization.

Why is a gem durable? Well, that depends on the way its atoms are connected to each other by electron interactions. Non-directional charge interactions lead to (weak) ionic bonds; directional charge interactions lead to (strong) covalent bonds; and atomic nuclei that swim in a sea of electrons are characteristic of metals (which are sometimes weak with respect to scratching, but also malleable, or loathe to be broken apart).

Why is a gem rare? Many gem minerals require a specific history to form within the earth. For example, corundum needs a starting material from which Si is leached or under-available relative to Al; it helps if the Mg content is low as well (to avoid crystallizing spinel). If the right trace elements are present in the right abundance, it may be a ruby, a blue sapphire, or a fancy-coloured sapphire. But if it embraces too much of its history, in the form of inclusions, clouds, fissures or stains, it will not be gemmy. Then, after its formation, it must finally be brought to the surface of the earth where it can be mined.

This book is profusely illustrated, with the captions expansively explanatory, which brings me to my main quibble with this book: its design. Often, the captions are too big to fit on the same or facing page as the illustration. Also, not only are concepts explained the same way in the text as in the captions, but sometimes these explanations are only a few lines apart.

Less significantly, there are a few notable errata. An attempt to explain refractive indices in uniaxial minerals in the caption of figure 3-16C, on page 76, leads to two different meanings of $n_\varepsilon$ in the same sentence ($n_\varepsilon$ is "some value between $n_\varepsilon$ and $n_\omega$"). On page 81, figures 3-21B and C are reversed in the caption. Yet, on the other hand, figure 5-4 on p. 106, illustrating how interference colours come about, is both beautiful and self-explanatory, and for the most part the figures are more helpful than confusing.

Of course knowledge is always increasing, and some exotic gems or treatments may go beyond the lessons in this book. One should always be suspicious—or at least curious—about new gem substances and locations, and strange gem appearances. Still, with careful attention to the text and figures, it should in principle be possible for the reader to gain a good education on the basic mineralogy of gems using this book alone.

*Mary L. Johnson*
*Mary Johnson Consulting*
*San Diego, California, USA*

# OTHER BOOK TITLES

## Coloured Stones

***Tanzanite: Born from Lightning***
By Didier Brodbeck and Hayley Henning, 2016. Watchprint, La Croix-sur-Lutry, Switzerland, 208 pages, ISBN 978-2940506118. CHF92.00 hardcover.

## Gem Localities

***Collector's Guide to the Black Tourmaline of Pierrepont, New York***
By Steven C. Chamberlain, George Robinson, Michael Walter and Jeffrey Chiarenzelli, 2016. Schiffer Publishing Ltd., Atglen, Pennsylvania, USA, 128 pages, ISBN 978-0764351990. US$24.99 softcover.

***The Mineralogy of Texas***
By Arthur Edward Smith Jr., 2016. Self-published using www.lulu.com, 226 pages, ISBN 978-1329804746. US$25.50 softcover.

## General Reference

***The Crystal Guide: Identification, Purpose, Powers and Values***
By Patti Polk, 2016. Krause Publications, Iola, Wisconsin, USA, 256 pages, ISBN 978-1440247187. US$19.99 flexibound.

***Gem: The Definitive Visual Guide***
Ed. by Anna Fischel, 2016. Dorling Kindersley Ltd., London, 440 pages, ISBN 978-1465453563. £25.00 hardcover.

***Gems aur Rocks***
By Gagan Choudhary, 2016. Self-published, 280 pages, ISBN 978-9352671700 (in Hindi). INR1000 hardcover.

***Jewel: A Celebration of Earth's Treasures***
Ed. by Anna Fischel, 2016. Dorling Kindersley Ltd., London, 360 pages, ISBN 978-0241226032. £25.00 hardcover.

***Mineral Collections in Hong Kong***
Ed. by Elissa Sz, Trudy Kwong, Lai Siu Kwong and Sam Yung, 2016. Mineralogical Society of Hong Kong, 91 pages. HK$200 hardcover.

***Secrets of the Gem Trade: The Connoisseur's Guide to Precious Gemstones*, 2nd edn.**
By Richard Wise, 2016. Brunswick House Press, Massachusetts, USA, 404 pages, ISBN 978-0972822329. US$99.95 hardcover.

## Jewellery and *Objets d'Art*

***Art Nouveau Jewelry Designs***
Ed. by René Beauclair, 2016. Dover Publications, Mineola, New York, USA, 48 pages, ISBN 978-0486810065. US$14.95 softcover or Kindle edition.

***Cartier Magician: High Jewelry and Precious Objects***
By François Chaille, 2016. Flammarion, Paris, France, 264 pages, ISBN 978-2080203076. €95.00 hardcover.

***Helga Zahn: Jewelry. One-Off and Series***
By Petra Hölscher, 2016. Arnoldsche Art Publishers, Stuttgart, Germany, 104 pages, ISBN 978-3897904811 (in English and German). €28.00 hardcover.

***Hidden Gems: Jewellery Stories from the Saleroom***
By Sarah Hue-Williams, 2016. Unicorn Publishing Group, London, 312 pages, ISBN 978-1910065990. £35.00 hardcover.

***Jewelry Appraisal Handbook*, 9th edn.**
2016. American Society of Appraisers, Reston, Virginia, USA, 50+ pages. US$127.00 three-ring binder, $95.00 PDF file or $167.00 for both.

***Keepsakes and Treasures: Stories from Historic New England's Jewelry Collection***
By Carl Nold and Laura E. Johnson, 2016. Historic New England, Boston, Massachusetts, USA, 64 pages, ISBN 978-0989059831. US$19.95 softcover.

***Lydia Courteille: Extraordinary Jewellery of Imagination and Dreams***
By Juliet Weir-de La Rochefoucauld, 2016. ACC Art Books, Suffolk, 240 pages, ISBN 978-1851498376. £26.00 hardcover.

***nsaio 6: Neuer Schmuck aus Idar-Oberstein (New Jewellery from Idar-Oberstein)***
By Ute Eitzenhöfer and Theo Smeets, 2016. Arnoldsche Art Publishers, Stuttgart, Germany, 368 pages, ISBN 978-3897904736 (in English and German). €34.00 hardcover.

## Social Studies

***Natural Resource Conflicts: From Blood Diamonds to Rainforest***
By Mark Troy Burnett, 2016. ABC-CLIO LLC, Santa Barbara, California, USA, 910 pages, ISBN 978-1610694643. US$189.00 hardcover or $145.08 Kindle edition.

Compiled by Angharad Kolator Baldwin and Brendan Laurs

# Literature of Interest

## Coloured Stones

**The bright purple garnet: A new find in Mozambique.** D. Schwarz, P. Danchalermnon and Z. Michelou, *InColor*, No. 32, 2016, 48–53.

**Comparison of univariate and multivariate analysis for jadeite using laser induced breakdown spectroscopy.** Y. Wang, B. Shi, X. Yuan and Q. Zhang, *Journal of Gems & Gemmology*, **18**(3), 2016, 31–36 (in Chinese with English abstract).

**Evolution of the inclusion illusion.** E. Skalwold, *InColor*, No. 32, 2016, 22–23.

**Gemological and chemical characteristics of green tourmaline from Madagascar, Mozambique, and Tanzania.** M. Kaewtip and P. Limtrakun, *Walailak Journal of Science and Technology*, **13**(12), 2016, 985–992, http://wjst.wu.ac.th/index.php/wjst/article/view/2381.*

**"Geuda" - A market update on this unborn sapphire.** G. Zoysa, *Journal of the Gemmological Association of Hong Kong*, **37**, 2016, 93–95, www.gahk.org/journal/2016/a16.pdf.*

**Golden sheen sapphire – Saphire mit goldfabigem Schimmer aus Kenia [Golden sheen sapphire from Kenya].** H.A. Hänni and U. Henn, *Gemmologie: Zeitschrift der Deutschen Gemmologischen Gesellschaft*, **65**(1–2), 49–52 (in German with English abstract).

**Grossular garnet - a market update.** J. Saltzman, *Journal of the Gemmological Association of Hong Kong*, **37**, 2016, 83–84, www.gahk.org/journal/2016/a14.pdf.*

**Grüner Türkis [Green turquoise].** U. Henn, *Gemmologie: Zeitschrift der Deutschen Gemmologischen Gesellschaft*, **65**(1–2), 2016, 47–48 (in German with English abstract).

**How structure compactness impacts the quantitative colour research of turquoise.** Z. Luo, A.H. Shen, Q. Zhu and L. Liu, *Journal of Gems & Gemmology*, **18**(2), 2016, 1–8 (in Chinese with English abstract).

**The influence of different standard illuminants on tourmaline color red.** Y. Yang, Y. Guo, Y. Tan and Z. Chen, *Acta Mineralogica Sinica*, **36**(2), 2016, 220–224 (in Chinese with English abstract).

**A look at emeralds [pricing].** S.M. Robertson and Ç. Lüle, *GemGuide*, **35**(6), 2016, 2–5.

**Looks like maw sit sit: Sannan skarn from Pakistan.** H.A. Hänni, *InColor*, No. 32, 2016, 34–36.

**Un oeil-de-chat sur un saphir noir étoilé de Thaïlande [A cat's-eye on a black star sapphire from Thailand].** T.N. Bui, A. Solyga, K. Deliousi and J.-P. Gauthier, *Revue de Gemmologie A.F.G.*, No. 197, 2016, 22–23 (in French with English abstract).

**On the trail of Blue John.** S. Steele, *Gems&Jewellery*, **25**(6), 2016, 22–28.

**Quarzo ametista dei graniti di Cuasso al Monte e di Brandberg: Un confront [Amethyst quartz from Cuasso al Monte and Brandburg granites: A comparison].** A. Guastoni and P. Gentile, *Rivista Mineralogical Italiana*, No. 3, 2016, 168–179 (in Italian with English abstract).

**Recent finds of ajoite-included quartz in the Artonvilla mine, Messina District, Limpopo Province, South Africa.** P. Mayer and T. P. Moore, *Mineralogical Record*, **47**(4), 2016, 461–473.

**Reversible color modification of blue zircon by long-wave ultraviolet radiation.** N.D. Renfro, *Gems & Gemology*, **52**(3), 2016, 246–251, http://dx.doi.org/10.5741/GEMS.52.3.246.*

**Le vanadium trivalent comme colorant du chrysoberyl [Trivalent vanadium as a chrysoberyl colorant].** E. Thoreux, *Revue de Gemmologie A.F.G.*, No. 197, 2016, 8–12 (in French).

**Zircon - a very old gemstone.** H.A. Hänni, *Journal of the Gemmological Association of Hong Kong*, **37**, 2016, 37–41, www.gahk.org/journal/2016/a7b.pdf.*

## Cultural Heritage

**Diamonds through antiquity.** J. Asplund, *Gemmology Today*, **1**(1), 2016, 5–7, www.worldgemfoundation.com/GTNov2016.*

**Les gemmes dans la civilisation minoenne [The gems of the Minoan civilization].** H.-J. Schubnel and E. Gonthier, *Revue de Gemmologie A.F.G.*, No. 197, 2016, 24–30 (in French).

**Die Verwendung von Schlottwitzer Amethyst bei Tabatieren des 18. Jahrhunderts [The application of Schlottwitz amethyst in reference to 18th century snuffboxes].** G. Holzhey, *Gemmologie: Zeitschrift der Deutschen Gemmologischen Gesellschaft*, **65**(1–2), 2016, 31–39 (in German).

## Diamonds

**Diamond demographics: Junior diamond producers.** E. Laniado, *World Diamond Magazine*, No. 8, 2016, 70–72.

**Feasibility study on evaluation of fire in round brilliant cut diamond.** P. Liu, X. Yuan and B. Shi, *Journal of Gems & Gemmology*, **18**(4), 2016, 47–54 (in Chinese with English abstract).

---

* Article freely available online, as of press time

**The juniors: Second tier diamond miners.** E. Laniado, *World Diamond Magazine*, No. 8, 2016, 80–82.

**Large gem diamonds from metallic liquid in Earth's deep mantle.** E.M. Smith, S.B. Shirey, F. Nestola, E.S. Bullock, J. Wang, S.H. Richardson and W. Wang, *Science*, **354**(6318), 2016, 1403–1405, http://dx.doi.org/10.1126/science.aal1303.

**Over grading of blue fluorescent diamonds revisited.** M.D. Cowing, *Gemmology Today*, **1**(1), 2016, 38–39, www.worldgemfoundation.com/GTNov2016.*

**Polishing mechanism and surface damage analysis of type IIa single crystal diamond processed by mechanical and chemical polishing methods.** N. Tatsumi, K. Harano, T. Ito and H. Sumiya, *Diamond and Related Materials*, **63**, 2016, 80–85, http://dx.doi.org/10.1016/j.diamond.2015.11.021.

**Sites of the N1 nitrogen paramagnetic centers in natural diamond crystals: Dissymmetrization of the structure as a result of plastic deformation.** S.V. Titkov, R.M. Mineeva, I.D. Ryabchikov and A.V. Speransky, *Doklady Earth Sciences*, **468**(1), 2016, 500–502, http://dx.doi.org/10.1134/s1028334x16050135.

**Temperature effects on luminescence centers in natural type IIb diamonds.** S. Eaton-Magaña and T. Ardon, *Diamond and Related Materials*, **69**, 2016, 86–95, http://dx.doi.org/10.1016/j.diamond.2016.07.002.

**Value effect of fluorescence.** R.B. Drucker, *GemGuide*, **35**(5), 2016, 7–9.

## Fair Trade

**Diamonds are forever? Press coverage of African conflicts and the Westphalian filter of resource wars.** C.R. Cook, *Journal of African Media Studies*, **8**(2), 2016, 109–126, http://dx.doi.org/10.1386/jams.8.2.109_1.

**The legendary gem mines of Mogok Myanmar (Burma): Is responsible sourcing possible beyond sanctions?** L.E. Cartier, *National Geographic Voices*, 29 October 2016, http://voices.nationalgeographic.com/2016/10/29/gem-mines-of-mogok-myanmar-burma.*

## Gem Localities

**Ethiopian opal.** G. Kratch, *GemGuide*, **35**(5), 2016, 10–11.

**Mogok: Mining beauties and beyond.** T. Hainschwang and F. Notari, *InColor*, No. 32, 2016, 38–50.

**A new deposit of gem-quality grandidierite in Madagascar.** D. Bruyère, C. Delor, J. Raoul, R. Rakotondranaivo, G. Wille, N. Maubec and A. Lahfid, *Gems & Gemology*, **52**(3), 2016, 266–275, http://dx.doi.org/10.5741/GEMS.52.3.266.*

**Peridot from the Central Highlands of Vietnam: Properties, origin, and formation.** N.T.M. Thuyet, C. Hauzenberger, N.N. Khoi, C.T. Diep, C.V. Lam, N.T. Minh, N. Hoang and T. Häger, *Gems & Gemology*, **52**(3), 2016, 276–287, http://dx.doi.org/10.5741/GEMS.52.3.276.*

**Rubis australasiens [Australian rubies].** L. Sutherland, I. Graham, S. Harris, K. Zaw, S. Meffre, T. Coldham, R. Coenraads and G. Sutherland, *Revue de Gemmologie A.F.G.*, No. 197, 2016, 13–20 (in French with English abstract).

**Sapphires from the Sutara placer in the Russian Far East.** S.Y. Buravleva, S.Z. Smirnov, V.A. Pakhomova and D.G. Fedoseev, *Gems & Gemology*, **52**(3), 2016, 252–264, http://dx.doi.org/10.5741/GEMS.52.3.252.*

## Instrumentation

**10 Years of laser ablation - ICPMS applied in gem labs.** D. Nyfeler, *Journal of the Gemmological Association of Hong Kong*, **37**, 2016, 73–75, www.gahk.org/journal/2016/a12.pdf.*

**GemTOF: A pioneering technique in gemology.** H.A.O. Wang, L.E. Cartier and M.S. Krzemnicki, *InColor*, No. 32, 2016, 40–46.

**Light and gemstones - Spectrometric identification tools.** J. Dyer, *Gemmology Today*, **1**(1), 2016, 62–65, www.worldgemfoundation.com/GTNov2016.*

## Miscellaneous

**Faceting as a factor of gemstone appraisal on tomorrow's market.** V. Tuzlukov, *InColor*, No. 32, 2016, 54–58.

**Gems & jewelry TV—A worldwide retail window.** C. Unninayar, *InColor*, No. 32, 2016, 26–39.

**Photomicrography - A world within a gem.** E. Gavrilenko, *Gemmology Today*, **1**(1), 2016, 40–47, www.worldgemfoundation.com/GTNov2016.*

## News Press

**The dark shadow of Myanmar's jade trade.** D. Pye, *Financial Times*, 26 September 2016, www.ft.com/content/cf46e086-6909-11e6-a0b1-d87a9fea034f.*

**De Beers harvests diamonds at the bottom of the sea.** A. Wexler, *The Wall Street Journal*, 20 October 2016, www.wsj.com/articles/de-beers-harvests-diamonds-at-the-bottom-of-the-sea-1476973582.*

**Diamond mining companies setting sights on the sea as land dries up in Africa.** A. Laing, *The Telegraph,* 12 September 2016, www.telegraph.co.uk/news/2016/09/11/as-the-land-dries-up-diamond-mining-companies-are-turning-their.*

**Miners find massive jade boulder worth $170M.** T. Nace, *Forbes*, 24 October 2016, www.forbes.com/sites/trevornace/2016/10/24/miners-find-massive-jade-boulder-worth-170-million/#6a6fc9cd407e.*

## Organic Gems

**A burning question [ivory].** M. Campbell Pedersen, *Gems&Jewellery*, **25**(6), 2016, 10–11.

**A feathered dinosaur tail with primitive plumage trapped in mid-Cretaceous amber.** L. Xing, R.C. McKellar, X. Xu, G. Li, M. Bai, W.S. Persons, T. Miyashita, M.J. Benton, J. Zhang, A.P. Wolfe, Q. Yi, K. Tseng, H. Ran and P.J. Currie, *Current Biology*, **26**, 2016, 1–9, http://dx.doi.org/10.1016/j.cub.2016.10.008.*

**Recycling process of wasted amber from Myanmar.** R. Huang and E. Zu, *Journal of Gems & Gemmology*, **18**(4), 2016, 41–46 (in Chinese with English abstract).

## Pearls

**Bead-cultured and non-bead-cultured pearls from Lombok, Indonesia.** N. Sturman, J. Bergman, J. Poli, A. Homkrajae, A. Manustrong and N. Somsa-ard, *Gems & Gemology*, **52**(3), 2016, 288–297, http://dx.doi.org/10.5741/GEMS.52.3.288.*

**Golden South Sea cultured pearls: Cultivation steps & gemmological investigations.** L.E. Cartier and M.S. Krzemnicki, *Journal of the Gemmological Association of Hong Kong*, **37**, 2016, 16–21, www.gahk.org/journal/2016/a5.pdf.

**Identification of dyed golden South Sea pearls using UV-Vis and PL tests.** K.-W. Kwak, J.-K. Lee and E.-A. Jeong, *Journal of the Gemmological Association of Hong Kong*, **37**, 2016, 58–61, www.gahk.org/journal/2016/a10.pdf.*

**Mabé pearls: A forgotten variety on the rise?** H.A. Hänni, *JNA*, No. 387, 2016, 58–59.

**Perlas del Mar de Cortez: Cultured pearls from Mexico.** E. Arizmendi, S. Karampelas and M. Nava, *InColor*, No. 32, 2016, 26–32.

## Simulants

**The gemmological characteristics of a new kind of imitation of turquoise** S. Li, J. Di, X. Wang and B. Cao, *Spectroscopy and Spectral Analysis*, **36**(9), 2016, 2978–2983 (in Chinese with English abstract).

## Synthetics

**Observations on CVD-grown synthetic diamonds: A review.** S. Eaton-Magaña and J.E. Shigley, *Gems & Gemology*, **52**(3), 2016, 222–245, http://dx.doi.org/10.5741/GemS.52.3.222.*

**Synthesis of diamonds with mineral, fluid and melt inclusions.** Y.V. Bataleva, Y.N. Palyanov, Y.M. Borzdov, I.N. Kupriyanov and A.G. Sokol, *Lithos*, **265**, 2016, 292–303, http://dx.doi.org/10.1016/j.lithos.2016.07.005.

## Treatments

**Effect of heat treatment and electron beam irradiation [of] tourmaline: UV-visible, EPR, and mid-IR spectroscopic analyses.** A. Maneewong, K. Pangza, N. Jangsawang and T. Charoennam, *Walailak Journal of Science and Technology*, **13**(12), 2016, 993–1003, http://wjst.wu.ac.th/index.php/wjst/article/view/2382.*

**Improving the color of diamonds through HPHT processing.** S. Pope, B. Deljanin and J. Chapman, *InColor*, No. 32, 2016, 15–19.

**Iron K-edge XANES study of heated green beryl from Madagascar.** C. Chankhantha, P. Thanasuthipitak and P. Kidkhunthod, *Walailak Journal of Science and Technology*, **13**(12), 2016, 977–983, http://wjst.wu.ac.th/index.php/wjst/article/view/2380.*

**Research on treatment method of electron irradiated blue diamond.** C. Zhang and M. Chen, *Journal of Gems & Gemmology*, **18**(4), 2016, 10–15 (in Chinese with English abstract).

## Compilations

***G&G* Micro-World.** Andradite in andradite • Growth zoning in beryl • Growth blockages in cat's-eye beryllonite • Iridescent cleavage in tanzanite • Mobile fluorite inclusion in quartz • Inclusions in spinel from Madagascar • Sphalerite in topaz • Tourmaline termination • Axinite in quartz. *Gems & Gemology*, **52**(3), 2016, 310–316, www.gia.edu/gems-gemology.*

**Gem News International.** Aquamarine from San Luis Potosí, Mexico • Colored stone mining in Tanzania • Purple garnet from Mozambique • Trapiche rhodochrosite • Rubies from Pokot, Kenya • Blue sapphires from Badakhshan, Afghanistan • 'Punsiri'-type spectral features in natural yellow sapphire • Large fluid inclusion in amethyst • Impregnated jadeite seen with DiamondView • Conference reports. *Gems & Gemology*, **52**(3), 2016, 317–330, www.gia.edu/gems-gemology.*

**Lab Notes.** Focused-beam irradiation of treated pink diamond • Treated pink type IIa diamond colored by red luminescence • 59.88 ct irradiated yellow diamond • Purple fluorite inclusion in emerald • *Spondylus calcifer* pearls • Lead-glass-filled black star sapphire • Green lead-glass-filled sapphire rough • Graphite inclusion in CVD synthetic diamond • Screening colourless diamond melee • Treated red and green HPHT-grown synthetic diamonds. *Gems & Gemology*, **52**(3), 2016, 298–309, www.gia.edu/gems-gemology.*

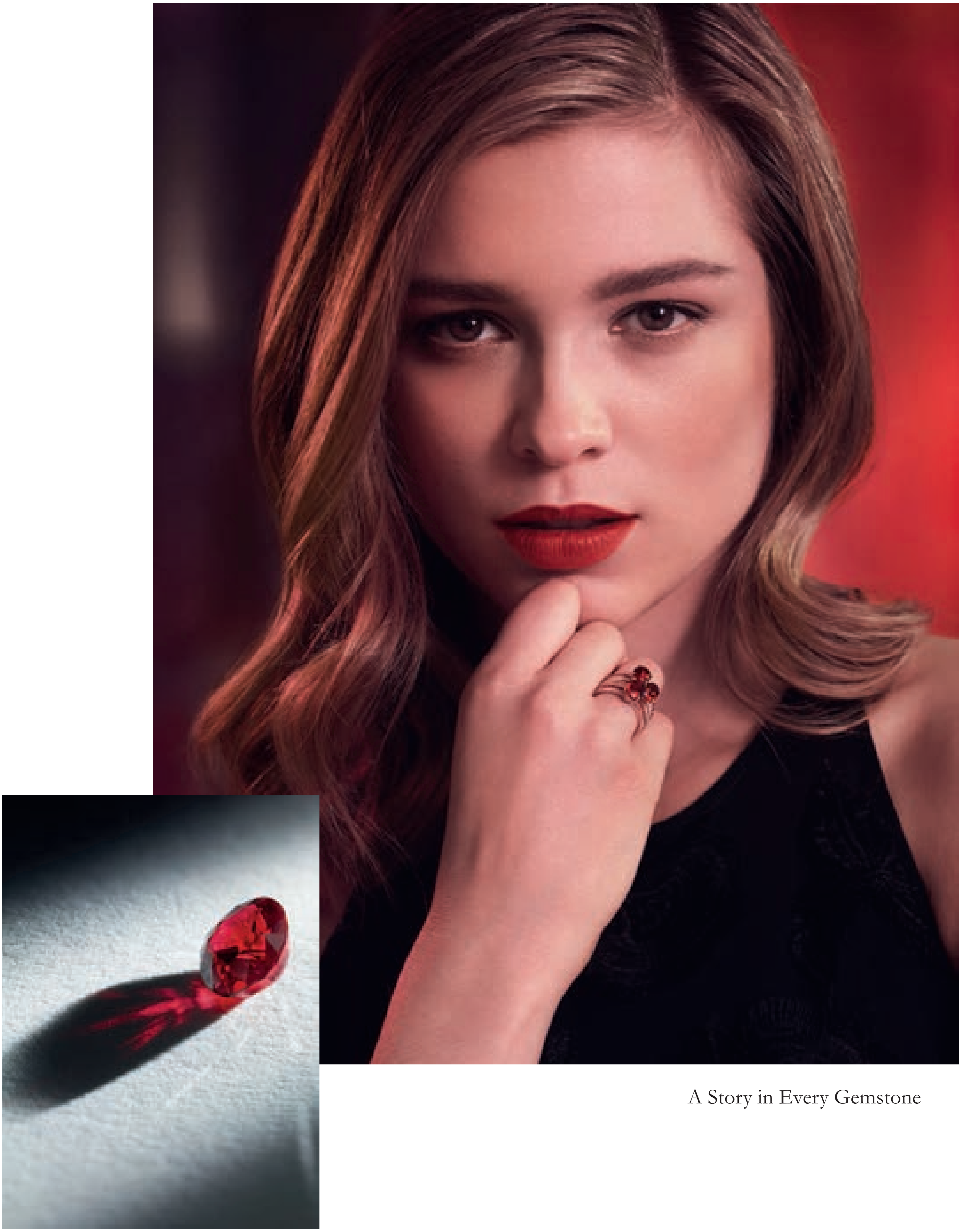
A Story in Every Gemstone

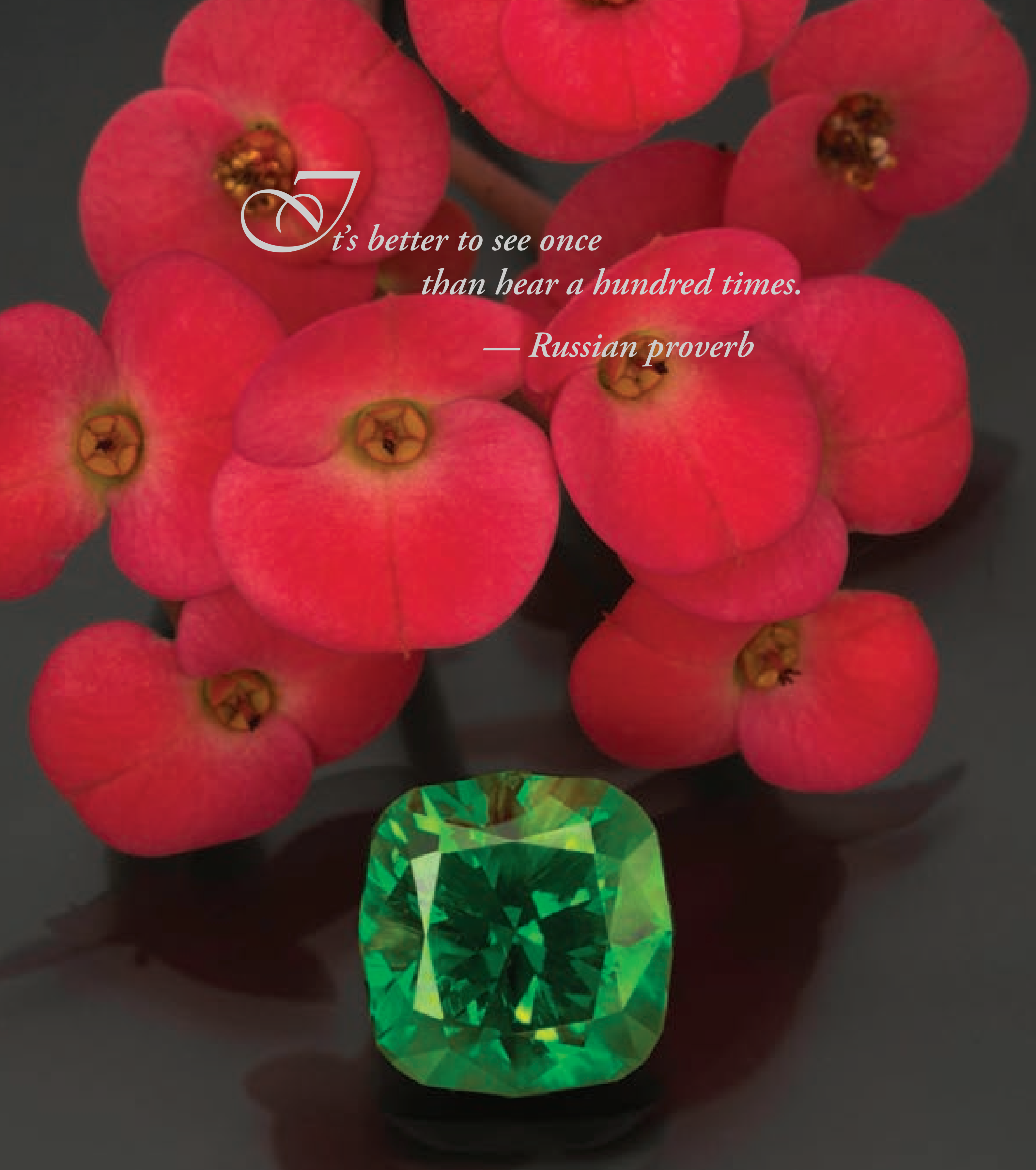

Demantoid Garnet from Russia • 6.97 ct • 10.88 x 11.16 x 7.26 mm
Blooms from Pala International Grounds • Photo: Mia Dixon